SHEAR STRENGTH OF PRESTRESSED CONCRETE BEAMS WITHOUT SHEAR REINFORCEMENT

by

MAHGOUB OSMAN MAHGOUB, B.Sc.,

being a thesis submitted for the degree of Doctor of Philosophy in the University of Glasgow.

Department of Civil Engineering

9th July, 1976.

CONTENTS

ACKNOWLEDGEMENTS

The work described herein was carried out in the Department of Civil Engineering at the University of Glasgow under the general guidance of Professor W.T. Marshall, until his sudden death at the end of 1975. The author would like to express his appreciation to Professor Marshall for the facilities of the Department and to Professor H.B. Sutherland for taking over the final stages of the supervision of the research.

The author is indebted to Dr. P.D. Arthur for his valuable supervision, encouragement and advice throughout the course of the investigation.

The author is grateful to Dr. P. Bhatt for useful discussions and criticisms, and to Dr. I.A.Smith for helping with computer work.

The author wishes to express his thanks to the concrete laboratory and workshop staffs for their interest and assistance. In particular, the help and interest of Messrs. J. Thomson, J. Coleman and A. Galt is gratefully acknowledged.

The author also wishes to thank Mrs. E. Carr, of 17 Woodbank Crescent, for typing the thesis.

Finally, thanks are extended to the Sudan Government for financial support during the period of the research.

SUMMARY

This thesis presents a detailed study, based on dimensional analysis and confirmed by experiment, of the factors which affect the shear strength of prestressed concrete beams without shear reinforcement. Sixty - eight pre-tensioned concrete beams of six different I - sections and one rectangular section were tested under one - or two-point loading and twenty-three pretensioned concrete beams of five different I - sections were tested under uniform loading.

The final mode of failure as well as the ultimate failure load were observed to be functions of many variables, some of which cannot be evaluated. As a result the shear force at diagonal tension cracking rather than the ultimate failure load was taken as the limit of the usefulness of the beam in shear. Accordingly an expression was developed for predicting the diagonal-tension cracking shear force under one - or two - point loads, and this expression was modified to predict the total uniform load at the diagonal tension crack in the case of a uniformly loaded beam.

Based on Mohr's failure theory, an expression for the shear - compression failure load was derived. It was shown that the ultimate strength of beams without shear reinforcement must be limited to the diagonal tension cracking load or the shear - compression load, whichever is the lesser.

The equations developed were compared, for specific

cases, with other published expressions and code design rules. Other published test results were shown to be in good agreement with the derived expressions.

NOTATION

All symbols used are the standard symbols of BSCP 110: Part 1: 1972[30] except as indicated below:-

a_v shear span.

C horizontal projection of a diagonal crack[28,29].

d′ distance between centroids of flanges[34].

E_{ci} static secant modulus of elasticity of concrete at transfer.

e eccentricity of the prestressing tendons from centroidal axis of beam.

f stress; concrete compressive stress at compression face at any stage of loading.

f_{av} average normal compressive stress in the compressive zone of beam.

f_c concrete compressive stress at compression face of section at failure (which corresponds to strain ε_c).

f'_c uniaxial compressive strength of concrete (taken as 0.8 f_{cu}).

f'_{ct} tensile strength of concrete (cylinder-splitting value).

f_{cu} characteristic concrete cube strength, taken as 1.25 x (compressive strength of 150 x 300 mm cylinders).

f_o maximum compressive strength of concrete in flexure (= 0.67 f_{cu} for CP 110).

f_{pb} tensile stress in prestressing tendons at beam failure.

f_{pi} stress in tendons before deduction of losses.

f_{ptr} stress in tendons after elastic shortening.

$f_{p.2\%}$ 0.2% proof stress of prestressing tendons.

f_{prism}	compressive strength of concrete prisms[25,28,29].
f_{sv}	permissible tensile stress in web reinforcement[83].
f'_t	uniaxial tensile strength of concrete.
f_{xx}	normal flexure stress in the compressive zone of beam (taken as f_{av}).
f_{yy}	stress normal to the longitudinal axis of the beam due to applied load and reaction.
f_1, f_2	principal stresses in a two dimensional stress system.
h	clear distance between flanges[34].
k_1	ratio of average normal flexure compressive stress to maximum normal flexure compressive stress.
k_2	ratio of the depth to the line of action of the normal compressive force to the neutral axis depth at failure.
k_3	ratio of the maximum normal flexure compressive stress, f_o, to compressive strength of concrete, $f_{cu}\left(= \frac{f_o}{f_{cu}} = 0.68 \text{ for CEB}^{(27)} \text{ and } = 0.67 \text{ for BSCP } 110^{(30)}\right)$
k_u	ratio of neutral axis depth at failure to effective depth.
l_t	transmission length[83].
M	bending moment at any stage of loading.
M_u	ultimate resistance moment at ultimate shear failure.
$\left(\frac{M}{V}\right)_c$	moment - shear ratio at failure.
Q	first moment of area of cross-section above and about the neutral axis.
q_c	uniformly distributed load per unit length of the span at diagonal tension crack.
$q_c l$	total uniformly distributed load at diagonal tension crack (written as W_c in the photographs).
$q_u l$	total uniformly distributed load at failure (written as W_u in the photographs).

V shear force at any stage of loading.

V_c ultimate shear resistance of concrete = shear force at diagonal cracking.

V_p vertical component of the effective prestress at the section considered(32).

V_s shear force resisted by web steel.

V_u shear force at failure.

v shear stress.

v_c ultimate shear stress in concrete (Table 5 of CP 110), nominal shear stress for concrete $\left(=\frac{V_c}{b_w d}\right)$

v_h horizontal shear stress.

$v_{max.}$ maximum shear stress.

v_{xy} average shear stress in the compression zone at failure.

v_{xymax} maximum shear stress in the compression zone or in the web at failure.

y distance from the centroid of concrete to centroid of the tensile reinforcement.

y_t distance from centroid axis of cross-section, neglecting the reinforcement, to extreme fibre in tension(32).

α $\varepsilon_c/\varepsilon_o$

γ ratio of uniaxial compressive strength to uniaxial tensile strength of concrete = f_c'/f_t'

ε strain; concrete compressive strain at compression face of section at any stage of loading.

ε_c concrete compressive strain at compression face of section at failure.

ε_u ultimate concrete strain in compression (= 0.0035 for CEB-FIP(27) and BSCP 110(30))

ε_o concrete compressive strain at compression face of section when f_o is reached (= 0.002 for CEB-FIP and $0.244 \times 10/\sqrt[3]{f_{cu}}$ for BSCP 110).

ε_{pa} strain in tendons produced by the applied loading.

ε_{pb} strain in tendons at beam failure.

ε_{pe} strain in tendons due to the effective prestress.

ε_{pi} strain in tendons before deduction of losses.

ε_{pt} strain in tendons due to concrete prestress at level of tendon $\left(= \frac{f_{pt}}{E_c}\right)$

θ slopes of cables[52].

$\lambda_c l$ distance of the critical section in shear from a support in a uniformly loaded beam failing by diagonal tension.

$\lambda_u l$ distance of the critical section in shear from a support in a uniformly loaded beam failing in shear compression.

ρ_v shear steel ratio $\left(= \frac{A_{sv}}{bd}\right)$

Φ reduction factor[32] (ACI (318 - 71) given as 0.85).

Note:- In Chapters 6 to 8, expressions containing the term $1000V_c$ will be dimensionally correct only when V_c is expressed in kN, f'_{ct} in N/mm^2, and other dimensions in mm.

CHAPTER 1

INTRODUCTION

In the design of concrete structures, it is generally desirable to ensure that ultimate strengths are governed by flexure rather than by shear.[1,2] A prestressed concrete beam under the combined action of a shear force and bending moment may fail in shear before its ultimate flexural strength is attained if it is not adequately designed for shear. The problem of shear failure in prestressed concrete beams is important mainly because, unlike flexural failure of correctly designed beams, it is characterised by small deflections and lack of ductility. Shear failure can occur very suddenly and without warning and it is sometimes violent and catastrophic as illustrated in Figures 5.1.d to 5.1.h.

The collapse of a large part of the roof of a U.S. Air Force warehouse in August 1955, due to the failure of the major structural frames by diagonal tension cracking, exposed the inadequacy of the design methods suggested in the then current codes and created fresh interest in the study of shear in reinforced concrete.[3] Nowadays the introduction of the concept of limit state design in the codes of practice requires a thorough knowledge of shear failure since design for the ultimate limit state results in size reduction which in turn may increase the danger of shear failure. In view of the large number of factors affecting the shearing strength, and the complexity of the stress conditions in the web of a cracked prestressed concrete I - beam, a fully mathematical solution is not a practical possibility.

As I - beams are in practice the most commonly used prestressed concrete structural members, the majority of the test specimens in this investigation were I - sections with differing geometrical properties. The dimensions were varied to permit a systematic study of the parameters affecting the shear strength of prestressed concrete beams without shear reinforcement under point loads and uniform loads, so as to establish an expression for predicting the shear force below which shear reinforcement is unnecessary. Beams without shear reinforcement are not common in practice, but they were used in this investigation because in them the diagonal cracking shear force could be defined clearly and the variables affecting it could be studied.

A shear failure in beams without shear reinforcement may be defined as a failure for which the primary cause is the formation of an inclined tension crack due to the combined action of a bending moment and shear force. In prestressed concrete beams without shear reinforcement the following types of failure have been observed:-

(a) Splitting of concrete due to diagonal tension crack.
(b) Web crushing under compression.
(c) The compressive zone is subjected to compression and shear and can fail either by splitting or crushing of concrete in the compressive zone.
(d) Splitting of concrete along the longitudinal reinforcement following the formation of the inclined tension crack.

The final mode of shear failure depends on various factors[4] which in turn govern the reserve capacity of a beam after the formation of the inclined tension crack-

ing. Some beams in this investigation carried a considerable load beyond the first inclined tension cracking load. In some instances the failure load V_u was 70% greater than the first inclined cracking load V_c, but the amount of this excess could not be predicted as it involves some unpredictable factors. Hence the shear force at the formation of the first diagonal crack rather than the actual maximum load has to be taken as the ultimate load for a beam without shear reinforcement. This load has been studied in this investigation using dimensional analysis and has been expressed in terms of the beam properties and either the a_v/d or the l/d ratio depending on the type of loading.

In some instances, such as beams with rectangular cross-sections tested at higher a_v/d or l/d ratios, shear-compression failure initiated by a flexure - shear crack has proved to be the dominant mode of failure. Kar's[42,43] prestressed rectangular beams were good examples of this type of shear failure. For such cases an expression based on Mohr's failure hypothesis with a straight line envelope to the failure stress circles was developed in this investigation to predict shear force at failure. Then the lesser of the first diagonal tension cracking load and shear - compression failure load is taken as a limit of the useful capacity of a beam without shear reinforcement in shear.

The expressions developed as described above were compared, for specific cases, with other published expressions and code design rules. The equations

developed were also compared with the test results published by other investigators and good agreement was observed.

CHAPTER 2.

HISTORICAL REVIEW

2.1 General:

The shear strength of concrete beams has been a subject of considerable interest to various investigators.[1,5-8] In 1973, an excellent report was published by the joint A.S.C.E. - A.C.I. Committee[2] which referred to over 200 documents and reviewed recent research results and design proposals concerning the shear strength of reinforced concrete structures. Despite the tremendous number of references in this subject, the Committee pointed out that " - - - - the question of shear strength is far from being settled. In some instances the explanations of behaviour and design concepts that are presented are somewhat speculative and may change as more information becomes available".

A comprehensive review of the published work on shear in concrete beams seems impossible to accomplish in a thesis of this nature, and accordingly reference will be made only to some major papers.

As shear strength of prestressed concrete beams can reliably be related to that of "unprestressed" beams, a review of some of these papers is necessary.

2.2 Shear in Reinforced Concrete Beams:

2.2.1 Concept of shear strength:

Controversy characterised the early development of shear design from 1900 to 1910[6]. Some engineers believed that horizontal shear, v_h, was the basic mechanism of shear

strength in reinforced concrete beams. Accordingly, shear stresses were computed by the equation:

$$v_h = \frac{VQ}{Ib} \qquad (2.1)$$

A second group of engineers recognised that the basic mechanism of shear strength is diagonal tension computed by:

$$v = \frac{V}{Zb} \qquad (2.2)$$

It took a full decade of heated discussion to arrive at diagonal tension and equation 2.2 as basic design tools. This was accomplished largely through the efforts of Mörsch in Germany and Talbot in United States.

2.2.2. In 1951 Clark[9] carried out 62 tests on beams with no web reinforcement and on beams with varying ratios of web reinforcement. From the test results, he derived the following semi-empirical expression for the maximum shear stress v_c as:

$$v_c = 17.3\sqrt{\rho_v} + \frac{0.12\ (0.8\ f_{cu})}{a_{v/d}} + 48.4\rho \qquad (2.3)$$

Clark was the first to include the $a_{v/d}$ ratio in shear equations and he was the first to account quantitatively for all the variables listed by Talbot[10] in 1909 as influencing the shear strength of reinforced concrete beams.

2.2.3 In an investigation sponsored by the Reinforced Concrete Research Council at the University of Illinois, U.S.A., Moody, Viest, Elstner and Hognestad presented a

series of tests in three reports [11,12] and these test results were analytically studied by Moody and Viest in the fourth report[13].

The authors observed that the phenomenon of diagonal cracking was one which involved the combination of flexural and shear stresses. Various attempts were made to express this phenomenon in terms of rational theory based on the ordinary theory of flexure and they have not yielded any solution. Hence an empirical equation for cracking load was reported. This equation includes both concrete strength and the $a_{v/d}$ ratio, and is as follows:

For $8.7 \leq f_{cu} \leq 43.3$ N/mm^2

$$v_c = \frac{V_c}{0.875\ bd} = 0.12x\left(0.8\ f_{cu}\right)\left(1 - \frac{0.8\ f_{cu}}{69.2}\right)\left(1 - 0.1\ \frac{a_v}{d}\right)$$

and for $43.3 \leq f_{cu} \leq 51.9$ N/mm^2

$$v_c = \frac{V_c}{0.875\ bd} = 0.12x\left(0.8 \times 43.3\right)\left(1 - \frac{0.8 \times 43.3}{69.2}\right)\left(1 - 0.1\ \frac{a_v}{d}\right) \qquad (2.4)$$

Equation 2.4 shows that the rate of increase of the nominal shearing stress, v_c, is decreasing with increasing concrete strength, and that for concrete strength greater than $f_{cu} = 43.3$ N/mm^2, the nominal shearing stress is independent of f_{cu}. This equation was derived from test data with a limited range of variables. The range of $a_{v/d}$ in test beams was 0.57 to 3.33, and hence equation 2.4 is not necessarily applicable to longer shear spans. For the ultimate shearing stress, they assumed that

the ultimate moment could be expressed by the same type of equation as for pure flexure (see Section 2.3).

2.2.4. Morrow and Viest[14] in their tests covered a wide range of $a_{v/d}$ ratios ranging from 0.96 to 7.79. As a result of this wide variation in $a_{v/d}$ ratios, different modes of failure were observed, which could be seen from their photographs. Analysing their test results, they reported that the concentration of concrete compressive stresses at a critical section was caused by concentrated rotations at the compressive end of the diagonal crack, the tensile stresses on the 'compression face' were caused by 'arch-action' present after the formation of the diagonal crack. The concentration of compressive strains at the critical section led to a premature crushing of the compressive zone of concrete and thus to failure before the flexural capacity was reached.

They gave two semi-empirical expressions similar to those of Moody and Viest. One for the diagonal tension crack load in terms of the nominal shearing stress which is given by:

$$v_c = \left[0.12 + \frac{3.19}{\frac{(M/Vd)_c}{(Es/Ec)\rho}}\right]\sqrt{0.8\, f_{cu}} \qquad (2.5)$$

where Ec is given from Kesler's[15] data as

$$460 \times (0.8\, f_{cu}) + 12456 \text{ N/mm}^2$$

The other for 'shear-compression' strength in terms of shear moment capacity.

They concluded that the presence of a diagonal tension crack is dangerous even in short beams. This is

because diagonal tension cracks in beams without shear reinforcement are considerably wider than flexural cracks; furthermore, a few repetitions of load may cause the diagonal tension crack to spread and possibly result in splitting along the reinforcement or in a premature shear failure. Accordingly for beams without web reinforcement, the diagonal tension cracking load may have to be considered in design as the ultimate capacity in shear.

2.2.5. Whitney[16] reported that the value of the unit shear at diagonal cracking is not a simple function of concrete strength, since it depends largely on the tension reinforcement. He proposed the following equations, for one-or two-point loads.

$$v_c = 0.346 \text{ N/mm}^2 + 0.26 \frac{M_u}{bd^2} \sqrt{\frac{1}{a_{v/d}}} \text{ N/mm}^2 \qquad (2.6)$$

and for uniformly distributed load

$$v_c = 0.484 \text{ N/mm}^2 + 0.54 \frac{M_u}{bd^2} \sqrt{\frac{1}{0.5\ l/d}} \text{ N/mm}^2 \qquad (2.7)$$

where

$\frac{M_u}{bd^2} = \frac{0.8\ fcu}{3}$ for over-reinforced beams.

$\frac{M_u}{bd^2} = \rho\ f_{yl} \left(1 - \frac{\rho\ f_{yl}}{1.7 \times (0.8\ f_{cu})}\right)$ for under-reinforced beams.

Balanced reinforcement is given by

$$\rho_o = 0.456 \times \frac{(0.8\ fcu)}{f_{yl}}$$

Like Morrow and Viest, Whitney considered the diagonal cracking load as the ultimate strength in shear of the beams without shear reinforcement.

2.2.6. In the United Kingdom, Taub and Neville[17]

conducted a large number of tests and they emphasised the importance of the moment-shear ratio. They showed also that the lattice analogy is not satisfactory for the design of bent-up bar reinforcement and recommended the use of a combination of bent-up bars and vertical stirrups to achieve the most effective resistance to shear failure.

2.2.7. Smith[18] devcloped an expression for the cracking load taking account of the influences of the ratio of the main reinforcement, ρ, and the $a_{v/d}$ ratio. Smith gives for sections already cracked in flexure:

$$\frac{V_c}{bh} = 0.79\sqrt{0.8\ f_{cu}}\left(0.186 + 0.00157\left(9 - \frac{a_v}{d}\right)^2\right)\left(1 + 7.5\ \rho\right) \qquad (2.8)$$

$a_{v/d} \geq 2.4$

where $0.79\sqrt{0.8\ f_{cu}}$ is the modulus of rupture.

On the basis of tests by Krefeld and Thurston[19], Smith concluded that the critical shear force at the critical section of a uniformly loaded simply supported beam can be expressed by the equation:

$$\frac{V_{c\ (U.D.L.)}}{bh} = 0.247\left(1 + 7.5\ \rho\right) \times 0.79\sqrt{0.8\ f_{cu}} \qquad (2.9.1)$$

where the critical section is at a distance x from the support and X is given by the following equation:

$$\frac{x\ (l - x)}{d\ (l - 2x)} = 1.2 \qquad (2.9.2)$$

Smith[1] later on revised equation 2.8 to give more weight to the influence of the ratio of main reinforcement and he gave the following:-

for $\rho \geq 1.25\%$

$$\frac{V_c}{bd} = 1.57 \times 0.79\sqrt{0.8\ f_{cu}}\left[0.13 + 0.0224\left(3 - \frac{a_v}{d}\right)^2\right]\left(1 + 14\rho\right) \qquad (2.10.1)$$

10

for $\rho \leq 1.25\%$

$$\frac{V_c}{bd} = 0.79 \sqrt{0.8\ f_{cu}} \left[0.13 + 0.0224 \left(3 - \frac{a_v}{d}\right)^2\right]\left(1 + 70\rho\right) \quad (2.10.2)$$

when $a_{v/d} > 3.0$, the second term in the square brackets of both equations is dropped.

2.2.8. Brock in a private communication to the Shear Study Group[1], presented a more general approach to the problems of shear in beams without shear reinforcement. This was in the form of an interaction diagram between the ultimate moment and the $a_{v/d}$ ratio.

This can be summarised by the following equations:

$$\frac{M_{flex}}{.8\ f_{cu}\ bd^2} = 0.456\left(\frac{\rho}{\rho_o}\right)\left(1 - 0.268\ \left(\frac{\rho}{\rho_o}\right)\right)$$

for under-reinforced sections, i.e. when $\rho < \rho_o$

and $$\frac{M_{flex}}{0.8\ f_{cu}\ bd^2} = 0.293 + 0.04\ \ (\rho/\rho_o)$$

for over-reinforced sections i.e. when $\rho > \rho_o$

where $\rho_o = 0.456 \times (0.8\ f_{cu})\ /\ f_{yl}$ (2.11)

The section attains its full flexural moment of resistance M_{flex} when

$$\frac{a_v}{d} > \frac{144\ f_{yl}}{8000}$$

where $\frac{a_v}{d}$ (or $\frac{M}{Vd}$ at the critical section) is less than $144\ f_{yl}/8000$ there is shear deterioration except for cases where $M_{flex}/(0.8\ f_{cu}\ bd^2) < 0.106$.

For very small values of $a_{v/d}$ there is a splitting type of failure which is assumed to be analogous to the Brazilian tensile test in which a cylinder of concrete is loaded along its sides. Recently this

approach was used by Desayi[20] too.

2.3. Shear-Compression Approach.

The commonest approach in determining the ultimate load capacity of beams failing in shear is the so-called shear-compression approach. This type of failure was envisaged by Laupa et al[21] as being essentially the same as flexural failure, the only difference being that the depth of the compressed zone was reduced by diagonal cracks extending considerably higher than flexural cracks at failure. This results in crushing of concrete at the head of critical shear crack.

In this approach, the dowel force is neglected, it being assumed that the stiffness of the dowel formed by the main steel is greatly reduced when the horizontal part of the crack is formed[22]. With this assumption the internal structural behaviour is similar to that of a simple tied arch. The external load is supported by an inclined, arch-like, thrust in the concrete above the shear crack, and the horizontal component of thrust at the support is resisted by the tension steel acting as a tie.

This concept of the structural behaviour of a beam containing a shear crack is supported by measurements of strains in the concrete which show that the centre of compression in the concrete falls as the support is approached[23].

Provided that the anchorage of the main reinforcement is sufficient for the tie-force, and that the geometry of the crack is such that the 'arch' does

not become unstable, i.e. fails by instability of the compression zone, collapse of the structure is caused by the crushing failure of the concrete at the crown of the arch. This ultimate compression load is given generally, by:

$$M_u = V_u \times a_v = k_1 k_3 f_{cu}\, b\, k_u\, d^2\, (1 - k_2 k_u) \qquad (2.12)$$

The coefficients $(k_1 k_3)$ and k_2 are generally ascribed values equal to normal flexural ones, viz.

Bjuggren[1] $k_1 k_3 f_{cu} = 0.5\, f_{cu}$ (2.13.1)

Moody and Viest[13] $k_1 k_3 f_{cu} = \left(1.121 - \frac{4.58 \times 144 \times (0.8 f_{cu})}{10^5}\right) \times (0.8\, f_{cu})$ (2.13.2)

Laupa et al[21] $k_1 k_3 f_{cu} = \left(1.37 - \frac{10.8 \times 144 \times (0.8\, f_{cu})}{10^5}\right) \times (0.8\, f_{cu})$ (2.13.3)

Regan[24] $k_1 k_3 f_{cu} = 0.67 \times (0.8\, f_{cu})$ (2.13.4)

Walther[25] and Ojha[26] have assumed that the capacity of the concrete to resist longitudinal stresses is reduced by the existence of a shear crack. Walther applied a biaxial failure criterion to the average compressive and shear stresses above the head of a shear crack and obtained:

$$k_1 k_3 f_{cu} = \frac{f_{prism}}{1 + 3.2\left(\frac{V_d}{M}\right)_c^2} \qquad (2.13.5)$$

where f_{prism} is the compressive strength of concrete prisms.

The main difficulty in equation 2.12 lies in a realistic assessment of the neutral axis depth $k_u d$. The neutral axis depth, $k_u d$, in equation 2.12 differs from the normal flexural one because the flexural

assumption that all sections plane before loading remain plane during loading is not valid in the presence of shear cracks. At the same time $k_u d$ is not generally equal to the ultimate flexural neutral axis depth because in most shear failures the main steel has not yet yielded at failure.

A detailed derivation of the expressions used in determining the neutral axis depth is beyond the scope of this review. The final expressions derived by some investigators in calculating M_u are shown as follows:-

Bjuggren:

$$\frac{M_u}{f_{cu} bd^2} = 0.5\, k_1 k_3 k_u\,(1 - 0.4\, k_u)$$

where $k_u = \dfrac{\rho E_s \varepsilon_u}{f_{cu}} \left(-1 + \sqrt{1 + \dfrac{2}{\dfrac{\rho E_s \varepsilon_u}{f_{cu}}}} \right)$ (2.14.1)

and $\varepsilon_u = 0.003$

Moody and Viest:

$$\frac{M_u}{f_{cu}\ bd^2} = \frac{\rho f_{st}}{f_{cu}} \left(1 - \frac{0.42\, \rho f_{st}}{k_1 k_3 (0.8\, f_{cu})} \right) \qquad (2.14.2)$$

where

$$f_{st} = 0.729 \times \left[6.9\ 10^{-4} E_s \left(-1 + \sqrt{1 + \frac{1450\, k_1 k_3 (0.8\, f_{cu})}{\rho E_s}} \right) \right]$$

Laupa et al:

$$\frac{M_u}{f_{cu}\ bd^2} = k_1 k_3 k_u\,(1 - 0.45\, k_u) \qquad (2.14.3)$$

where $k_u = 1.11 - \sqrt{1.23 - 0.92\, k'_u}$

and $k'_u = -np + \sqrt{(np)^2 + 2np}$

where $n = \dfrac{E_s}{E_c} = 5 + \dfrac{10000}{144 \times 0.8\, f_{cu}}$

Laupa's equation appears to predict a decrease of beam strength with increasing concrete strength, (see equation 2.13.3), but it is not intended to be applicable in such cases.

Regan:

$$\frac{M_u}{f_{cu} bd^2} = k_1 k_3 k_u (1 - 0.375\, k_u) \qquad (2.14.4)$$

where $k_u = \dfrac{n_o^2}{n_o + 1}$

$$\frac{n_o^2}{1 - n_o} = \frac{3\rho E_s \varepsilon_u}{2 \times 0.8\, f_{cu}}$$

and $\varepsilon_u = 0.0035$

The values of $k_1 k_3$ are given by equations 2.13.2 - 2.13.4

2.4. Some Code Approaches to Design of Beams for Shear Strength:

2.4.1. European Concrete Committee - International Federation of Prestressing.

The 1970 CEB - FIP Recommendations[27] state that the resistance mechanism of a beam or slab subject to shear loading depends essentially on the mode of cracking under design loads. The Committee recognises three cases of behaviour, but from a practical point of view only two are discussed, viz. AB and C.

Case AB is characterised by the development of web-shear cracks without flexural cracks at ultimate. In the region in which web-shear cracks occur, web reinforcement must be provided for the difference between the principal tensile stress at ultimate and a reduced

value of the tensile strength of concrete (Clause R 43 · 132). Failure due to crushing of the web should be prevented (Clause R 43.131).

Case C corresponds to those regions having flexure-shear cracking (Clause R43.14). The maximum shear is limited to prevent crushing of the web. The shear, V_c, carried by concrete is a function of the amount of longitudinal reinforcement and the square root of concrete strength.

For prestressed concrete beams the design procedure involves checking Case AB and C. In Case C the shear, V_c, carried by the concrete is increased as a function of average prestress.

2.4.2. U.S.S.R. Building Codes:

The shear strength carried by concrete is assumed[28,29] to be a function of the tensile strength of concrete and the horizontal projection of the diagonal crack, 'C'. The value of 'C' is taken as that length giving the minimum value of $(V_c + V_s)$, and these are given by:

$$V_c = \frac{0.15\ f_{prism}\ bh^2}{C}$$

$$C = \sqrt{\frac{0.15\ f_{prism}\ bh^2}{A_{sv}\ f_{yv}/S_v}}$$

$$\text{or } V_c + V_s = \sqrt{\frac{0.6\ f_{prism}\ A_{sv}\ f_{yv}\ bh^2}{S_v}} \qquad (2.15)$$

where f_{prism} is the strength of concrete prisms. The maximum shear stress on the web is limited to prevent crushing of the inclined concrete struts in the web.

2.4.3. British Code of Practice.

The provisions for shear in the new code BSCP 110: Part 1: 1972[30] differ considerably from those in BSCP 115: 1959[31]. BSCP 115: 1959 treats shear by limiting the principal tensile stress in regions of a member uncracked in flexure to values given in Table (6) of the Code. For regions cracked in flexure this Code is very vague and only gives the warning that "special consideration should be given to the shear resistance under ultimate load conditions where the section is cracked in bending". However, the new Code, BSCP 110: Part 1: 1972 gives separate expressions for the shear carried by the concrete in regions of a member uncracked in flexure and regions cracked in flexure.

For regions uncracked in flexure the BSCP 110 limits the tensile stress at the centroidal axis to $0.24\sqrt{f_{cu}}$. The shear force, V_{co}, corresponding to this principal tensile stress, is the shear force carried by the concrete at the limit state of collapse. From elastic theory, and neglecting the stress normal to the longitudinal axis, f_{yy}, due to applied load and reactions, V_{co}, is given as:

$$V_{co} = 0.67\ bh\sqrt{f_t^2 + 0.8\ f_t\ f_{cp}} \qquad \text{Code equation (45)}$$

where $f_t = 0.24\sqrt{f_{cu}}$

For regions cracked in flexure, the BSCP 110 gives the value of shear force carried by the concrete as V_{cr}, given by:

$$V_{cr} = \left(1 - 0.55\frac{f_{pe}}{f_{pu}}\right) v_c\ bd + \frac{M_o\ V}{M} \qquad \text{Code equation (46)}$$

$$\not< 0.1\ b_w d\ \sqrt{f_{cu}}$$

where v_c is the ultimate shear stress and is given as a function of ρ and f_{cu} in Table (5) of BSCP 110, and M_o is the moment necessary to produce zero stress in the concrete at the depth d, given by $M_o = 0.8\ f_{pt} \frac{I}{y}$

The shear force at the inclined crack should be taken as the lesser of the Code equations (45) and (46).

2.4.4. American Building Code:

The American Building Code ACI (318 - 71)[32], has two alternative methods for calculating the shear force carried by the concrete in regions of a member not cracked in flexure. One given in terms of average shear stress, v_{cw}, derived from the principal tensile stress equation as:

$$v_{cw} = \phi \left(0.29 \sqrt{0.8\ f_{cu}} + 0.3\ f_{cp} + \frac{V_p}{b_w d}\right)$$ Equation (11.12) of ACI (318-71)

and the other by limiting the principal tensile stress at the beam centroid to $0.33 \sqrt{0.8\ f_{cu}}$.

For regions cracked in flexure, it gives v_{ci} as the average shear stress at diagonal cracking. Neglecting the dead load, v_{ci}, is given by the following expression:

$$v_{ci} = \phi \left[0.05 \sqrt{0.8\ f_{cu}} + \frac{I}{y_t} \left(\frac{0.5 \sqrt{0.8\ f_{cu}} + f_{pe}}{b_w d^2\ (a_{v/d})}\right)\right]$$

Equation (11.11) of ACI (318-71)

ϕ is a reduction factor of 0.85

2.5. Shear in Prestressed Concrete Beams:

2.5.1. Prestressing introduces extra compressive stresses which are expected to reduce the final tensile stress resulting from shear. Thus the prestressing force creates a new variable in addition to those already mentioned for ordinary reinforced concrete beams. The factors affecting the shear of prestressed concrete beams and their behaviour under various conditions of loading and levels of prestressing have been discussed in various papers[33-54].

The shear strength of simply supported prestressed concrete beams without shear reinforcement under one-or two-point loads have been studied by Hicks[33], Sethunarayanan[34,35], Sozen, Zwoyer and Siess[36], Evans and Hosny[37], Walther[38], Warner and Hall[39], Evans and Schumacher[40], Swamy[41], Kar[42,43], Arthur[44] and Arthur and Mahgoub[45].

Kar[42,43], Wilby and Nazir[46], Hanson and Hulsbos[47], and Arthur, Bhatt and Duncan[48] made investigations on uniformly loaded beams. Bennett, Abdul-Ahad and Neville[49] have studied the problem of moving loads.

Among the investigators who studied the effect of shear reinforcement on the shear strength of prestressed concrete beams were MacGregor, Sozen and Siess[50]. and they also reported on the behaviour of prestressed concrete beams with draped reinforcement[51]. A paper which dealt with the shear strength of continuous beams of prestressed concrete

was by Jena and Pannell[52].

Now some of the papers which dealt with the shear strength of prestressed concrete beams without shear reinforcement will be reviewed in more detail.

2.5.2. Shear strength under one- or two-point loads:

2.5.2.1. Hicks[33] in his tests covered a wide range of $a_{v/h}$ ratios in an attempt to relate $a_{v/h}$ to the various types of failure and to investigate the effect of shear span and concrete strength on shear strength. The specimens were 16 pre-tensioned concrete beams. One cross-section of unsymmetrical I - section was used. The bottom and top flange breadths were 127 and 178 mm respectively, the web breadth was 38 mm, the flange thickness was 70 mm and overall depth was 254 mm.

The prestressing force was developed by using ten - 5 mm diameter indented wires having an ultimate strengtn of 1590 N/mm^2. The wires were distributed in such a way to give zero and 13.8 N/mm^2 compressive stress at the top and bottom fibres respectively and this was regarded as constant in all the beams. The concrete strength, which was one of the main variables, was varied between 34.0 and 47.0 N/mm^2.

By varying the $a_{v/h}$ ratio between zero and 8.15, four types of failure were observed which gave Hicks his limits of the $a_{v/h}$ ratio within which each type of failure occurred. For $a_{v/h}$ = 1.5, 'shear distortion' would prevail which describes the state of web

cracking and crushing followed by failure of the separate flanges in flexure, cracks appear at the top flange above the reaction and in bottom flange below the load. 'Diagonal compression' would be the failure pattern for $a_{v/h}$ between 1.5 and 4.5. The main difference between this type of failure and the shear distortion was that, in the diagonal compression failure the vertical cracks in the top and bottom flanges occurred away from the reaction and load points. At higher $a_{v/h}$ ratios, between 4.5 to 9.0, failures tended to resemble the 'diagonal tension' type. This occurs by a sudden splitting of the web and causes the beam to fail immediately without any traces of web crushing. Above $a_{v/h} = 9.0$ flexure failure would be expected.

For those beams failing in diagonal tension, Hicks suggested the following equation for the principal tensile stress at failure at the neutral axis:

$$f_t = f'_{ct} - 0.187\left(\frac{a_v}{h} - 2\right) \qquad a_{v/h} \leq 2 \qquad (2.16)$$

He concluded his investigation by suggesting a reduction factor of 0.7 to be applied to the ultimate flexural moment for $a_{v/h} < 7.0$ for design purposes.

This was an investigation of restricted scope since Hicks used only one type of cross-section with a constant prestressing force.

2.5.2.2. On the other hand tests reported by Sethunarayanan[34] on pre-tensioned I beams with various cross-sections revealed that the transition from one mode of failure to another depended not only on $a_{v/h}$ ratio, but also on the amount of pre-stress and strength of concrete. This was later confirmed by Arthur's[44] tests.

Sethunarayanan's tests were conducted on 32 pretensioned I beams with top flange breadth ranging from 127 to 178 mm and with a constant bottom flange breadth of 178 mm. The thickness of the top flange ranged from 50.8 to 81.2 mm and that of the bottom flange was constant at 63.5 mm. The web breadth ranged from 35.0 to 62.2 mm. The distance between the centroids of the flanges was taken as the effective depth and this ranged, accordingly, between 171 and 184 mm.

The prestressing force was developed through 5 mm diameter indented wires varied in number between 5 and 10. The wires were stressed and distributed over the cross-section to give a variation in f_{cp} ranging from zero to 7.75 N/mm^2. The concrete strength, f_{cu}, varied from 34.4 to 41.6 N/mm^2.

From his test results Sethunarayanan developed the following expression for the diagonal cracking load:-

$$V_c = f'_{ct}\left(1 + \frac{1 + f_{cp}/f'_{ct}}{\sqrt{a_{v/d'}}}\right) h' b_w \qquad (2.17)$$

Equation 2.17 shows that V_c is inversely proportional

to flange thickness which conflicts with Arthur's[44] findings. He also developed an analysis based on the truss analogy for the cases in which web crushing followed the initial inclined cracks.

2.5.2.3. As a part of an investigation of prestressed concrete for highway bridges, Sozen, Zwoyer and Siess[36] carried out tests on 43 and 56 rectangular and I-section concrete beams respectively. All the beams were 152 by 304 mm overall in cross-section. For I-beams the $b_{w/b}$ ratio had values of 0.29 and 0.50, and the $h_{f/d}$ ratio ranged from 0.28 to 0.50. The end-blocks were 456 mm long.

5 mm diameter hard drawn wire was used with f_{pu} varying from 1660 to 1870 N/mm^2. The stress in the prestressing wires, at test, varied between zero and 970 N/mm^2 and the prestressing steel ratio, ρ, varied from 0.10% to 0.96% giving a variation in f_{cp} between zero and 6.23 N/mm^2.

All the I-beams and eight of the rectangular beams were pre-tensioned, the rest being post-tensioned and grouted. All but three of the I-beams had prestressed external stirrups to prevent propagation of cracks into the end-block. Those external stirrups were placed, one at each junction of the web and the end-block and one immediately on the outside of each reaction block.

The beams were tested simply supported with $a_{v/d}$ ranging from 2.7 to 5.4 and most of the tests were conducted between $a_{v/d} = 3.2$ and 4.2.

The strain measurements in the top surface of the beam showed that after web cracking, the longitudinal

strains adjacent to the load points were higher than in the zone between them, which led to the conclusion that web cracking effect was to cause concentrations of strains leading to crushing of concrete.

Ninety beams failed in shear and the remaining nine failed in flexure either by crushing of the concrete or fracture of the steel. The modes of shear failure observed were given a detailed description in their bulletin. They classified the shear failures into two categories: 'shear-compression' and 'web-distress'. The shear-compression failure was described as similar to flexural compression failure except that the concrete crushed at the upper end of the inclined crack where there was a very high strain concentration. This mode of failure was observed in both rectangular and I beams.

On the other hand web-distress could take any one of the following forms:

(i) Secondary inclined tension cracks formed near the supports and above mid-height of the beam, which separate the compression flange from the web, leading to violent failure.

(ii) Inclined cracks near the loading points extending horizontally toward the supports tending to separate the web from the bottom flange entirely, or

(iii) Crushing of the web under high compressive stresses due to 'arch action' created by the loss of shear flow between the steel and compression flange.

Based on their definition of the inclined tension cracking load as the load at which the inlined crack started to affect the behaviour of the beam, they

analysed their test results and derived the following semi-empirical expression for the inclined cracking load:

$$V_c = \frac{f'_t \left(1 + \frac{f_{cp}}{f'_t}\right) \sqrt{b_w b}\ d}{a_{v/d}} \qquad (2.18)$$

where f'_t was given as a function of $(0.8\ f_{cu})$ as

$$f'_t = \frac{6.92}{B + \frac{41.5}{0.8\ f_{cu}}}\ N/mm^2 \qquad (2.19)$$

They gave B = 1.0 for concrete with regular coarse aggregate (maximum size 38 mm) and B = 2.0 for small size coarse aggregate (maximum size 10 mm).

They concluded that the inclined cracking load should be taken as the limit of the usefulness of a beam in shear since the development of inclined cracks was unstable.

The limited number of tests outside the range of $a_{v/d}$ ratio of 3.2 to 4.2, means that the confidence which can be placed in equation 2.18 is limited, and may lead to seriously unsafe overestimates of the strength particularly for low values of $a_{v/d}$[45].

2.5.2.4. Evans and Hosny[37] analysed the test results carried out by Hosny on post-tensioned prestressed concrete beams, together with the results of similar tests reported by Zwoyer[36] and Thornton[37].

Hosny's beams were 3 rectangular and 17 I beams. The specimens were 101 by 304 mm in overall. The I section had its top and bottom flange thicknesses as 62 and 70 mm respectively and the web breadth was 47.0

to 50.8 mm. This gave a variation in $h_{f/d}$ of 0.240 to 0.245 and in $b_{w/b}$ from 0.46 to 0.50.

The prestressing force was developed through Macalloy bars. All the beams were grouted except two. The percentage of the prestressing steel, ρ, ranged from 2.453 to 2.987. The average prestress in the concrete at test, f_{cp}, ranged from 1.72 to 5.25 N/mm^2. The concrete strength measured as (0.8 f_{cu}) ranged from 34.7 to 58.1 N/mm^2.

Thornton's beams were 13 pretensioned I beams with prestressed compression reinforcement placed at 11.0 mm below the top fibres. Two cross-sections were basically used with $b_{w/b}$ as 0.375 and a variation in $h_{f/d}$ of 0.188 to 0.210. The percentage of the prestressing steel wires, ρ, was 0.437 and 0.485 giving a value of f_{cp} ranging from 0.61 to 3.16 N/mm^2. The strength of the concrete was intended to be constant and was 42.6 (=0.8 f_{cu}) N/mm^2. The $a_{v/d}$ ratio ranged from 2.32 to 3.48.

Evans and Hosny gave a full description of the modes of failure observed in Hosny's tests which were: Shear-compression, diagonal crushing of the web and shearing of the compression zone, the last being observed in I sections with web reinforcement. In their analysis of these test results, they took the nominal shear stress to be a function of $\sqrt{0.8\ f_{cu}}$, the cross-section properties, the prestressing force and $a_{v/d}$ ratio and gave the following expression for ultimate shear force:-

For rectangular section where $\rho \not< 0.350$ and $2.57 \leq \frac{a_v}{d} \leq 6.70$

$$V_u = \frac{(0.83 + 0.15\ \rho\ f_{pe})\sqrt{0.8\ f_{cu}}\ b_w\ Z}{(a_v/d)} \qquad (2.20)$$

For an I section where $2.32 \leq \frac{a_v}{d} \leq 3.60$

$$V_u = \frac{(1.91 + 0.15\ \rho\ f_{pe})\sqrt{0.8\ f_{cu}}\ b_w\ Z}{(a_v/d)} \qquad (2.21)$$

From their analysis of the I section results, they noticed that the ratio of maximum principal tensile stress to the tensile strength of concrete was constant for $a_{v/d} \geq 3.0$. They gave the following relationships for the value of the maximum principal tensile stress, f_t as:-

$$f_t = \left(\frac{4.99}{1.75 + a_{v/d}} - 0.624\right)\sqrt{0.8\ f_{cu}} \quad \text{for } \frac{a_v}{d} \leq 3.0 \qquad (2.22)$$

$$f_t = 0.312\sqrt{0.8\ f_{cu}} \quad \text{for } \frac{a_v}{d} \geq 3.0 \qquad (2.23)$$

The applicability of equations 2.21 - 2.23 is rather limited since they are based on a very narrow range of $a_{v/d}$ values.

2.5.2.5. Warner and Hall[39] developed expressions for the principal tensile stress, f_t, as a function of $a_{v/d}$ and the concrete strength.

For $f_{cu} \geq 43.3$ N/mm^2

$$f_t = 0.034\ f_{cu}\ (6.85 - 3.9\ a_{v/d}) \quad \text{for } \frac{a_v}{d} < 1.5$$

$$f_t = 0.034\ f_{cu} \quad \text{for } \frac{a_v}{d} > 1.5$$

For $f_{cu} < 43.3$ N/mm^2

$$f_t = (6.85 - 3.9\ \frac{a_v}{d})(0.077 - 0.001\ f_{cu})f_{cu} \quad \text{for } \frac{a_v}{d} < 1.5$$

$$f_t = (0.077 - 0.001\ f_{cu})f_{cu} \quad \text{for } \frac{a_v}{d} \geq 1.5 \qquad (2.24)$$

2.5.2.6. Evans and Schumacher[40] conducted tests on 5 rectangular and 49 I section fully bonded post-tensioned concrete beams. The percentage of the pre-stressing steel, length of shear span, shape of beam cross-section and curing method were taken as major variables.

Basically three shapes of cross-sections were employed, rectangular and two I-sections with nominal $b_{w/b}$ ratio of 0.34 and 0.50 and $h_{f/d}$ ratio was found to range from .29 to .31. The I beams had solid end -blocks broader than flange breadth.

Three types of steel were used, viz, Lee-McCall bars or Gifford-Udall cables of 7 and 5 mm diameter hard drawn prestressing wires. The percentage of the prestressing steel, ρ, was varied between 0.21 and 4.77. The beams were stressed, at minimum, 10 days after casting and grouted immediately afterwards. f_{cp} values ranged from 1.45 to 5.60 N/mm^2 and f_{cu} ranged from 40.5 to 69.5 N/mm^2.

Most of the beams failed by shear-compression, diagonal cracking alone, diagonal cracking followed by web-crushing, or flexural failure. 13 of the beams failed in flexure and two showed failure of the web following the formation of cracks at the upper web flange junction.

They analysed their test results and came out with two expressions, one for shear-compression failure and the other for diagonal cracking failure.

For rectangular sections failing in shear-compression, they gave:

$$V_u = \left(1.400 - 1.388\rho\frac{f_{pu}}{f_{cu}}\right) \frac{k\ b\ d}{a_v/d}\ f_{cu}\ k_u\ (1.00 - .42\ k_u) \qquad (2.25)$$

where $\rho f_{pu}/f_{cu} \angle 0.72$

For I-section failing in shear-compression,

$$V_u = (1.400 - 1.388\rho\frac{f_{pu}}{f_{cu}})(3.45\rho\frac{f_{pu}}{f_{cu}} - 0.19)\frac{k\,bd}{a_v/d}\ f_{cu}k_u(1-.42k_u) \qquad (2.26)$$

where $0.24 \angle \rho\frac{f_{pu}}{f_{cu}} \angle 0.8$

in the above two equations 2.25 and 2.26:

$$k = 1.2 - 0.661 \times 10^{-2} f_{cu} \qquad (2.27)$$

$$\text{and } k_u = \rho\frac{f_{pu}}{f_{cu}}\ (0.534 + 0.063\,\rho f_{pe}) \qquad (2.28)$$

$$\leq \frac{h_f}{d} \quad \text{for I-sections.}$$

For diagonal cracking load, they gave:

$$V_c = 3.33\ f'_{ct} \left(1 + \frac{f_{cp}}{f'_{ct}}\right)\ b_w d \left(0.10 + \frac{0.275}{a_v/d}\right) \qquad (2.29)$$

They concluded that the lesser of the shear-compression load and the diagonal cracking load should be taken as the limit of usefulness of a beam failing in shear.

The authors realised that equation 2.29 might not be applicable to other I - sections because the ratio $\frac{h_f}{d}$ was not varied in their tests, although it would be expected to have an influence on the diagonal cracking load.

2.5.2.7. Swamy[41] carried out a preliminary investigation on seven post-tensioned, unbonded, hollow rectangular beams to study diagonal cracking failure.

All the beams were 229 mm by 152 mm overall with effective depth of 203 mm, having $b_{w/b}$ = 0.25 and $h_{f/d}$ = 0.25. The prestressing steel used was Macalloy high tensile steel bars and the percentage of the prestressing steel, ρ, ranged from 0.770 to 1.540, giving a variation in f_{cp} from 4.43 to 8.23 N/mm^2. The concrete strength, f_{cu}, ranged from 59.2 to 73.4 N/mm^2. The beams were loaded at third-points giving $a_{v/d}$ as 3.75.

The tensile steel and the compressive concrete strains and deflections all showed essentially elastic behaviour until failure occurred. The principal tensile stress obtained from the strain gauge readings taken in three directions at the centre of the web at the mid-point of the shear span were found to bear little relation to either the theoretical stresses or the tensile stress of concrete. Accordingly Swamy concluded that the principal tensile stress was an unsuitable criterion for predicting the cracking load.

Failure took place by diagonal cracking in all the beams except two which failed by flexure initiated by yielding of steel and they gave warning of distress before failure. There was practically no difference between the cracking load and the ultimate load, so Swamy considered the diagonal cracking load as a measure of shear capacity of the beam. Because of

the small number of the test beams no attempt was made to develop an expression for the diagonal cracking load.

2.5.2.8. Kar[42,43] conducted tests on 26 rectangular and 9 I-beams which were all post-tensioned and grouted.

The rectangular beams were composed of ten 125 by 250 mm, nine 125 by 300 mm and seven 100 by 200 mm. The I-beams were all 150 by 300 in overall with $b_{w/b}$ as 0.254 and $h_{f/d}$ ranging from 0.358 to 0.383. The prestressing steel was 5 mm diameter and 7 mm diameter high tensile steel wires. The concrete strength, measured as $(0.8\ f_{cu})$, was varied between 27.9 and 38.9 N/mm^2 and the $a_{v/d}$ ratio ranged from 2.0 to 6.0.

The majority of beams failed by shear-compression and the rest by web-crushing. For the prediction of the shear-compression failure load, Kar based his analysis on a modified linear strain diagram, equilibrium of internal forces and equilibrium of internal and external moments. Then he developed expressions which require a trial and error procedure to determine V_u for rectangular beams.

Kar[42] examined the web of the I-beam and found that the plane of rupture prior to cracking was subject to non-uniform longitudinal compressive stress. Accordingly Kar proposed Seth's[42] failure criterion under combined stresses which is identical in nature with Coulomb's internal friction theory for biaxial stress

conditions, to be applied to the rupture conditions on the web of the I beam. Using the experimental results, Kar[42] modified Seth's failure criterion to take into account the influence of $^{a}v/d$ and developed the following equation for predicting the web-shear cracking shear force:

$$V_c = \frac{Cr\ I\ b_w(0.8\ f_{cu})}{2\ Q}\left[(1 + C_1)^2 - 2C_1(1 + C_1)\left(\frac{f_{cp}}{0.8f_{cu}}\right) - (1 - C_1^2)\left(\frac{f_{cp}}{.8\ f_{cu}}\right)^2\right]^{1/2}$$

where $Cr = 0.953 - 0.0565\ \frac{a_v}{h}$ $\quad \frac{a_v}{h} \geq 2.0$

or

$$Cr = 1.88 - 0.52\ \frac{a_v}{h} \qquad \frac{a_v}{h} \leq 2.0$$

and $C_1 = -\frac{0.8\ f_{cu} + f_t}{0.8\ f_{cu} - f_t}$ where $f_t = 0.624\sqrt{0.8\ f_{cu}}$

(2.30)

2.5.2.9. Arthur[44] carried out tests on 55 pretensioned concrete I beams, treating as major variables the solid end-blocks, the strength of concrete, prestressing force, beam cross-section and $^{a}v/d$ ratio.

Basically four cross-sections were used. Three of the cross-sections were 152 by 304 mm in overall with an effective depth of 272 mm. The fourth one was 152 by 228 mm with an effective depth of 200 mm. The ratio of $^{b}w/b$ was varied between 0.33 and 0.50, three different values were chosen and $^{h}f/d$ was 0.19 and 0.25. The prestressing steel was indented tensile steel wires with diameters of 2.65 mm and 5 mm. The average effective prestress, ^{f}cp, ranged from 4.17 to

6.20 N/mm^2. The concrete strength, f_{cu}, varied between 36.5 and 68.9 N/mm^2.

The $a_{v/d}$ ratios covered ranged from 1.12 to 4.57. The mode of failure observed was mainly diagonal cracking either alone or followed by either web distortion, web crushing or flexural compression. Shear-compression failure initiated by a flexure-shear crack was also observed in some cases.

The solid end-blocks were found to have no effect on the cracking load. In 86% of the tests conducted, the shear loads carried by the beams exceeded the diagonal cracking load, but this excess could not be predicted. Accordingly Arthur limited the useful capacity of a beam failing in shear to the diagonal cracking load. The following expression was developed for its prediction.

$$V_c = f'_{ct}\left(1 + \frac{f_{cp}}{f'_{ct}}\right) b_w h_f \left(0.73 + \frac{3.34}{a_{v/d}}\right) \qquad (2.31)$$

for $h_{f/d} \not< 0.19$

where the f'_{ct} values are those given by Dewar's[55] expressions:

$$f'_{ct} = 0.25\, f_{cu}^{2/3} \quad \text{for crushed rock}$$

$$\text{or} \quad f'_{ct} = 0.23\, f_{cu}^{2/3} \quad \text{for gravel} \qquad (2.32)$$

Equation 2.31 above is based on two values of $h_{f/d}$ so its applicability is rather limited, and it tends to over-estimate the value of V_c at high values of $h_{f/d}$ (see Section 7.2). It is not applicable in the

case of a rectangular beam. Arthur suggested a reduction factor of 0.7 to equation 2.31 for design purposes.

2.5.2.10. Jena and Pannell[52] carried out tests on two series of 20 two-span unbonded prestressed concrete I-beams of b_w = 76.0 mm. The first series was 152 mm wide by 229 mm deep overall, with h_f = 57.5 and the second series 152 mm wide by 305 mm deep overall, with h_f = 70.5. Each of the twenty beams had a total length of 4.9 m and was continuous over two spans of 2.3 m each. The prestressing steel was two strands of 12.7 mm nominal diameter. The cable profile is shown in Figure 2.1. The effective prestress in the strands ranged from 765 to 1061 N/mm^2. The concrete strength, f_{cu}, varied between 35.9 to 56.2 N/mm^2.

Two-point loads were applied, at equal distances on either side of the central support. Of the 20 beams tested, 17 failed in shear, remainder failing in bending. Jena and Pannell compared the limiting principal tensile stresses at the centroids of the 17 unbonded prestressed concrete beams failing by diagonal tension cracking with others obtained from pretensioned and post-tensioned I beams with similar modes of failure and found that there was no distinguishable difference between the data derived from both cases. During their tests they observed that the diagonal tension crack appeared suddenly in the web at or near the point of contraflexure and very

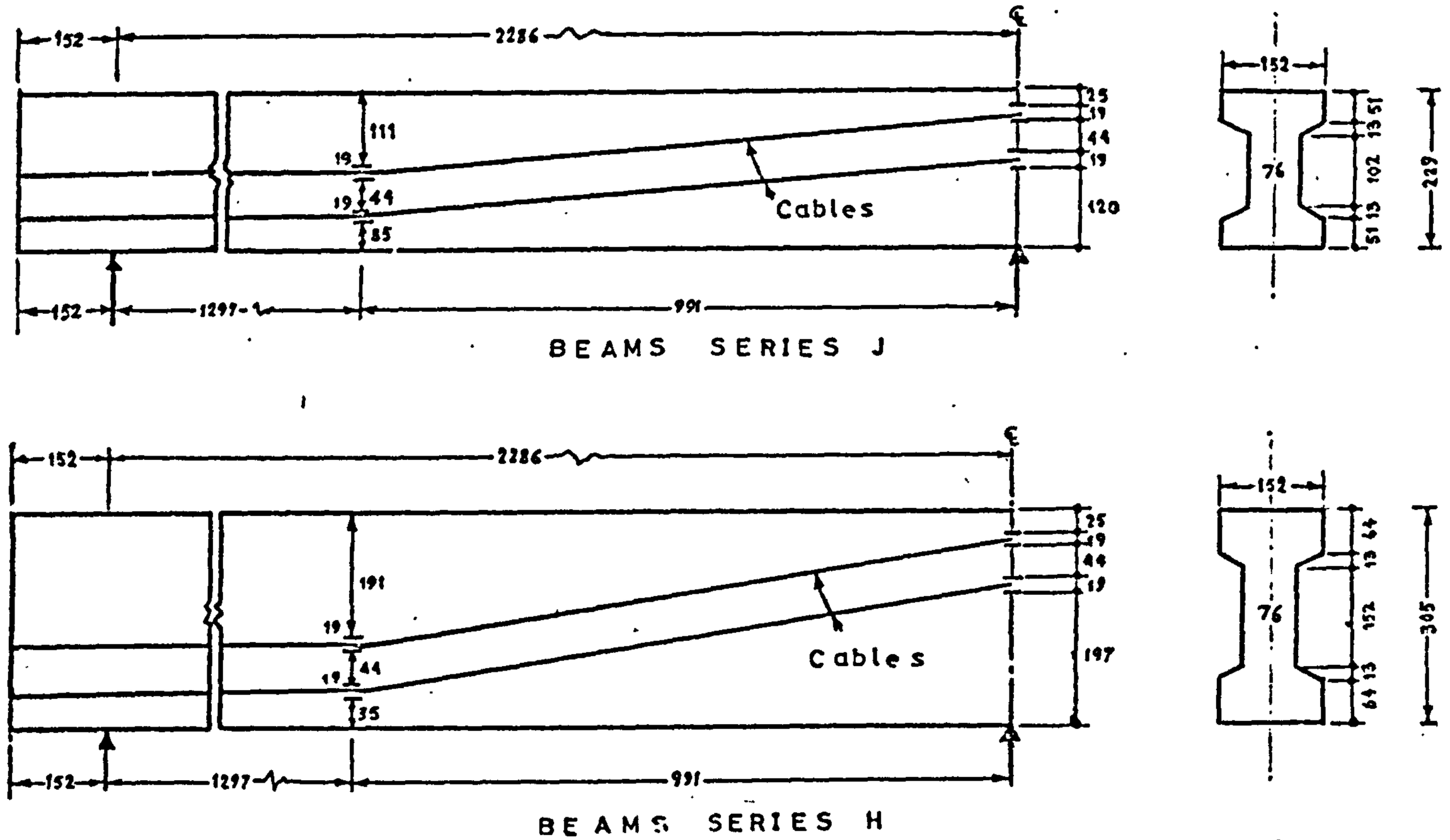

Figure (2.1): Cable profiles in Jena and Pennell's[52] two series of beams.

close to the centroidal axis of the uncracked section. Thus basing their analysis on the principal tension theory, Jena and Pannell using their own results and those of others[33,34,42], derived expressions for the maximum principal tensile stress at the neutral axis as a function of $a_{v/h}$ and concrete strength. They gave the following expression for calculating the cracking shear force:-

$$V_c = \frac{I\, b_w}{Q}\sqrt{f_t^2 + f_t\, f_{cp}} + A_s\, f_{pe} \sin\theta \qquad (2.33)$$

where f_t is equal to $\frac{0.55\sqrt{f_{cu}}}{a_{v/d}}$

2.5.2.11. Borišanskij and Nikolaev[8] at the NIŽB (Reinforced Concrete Institute) in Moscow studied the conditions for the formation of diagonal cracks in beams. As well as I beams, prestressed T beams were studied with flanges in the tension or the compression zone. It was shown that diagonal cracks in the web do not develop at the places where the principal stresses, as calculated for elastic behaviour, are assumed to be greatest.

Gvozdev[8] in calculating the principal tensile stress took into consideration the compressive stresses acting on the horizontal planes near the points of application of loads and reactions. By using the data from Paduart's theoretical studies[8] and the results of the deformation tests on beams by Borisanskij and Nikolaev, Gvozdev proposed the following expressions for determining local compressive stresses:

$$f_{yy} = \frac{P}{2b_w h}\left(\frac{h}{y'} - 1\right)\left(1 - \frac{x'}{2y'}\right) \text{ for } y' < 0.4\ h \text{ and } x' \leq 2y'$$

$$f_{yy} = \frac{P}{0.8\ b_w h}\left(1 - \frac{y'}{h}\right)\left(1 - \frac{x'}{0.8h}\right) \text{ for } y' \geq 0.4\ h \text{ and } x' \leq 0.8\ h \quad (2.34)$$

where P is the value of point load, y' is the distance between the point on the beam from the compression face and x' is the distance between the point on the beam and the section where the load is applied. Equation 2.34 predicts a zero value for f_{yy} at the mid of shear span at centroidal axis for $a_{v/d} = 2.0$ ($d = 0.8\ h$).

2.5.3. Shear strength under uniformly distributed load.

2.5.3.1 Wilby and Nazir[46] conducted tests on 5 post-tensioned prestressed concrete I beams, 4 of them with grouted ducts and all with unreinforced webs to study their behaviour and strength under multiple point loads. The beams were all simply supported on spans corresponding to $l/d = 5.4$. The beams were 152 by 304 mm overall. Only one cross-section, with $\frac{b_w}{b} = 0.33$, $\frac{h_f}{d} = 0.25$ and effective depth = 254 mm, was used, The prestressing force was developed through Lee-McCall bars, which were stressed initially to 413 N/mm^2. The only variable was the concrete strength which varied between 28.0 and 58.0 N/mm^2.

The modes of failure observed were the destruction of the web either by splitting along the line of the diagonal crack or by the crushing of concrete due to the arch action. It was found that the critical

diagonal crack crossed the neutral axis at an average distance of 0.22l from a support. Strain measurements were taken with electrical strain gauges forming an equilateral triangle at points on the centroidal axis 0.22 l from each support. Those measurements showed that the discrepancy was quite appreciable when compared with the theoretical values of the principal tensile stress. This led Wilby and Nazir to conclude that the theoretical principal tensile stress as a means of predicting the initial diagonal cracking load has no meaning. They also found that the principal tensile stress calculated from the measured strains corresponding to the formation of the first diagonal cracks did not compare with the tensile strength of concrete. In this respect their results were in good agreement with those obtained by Swamy[41], although they pointed out that their experimental measurements were susceptible to some slight amount of error because the strains at a point were measured along the three sides of an equilateral triangle enclosing, instead of precisely, at the point. Also they mentioned that owing to the short span, the portion undergoing diagonal failure experiences some of the vertical stresses due to the load points.

Although their tests were restricted in number and the concrete strength was the only variable, they derived the following expression for web-cracking load

$$q_c^l = 4.94\, f_{cu} + 61.3 \quad KN \qquad (2.35)$$

2.5.3.2. Kar[43] carried out tests on 14 post-tensioned prestressed rectangular concrete beams under uniformly distributed load with simply supported ends. The specimens were four beams 100 by 200 mm overall with l/d = 15.3 and ten 125 by 300 mm overall with l/d = 13.1. He found that the critical section in shear-compression type of failure lay at 0.315 l from the nearest support, and this confirms Hanson and Hulsbos[47] observations on two pre-tensioned I-beams under the same type of loading who found the critical section in his I - beams lay at 0.33 l from the nearest support.

Kar gave the following relationship between the point-load case and the uniformly distributed load case for use in prediction of the shear-compression failure load of the latter:

$$q_u l = \frac{8.33\ V_u\ (a_v/d)}{(l/d)} \qquad (2.36)$$

2.5.3.3. Arthur , Bhatt and Duncan[48] studied the strength in shear of 19 pretensioned concrete I-beams with unreinforced webs under uniformly distributed load with simply supported ends. The uniformly distributed load was applied using the fire-hose technique used by Hanson and Hulsbos[47], and by Leonhardt and Walther[61].

Basically three different cross-sections were employed. The specimens were 153 by 304 mm overall with $b_{w/b}$ ranging from 0.416 to 0.500, $h_{f/d}$ = 0.187 and the effective depth, d = 272 mm. All the beams were pre-stressed by nine 5 mm diameter high tensile

steel wires. The value of prestressing force at test ranged from 134 to 184 KN giving a variation in f_{cp} between 5.40 and 7.00 N/mm^2. The concrete strength, given as tensile strength derived from split cylinder value, ranged from 2.84 to 3.93 N/mm^2. The l/d ratio covered ranged from 6.18 to 9.52.

It was observed that all the beams cracked on a line through a reaction. In 9 beams the ultimate load was the same as or only slightly greater than the web-cracking load. Thus Arthur et al regarded the web-cracking load as the ultimate load for failure in shear with unreinforced webs. The following semi-empirical expression was developed for predicting the web-cracking load.

$$q_c l = f'_{ct} \left(1 + \frac{f_{cp}}{f'_{ct}}\right) b_w d \left(0.1 + 0.5\frac{h_f}{d}\right)\left(9.85 - 0.79 \frac{l}{d}\right) l \qquad (2.37)$$

The constant and the coefficient of $\frac{h_f}{d}$ in the second bracket were chosen arbitrarily as only one value of $h_{f/d}$ was used. Equation 2.37 predicts a zero value for the cracking load at $l/d = 12.47$ which restricts its applicability at high values of l/d.

Arthur, Bhatt and Duncan in their analytical approach, took the principal tensile stress theory as a criterion for failure. A computer programme based on the simple theory of bending of beams was first prepared to search the web for the position of maximum principal tensile stress. The results obtained showed the maximum occurring either over the supports

at 3 — 5 mm above the centroidal axis or at mid-span depending on the value of the load and the length of span. From this it was concluded that the simple bending theory approach which neglected the effect of local stresses due to the reactions gave misleading information for maximum principal tensile stress in value and position. Then another approach was attempted based on elastic stress analysis which allowed approximately for the effect of the reactions, and vertical stresses due to the loading, in addition to normal bending and shear stresses. The reactions were treated as point loads on an infinite wedge. By equating the resulting maximum principal tensile stress in the web to the tensile strength of the concrete, a reasonable agreement with their experimental results was obtained.

2.6. Analytical Approach Using Finite Element:

Any attempt at a detailed analytical stress analysis over the whole loading range of a prestressed concrete beam has to recognise the non-linear behaviour of the beam due to cracking as well as non-linear material properties.

The advent of computers and modern methods of analysis, such as the finite element method[56] led to attempts by some investigators[57-59] to achieve the above objective.

An accurate analytical determination of the displacements and the internal stresses and deform-

ations in a reinforced or a prestressed concrete structure throughout its load history is complicated by a number of factors:(58)

1. The structural system is composed of two materials, concrete and steel.
2. The structural system has a continuously changing topology due to the cracking of concrete under increasing load.
3. Governing relationships and failure criteria under combined stress states are difficult to obtain. (See Section 3.6).
4. The stress-strain relationship for concrete is non-linear and is a function of many variables. (See Section 6.2.2.).
5. Concrete deformations are influenced by shrinkage and creep.
6. Deformations and stress are time-dependent on load and environmental history.
7. The effect of dowel action in the steel reinforcement, bond between the reinforcement and concrete, bond slip, and aggregate interlock at cracks are difficult to incorporate into a general analytical model.

Although no attempt has been made to include all the above factors in an analytical model, it seems that there is a potential for this finite element technique, mainly as a research tool, to explore the behaviour of reinforced and prestressed concrete beams under the combined action of shear and bending when more information concerning the above mentioned factors becomes available.

2.7. Concluding Remarks:

The review of previous work on the shear strength of prestressed concrete beams without shear reinforcement shows that:

2.7.1. None of the existing expressions is generally applicable because:

1. The geometric properties of the cross-section were treated differently. All but Sethunarayanan[34] and Arthur[44] ignore the flange thickness, h_f, as a variable. Sethunarayanan included the effect of the flange thickness in his equation 2.17 in terms of the clear distance between flanges. On the other hand Arthur used a constant value of the flange thickness, h_f, throughout his tests and he included h_f as a variable directly proportional to V_c in his equation 2.31 . Sethunarayanan and Arthur's equations are of contradictory nature a) with respect to the variable h_f.
2. All but Sozen et al[36] did not include the effect of b/b_w in their expressions.
3. The data recorded in the literature for concrete strength is not uniform. A wide range of expressions is used for the tensile strength of concrete.
4. Most of the tests were conducted at $a_{v/d}$ ratios between 2.5 and 4.2 except a few cases[33,34,44] which dealt with values of $a_{v/d}$ less than 2.5. Sozen et al conducted tests on 99 beams, the

majority of them with $a_{v/d}$ between 3.2 and 4.2, which makes equation 2.18 of a restricted scope[45].

2.7.2. Although only uniformly distributed load constitutes a practical type of loading, we find that most of the available test data relate to beams under one- or two-point load.

2.7.3. The well-known failure criteria for concrete subjected to normal and shear stresses cannot be applied in the case of beams without being modified to take into account the affect of $a_{v/d}$[25,42].

2.7.4. A fully mathematical solution is not practicable in case of prestressed concrete beams subjected to combined bending and shear.

2.7.5. There are gaps in the experimental results available which indicate that a wider range of variables needs to be covered in a systematic way.

CHAPTER 3

STUDY OF THE PARAMETERS AFFECTING THE SHEAR STRENGTH OF PRESTRESSED CONCRETE BEAMS AND CRITERIA USED IN PREDICTING FAILURE OF CONCRETE

3.1 Introduction:

The review in the foregoing Chapter showed that the parameters which seem to affect the shear strength of prestressed concrete beams without shear reinforcement are : the geometric configuration of the cross-section, the concrete strength, the intensity of the prestressing force, the position of the prestressing tendons and the shear span.

Professor R. Walther, in a lecture on 'shear problems in reinforced concrete beams' given on 31st October 1972 in the Department of Civil Engineering at the University of Glasgow, disagreed with Table 5 of B.S.C.P. 110 : part 1: 1972,[30] which takes the shear stress as a function of the longitudinal steel ratio. He claimed that the shear stress was a function of the amount of longitudinal steel in excess of that needed for bending, i.e. shear stress is a function of $\left(\frac{A_s \text{ prov.}}{A_s \text{ req.}}\right)$. In dealing with prestressed concrete beams the above ratio will have little influence on diagonal tension cracking since the area of excess longitudinal steel likely to be used is small compared with that likely to be used in reinforced concrete beams. Hence that factor will be neglected and factors mentioned above will be discussed in more detail.

3.2. The Geometric Configuration of the Cross-section:

The effect of the cross-section configuration on shear strength has been shown by test results obtained by several investigators[17,60-62]. Ferguson and Thompson[60] and Leonhardt and Walther[61] showed that failure loads increase with increasing web breadth. For instance, Ferguson and Thompson's beams A1 and D2 differed only in web breadths, which were in the ratio of 1.75 : 1. The ultimate shears of these two beams were found to be in the ratio of 1.79 : 1, i.e. the ultimate shear strength was directly proportional to the web breadth.

The effect of flange dimensions on the shear strength was demonstrated by Taub and Neville[17] on rectangular and T beams with comparable web breadths. Similar tests on flange width were reported by Placas and Regan[62] on T beams with 150 mm web breadth. It was found that the beams with 300 mm or wider flanges had about 20% greater ultimate shear strength than rectangular beams. It was concluded that only the portion of the flange immediately adjacent to the web could transmit a component of the shear in the compression zone.

The effect of beam size was shown by Leonhardt and Walther's[61], Kani's[63] and Taylor's[64] tests. Leonhardt and Walther concluded that in beams with external similarity but constant bond quality, shear strength was fairly independent of the beam size.

Kani, using beams differing only in depth, found that the shear stress at failure decreased with increasing beam depth. Kani concluded that as the depth increased, the splitting forces due to the 'wedging bond action' of the reinforcement increased, and as a result, the failure of the two deeper series of Kani's beams involved splitting along the reinforcement while the smaller beams did not. Taylor showed that the size effect could be reduced if the size of the coarse aggregates was changed in proportion to the beam size. Taylor suggested a reduction factor of 0.6 to the shear stress carried by a concrete beam with $\frac{d}{b} > 4.0$.

3.3. Concrete Strength.

Shear does not directly cause the failure of reinforced or prestressed concrete beams, but its effects appear as tensile stress leading to diagonal tension cracks. Although the tensile strength of concrete is not convenient for use in design, as the compressive strength is the usual property specified, it sounds reasonable to relate the diagonal cracking load to the tensile strength of concrete. The values for the tensile strength of concrete reported in the literature were obtained in a variety of ways.

Sethunarayanan used the cylinder splitting value. Sozen et al related the modulus of rupture of concrete to cylinder compressive strength and used two-thirds of this derived modulus of rupture as a measure of the tensile strength of concrete. Evans and Hosny took the tensile strength of concrete as directly proportional to $\sqrt{0.8\, f_{cu}}$ and Evans

and Schumacher used 0.72 of the tensile strength obtained from briquette tests. Arthur used values derived from Dewar's expressions.

As the indirect tensile strength of concrete derived from the split cylinder value tends to give more uniform results than other types of tensile tests,[65,66] it is used in this investigation as a measure of the tensile strength of concrete.

3.4 Prestressing Force:

As already mentioned the prestressing force induces extra compressive stresses which reduce the final tensile stress resulting from shear. The position of the prestressing force creates a variation across the depth of the beam in the value of the prestress in the concrete. Since the position at which the crack will open is unknown, the value of the prestressing stress at that point will be taken to be proportional to the average prestress in the concrete, f_{cp}. Also, as the value of the inclined tension cracking load depends to some degree on the presence or absence of flexural cracks, it is expected that the eccentricity of the prestressing force should have some effect. So the effective depth, d, rather than the overall depth, h, will be considered as a variable. Some investigators[42,52] took h as a variable where no flexural cracks were expected.

3.5 The Shear Span:

The importance of this variable on the shear strength has been emphasised by the majority of investigators. Thus the effect of the bending moment and the vertical stresses

due to the relative positions of the failure plane, the load and the reaction will be introduced by considering the shear span, a_v.

3.6 A Failure Criterion for Concrete.

The various modes of shear failure all involve cracking or crushing of concrete under complex state of stress as, e.g., when diagonal cracking, shear-compression failure, splitting or web crushing occurs. Several studies have attempted to determine which of the classical failure theories is most applicable to concrete, but Goode and Helmy[67] state that none of these theories successfully predicts its failure under all complex states of stress. The strength of concrete under combined shear and direct stresses seems to be well predicted by the octahedral stress theory[68]. The simplest cracking criterion is based on the principal tensile stress or principal tensile strain theories of failure. These approaches have been shown to be useful in predicting tensile failure when applied to certain simple state of stress[69,95] and have been shown to give reasonable results when applied to the tensile cracking of a reinforced concrete beam under combined shear and bending moment[70]. Frequently the stresses in a structure can be idealized to a biaxial state of stress with the stress in the third direction equal to zero as shown in Figure 3.1. Kupfer, Hilsdorf and Rüsch[71] and later, in 1972, Liu, Nilson and Slate[72] have shown that as f_1 and f_2 are varied, the element shown in Figure 3.1.a will have the strengths shown by the solid lines in Figure 3.2. Figure 3.2 is symmetrical

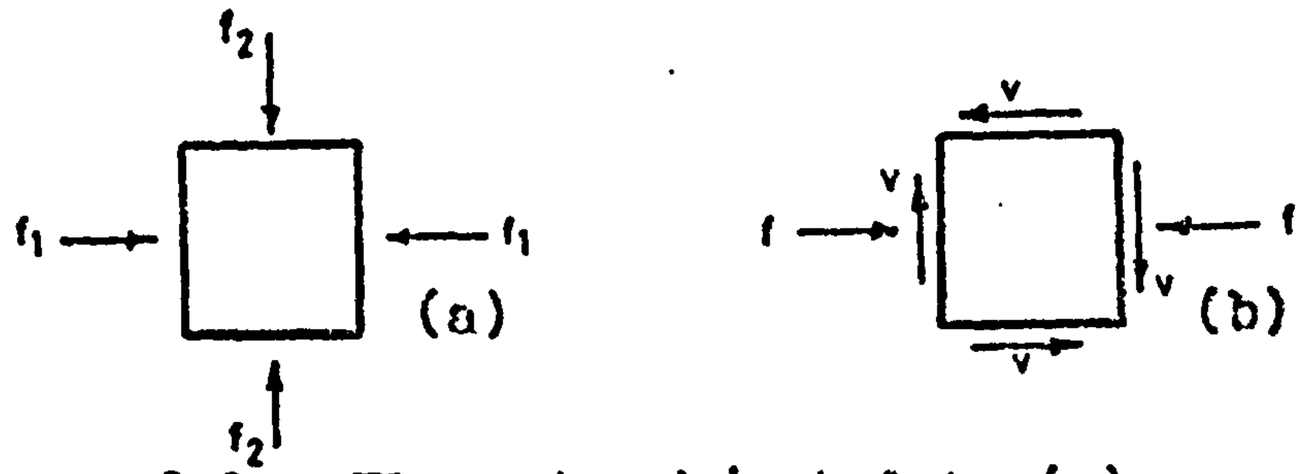

Figure 3.1: Element subjected to (a) normal stresses (b) normal and shear stresses.

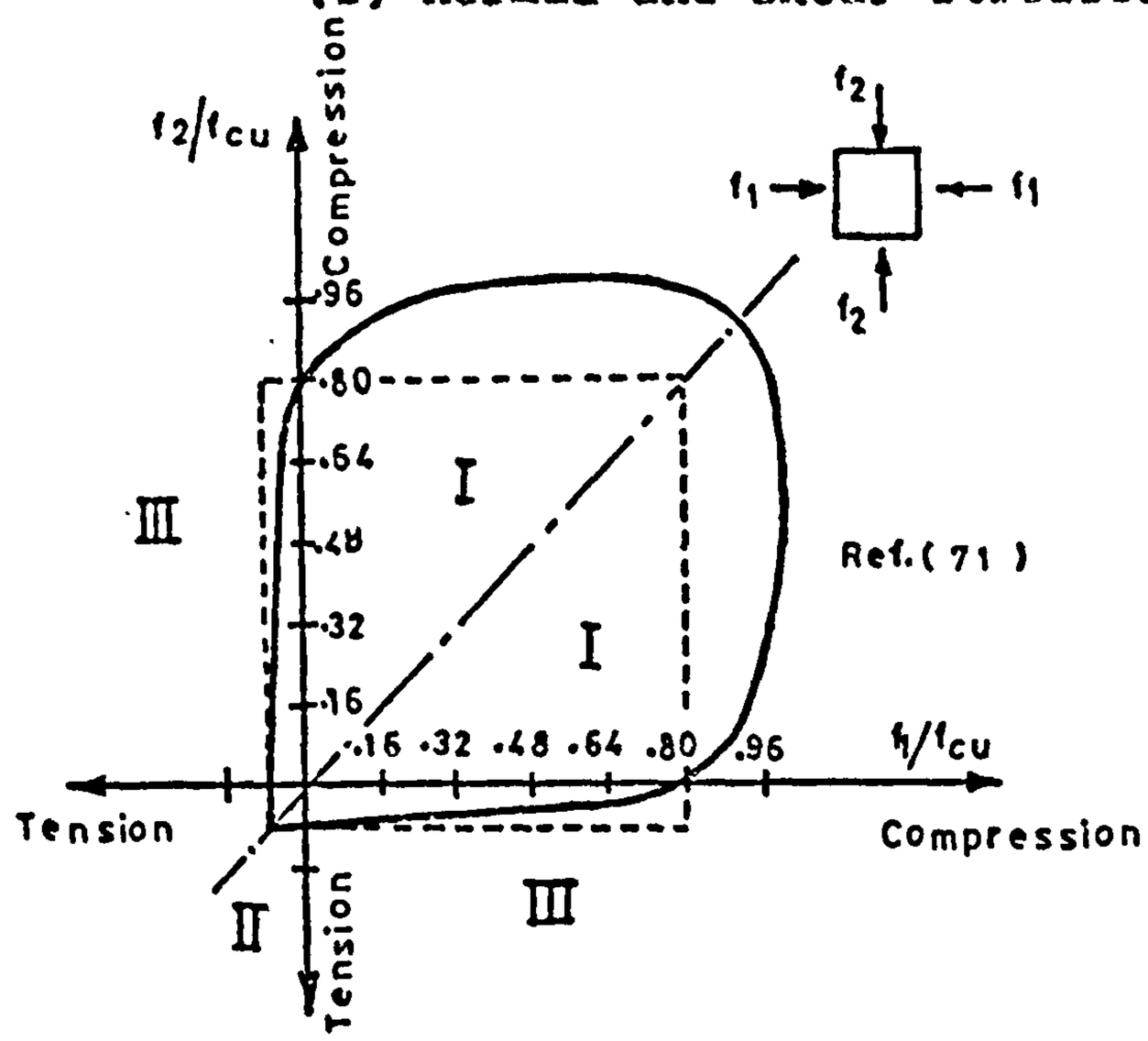

Figure 3.2: Biaxial strength of concrete

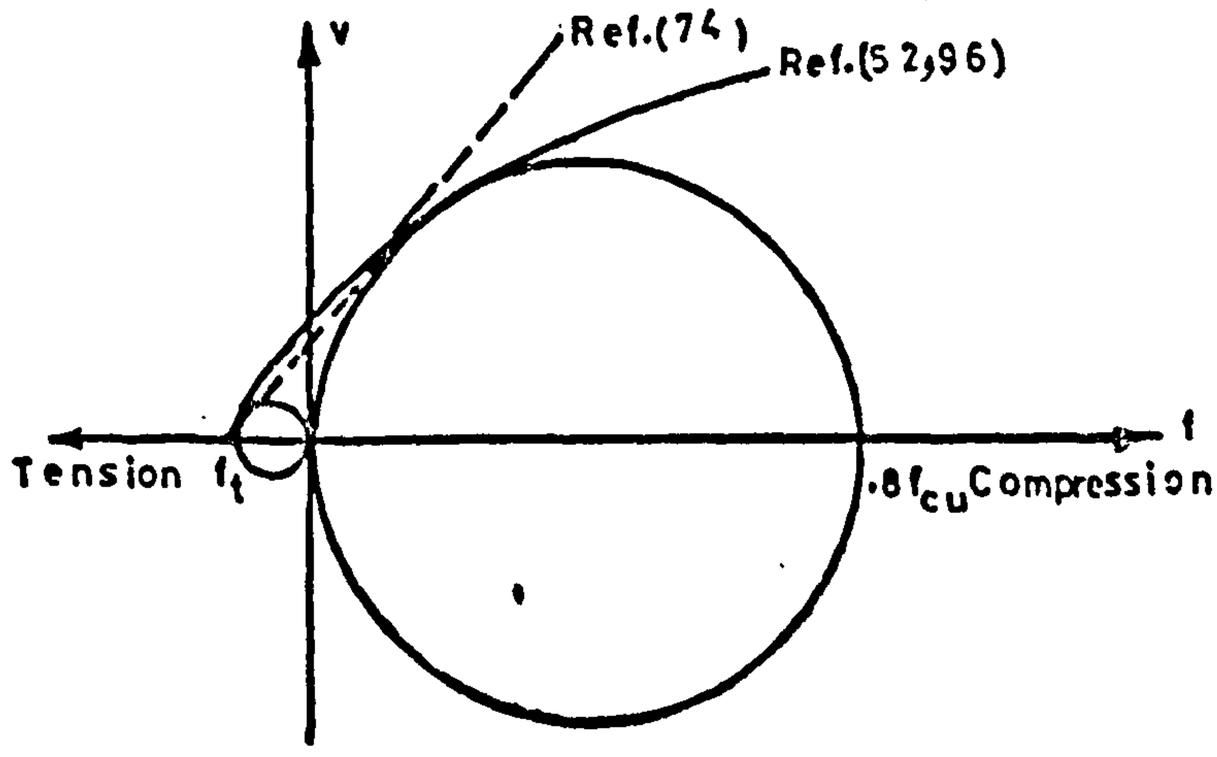

Figure 3.3: Possible Mohr's rupture envelopes for concrete

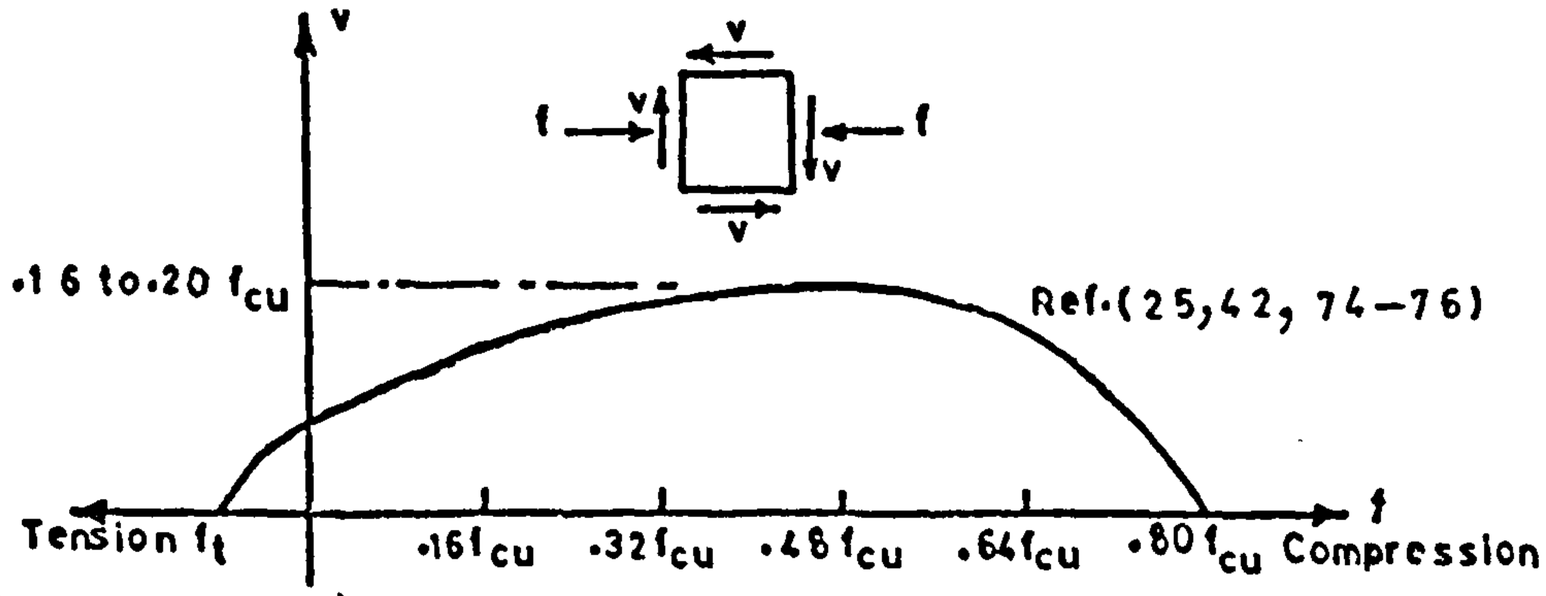

Figure 3.4: Failure of concrete under combined direct and shear stresses.

about a 45^{o} axis and it may be divided into three regions: (I): biaxial compression, (II) biaxial tension, and (III) combined compression and tension. The failure criterion based on uniaxial strengths is given by the rectangle indicated by dashed lines.

Several observations can be made: (a) In Region I biaxial compression increases the compressive stress at failure above the uniaxial compressive stress, (b) In Region II biaxial tension has little effect on the tensile stress at failure, and (c) Region III shows that the combined compression and tension may appreciably reduce both the tensile and the compressive stresses at failure.

Alternatively, Mohr's theory of failure[73] yields acceptable strength predictions for either of the cases shown in Figure 3.1. Parabolic[52,96] and straight line[74] envelopes have been proposed for the family of Mohr's circles representing failure conditions. Any stress condition that corresponds to a Mohr's circle that is tangent to or intersects this envelope is assumed to represent a failure condition.

Based on either the Mohr theory of failure or the Kupfer, Hilsdorf and Rüsch diagrams, relationships have been derived,[25,42,74-76] Figure 3.4,for the strength of elements stressed as shown in Figure 3.1.b. This envelope, Figure 3.4, represents all the combinations of shearing and axial stresses on the vertical plane of the element shown in Figure 3.1.b which results in failure of the element. The implication of such diagram

is that the presence of shearing stresses will reduce the compressive strength of concrete[25]. Combined shear and compressive stresses occur in the compression zone of beams except in regions of constant moment.

3.7. Principal Tensile Stress and Diagonal Tension Cracking.

Guyon[77] found that the diagonal tension cracks always coincided with the paths of stress trajectories, but he did not show at which positions the principal tensile was critical. MacGregor et al[51] regarded the principal tensile stress at the elastic centroid as critical, whilst others[33,37,39,41,52] believed that this principal tensile stress should be related to concrete strength and the $a_{v/d}$ ratio. However, when Kar[42] tried to relate the principal tensile stress to $\sqrt{0.8\ f_{cu}}$ and to $a_{v/d}$ using his own results and those of others[33,34,36] the plotting showed a considerable scatter even for the same value of $a_{v/d}$. He obtained slightly better predictions of the cracking load by the use of Mohr's failure theory for concrete subjected to combined shear and normal stresses after he introduced a correction factor evaluated from the experimental data. This was a function of $a_{v/d}$, equation 2.30.

Bhatt[53] by using a method which allows approximately for the effect of local stress concentrations on the normal bending and shear stresses in a pre-tensioned I-beam, took the maximum principal tension in the web as a criterion and this was found to occur at the lower web - flange junction for the majority of cases analysed. He concluded that the maximum principal tension cannot

be the only criterion in the case of the diagonal cracking of the web. Then he used the maximum principal tension and the Bresler - Pister[68] criterion to determine failure loads in tests carried out by several other investigators.[34,36,44] He found that both criteria predicted approximately equal failure loads and the Bresler - Pister criterion always predicted failure at mid-shear-span along the lower web-flange junctions. He also found that both approaches showed that the $a_{v/d}$ ratio had an important effect on the predicted failure load.

From the above discussion it emerges that the stress conditions in the web of a prestressed concrete I-beam are extremely complex. It is, however, reasonable to assume that failure will occur when a failure criterion for concrete is reached at some point in the shear span. In the circumstances, a rational semi-empirical approach based on dimensional analysis has been adopted.

3.8. Semi-empirical Approach Based on Dimensional Analysis.

By applying the dimensional analysis technique to the variables that seem to affect the value of the diagonal cracking load, the basic format of the expression can be obtained; then regression analysis can be applied to determine the empirical constants and their relationship in order to obtain agreement with test data.

Referring to Section 3.1, the relationship connecting the variables that seem to affect the value of the diagonal cracking load for simply supported prestressed concrete beams under one- or two-point loading is indicated by the equation,

$$f\ (V_c, f_{cp}, b, b_w, d, f'_{ct}, a_v, h_f\ ) = 0 \quad (3.1.1)$$

By applying Buckingham's Pi theorem[78], equation 3.1.1. can be expressed in terms of a complete set of dimensionless products. Any product Π of these variables has the following form:-

$$\Pi = V_c^{k_1} f_{cp}^{k_2} b^{k_3} b_w^{k_4} d^{k_5} f'^{k_6}_{ct} a_v^{k_7} h_f^{k_8} \quad (3.1.2)$$

where $k_1, k_2, - - - - - -, k_8$ are the exponents of a dimensionless product.

If F (= Force) and L (= Length) are the basic dimensions, then the dimensions of the variables in equation 3.1.1 are:

$V_c = F$, $f'_{ct} = F\ L^{-2}$, $f_{cp} = F\ L^{-2}$ and $b_w = b = h_f = d = a_v = L$

Applying Buckingham's theorem,

No. of variables = 8

No. of basic dimensions = 2

No. of dimensionless ratios = 8 - 2 = 6.

Then a complete set of 6 dimensionless products of the variables can be derived. Since a_v/d and $h_{f/d}$ are seen to be dimensionless products, the variables a_v and h_f may be tentatively disregarded. Then the dimensional matrix is

	V_c	f_{cp}	b	b_w	d	f'_{ct}
F	1	1	0	0	0	1
L	0	-2	1	1	1	-2

where each column consists of the exponents in the dimensional expression for the corresponding variable. In the above dimensional matrix, the rank is two and

the number of variables is six. Consequently, there are four dimensionless products in a complete set. The equations corresponding to the dimensional matrix are:

$$\begin{aligned} k_1 + k_2 + k_6 &= 0 \\ -2k_2 + k_3 + k_4 + k_5 - 2k_6 &= 0 \end{aligned} \qquad (3.2)$$

The matrix solution is:

	V_c	f_{cp}	b	b_w	d	f'_{ct}
Π_3	1	0	0	0	-2	-1
Π_4	0	1	0	0	0	-1
Π_5	0	0	1	0	-1	0
Π_6	0	0	0	1	-1	0

Accordingly, a complete set of dimensionless products is:

$$\Pi_1 = \frac{a_v}{d}\ ,\ \Pi_2 = \frac{h_f}{d}\ ,\ \Pi_3 = \frac{V_c}{d^2 f'_{ct}}\ ,\ \Pi_4 = \frac{f_{cp}}{f'_{ct}}$$

$$\Pi_5 = \frac{b}{d} \quad \text{and} \quad \Pi_6 = \frac{b_w}{d}$$

By referring to Section 3.2, the following transformation is made to achieve greater experimental control of the variables:-

$$\Pi_1' = \frac{a_v}{d}\ ,\ \Pi_2' = \frac{h_f}{d}\ ,\ \Pi_3/\Pi_6 = \frac{V_c}{b_w d\ f'_{ct}} = \Pi_3'\ ,$$

$$\Pi_4' = \frac{f_{cp}}{f'_{ct}},\ \Pi_5/\Pi_6 = \frac{b}{b_w} = \Pi_5' \text{ and } \Pi_6' = \frac{b_w}{d}$$

The justification of replacing $f(\Pi_1, \Pi_2, \ldots, \Pi_6)$

by f (Π_1', Π_2', -----, Π_6') is that the relationship among Π_1, Π_2, ----- and Π_6 is unknown, all that is known is that a relationship exists. A relationship among Π_1, Π_2, ------ and Π_6, implies a relationship among Π_1', Π_2', -----and Π_6' since the variables Π_1, Π_2, ------ and Π_6 are determined by Π_1', Π_2', -------and Π_6' and vice versa.

Consequently there is a function F_o, such that

$$F_o\left(\frac{V_c}{b_w d\ f'_{ct}}, \frac{f_{cp}}{f'_{ct}}, \frac{b}{b_w}, \frac{h_f}{d}, \frac{a_v}{d}, \frac{b_w}{d}\right) = 0 \qquad (3.3)$$

This may be written in the explicit form:

$$\frac{V_c}{b_w d\ f'_{ct}} = F_1\left(\frac{f_{cp}}{f'_{ct}}, \frac{b}{b_w}, \frac{h_f}{d}, \frac{a_v}{d}, \frac{b_w}{d}\right) \qquad (3.4)$$

where F_1 is a functional notation.

The term $\frac{b_w}{d}$ will be dropped because of its negligible effect on the value of the cracking load within the practical range of normal proportions[63,79]. Kani[63] did not find any significant change in shear stress when the beam breadth was changed from 150 to 600 mm and statistical studies by Iyengar et al[79] on a large amount of data showed no significant effect of $\frac{b_w}{d}$ in the range from $0.25 \leq \frac{b_w}{d} \leq 1.0$.

Consequently equation 3.4 will take the more specific form:

$$\frac{V_c}{b_w d\ f'_{ct}} = F_2\left(\frac{f_{cp}}{f'_{ct}}, \frac{b}{b_w}, \frac{h_f}{d}, \frac{a_v}{d}\right) \qquad (3.5)$$

where F_2 is a functional notation.

CHAPTER 4

EXPERIMENTAL WORK

4.1. Test Specimens:

The experimental programme was planned to demonstrate the effect of each of the dimensionless parameters shown in equation 3.5 on the value of the cracking load, V_c. The grouping of the variables in the manner shown in equation 3.5 requires a wide variation in the cross-sectional properties of the beam. As design formulae should be the logical outcome of any research of this nature, the test specimens were designed to resemble as far as possible, those which could be used in practice. Accordingly $h_{f/d}$ and $b_{/bw}$ were allowed to vary systematically within the bounds of realistic values. $h_{f/d}$ was varied from zero to 0.33 and $b_{w/b}$ from 0.25 to 1.00. The $a_{v/d}$ ratio ranged from 1.25 to 6.00 and the $l_{/d}$ ratio from 6.0 to 17.78. The overall cross-section dimensions were 200 by 300 mm, and the specimens were 3.25 m and 4.75 m in length; the latter being used with $l_{/d}$ ratio of 17.78. Seven different cross-sections were tested under one-or two-point loading, and five cross-sections, under uniformly distributed load. Full details of the test specimen cross-sections and geometric properties are given in Figures 4.1, 4.2 and Table 4.1

4.2. Materials:

4.2.1. Cement:

"Ferrocrete" rapid-hardening Portland cement and "Blue Circle" ordinary Portland cement were used; the

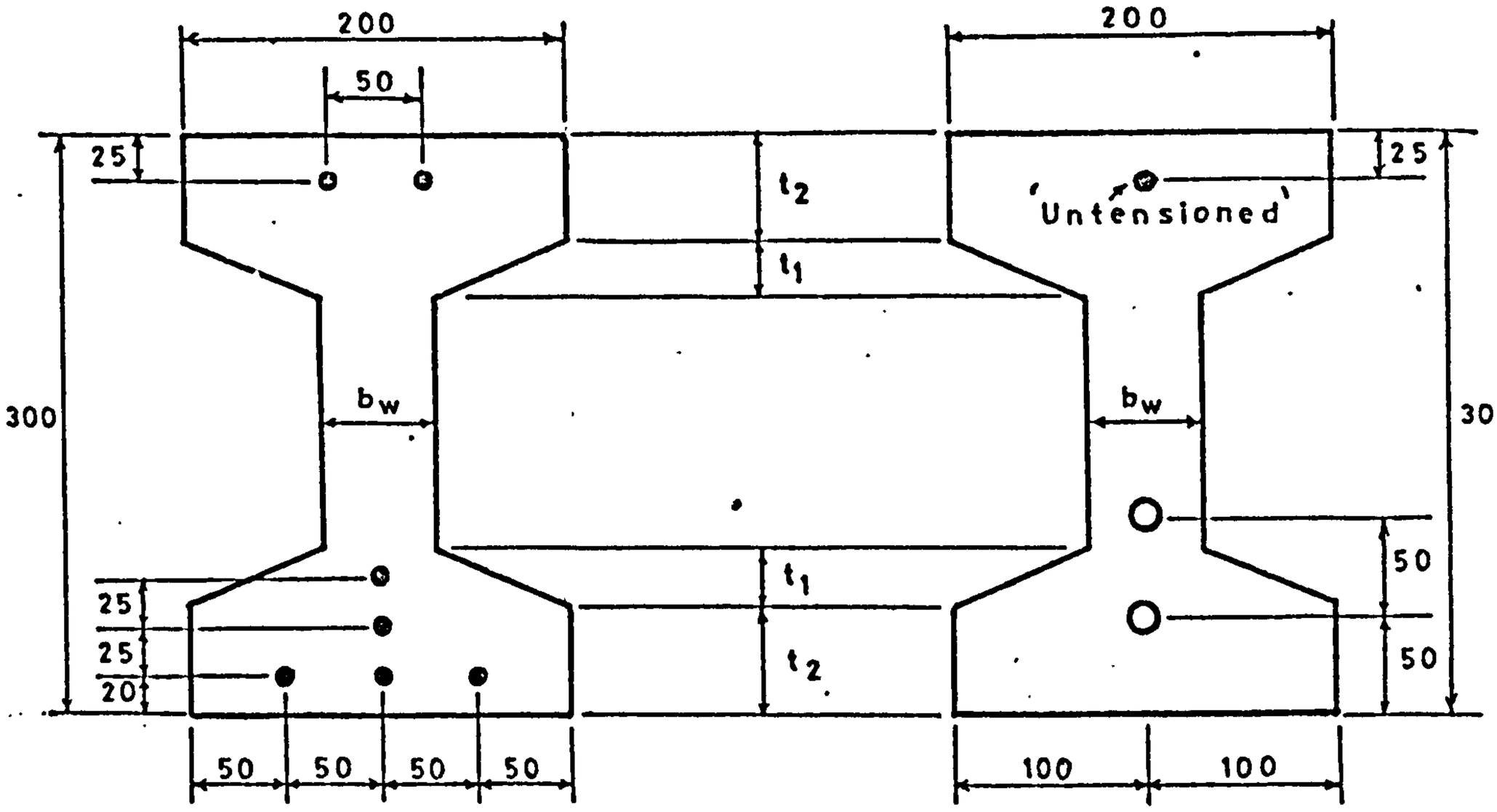

Figure 4.1

Figure 4.2

Table 4.1

Geometric properties of cross-section of the specimens

Beam mark	t_1 mm	t_2 mm	b_w mm	$A_c \times 10^{-3}$ mm^2	$I_c \times 10^{-7}$ mm^4
A	37.5	12.5	75	33.44	34.97
B	"	20.0	50	29.25	34.13
C	57.5	12.5	75	38.44	39.63
D	"	20.0	50	35.25	39.30
E	77.5	12.5	75	43.44	42.56
F	"	20.0	50	41.25	42.50
G	00.0	00.0	200	60.00	45.00

latter was used owing to difficulty in obtaining the rapid-hardening Portland cement at one period.

4.2.2. Aggregates:

Mid-Ross sand and gravel were used for all beams but six. When Mid-Ross stopped production, Hyndford sand was used for beams D11 to D14. The maximum size of the aggregate used was 10 mm. Both of these materials are of morainic origin, and the gravels are irregular in shape.

4.2.3. Concrete Mix:

The mix was designed[80] to attain about 35 N/mm^2 cube compressive strength in 5 days. Slight differences in the mix proportions were required from time to time to achieve this strength. Full details of mix proportions and their properties are given in Table 4.2.

4.2.4. Prestressing Steel:

In 72 of the beams, the prestressing steel was seven 7 mm diameter indented (Belgian pattern) high tensile steel wires. Plain wires of the same diameter had to be used in six beams owing to difficulty in obtaining indented wires at one period. At a later stage 12.5 mm diameter strands were used with 13 beams so as to cover high ratios of $a_{v/d}$ and $L_{/d}$ and to see the effect of different arrangements of prestressing tendons. Figures 4.3 shows the stress-strain behaviour and the properties of a typical batch of each type.

4.3. Fabrication of Specimens:

4.3.1. The formwork was designed[81] sufficiently rigid

TABLE 4.2

Concrete Properties and
Details of Prestress.

Beam mark	Age at test in days	Mix proportions W	C	S	G	Slump mm	C.F	f_{cu} 28 N/mm^2	f_{ci} N/mm^2	f_{cu} at test N/mm^2	f'_{ct} at test N/mm^2	Type of tendons	Apsfpe max. KN
A 1	26	.40	1.00	.80	2.50	20	.88	54.5	43.4	51.3	3.50	7P	247.5
2	137	"	"	"	"	35	.94	58.8	44.0	54.3	3.49	7I	225.7
3	20	"	"	"	"	25	.91	54.5	42.8	55.3	3.41	"	249.5
4	29	"	"	"	"	-	-	53.8	45.5	52.8	3.12	"	247.5
5	29	"	"	"	"	-	-	57.8	43.0	55.6	2.94	"	243.4
6	42	"	"	"	"	-	-	54.0	40.8	59.0	3.43	"	258.3
7	27	"	"	"	"	20	.85	60.3	40.5	51.0	3.68	"	251.5
8	13	.44	1.00	.95	3.00	20	.92	50.1	34.2	43.7	2.71	"	258.0
9	28	"	"	"	"	25	.91	53.0	34.5	42.8	3.15	"	246.5
10	27	"	"	"	"	-	-	53.8	37.3	45.2	3.45	"	219.4
11	25	.40	1.00	1.24	1.86	35	.92	52.6	38.3	40.9	3.08	"	179.9
12	14	.44	1.00	.95	3.00	-	-	49.1	31.5	36.5	2.59	"	197.0
B 1	35	.40	1.00	1.24	1.86	45	.90	50.2	36.0	46.3	3.36	7I	206.8
2	36	"	"	"	"	50	.96	50.3	37.8	50.5	2.86	"	215.9
3	35	"	"	"	"	35	.92	59.5	41.3	58.0	3.15	"	209.1
4	27	"	"	"	"	35	.86	51.3	33.0	48.8	3.30	"	214.7
5	64	"	"	"	"	45	.95	-	38.0	46.4	3.26	"	164.1
6	49	.40	1.00	.80	2.50	30	.90	-	37.0	52.1	3.30	"	194.6
7	23	"	"	"	"	35	.88	-	39.0	50.6	3.52	"	209.7
8	28	"	"	"	"	25	.89	-	38.0	41.8	3.04	"	204.8
9	33	"	"	"	"	30	.87	54.8	47.0	52.8	3.01	"	165.0
10	19	"	"	"	"	45	.91	-	40.0	53.5	3.72	"	219.1
11	184	"	"	"	"	45	.89	-	41.0	53.5	3.51	"	229.9
12	26	.41	1.00	.84	2.61	-	-	-	34.5	46.0	3.00	"	141.7
13	18	"	"	"	"	-	-	-	29.5	41.5	2.90	"	144.1
14	24	"	"	"	"	-	-	-	33.5	47.0	2.76	"	177.5
15	13	"	"	"	"	-	-	-	31.0	41.4	2.91	"	184.0

TABLE 4.2 (Cont'd)

Beam mark	Age at test in days	Mix proportions W	C	S	G	Slump mm	C.F.	f_{cu} 28 N/mm^2	f_{ci} N/mm^2	f_{cu} at test N/mm^2	f'_{ct} at test N/mm^2	Type of tendons	Apsfpe max. KN
C 1	21	.40	1.00	.80	2.50	20	..88	54.5	43.4	50.0	3.52	7P	257.9
2	120	"	"	"	"	20	.88	58.8	44.0	46.5	3.33	7I	240.4
3	26	"	"	"	"	25	.91	54.5	42.8	55.9	3.68	7I	242.6
4	25	"	"	"	"	-	-	53.8	45.5	53.1	3.01	"	246.0
5	27	"	"	"	"	-	-	57.8	43.0	51.0	3.29	"	241.7
6	42	"	"	"	"	30	.89	54.0	40.8	59.0	3.43	"	258.4
7	28	"	"	"	"	20	.85	60.3	40.5	50.8	3.40	"	250.7
8	15	.44	1.00	.95	3.00	20	.82	50.1	34.2	45.0	2.74	"	252.5
9	29	.44	1.00	.95	3.00	25	.91	53.0	34.5	43.8	3.17	"	244.3
10	23	"	"	"	"	-	-	53.0	37.3	42.3	3.22	"	221.8
11	21	.40	1.00	1.24	1.86	35	.92	52.6	38.3	45.0	3.14	"	188.4
12	13	.44	1.00	.95	3.00	-	-	49.1	31.5	35.0	2.49	"	200.3
13	20	.41	1.00	.84	2.61	25	.95	-	34.5	46.9	3.48	"	153.4
14	26	"	"	"	"	40	.92	-	29.5	46.5	3.14	"	154.6
15	23	"	"	"	"	-	-	-	33.5	47.0	3.45	"	194.9
16	14	"	"	"	"	-	-	-	31.0	41.4	2.91	"	207.2
17	28	.40	1.00	.84	2.61	-	-	-	30.9	37.2	2.70	2S	98.0
18	31	"	"	"	"	-	-	-	34.0	45.8	2.89	"	95.7
19	36	"	"	"	"	-	-	-	37.0	51.0	3.01	"	94.2
20	379	.41	1.00	0.81	2.61	-	-	-	34.0	34.2	2.97	"	108.0
D 1	26	.40	1.00	.80	2.5	30	.90	-	37.0	48.6	2.94	7I	224.9
2	13	"	"	"	"	30	.90	-	39.0	49.4	3.05	"	227.3
3	30	"	"	"	"	35	.88	-	38.0	53.3	3.10	"	188.9
4	34	"	"	"	"	30	.88	54.8	47.0	51.5	3.30	"	176.9
5	726	"	"	"	"	45	.91	-	40.0	45.0	3.55	"	187.2
6	611	"	"	"	"	45	.89	-	41.0	54.1	3.52	"	188.6
7	28	.40	1.00	.84	2.61	-	-	-	30.9	37.2	2.70	2S	98.7
8	31	"	"	"	"	-	-	-	34.0	45.8	2.89	"	95.9
9	36	"	"	"	"	-	-	-	37.0	51.0	3.01	"	95.2

TABLE 4.2 (Cont'd)

Beam mark	Age at test in days	Mix proportions W	C	S	G	Slump mm	C.F.	$f_{cu_{28}}$ N/mm^2	f_{ci} N/mm^2	f_{cu} at test N/mm^2	f'_{ct} at test N/mm^2	Type of tendons	Apsfpe max. KN
D10	378	.41	1.00	.81	2.61	45	.89	54.8	34.0	34.2	2.97	2S	104.8
11a	14	"	"	"	"	-	-	-	46.5	56.0	3.45	"	109.3
11b	30	"	"	"	"	-	-	-	43.5	54.8	3.29	"	108.2
12	22	.40	1.00	.81	2.50	-	-	-	46.0	61.3	3.34	"	119.9
13	15	"	"	"	"	-	-	-	34.2	46.5	2.52	"	116.0
14	14	.40	1.00	.81	2.50	-	-	-	36.9	43.9	2.88	"	121.4
E 1	42	.40	1.00	.80	2.50	20	.91	57.1	41.0	64.1	3.73	7I	190.3
2	11	"	"	"	"	15	.92	53.2	41.8	52.7	3.17	"	160.8
3	11	"	"	"	"	20	.85	56.5	42.3	55.7	3.37	"	224.2
4	11	"	"	"	"	20	.96	54.0	45.5	50.0	3.29	"	225.0
5	8	"	"	"	"	30	.90	55.3	40.4	53.1	3.17	"	245.9
6	14	"	"	"	"	20	.87	53.2	40.8	50.0	3.22	"	274.5
7	15	"	"	"	"	20	.91	53.1	38.8	46.0	3.10	7P	242.4
8	138	"	"	"	"	25	.90	54.0	47.0	57.2	3.55	"	233.0
9	20	.40	1.00	.84	2.61	-	-	-	30.0	40.8	2.93	7I	189.3
10	20	"	"	"	"	-	-	-	37.1	42.1	3.31	"	195.5
11	27	.40	1.00	.84	2.61	-	-	-	32.5	39.5	2.87	"	216.8
12	47	"	"	"	"	-	-	-	31.7	43.5	2.70	"	194.2
F 1	33	.40	1.00	1.24	1.86	45	.90	50.2	36.0	47.5	3.14	7I	187.7
2	34	"	"	"	"	50	.96	50.3	37.8	49.3	3.30	"	193.5
3	41	"	"	"	"	35	.92	59.5	41.3	54.9	3.30	"	220.7
4	21	"	"	"	"	35	.86	51.3	33.0	49.4	3.08	"	242.1
5	62	"	"	"	"	45	.95	-	38.0	52.6	3.03	"	137.4
6	21	.41	1.00	.81	2.61	-	-	-	30.0	42.3	3.10	"	178.9
7	20	"	"	"	"	-	-	-	37.1	40.9	3.03	"	188.0
8	28	"	"	"	"	-	-	-	32.5	42.1	2.99	"	207.5
9	47	"	"	"	"	-	-	-	31.7	43.7	2.80	"	186.0

TABLE 4.2 (Cont'd)

Beam mark	Age at test in days	Mix-proportions W	C	S	G	Slump mm	C.F.	$f_{cu_{28}}$ N/mm^2	f_{ci} N/mm^2	f_{cu} at test N/mm^2	f'_{ct} at test N/mm^2	Type of tendons	^1Apsfpe max. KN
G 1	40	.40	1.00	.80	2.50	20	.91	57.1	41.0	65.8	3.69	7I	192.0
2	13	"	"	"	"	15	.85	56.5	42.3	54.5	3.45	"	224.4
3	14	"	"	"	"	15	.95	53.2	41.8	53.0	3.64	"	139.8
4	12	"	"	"	"	20	.96	54.0	45.5	53.2	3.30	"	213.0
5	7	"	"	"	"	30	.90	55.3	40.4	43.4	2.71	"	223.0
6	12	"	"	"	"	20	.87	53.2	40.8	49.7	3.48	"	252.0
7	20	"	"	"	"	20	.97	53.1	38.8	46.0	3.11	7P	239.3
8	903	"	"	"	"	25	.90	54.0	47.0	54.4	3.94	"	230.0

Notes.

1. Mix proportions were by weight. W = water, C = cement, S = sand G = gravel (10mm maximum). Where the cement proportion is underlined the cement used was ordinary Portland Cement, otherwise R.H.P.C. was used. C.F. = compacting factor.
2. $f_{cu_{28}}$ = compressive strength on 100 mm cubes at 28 days. (Average of 3).
   f'_{ct} at test = tensile strength of concrete (Cylinder split test).
3. 7I = Seven 7 mm indented prestressing wires.
   7P = " " plain " "
   2S = Two 12.5 mm prestressing strands.

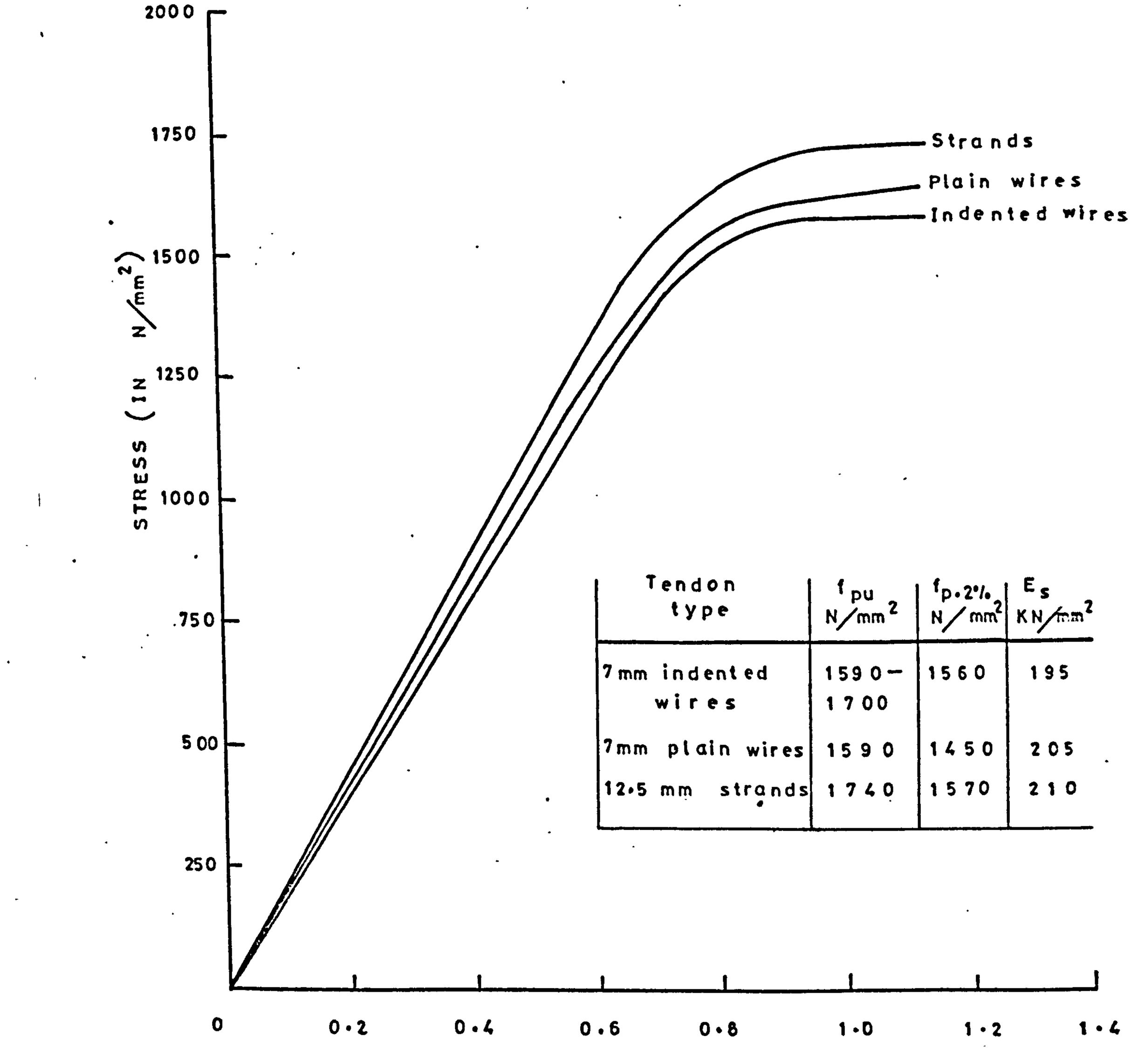

Tendon type	f_{pu} N/mm²	$f_{p\cdot2\%}$ N/mm²	E_s KN/mm²
7mm indented wires	1590–1700	1560	195
7mm plain wires	1590	1450	205
12·5 mm strands	1740	1570	210

Figure 4.3: Typical stress-strain curves for tendons used.

and tight to prevent loss of mortar from concrete at all stages and to maintain the forms in their correct position, shape and profile.

Specimens were cast in pairs in a semi-long-line process in rectangular steel moulds with timber web-formers fixed inside to give the required I-sections. Seven wires were used in the wire-stressed beams, two being placed in the top flange to give the correct distribution of prestress, as shown in Figure 4.1. Later on, two 12.5 mm diameter strands were used, as shown in Figure 4.2, together with one untensioned 7 mm diameter wire placed in the top flange to provide an anchorage for the end zone stirrups. The prestressing tendons for the manufacture of a pair of beams were tensioned and the two beams were cast at the same time using the same mix. The prestressing tendons were passed through the bearing plates, shown in Figure 4.4, of the prestressing frame and the end plates of the forms; the former provided the reaction for the tensioning force. The anchorage was provided by the use of split-wedge and barrel-type anchor grips. Before tensioning, the tendons were free of rust and were cleaned of surface oil. No other reinforcement was used except in the end zones where 3 mild steel stirrups of 3.2 mm diameter were provided. These stirrups were designed according to Marshall and Mattock's[82] formula given by:

$$A_t = \frac{0.02\, A_{ps} f_{pi}}{f_{sv}\, l_t} \qquad (4.1)$$

where A_t = total cross-sectional area of web reinforcement.

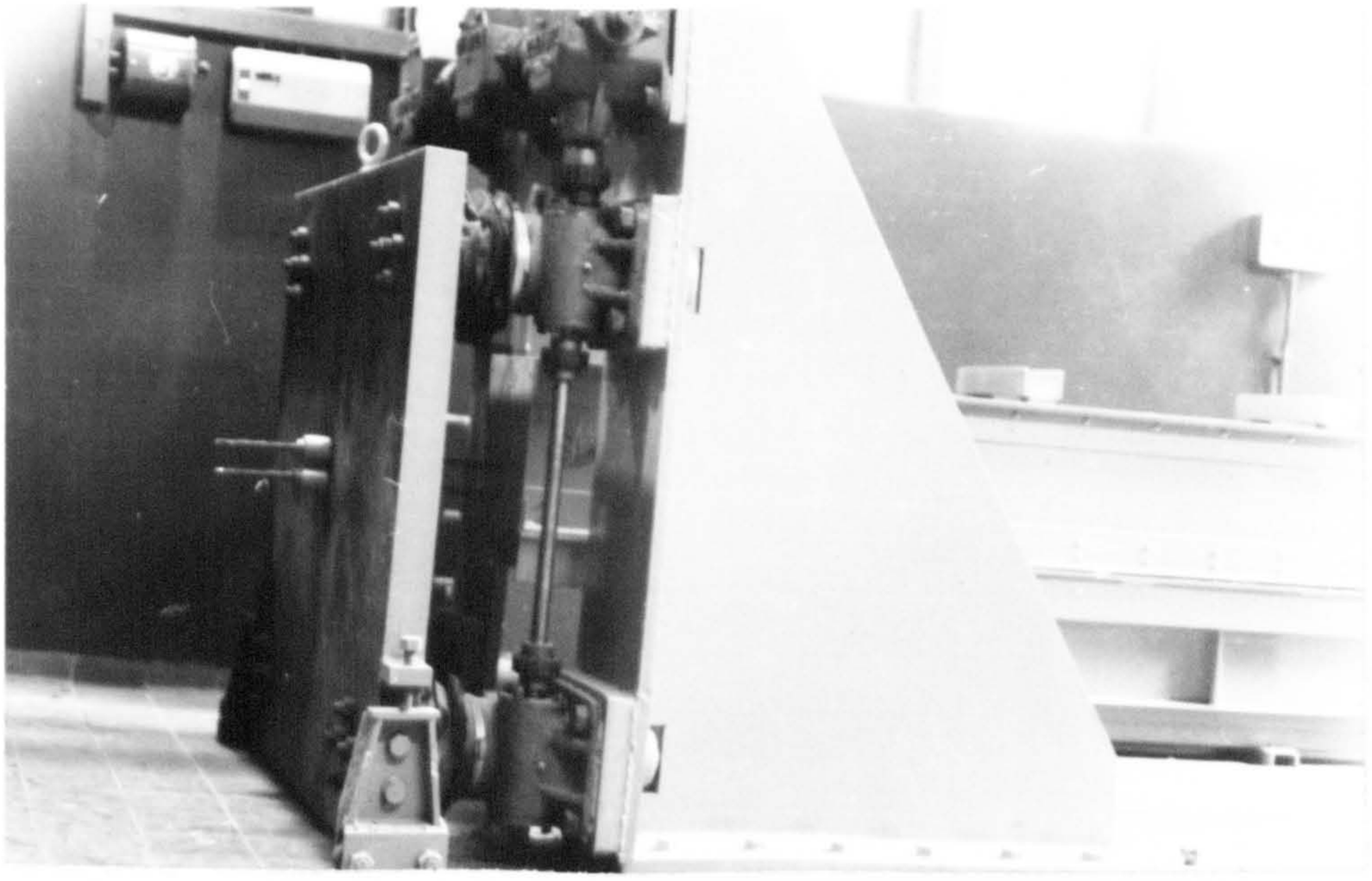

(a) Jack Anchor Bracket and Jack Faceplate

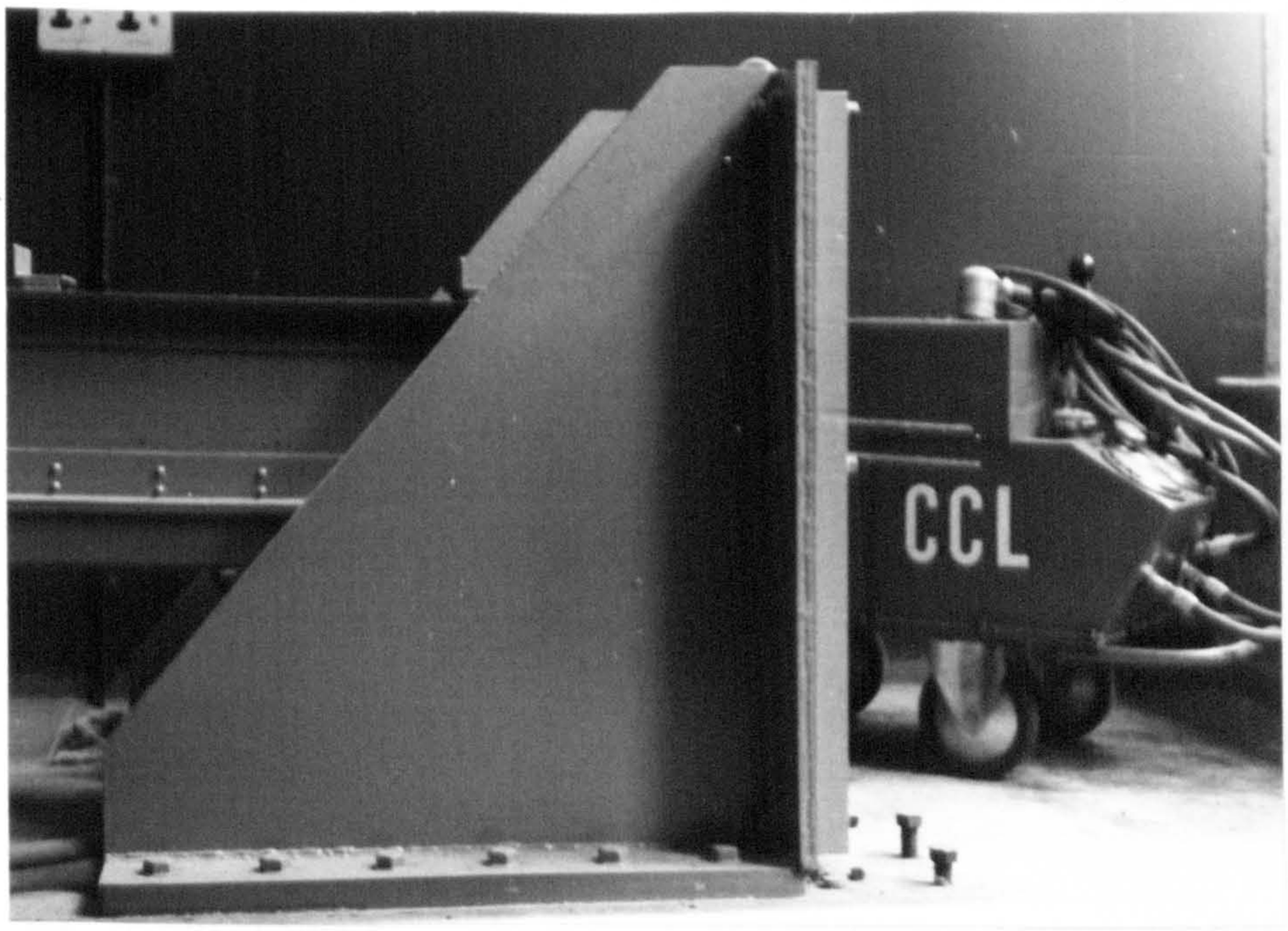

(b)Dead Anchor Bracket and Faceplate

Figure 4.4: The Bearing Plates of the Pre-stressing Bed

One stirrup at each end was extended to form a hook for lifting the beam.

4.3.2. Tensioning apparatus:

Two alternative tensioning devices were employed, one for the wires and the other for the strands. For the wires a hand-controlled P.S.C. monowire jack operated by a motor-driven hydraulic pump with a delivery pressure of 70 N/mm^2 was used. A C.C.L. 160 KN Stress-O-Matic Jack was used to stress the 12.5 mm strands. This Jack operates with a calibrated load-cell. Figure 4.5 shows the two tensioning devices.

4.3.3. Tensioning process:

The distance between the outer faces of the bearing plates was approximately 7.3 m. All the tendons were straight and/ /stressed individually. The stress in each tendon was increased at a gradual and steady rate. The tendons were overstressed by about 5% for two minutes to reduce stress loss due to relaxation of the prestressing steel[83]. Then the stress was reduced to the required level and the tendon was anchored. After the anchorage of the tendon, the force exerted by the tensioning apparatus was decreased gradually to avoid any shock to the tendon or anchorage.

The prestressing force applied was checked by strain measurements on the wires by means of 203 mm Demec gauge readings on collars attached to the wires. The strain developed in the wires was taken as the difference in strain readings, after the slack was removed and the tendons were locked. This was checked against extension

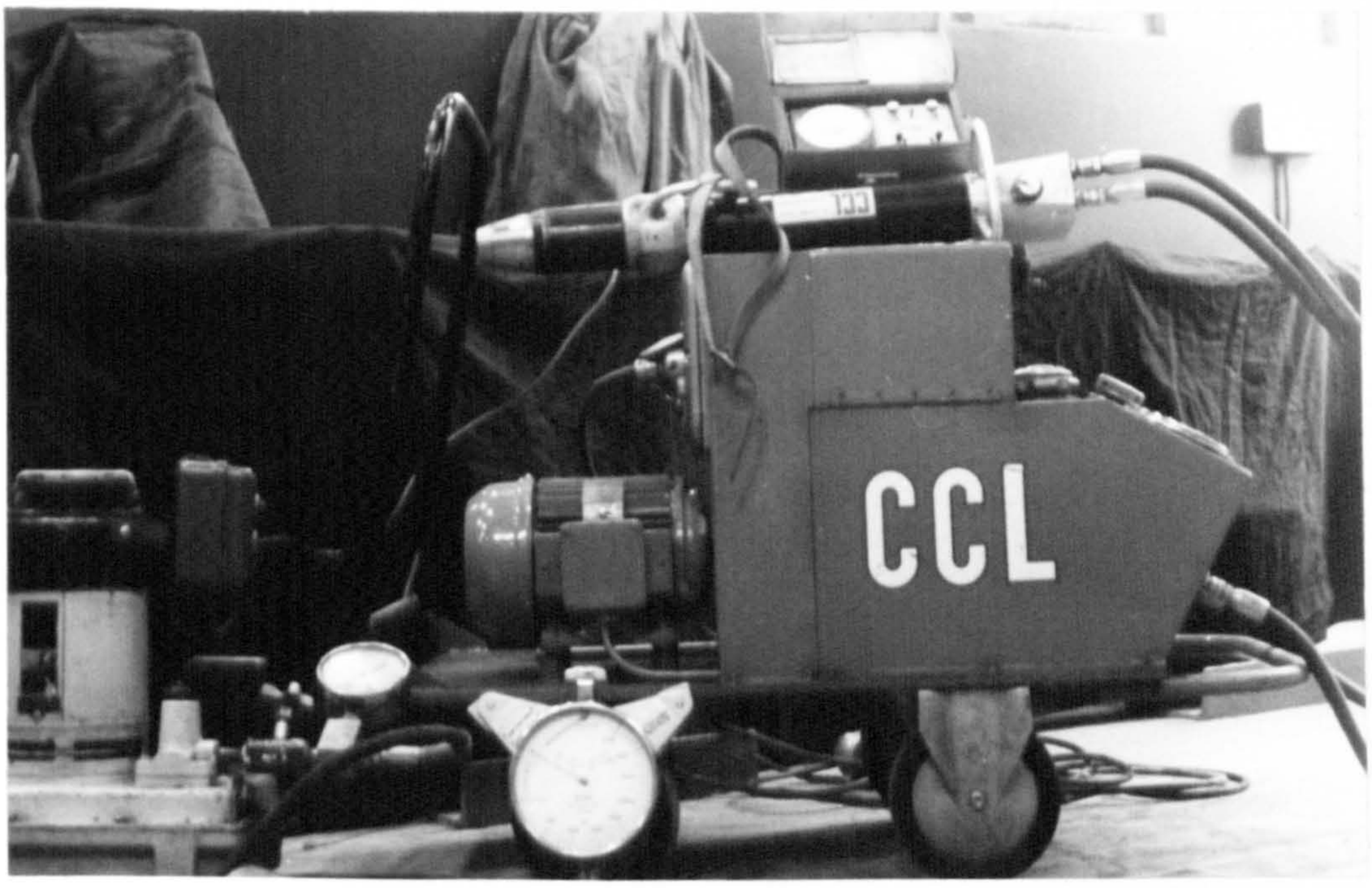

Figure 4.5: Tensioning Devices

(A hand-controlled P.S.C. monowire jack and a C.C.L. 160 KN Stress-o-Matic Jack)

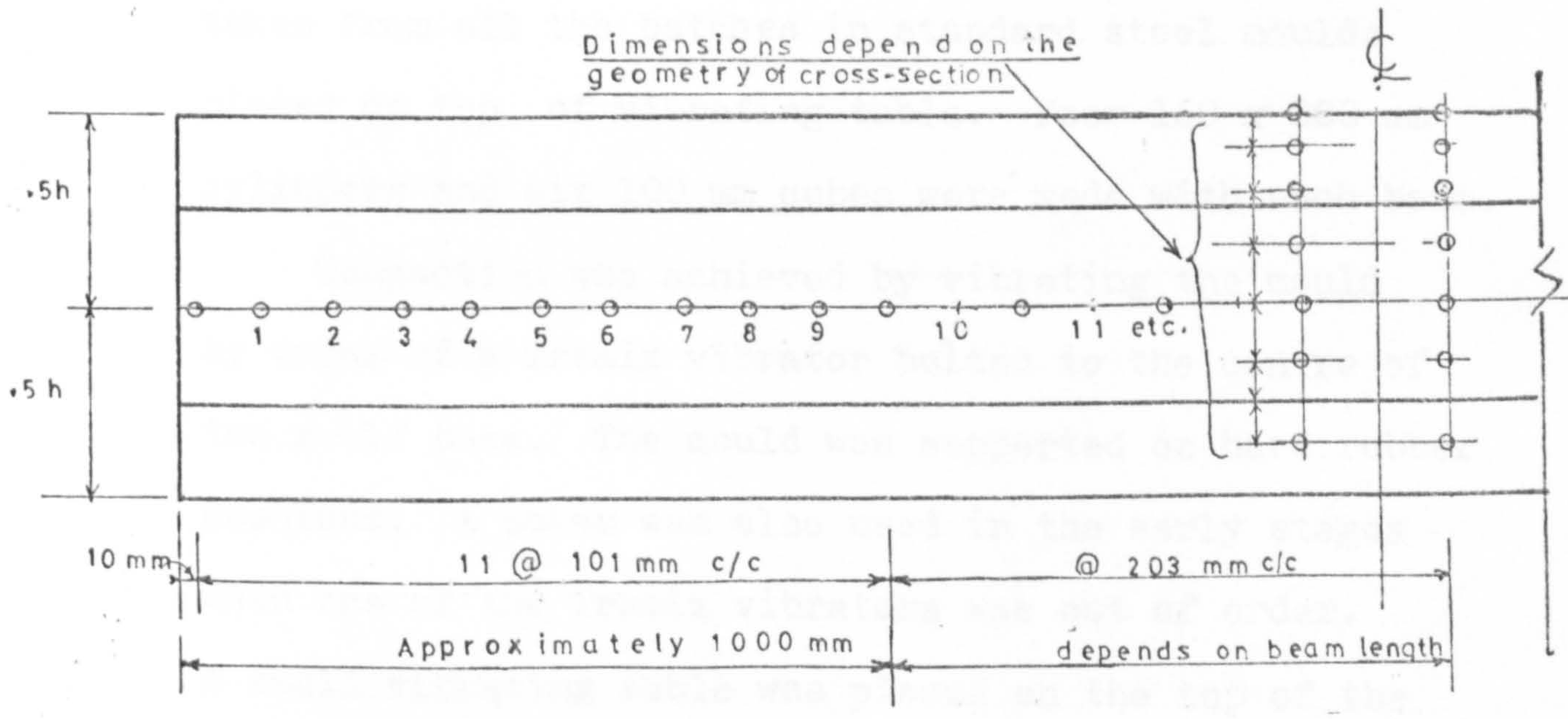

Figure 4.6. Arrangement of gauge marks for measuring the concrete strain.(The gauge marks were glued to both sides of the beam).

measurements taken for the wires by a scale attached to the wire and the jack. The calibrated pressure gauge built in the hydraulic system and Vogtmeter were used also to check the wire force. For the strands, the tendon force was checked against extension measurements, the calibrated pressure gauge reading and the load-cell attached to C.C.L. device reading.

4.3.4. Mixing and casting:

The concrete was cast after the stressing of the tendons. It was mixed in a pan-type mixer. The aggregates and cement were mixed dry, then water was added. Slump and compacting factor were determined immediately after mixing. The number of batches needed for a pair of beams varied between 8 and 12. The batches were placed in layers of uniform height through the beam. Meanwhile control specimens were made with concrete taken from all the batches in standard steel moulds placed on top of vibrating table. Four 150 x 300 mm cylinders and six 100 mm cubes were made with each beam.

Compaction was achieved by vibrating the mould by means of a Tremix vibrator bolted to the centre of the mould base. The mould was supported on hard rubber cushions. A poker was also used in the early stages when one of the Tremix vibrators was out of order. A small vibrating table was placed on the top of the specimen near the end zones to improve compaction in those zones.

After casting was complete, the tops of the cast specimens were trowelled smooth. After 6 hours, the

bolts on the sides of the shutters were loosened and the specimens were covered with damped sacks.

After 24 hours, the side shutters were removed. Experience showed that the removal of the form sides could be achieved without damaging the specimens by attaching two steel plates of appropriate dimensions to the surface of the timber in contact with concrete near the ends of the form sides and then by jacking against those plates through a bolt acting in a nut welded to the outside of the form.

The control specimens were then demoulded and placed on the top of the specimens, and all were then cured under damp sacking covered with polythene for 3 days.

After 5 days, and provided that a cube test indicated that the required strength had been reached[30], the wires were released all together and uniformly by an inward movement of one of the bearing plates. Before and after transfer, readings were taken on Demec points which had been fixed to the specimens for estimating the prestressing losses and to investigate the transmission length as shown in Figure 4.6. The results of these are shown in Figures A.1 and A.2 in Appendix A.

4.4. Instrumentation, Loading Apparatus and Test Procedure:

4.4.1. Instrumentation is required to give quantitative results to test the theoretical work involved. In concrete structures due to local cracking and uncertainty

about the stress-strain relationship of concrete, the instrumentation can hardly be as efficient as desired. Despite this some instrumentation intended to reveal the behaviour at different stages of loading was undertaken. Load-deflection curves for the mid-span were recorded for all the beams. Those load-deflection curves were used in the way described by Morice[84] to obtain an estimate of the prestressing force actually present at the time of test whenever this was possible. The shapes of these plots were not always sufficiently clearly defined, so in the final calculations, the effective prestressing force estimated from the surface strain measurement was used. A typical example of calculating the prestressing losses using C.E.B. - F.I.P.[27] and B.S.C.P. 110[30] Recommendations are shown in Appendix B.

4.4.2. All the beams were tested simply supported. The majority under either central point loading or symmetrical two-point loading in a 900 KN capacity Olsen crew-type universal testing machine. Later on, 23 tests were conducted on beams under uniformly distributed load. The load was uniformly distributed over the entire beam span surface by means of the water-filled fire-hose technique[47,48,61]. These specimens were tested at six span to effective depth ratios ranging from 6.00 to 17.78. Typical testing arrangements are shown in Figure 4.7.

4.4.3. The specimen was set centrally in the testing

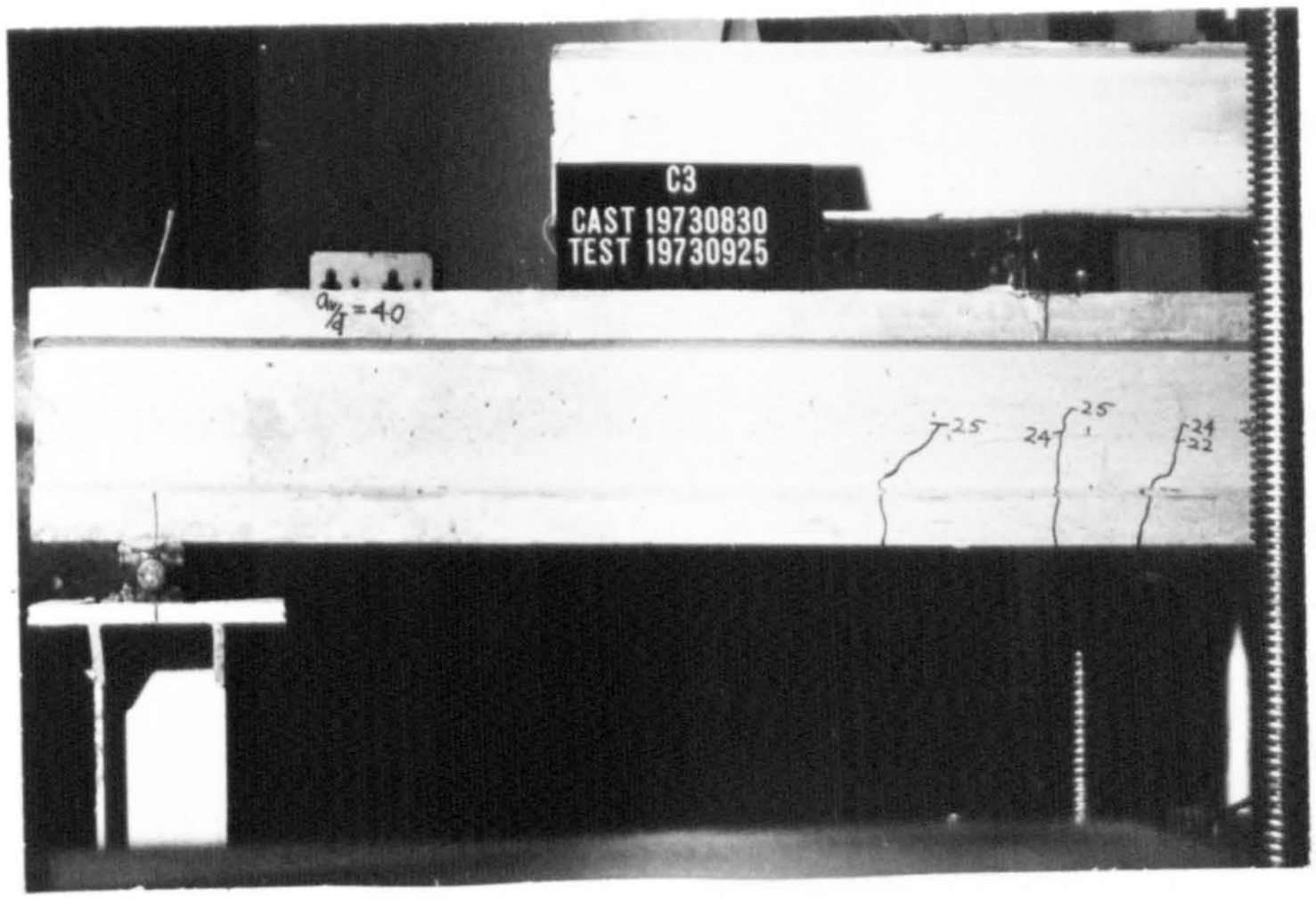

(a) Under two-point loading.

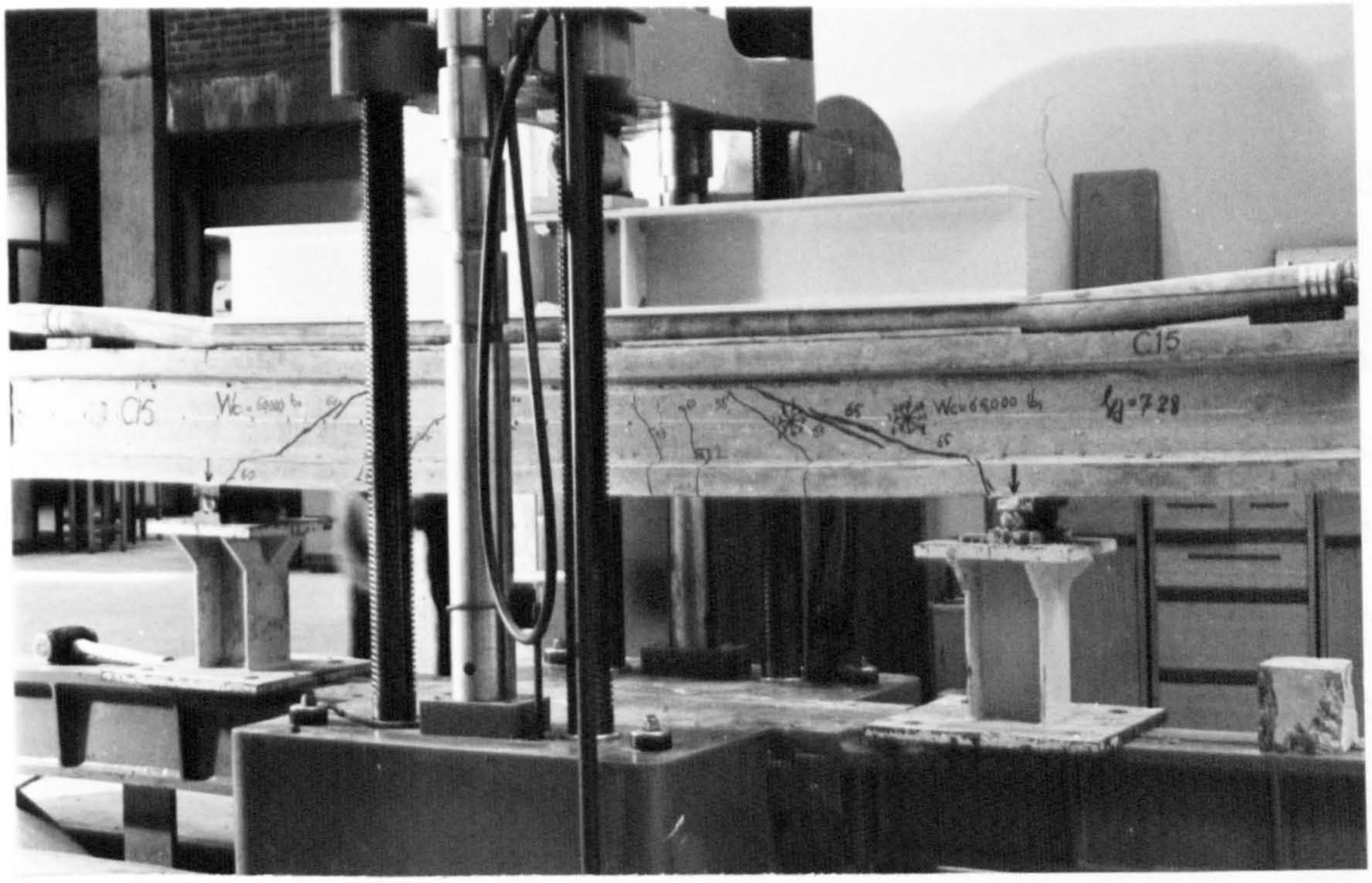

(b) Under uniformly distributed load.
(using water-filled fire-hose technique)

Figure 4.7: Typical Testing Arrangements

machine on pads of wet plaster which accommodated any irregularities of the beam shape. After the plaster had set, the load was applied in suitable increments. After each increment of loading, the load was held constant while strains were measured and any cracks marked. The magnitude of the increments in loading depended on the development of the crack pattern. The loading measuring apparatus was flexible enough to follow up any change in the beam behaviour; the inclined cracking loads after which the behaviour of the beam would be affected were easily obtained from an autographic plot of the central deflection against load for each specimen. Some typical plots are shown in Figures 5.2 and 5.3.

In some cases where diagonal cracking was observed in one of the shear spans of the test specimen, the shear span showing the cracking was clamped externally by channels and threaded steel rods. By so restraining the development of failure in the span already cracked, the other shear span frequently showed diagonal tension cracking. When the beam failed suddenly by a diagonal crack in one of the shear spans, it was sometimes possible to make more than one test in the intact portion, thus making extra useful results available.

During testing, the development of crack patterns was carefully studied, the distance of the intersection of the critical crack with the centroidal axis in the case of a uniformly distributed load being measured (see Figure 6.8). The load at the first inclined

tension crack and ultimate load were noted. All the results are shown in Tables 5.1 and 5.2. Photographs were taken of each beam after the completion of the test. Some typical examples of different types of shear failure are shown in Figures 5.1.a to 5.1.l and Figure 6.7.

For each beam, four 150 x 300 mm cylinders were split and four 100 mm cubes were crushed in accordance with B.S. 1881; Part 4: 1970. A relationship between the tensile strength of concrete, f'_{ct}, derived from cylinder split tests, and the cube strength of concrete, f_{cu}, was developed and the following expressions were obtained:

$$f'_{ct} = \frac{f_{cu}}{28} + 1.45 \quad N/mm^2 \qquad (4.2)$$

$$\text{or } f'_{ct} = 0.456 \sqrt{f_{cu}} \qquad (4.3)$$

and equation 4.2 was used in the final calculations. Figure 4.8 shows equations 4.2 and 4.3 compared with other equations for predicting the tensile strength of concrete[27,30,36,55] against the experimental results obtained in this investigation.

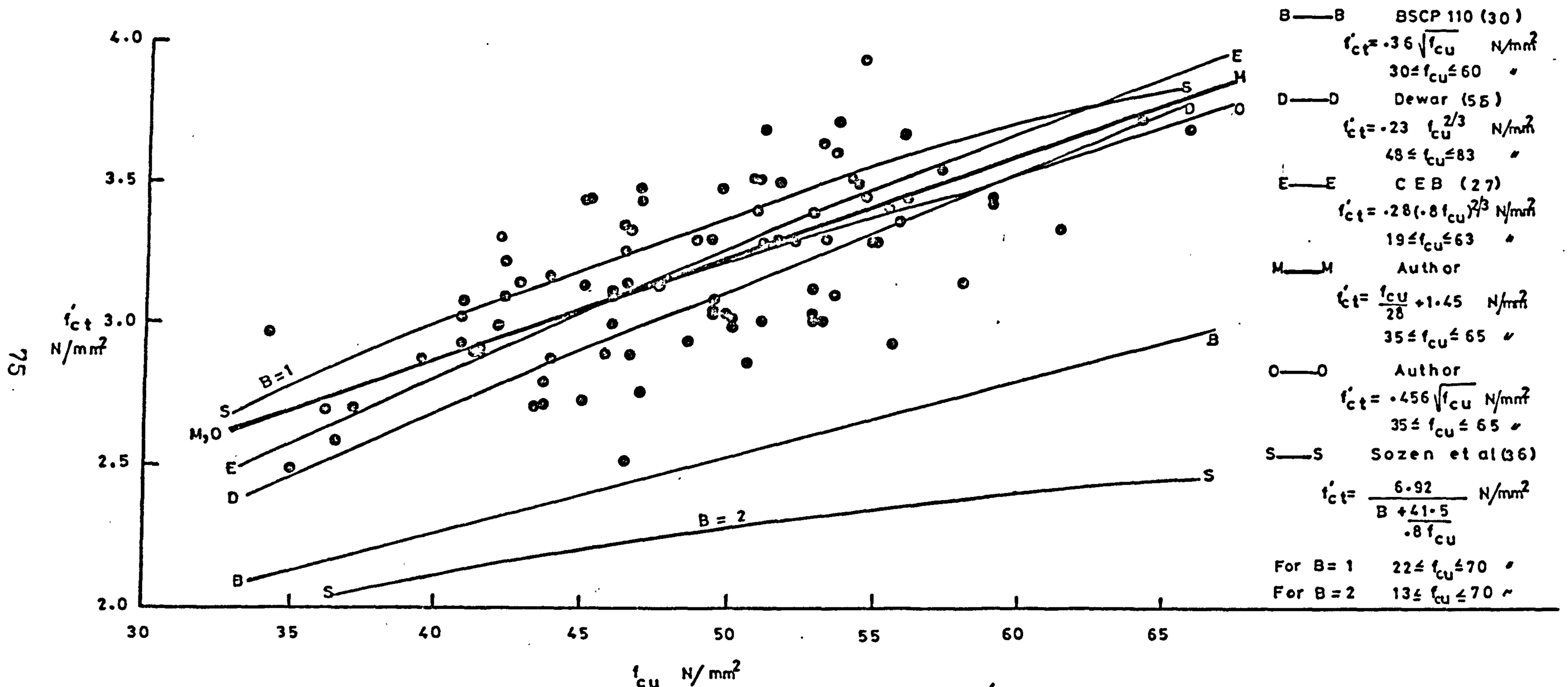

Figure 4.8 : Tensile strength of concrete, f'_{ct}, as a function of f_{cu}.

CHAPTER 5

DESCRIPTION of TESTS

5.1 Introduction:

Distress in shear begins with shear cracking. Two types of shear cracks are distinguished : web-shear cracks and flexure-shear cracks[32,85]. The web-shear cracks originate independently in the web and they may lead to the type of shear failure shown in Figure 5.1.a. Flexure-shear cracks occur in regions already cracked in flexure and these shear cracks are extensions of the flexure cracks and they may bring about the type of shear failure illustrated in Figure 5.1.b.

5.2. Development of the Shear Crack Patterns and the Observed Modes of Shear Failure:

5.2.1. Shear failures developed from web-shear cracks:

In the majority of the tests carried out in this investigation the shear crack started as a web-shear crack. These web-shear cracks can be divided into two types depending on the speed of their formation. In one type the formation of the web-shear crack is a gradual process and in the other it is sudden, explosive and destructive.

The gradual formation of the web-shear crack starts with very minute inclined web cracks in the middle of the web without any appreciable change in the load - deflection curve being observed. As the load increases these minute cracks start to link up

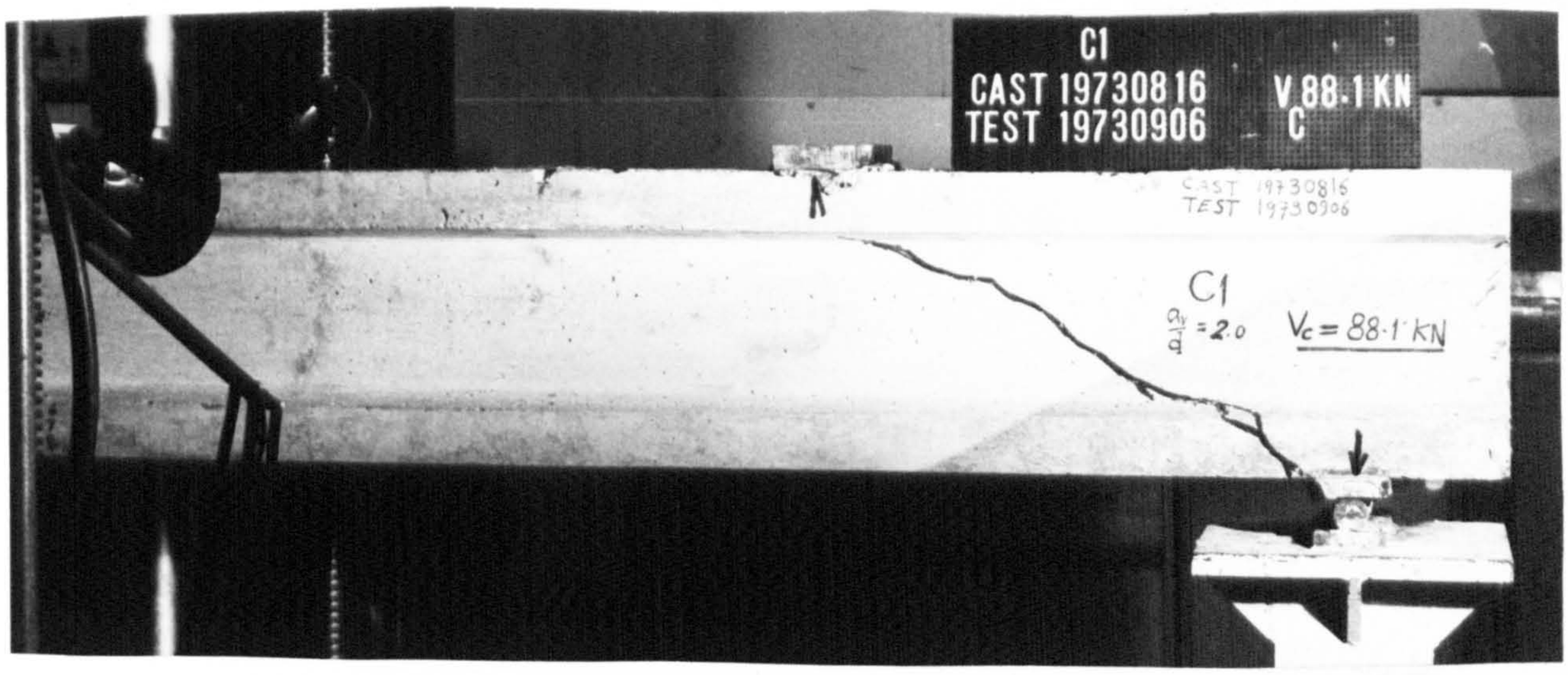

Figure 5.1.a. Shear failure as a result of web-shear crack followed by bond failure (mode of failure classified as diagonal crack and bond failure).

$a_{v/d} = 2.0$, $\frac{V_u}{V_c} = 1.00$, $\frac{V_{c\ Expt.}}{V_{c\ Calc.}}^{*} = 1.01$

Figure 5.1.b. Shear failure initiated by a flexure-shear crack (mode of failure classified as shear-compression).

$a_{v/d} = 2.0$, $\frac{V_u}{V_c} = 1.61$, $\frac{V_{c\ Expt.}}{V_{c\ Calc.}} = 0.77$

Note:
In the photographs the standard international form of the date is used, i.e. Year/Month/Day.

* See Page 82.

to form a continuous web-shear crack as illustrated in Figure 5.1.c and the load sustained by the beam suddenly drops as shown by the load-deflection curve of Beam B 7 in Figure 5.2. At this stage the principal tensile stress might be equated to the tensile strength of concrete. This was observed with I-beams at $a_{v/d}$ = 1.25. Depending on the quality of bond, further increase in loading may lead to the formation of more parallel inclined cracks and eventually web-crushing which was observed to be the predominant mode of failure in such cases as shown in Figure 5.1.c for Beam B 6 and Beam B 7 and other examples as given in Table 5.1. The web-crushing failure in itself is a gradual process by which the load decreases gradually as the web starts to crush as shown by the inclined curve of upper part of the load-deflection curve of Beam B 7 shown in Figure 5.2. In these cases the ultimate load could be as high as 1.7 of the first inclined cracking load.

The second type of web-shear crack appears suddenly and without warning in the uncracked web-zone traversing a considerable height of the web and extending rapidly both ways followed immediately by an explosive collapse of the beam along the inclined crack. With I - sections and depending on the value of f_{cp} and the $a_{v/d}$ ratio, the sudden formation of this web-shear crack (diagonal tension crack) will take place before any vertical flexure crack appears in

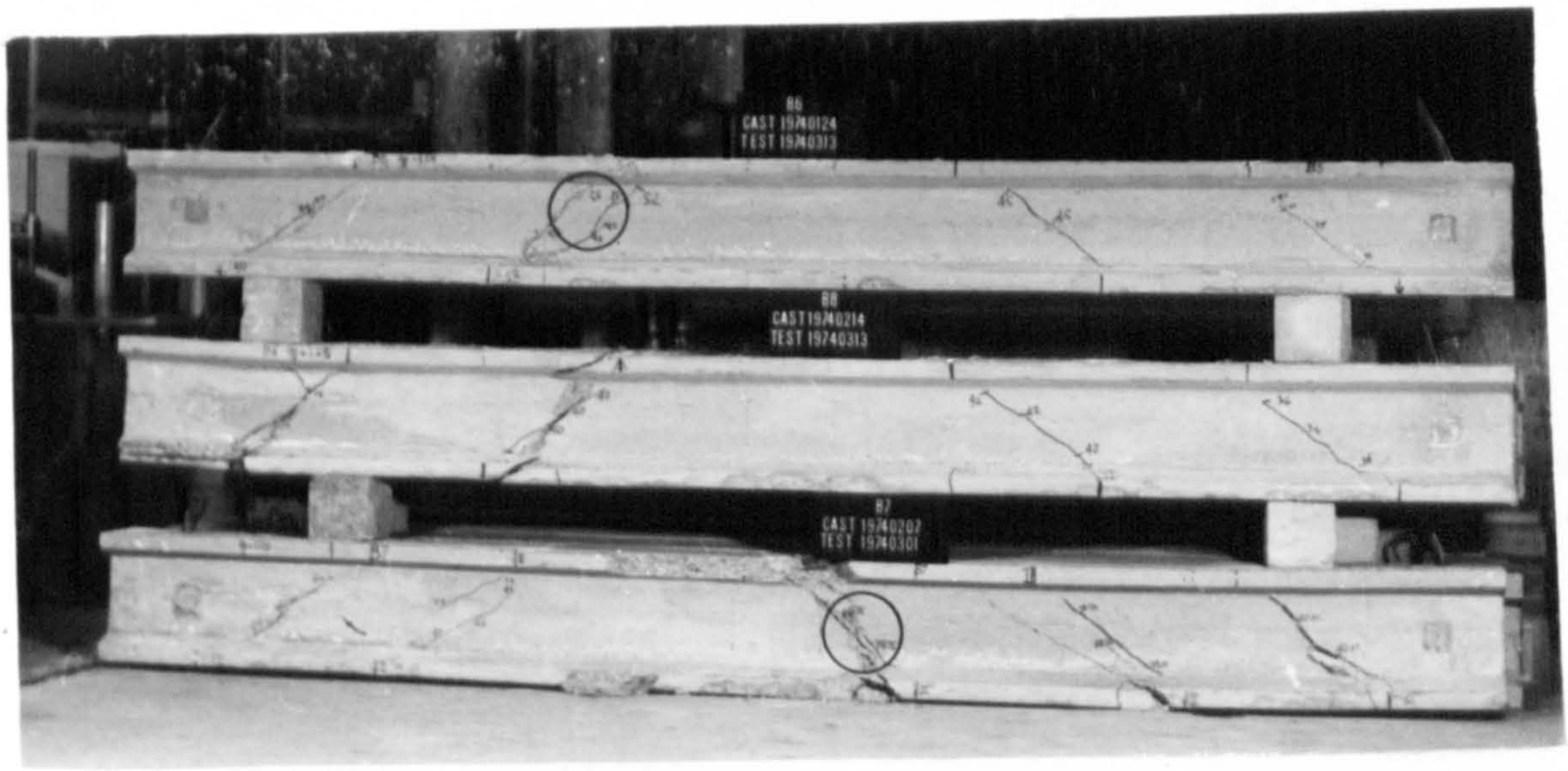

Figure 5.1.c. Showing (a) Non-explosive web-shear crack formation (b) web crushing mode of failure as shown by circles in 'B6' and 'B7' .

$a_{v/d} = 1.25$, $\frac{V_u}{V_c} = 1.17 - 1.69$, $\frac{V_{c\ Expt.}}{V_{c\ Calc.}} = 0.87 - 1.13$

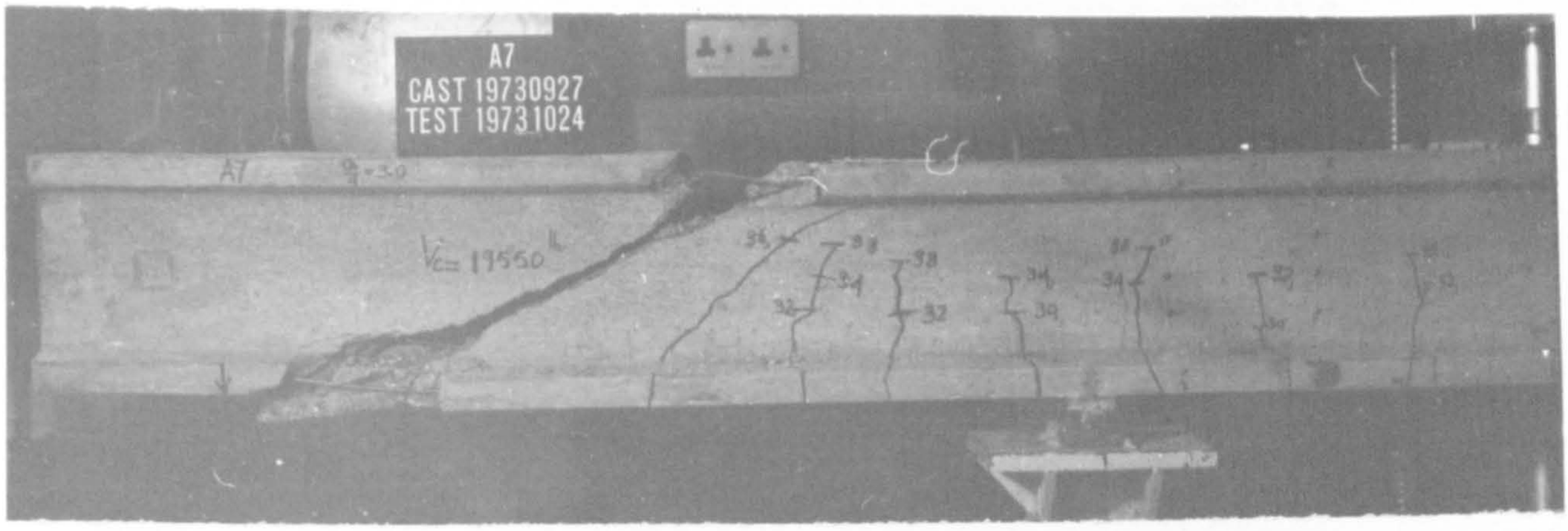

Figure 5.1.d. Sudden explosive formation of a diagonal tension crack in an uncracked web zone. No slipping was observed.

$a_{v/d} = 3.0$, $f_{cu} = 51.0\ N/mm^2$, $f_{cp} = 7.52\ N/mm^2$. $\frac{V_u}{V_c} = 1.09$, $\frac{V_{c\ Expt.}}{V_{c\ Calc.}} = 1.03$

Note: The figures indicate the load (=2V) in kips at which a crack had penetrated as far as the horizontal line indicated.

the beam. This is shown in Figure 5.1.a for Beam C 1 at $a_{v/d}$ = 2.0. However, with greater values of $a_{v/d}$, i.e. $a_{v/d} \geq 3.0$ flexure cracks first start to form in the flexure span and as the load is increased, flexure cracks appear in the shear span in the regions of maximum bending moment or a distinct flexure-shear crack might take place at a distance from the load point greater than or equal to the effective depth, depending on the $a_{v/d}$ ratio. While the flexure - shear crack is gradually widening and proceeding towards the point load, a sudden opening of an explosive destructive diagonal tension crack may take place in the uncracked web. This extends from the support to the load point and sometimes results in the destruction of bond between the concrete and steel leading to immediate collapse of the beam. Examples of these are shown in Figures 5.1.d to 5.1.f. In some instances it was observed that, while the load was held constant for a few minutes while readings were taken, this sudden explosive diagonal crack formed, as shown by Beam E 4 at $a_{v/d}$ = 4.0 in Figure 5.1.g. This was also observed by Sozen et al[36] in their tests.

5.2.2. Shear failures developed from flexure-shear cracks.

The development of shear failures from flexure-shear cracks was observed in this investigation in all ranges of $a_{v/d} \geq 2.0$ depending on the cross-sectional properties and f_{cp} values. With the rectangular

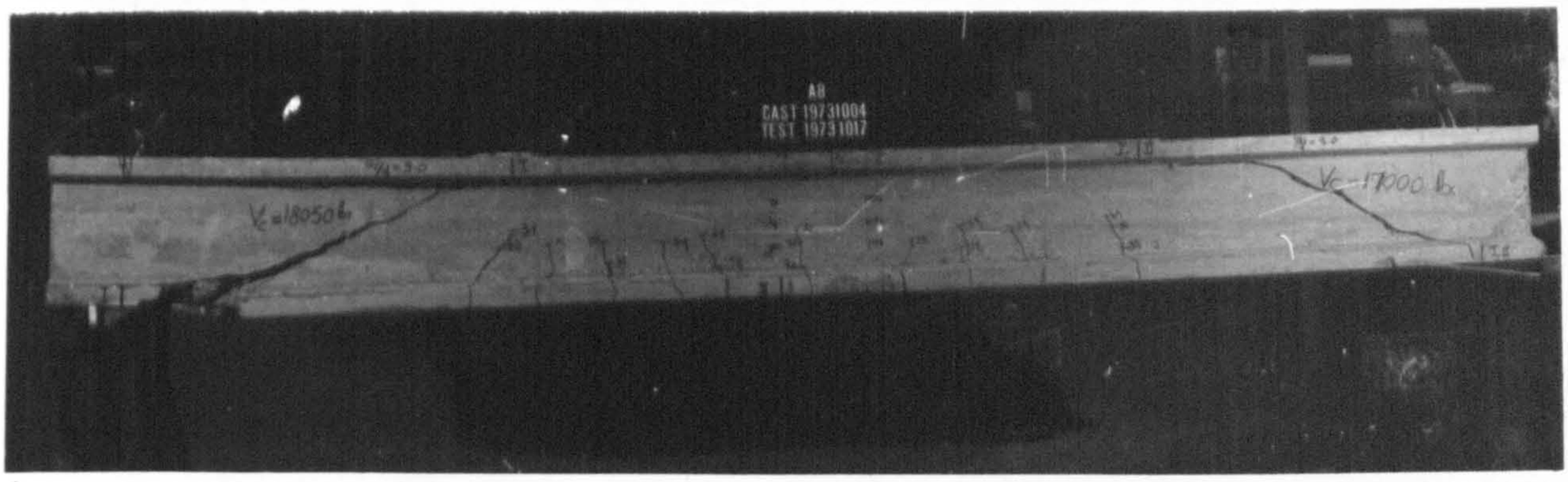

Figure 5.1.e. Sudden explosive formation of a diagonal tension crack in an uncracked web-zone. Slipping of wires was observed.

$\frac{a_v}{d}$ = 3.0, f_{cu} = 43.7 N/mm^2 and f_{cp} = 7.43 N/mm^2.

$\frac{V_u}{V_c}$ = 1.00, $\frac{V_c \text{ Expt.}}{V_c \text{ Calc.}}$ = 1.08 - 1.13

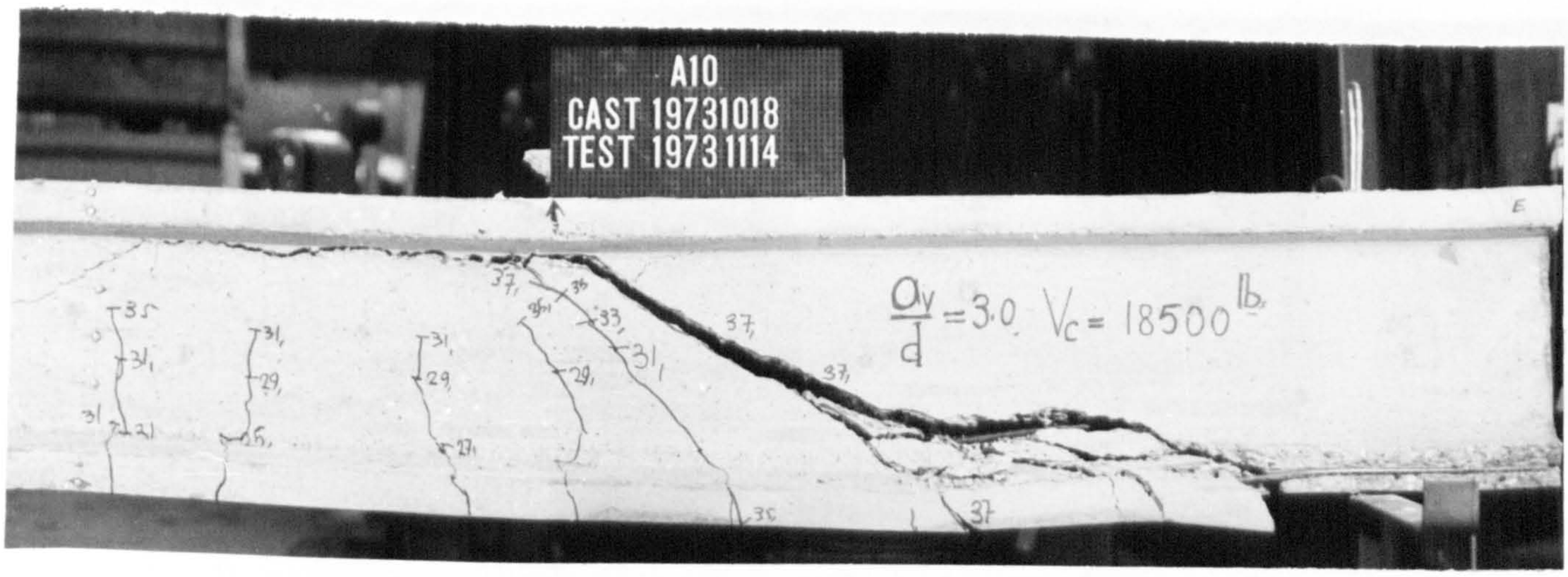

Figure 5.1.f. Mode of failure in A10. Sudden formation of a diagonal tension crack followed by bond destruction.

$\frac{a_v}{d}$ = 3.0, f_{cu} = 45.2 N/mm^2 and f_{cp} = 6.56 N/mm^2.

$\frac{V_u}{V_c}$ = 1.00, $\frac{V_c \text{ Expt.}}{V_c \text{ Calc.}}$ = 1.19.

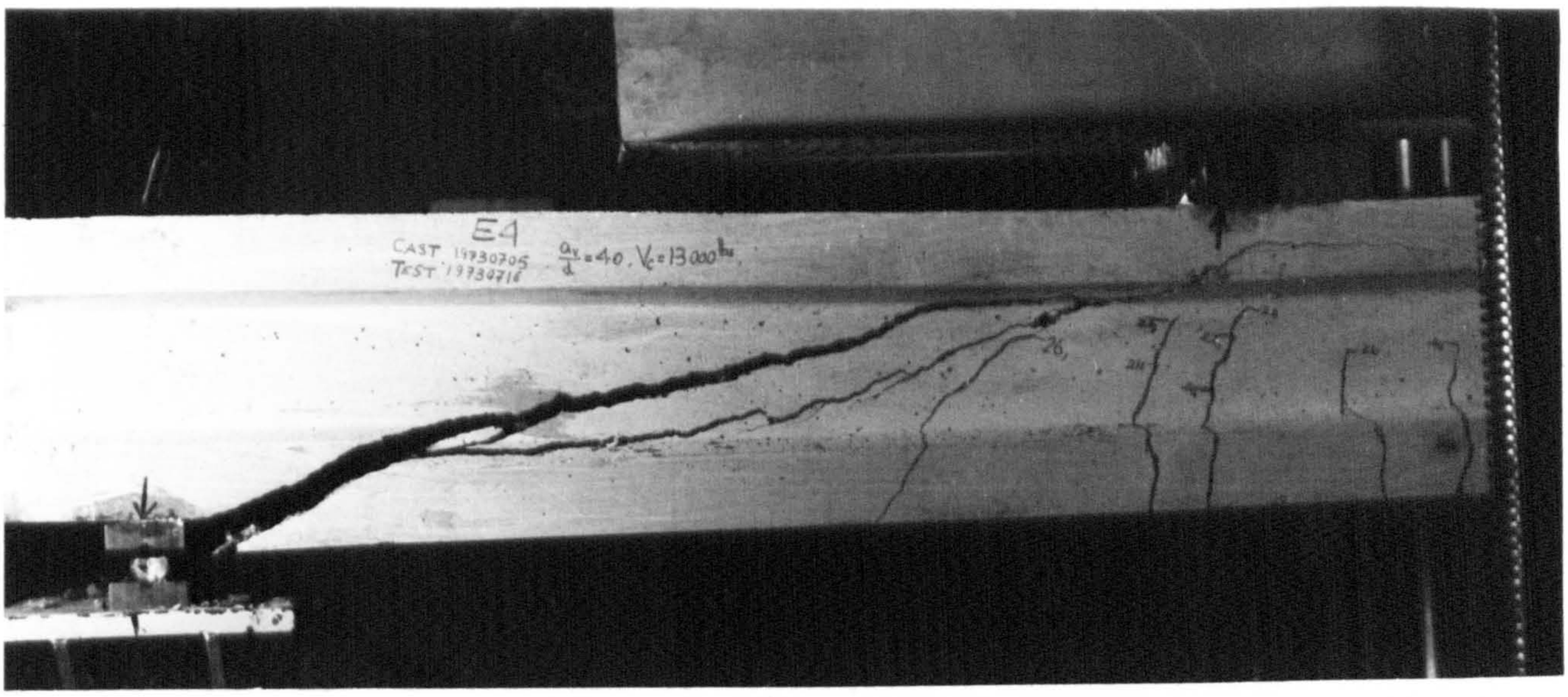

Figure 5.1.g. Sudden formation of diagonal tension crack in E4 while the load was held constant for few minutes.

$a_{v/d}$ = 4.0, f_{cu} = 50.0 N/mm^2 and f_{cp} = 5.18 N/mm^2.

$\frac{V_u}{V_c}$ = 1.00, $\frac{V_c \text{ Expt.}}{V_c \text{ Calc.}}$ = 0.96

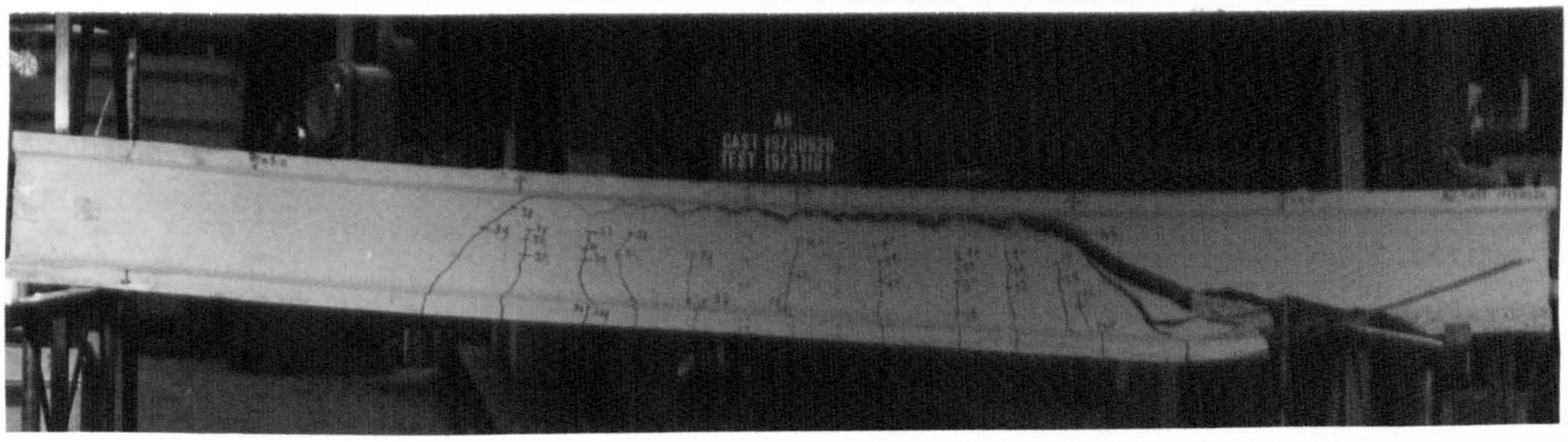

Figure 5.1.h. Mode of failure in A6. Explosive opening of a diagonal tension crack originating from a flexure crack, accompanied by bond destruction and separation of the top flange.

$\frac{a_v}{d}$ = 3.0, f_{cu} = 59.0 N/mm^2 and f_{cp} = 7.34 N/mm^2.

$\frac{V_u}{V_c}$ = 1.17, $\frac{V_c \text{ Expt.}}{V_c \text{ Calc.}}$ = 1.02

* Note $\frac{V_c \text{ Expt.}}{V_c \text{ Calc.}} = \frac{V_c \text{ Experimental}}{V_c \text{ Calculated using equation 6.5}}$

cross-section at $a_{v/d}$ = 2.0, vertical flexure cracks appeared first in the flexure span. With increase in load, a flexure crack might appear in the shear span in the regions of maximum bending moment or a distinct flexure-shear crack might take place at a distance equal to or less than the effective depth ($a_{v/d}$ = 2.0), followed by an appreciable drop in the load. Further increase in loading would lead to a gradual widening of the crack which in turn would start a process of internal redistribution of stress between concrete and steel resulting in strain concentration at the top of the inclined crack[11,36,42]. At this stage the crack would become sufficiently inclined and start to extend downwards. The beam could either fail very gently with crushing of concrete near the point load or by the sudden opening and extension of the flexure-shear crack both ways resulting in the explosive destruction of the beam. This is exemplified by Beam G 3 tested at $a_{v/d}$ = 2.0, which also showed some traces of crushing near the point load as shown in Figure 5.1.b. Similar behaviour and crack patterns were observed with an I - section A 6 at $a_{v/d}$ = 3.0, f_{cu} = 59.0 N/mm^2 and f_{cp} = 7.34 N/mm^2. The diagonal crack opened suddenly with propagation along the level of tension reinforcement. The increased shear force pressed down the longitudinal steel and caused the destruction of the bond between the concrete and steel which led to splitting of the concrete as illustrated

in Figure 5.1.h. This case could be compared with Beam A 10 with similar properties to Beam A 6 except for f_{cu} and f_{cp}. Beam A 6 had a higher value of $(f_{cp} + f'_{ct})$ compared with either A 7, A 8 or A 10 and this might explain why the diagonal tension cracks in these three beams formed independently of the existing flexure-shear crack. This behaviour is reflected also in their load-deflection curves as shown in Figure 5.3 for Beam A 6 and Beam A 10.

With $a_{v/d}$ increasing to 4.0, f_{cp} ranging between 5.21 and 5.77 N/mm^2 and f_{cu} from 35.0 to 42.3 N/mm^2, diagonal tension cracks originating from flexure cracks were found to initiate shear failure in many cases. The inclined crack showed a distinct tendency to become horizontal toward the nearest support at the level of the bottom web-flange junction. However in some instances, a series of horizontal cracks, which seemed to extend from the inclined crack, developed along the bottom web-flange junction. With increase in load, these cracks linked up and widened so leading to loss of bond. This resulted in the separation of the bottom flange from the web and eventually failure of the beam as shown for type C beam in Figures 5.1.i and 5.1.j. The corresponding load - deflection curves for Beam C 10 and Beam C 12 are shown in Figure 5.3. It is possible that this horizontal cracking was initiated by microscopic 'bond' cracking caused by the drying shrinkage of cement paste, which induces high

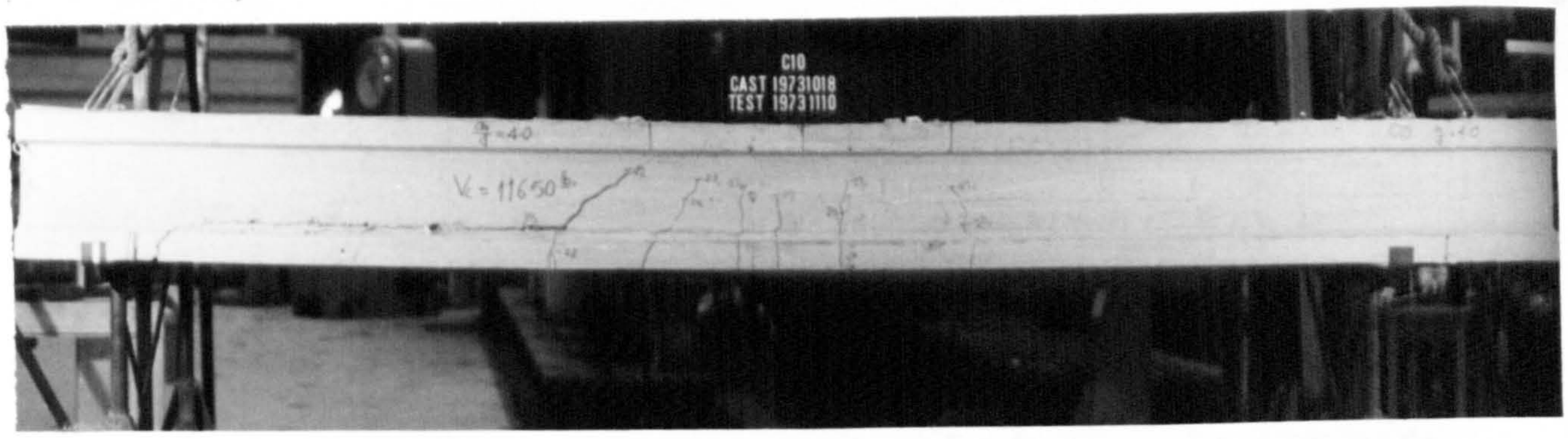

Figure 5.1.i. Mode of shear failure in C10. Diagonal tension crack originating from a flexure crack led to the separation of bottom flange from the web and was followed by bond failure.

$a_{v/d}$ = 4.0, f_{cu} = 42.3 N/mm^2 and f_{cp} = 5.77 N/mm^2.

$\frac{V_u}{V_c}$ = 1.00, $\frac{V_{c\ Expt.}}{V_{c\ Calc.}}$ = 0.90

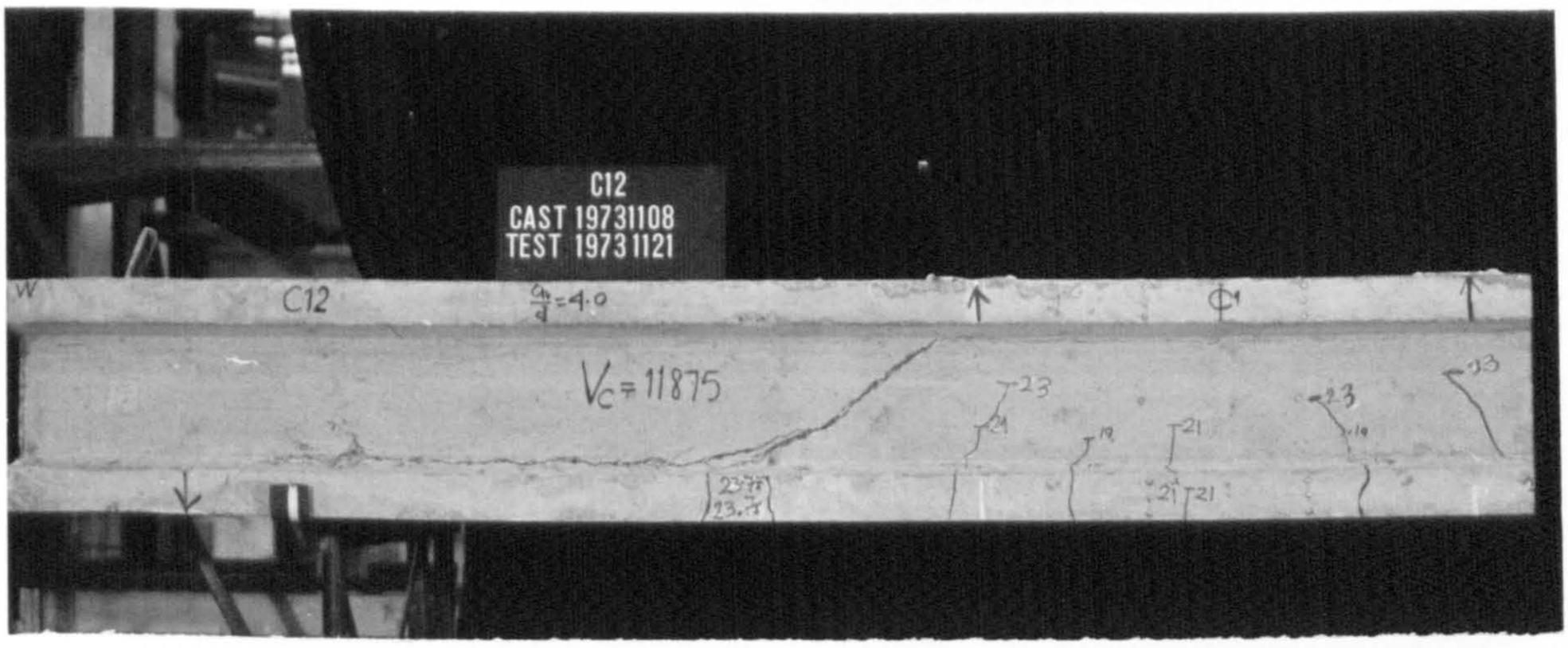

Figure 5.1.j. Mode of shear failure in C12. Diagonal tension crack developing from a flexure crack and extending along the bottom web-flange junction leading to the separation of the bottom flange from the web. The 'arching' effect and the crushing of the web near the reaction was observed.

$a_{v/d}$ = 4.0, f_{cu} = 35.0 N/mm^2 and f_{cp} = 5.21 N/mm^2.

$\frac{V_u}{V_c}$ = 1.00, $\frac{V_{c\ Expt.}}{V_{c\ Calc.}}$ = 1.00

internal tensile stresses at the mortar-aggregate interface[86-88]. Beam C 11 in Figure 5.1.k. shows an example of the effect of reducing f_{cp} from 5.77 N/mm^2, Beam C 10 case, to 4.90 N/mm^2 on the initiation of shear failure compared with Beam C 10. In the case of Beam C 11 the diagonal tension crack formed independently of any flexure crack and its behaviour afterwards with increase in load was similar to that described above for Beam C 10 and Beam C 12.

5.2.3. Shear failures developed from secondary inclined tension cracking.

What is described as a secondary inclined tension cracking[36] was observed in Beams A 12, B 1 and F 1. With Beam B 1 tested at $a_{v/d}$ = 4.0, an inclined tension crack opened suddenly in the vicinity of the support at a shear force of 39.9 KN, and a series of short inclined cracks followed immediately thereafter along the upper web-flange junction. With increase in load these short inclined cracks linked up and widened. Then this damaged shear span was strengthened by clamping it by channels and threaded rods to force shear failure on the other shear span and the test continued from this stage. At a shear force of 44.5 KN a non-explosive inclined tension crack opened in the vicinity of the reaction and propagated just beneath the upper web-flange junction towards the load point and the shear force dropped to 35.6 KN. Further attempts to increase the load led to the formation of an inclined crack extending from the support to the load point

followed by crushing at its upper end near the upper web-flange junction and the formation of a horizontal tension crack in the top flange near the middle of the shear span. The load then dropped to zero. A load-deflection of behaviour of Beam B 1 is shown in Figure 5.2.

With Beam A 12 tested at $a_{v/d}$ = 3.0, an inclined tension crack opened suddenly in the web at a shear force of 60.1 KN just over the reaction and propagated along the upper web-flange junction. This was followed immediately by the formation of another inclined tension crack in the uncracked part of the web in the same shear span which extended along the upper web-flange junction into the flexural span and backwards along the lower bottom web-flange junction to the support as shown on the L.H.S. of Figure 5.1.1. The load-deflection curve is shown in Figure 5.3. This damaged shear span was clamped and the test was repeated to force the shear failure to occur in the intact shear span. A similar behaviour and crack patterns were observed in the unclamped shear span, but at a shear force of 55.6 KN. Some crushing was observed in the upper web-flange junction as shown on the R.H.S. of Figure 5.1.1.

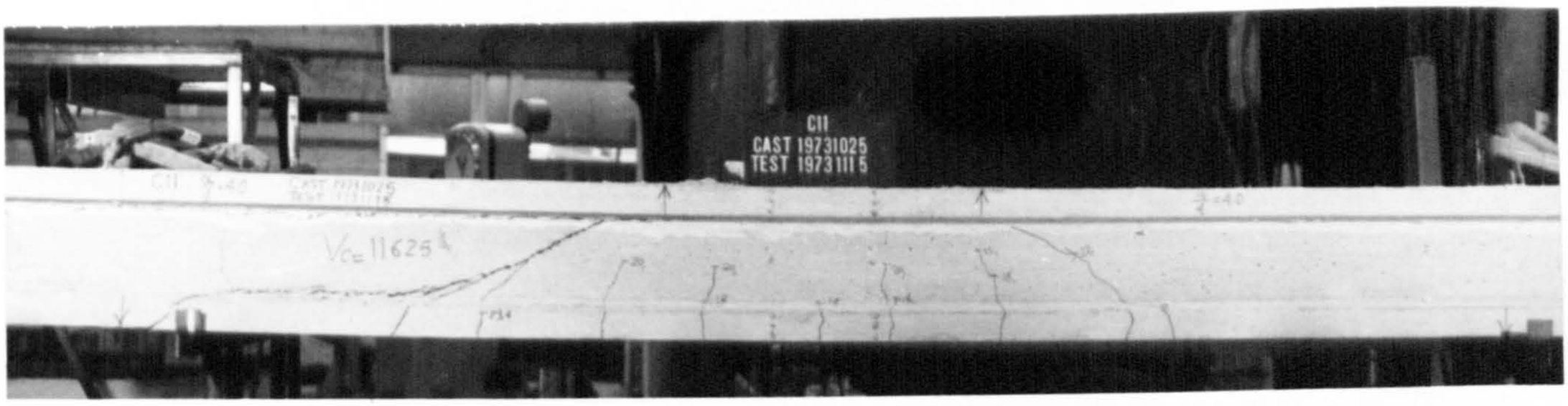

Figure 5.1.k. Mode of shear failure in C11. Diagonal tension crack developed independent of any flexure crack and extending along the bottom web-flange junction separating the bottom flange from the web. No slipping was observed.

$\frac{a_v}{d}$ = 4.0, f_{cu} = 45.0 N/mm^2 and f_{cp} = 4.90 N/mm^2.

$\frac{V_u}{V_c}$ = 1.07, $\frac{V_c \text{ Expt.}}{V_c \text{ Calc.}}$ = 0.97

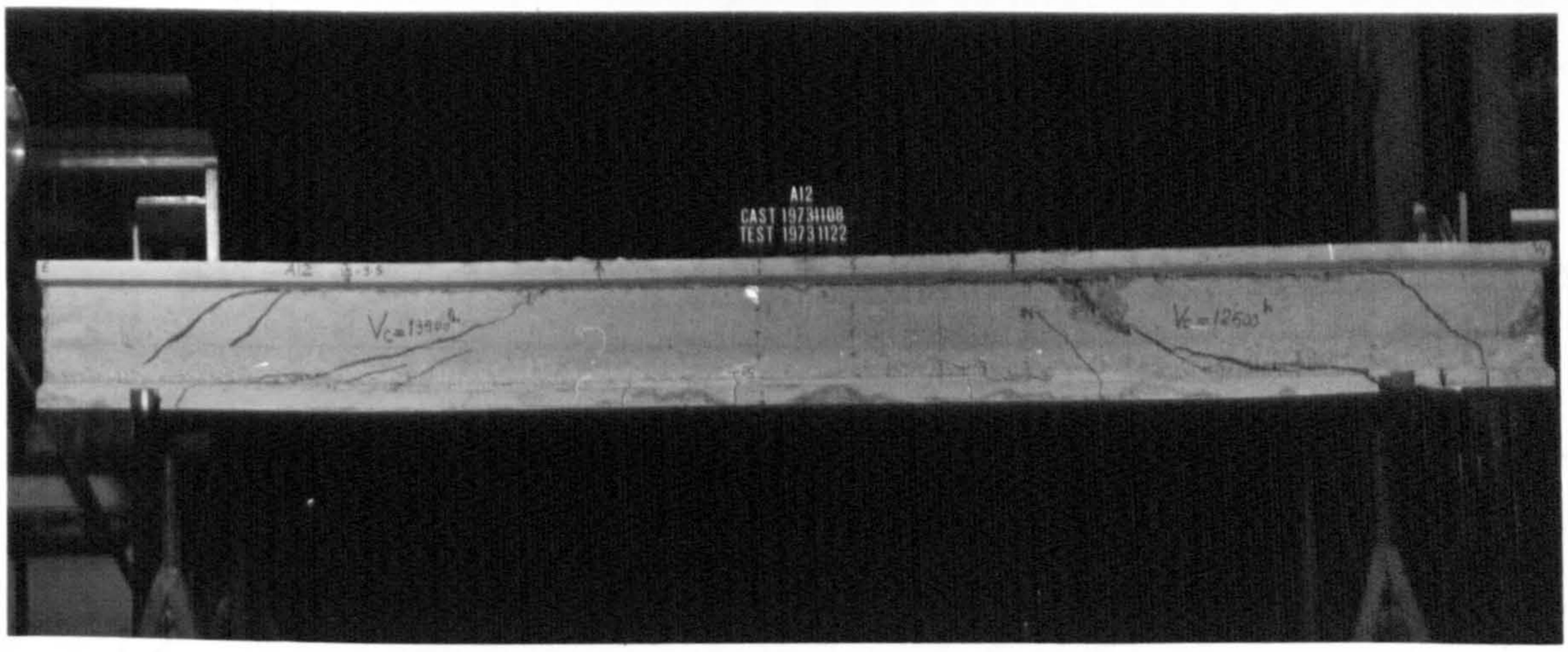

Figure 5.1.l. Shear failure in A12 as a result of secondary inclined tension cracking.

$\frac{V_u}{V_c}$ = 1.00, $\frac{V_c \text{ Expt.}}{V_c \text{ Calc.}}$ = 0.97 - 1.05

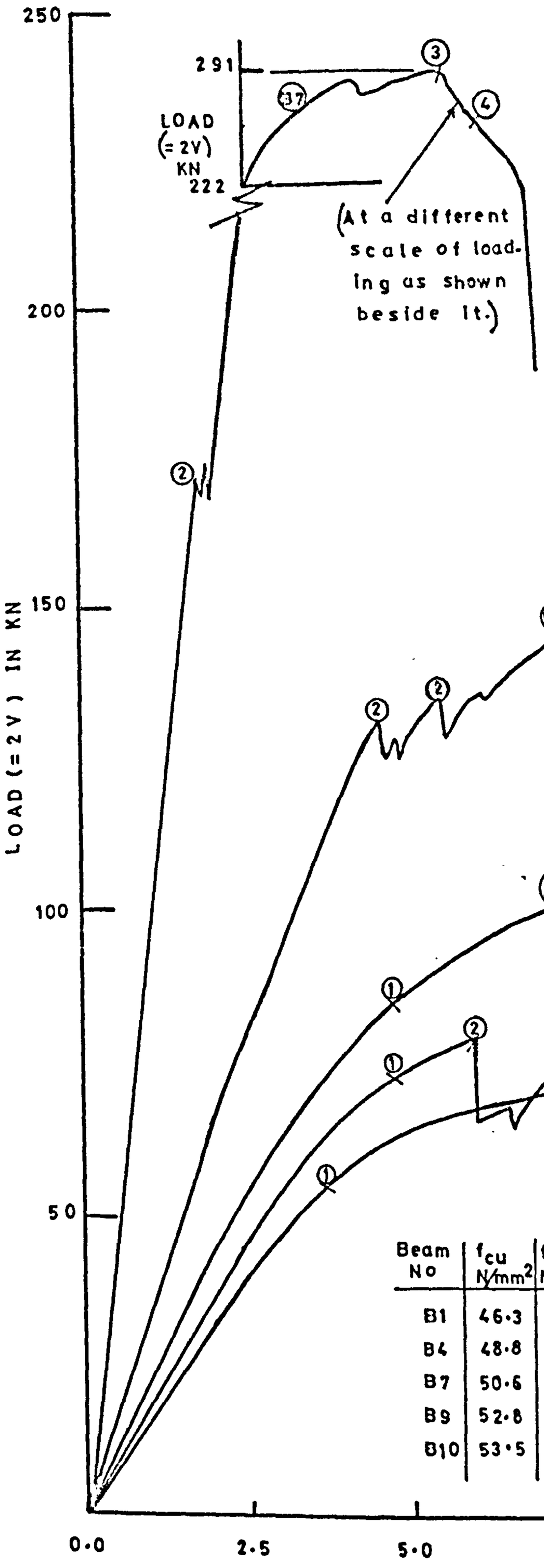

① - Appearance of flexure crack.
② - Diagonal tension crack formation.
③ - Ultimate shear failure load.
④ - Web-crushing.
⑤ - Web-distortion.
⑥ - Horizontal-tension crack in the upper flange (arching effect).
⑦ - Wires-slipping.

Beam No	f_{cu} N/mm²	f_{cp} N/mm²	a_v mm	$(1-a_v)$ mm	a_v/d
B1	46·3	5·89	1060	630	4·0
B4	48·8	7·05	530	1690	2·0
B7	50·6	6·45	330	597	1·25
B9	52·8	5·64	1190	570	4·5
B10	53·5	7·49	930	890	3·5

Figure 5.2 Load-deflection curves for type B beam.

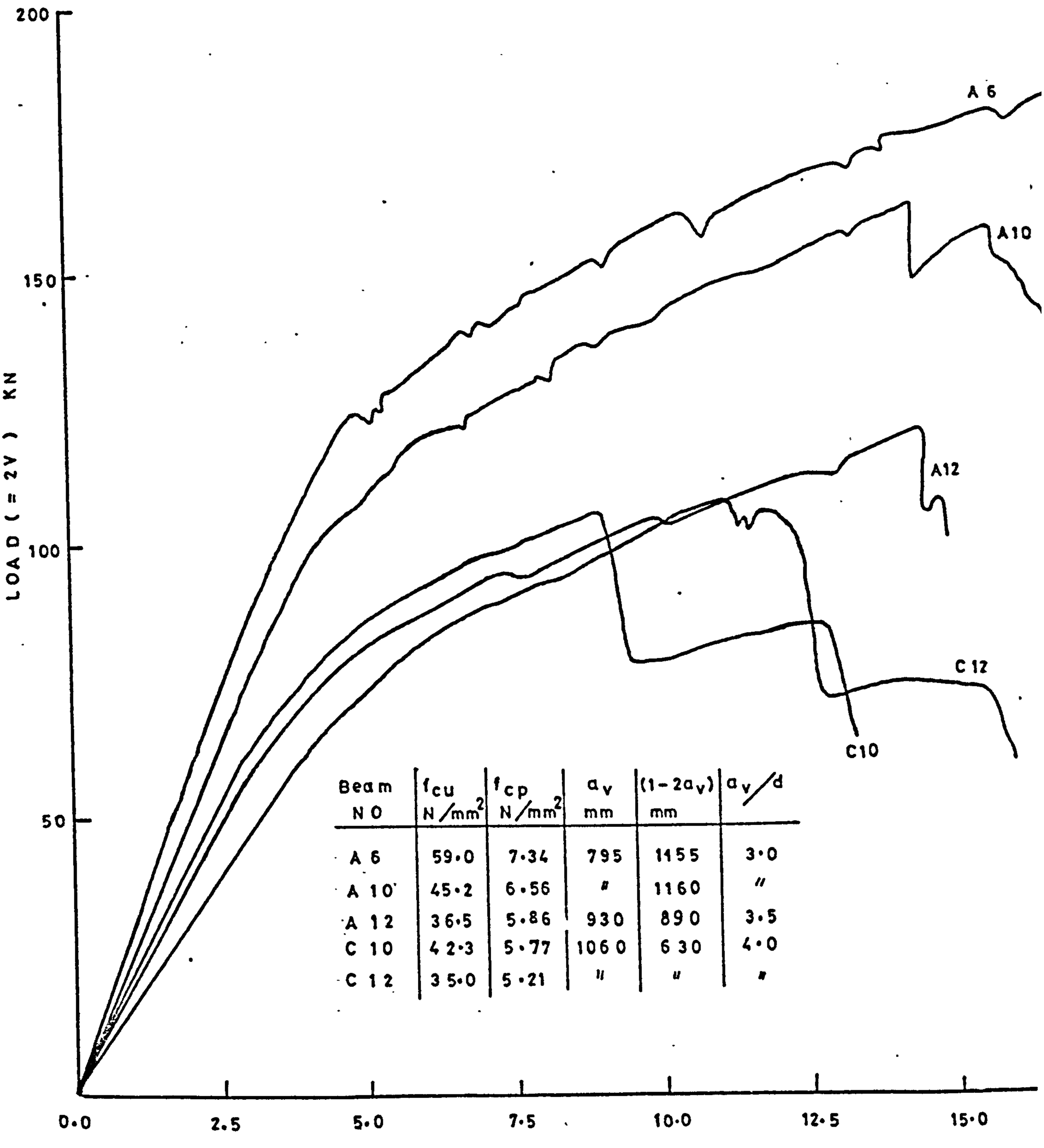

Beam NO	f_{cu} N/mm^2	f_{cp} N/mm^2	a_v mm	$(1-2a_v)$ mm	a_v/d
A 6	59·0	7·34	795	1155	3·0
A 10	45·2	6·56	〃	1160	〃
A 12	36·5	5·86	930	890	3·5
C 10	42·3	5·77	1060	630	4·0
C 12	35·0	5·21	〃	〃	〃

Figure 5.3: Typical load deflection curves
(Types A and C beams)

TABLE 5.1

Experimental results under one - or two-point loads.

Beam mark	a_v mm	$(l-2a_v)$ mm	d mm	$\frac{a_v}{d}$	$f^{\wedge}_{ct}$ N/mm^2	f_{cp} N/mm^2	V_c KN East	V_c KN West	V_u KN East	V_u KN West	$\frac{V_u}{V_c}$	Mode of failure
A1	795	1360	265	3.00	3.29	7.40	87.1	-	87.1	-	1.00	DC/WD
"	"	0	"	"	"	"	-	86.7	-	86.7	1.00	DC
2	930	890	"	3.50	3.39	6.75	64.5	-	77.5	-	1.20	DC/WD
3	530	1885	"	2.00	3.42	6.33	77.8	-	77.8	-	1.00	DC
"	"	810	"	"	"	"	-	76.4	-	76.4	1.00	DC/BF
"	"	0	"	"	"	7.46	101.2	-	101.2	-	1.00	DC
4	"	1890	"	"	3.34	6.81	101.3	-	104.5	-	1.03	DC/WD
"	"	820	"	"	"	"	-	81.4	-	81.4	1.00	DC
"	"	0	"	"	"	"	94.3	90.1	-	100.1	1.11	DC/WD
5	"	1890	"	"	3.42	6.67	87.8	-	87.8	-	1.00	DC
"	"	1355	"	"	"	"	-	94.5	-	94.5	1.00	DC
"	"	830	"	"	"	7.28	102.3	95.6	-	109.0	1.14	DC
"	"	0	"	"	"	"	98.7	-	98.7	-	1.00	DC
6	795	1155	"	3.00	3.56	7.34	-	80.1	-	93.4	1.17	DC/TFS
7	"	1160	"	"	3.27	7.52	79.5	-	87.0	-	1.09	DC
"	"	0	"	"	"	"	74.5	87.9	-	87.9	1.00	DC
8	"	1355	"	"	2.47	7.43	-	80.3	-	80.3	1.00	DC
"	"	0	"	"	"	"	75.6	-	75.6	-	1.00	DC
9	"	1160	"	"	2.98	7.37	-	79.0	-	80.1	1.01	DC/BF
"	"	0	"	"	"	"	-	79.4	-	79.8	1.01	DC
10	"	1160	"	"	3.05	6.56	82.3	70.1	82.3	-	1.00	DC/WD
11	930	890	"	3.50	2.91	5.38	53.4	58.5	71.2	-	1.33	DC
"	"	0	"	"	"	"	55.6	-	64.5	-	1.16	DC
12	"	890	"	"	2.75	5.86	60.1	55.6	60.1	-	1.00	DC/WD
B1	1060	630	265	4.00	3.10	5.89	38.9	44.5	-	44.5	1.00	DC/WD/TFS
2	"	"	"	"	3.26	7.07	47.4	48.9	-	48.9	1.00	DC/WD
3	530	1690	"	2.00	3.52	6.79	66.7	71.2	-	76.1	1.07	DC/SCC
"	"	630	"	"	"	"	-	74.5	-	74.5	1.00	DC/SCC
4	"	1690	"	"	3.19	7.05	66.2	67.7	80.1	-	1.21	DC/WD
"	"	630	"	"	"	7.34	83.4	67.7	83.4	-	1.00	DC/WD
5	1193	560	"	4.50	3.28	5.61	40.0	-	40.0	-	1.00	DC/BF

TABLE 5.1 (Cont'd)

Beam mark	a_v mm	$(1-2a_v)$ mm	d mm	$\frac{a_v}{d}$	f'_{ct} N/mm^2	f_{cp} N/mm^2	V_c KN		V_u KN		$\frac{V_u}{V_c}$	Mode of failure.
							East	West	East	West		
B 6	330	2090	265	1.25	3.31	5.99	80.1	77.8	-	117.0	1.50	DC/WD
"	"	1430	"	"	"	"	93.4	89.0	-	149.9	1.68	DC/WC
7	"	2085	"	"	3.26	6.45	90.1	90.1	-	122.3	1.36	DC/WD /BF
"	"	1200	"	"	"	"	102.3	85.1	-	111.2	1.31	DC/WD /BF
"	"	597	"	"	"	"	-	86.2	-	145.4	1.69	DC/WC
8	"	2085	265	1.25	3.23	6.30	78.1	78.1	-	99.5	1.27	DC/WD /BF
"	"	1445	"	"	"	"	83.7	100.4	-	117.0	1.17	DC/WD
9	1190	570	"	4.50	3.30	5.64	37.2	-	37.2	-	1.00	DC/BF
10	930	890	"	3.50	3.23	7.49	-	55.6	-	55.6	1.00	DC/BF
"	400	680	"	1.50	"	"	71.2	84.5	-	84.5	1.00	DC/BF
11	730	1190	"	2.75	3.36	7.86	57.8	-	57.8	-	1.00	DC/BF
"	"	0	"	"	"	"	58.9	62.3	-	62.3	1.00	DC
C 1	530	1890	265	2.00	3.24	5.77	87.3	87.8	clamped	87.8	1.00	DC/BF
"	"	530	"	"	"	6.71	102.3	87.8		123.2	1.40	DC/WD
2	330	1890	"	1.25	3.11	5.94	93.7	122.3	151.2	-	1.62	DC/WD
"	"	715	"	"	"	"	129.0	129.0	189.0	-	1.47	DC/WC
3	1060	810	"	4.00	3.45	6.31	-	60.0	68.9		1.15	F
4	"	"	"	"	3.35	6.40	-	57.8	66.7		1.15	F
5	530	1890	"	2.00	3.27	5.66	-	77.8	-	77.8	1.00	DC/BF
"	"	1358	"	"	"	"	87.0	85.4	87.0	-	1.00	DC/BF
"	"	830	"	"	"	"	81.0	-	96.7	-	1.19	DC/WD
"	"	0	"	"	"	"	93.4	-	124.5	-	1.33	DC
6	330	2090	"	1.25	3.33	6.46	120.1	129.0	-	137.9	1.07	DC/WD
"	"	1430	"	"	"	"	-	111.2	-	111.2	1.00	DC/BF
"	"	1100	"	"	"	"	-	109.0	-	133.5	1.22	DC/BF
"	"	640	"	"	"	"	142.4	133.5	-	169.1	1.27	DC
7	"	2090	"	"	3.26	5.87	101.2	115.7	133.5	-	1.32	DC/BF
"	"	1430	"	"	"	"	100.1	-	113.4	-	1.13	DC/WD /BF
"	"	770	"	"	"	"	120.1	127.7	-	209.1	1.64	DC/WC

TABLE 5.1 (Cont'd)

Beam mark	a_v mm	$(1-2a_v$ mm	d mm	$\frac{a_v}{d}$	f'_{ct} N/mm^2	f_{cp} N/mm^2	V_c KN East	V_c KN West	V_u KN East	V_u KN West	$\frac{V_u}{V_c}$	Mode of failure
C8	530	1890	265	2.00	3.06	6.24		74.9		74.9	1.00	DC/BF
"	"	1355	"	"	"	"	82.3	-	82.3	-	1.00	DC/BF
"	"	640	"	"	"	"	-	94.5	-	98.4	1.04	DC/WD
9	330	2110	"	1.25	3.01	5.72	105.2	105.2	-	117.5	1.12	DC/WD/BF
"	"	960	"	"	"	"	124.6	124.6	-	195.8	1.57	DC/WC
10	1060	630	"	4.00	2.96	5.77	-	52.5	-	52.5	1.00	DC/BFS
11	"	"	"	"	3.06	4.90	51.7	48.9	-	52.1	1.07	DC/BFS
12	"	"	"	"	2.70	5.21	51.2	52.8	-	52.8	1.00	DC/WD
17	1350	0	225	6.00	2.73	2.55	27.8	-	40.9	-	1.47	DC/WD
18	"	0	"	"	3.04	2.49	-	25.6	-	40.0	1.56	DC/BFS
19	1180	490	"	5.25	3.27	2.45	-	31.1	-	54.5	1.75	SC
D1	530	1690	265	2.00	3.19	6.38	66.7	66.7	-	-	-	DC
"	"	630	"	"	"	"	71.2	66.7	86.5	-	1.21	DC/WC
2	"	1690	265	2.00	3.21	6.45	-	68.9	-	68.8	1.00	DC
3	795	1230	"	3.00	3.35	5.36	38.9	45.6	-	45.6	1.00	DC/BF
4	570	1190	"	4.50	3.29	5.02	36.1	36.1	36.1	clamped	1.00	DC/WD
5	1060	530	"	4.00	3.06	5.31	43.9	clamped	43.9	"	1.00	DC/WD
6	795	1230	"	3.00	3.39	5.35	51.2		51.2	-	1.00	DC/WD
7	1350	0	225	6.00	2.73	2.80	35.0	23.4	35.0	-	1.00	DC/TFS
8	"	"	"	"	3.04	2.72	-	23.4	26.7	-	1.14	DC/WD
9	1180	490	"	5.25	3.27	2.70	24.5	-	36.1	-	1.47	DC/WD
E1	795	1360	265	3.00	3.74	4.38	70.6	71.2	-	75.9	1.07	DC
"	"	415	"	"	"	"	72.3	-	72.3	-	1.00	DC
"	530	0	"	2.00	"	"	85.6	81.0	85.6	-	1.00	DC
2	"	1890	"	"	3.33	3.33	-	69.1	-	73.6	1.07	DC
"	"	1240	"	"	"	"	75.8	-	75.8	-	1.00	DC
"	"	0	"	"	"	"	-	69.9	-	75.8	1.08	DC
3	"	1880	"	"	3.37	4.88	-	86.2	-	86.2	1.00	DC
"	"	1240	"	"	"	"	-	86.7	-	86.7	1.00	DC
"	"	680	"	"	"	5.16	88.4	98.4	153.5	-	1.74	DC/WC
4	1060	830	"	4.00	3.29	5.18	56.2	57.8	-	57.8	1.00	DC/WD
5	"	"	"	"	3.17	5.66	-	68.9	-	68.9	1.00	DC/WD
"	530	530	"	2.00	"	"	84.5	92.3	-	92.3	1.00	DC

TABLE 5.1 (Cont'd)

Beam mark	a_v mm	$(1-2a_v)$ mm	d mm	$\frac{a_v}{d}$	f'_{ct} N/mm^2	f_{cp} N/mm^2	V_c KN		V_u KN		$\frac{V_u}{V_c}$	Mode of Failure
							East	West	East	West		
E6	795	1360	265	3.00	3.22	6.32	92.3	80.1	92.3	-	1.00	DC
7	"	"	"	"	3.10	5.58	-	66.7	-	66.7	1.00	DC
"	"	448	"	"	"	"	68.9	-	68.9	-	1.00	DC
"	"	0	"	"	"	"	72.1	-	81.0	-	1.12	DC/WD
8	1060	630	"	4.00	3.52	5.32	-	-	68.	9	-	F
F1	1060	630	265	4.00	3.14	4.55	41.4	29.7	41.4	-	1.00	DC/TFS/ BF
2	"	635	"	"	3.21	4.69	41.1	39.5	41.1	-	1.00	DC/WD
3	530	1690	"	2.00	3.41	5.12	64.5	66.7	-	98.5	1.48	DC/WC
"	"	400	"	"	"	5.35	71.2	75.9	-	105.3	1.39	DC/WC
4	"	1690	"	"	3.28	5.58	66.7	66.7	-	93.0	1.39	DC/WC
"	"	630	"	"	"	5.87	71.2	79.0	-	87.2	1.10	DC/WC
5	1200	570	"	4.5	3.33	3.33	-	31.1	-	32.8	1.05	DC/TFS
G1	530	1890	"	2.00	3.80	3.04	126.8	-	126.8	-	1.00	DC
"	"	595	"	"	"	"	136.6	-	136.6	-	1.00	DC
2	"	1880	"	"	3.40	3.74	144.6	-	151.6	-	1.05	SC
3	"	1890	265	2.00	3.34	2.00	-	84.5	-	136.0	1.61	SC
"	"	880	"	2.00	"	"	-	97.9	-	129.3	1.32	SC
"	"	0	"	"	"	2.33	122.3	-	122.3	-	1.00	DC
4	1060	830	"	4.00	3.35	3.55	-	-	75.	3	-	F
5	530	1890	"	2.00	2.94	3.73	-	108.4	-	108.4	1.00	DC
"	"	0	"	"	"	3.73	-	120.1	-	120.1	1.00	DC
6	795	1355	"	3.00	3.23	3.88	94.5	-	98.0	-	1.04	SC
"	530	0	"	2.00	"	"	-	111.2	-	-	-	
"	"	0	"	"	"	4.20	160.1	-	165.0	-	1.48	SC
7	400	2150	"	1.50	3.26	3.39	-	-	174.	1	-	BF
8	560	1790	"	2.00	3.39	3.83	-	-	147.	7	-	F

TABLE 5.1 (Cont'd)

Notes.

1. $f'_{ct} = \frac{f_{cu}}{28} + 1.45\ N/mm^2$ - Equation (4.2).

2. Mode of failure:

BF = bond failure (observed by the slipping of the tendons after the formation of the diagonal tension crack).

BFS = bottom flange separation.

DC = diagonal tension cracking.

F = flexure failure.

SC = shear compression.

SCO = shrinkage crack opened.

TFS = top flange separation.

WC = web crushing.

WD = web distortion.

/ = followed by.

$\frac{V_u}{V_c}$ = $\frac{\text{Ultimate failure load}}{\text{Diagonal cracking load}}$

TABLE 5.2

Experimental results under uniformly distributed load.

Beam mark	b_w mm	l mm	d mm	$\frac{l}{d}$	f'_{ct} N/mm^2	f_{cp} N/mm^2	q_{cl} KN		q_{ul} KN		$\frac{q_{ul}}{q_{cl}}$	Mode of failure
							East	West	East	West		
B12	50.0	2650	265	10.0	3.09	4.48	153.5	133.4	-	181.3	1.36	DC
13	"	2120	"	8.0	2.93	4.73	166.8	180.1	-	235.7	1.31	DC/WC
14	"	1930	"	7.28	3.13	6.07	200.2	220.2	-	314.9	1.43	DC/WD
15	"	1590	"	6.0	2.93	6.29	231.0	209.0	-	275.8	1.32	DC/TFS
C13	75.0	2650	265	10.0	3.13	3.79	199.0	-	267.0	-	1.34	DC/BF
14	"	2120	"	8.0	3.11	3.86	222.4	235.7	-	315.8	1.34	DC/TFS
15	"	1930	"	7.28	3.13	5.07	266.9	289.1	-	346.9	1.20	DC/WD
16	"	1590	"	6.0	2.93	5.39	275.0	275.0	-	360.3	1.31	DC/ TFS
20	"	2650	225	11.78	2.67	2.81	152.3	-	187.9	-	1.25	DC/WD
D10	50.0	2650	225	11.78	2.67	2.97	126.3	-	154.6	-	1.22	DC/WD
11a	58.0	4000	"	17.78	3.45	3.10	114.0	-	114.0	-	1.00	DC/WD
11b	"	"	"	"	3.41	3.07	100.1	115.6	146. 8		1.27	DC/TT
12	"	2650	"	11.78	3.64	3.40	160.0	129.0	222.4	-	1.39	DC/WD
13	"	3930	"	17.47	3.11	3.29	91.2	-	103.4	-	1.13	DC/WD
14	"	"	"	"	3.02	3.45	-	104.5	-	111.2	1.06	DC/WD
E 9	75.0	2650	265	10.0	2.91	4.14	213.5	-	271.1		1.27	DC
10	"	2120	"	8.0	2.95	4.32	240.2	246.7	346. 9		1.41	DC/TT
11	"	1590	"	6.0	3.10	4.99	311.4	311.4	378. 1		1.21	DC/TT
12	"	1930	"	7.28	3.00	4.47	298.0	275.8	299.8		1.01	DC/BF
F 6	50.0	2650	265	10.0	2.98	4.12	177.9	169.0	249.1	-	1.40	DC/WD
7	"	2120	"	8.0	2.91	4.42	213.5	213.5	-	258.0	1.21	DC/WD
8	"	1590	"	6.0	2.75	5.03	235.7	231.3	-	342.5	1.48	DC/ TFS
9	"	1930	"	7.28	3.01	4.57	200.1	204.6	-	235.7	1.15	DC/ TFS

Note.

Symbols for mode of failure are as shown on page 95

TT = test terminated.

5. 3. Prediction of Shear Failure Type:

The above analysis of the occurrence of shear failures and the photographs provided show that, within the range of variables covered in this investigation, the final mode of shear failure and hence the ultimate shear failure load could be affected by [4] (a) the location of the diagonal tension crack in the shear span, (b) the position of the upper end of the inclined crack with respect to the compression face, and (c) the quality of bond. The first two factors can be considered to be functions of the cross-sectional properties, the $a_{v/d}$ ratio, the prestressing force and the concrete strength. Bond, the failure of which is characterised by the longitudinal splitting of concrete along the tendons, is an indeterminate quantity because of the many factors affecting its quality.

Although all shear failures in I-sections originating from flexure cracks took place in the higher range of values of $a_{v/d}$, and all the shear failures initiated by the simple diagonal crack (web-shear crack) occurred in the lower range of values of $a_{v/d}$, the two categories overlapped in the middle of the range. Web-crushing following the formation of a diagonal crack was observed to be the predominant mode of failure for I-sections at lower ranges of $a_{v/d}$, i.e. $a_{v/d} = 1.25$, provided that there was a good bond between concrete and steel; but it was also

observed that the web-crushing also took place at the upper range of $a_{v/d}$ accompanied by 'arching' effect.

From the above discussion and the photographs shown in Figures 5.1.a to 5.1.l , it is clear that the value of $a_{v/d}$ at which the change from one type of shear failure to the other depends on several indeterminate factors in addition to the properties of the beam. Thus it is not possible to predict with any certainty what will follow the formation of a diagonal crack from a knowledge of only one variable, namely $a_{v/d}$.

5.4. Comparison between the Shear Crack Patterns observed under Uniform Loading and Point Loading:

The photographs (Figures 5.1.a. to 5.1.l) show that under point loading the diagonal tension crack generally forms in such a position that the upper end of the crack points towards the point of application of the load. The lower end of the diagonal crack extends in the direction of the support, and this extension may be in the form of a nearly straight line continuation of the diagonal tension crack as shown in Figures 5.1.a, 5.1.c, 5.1.d, 5.1.e and 5.1.g. In contrast, in some cases, the inclined crack continues down to the lower web-flange junction or to the level of the tendons and thence along the lower web-flange junction to the support, as shown in Figures 5.1.b, 5.1.f, 5.1.h, 5.1.i, 5.1.j and 5.1.k.

All the beams tested under uniform loading in this investigation showed similar shear crack patterns to those observed under point loading and the crack pattern seems therefore to be unaffected by the arrangement of loading. This similarity in behaviour and mode of failure implies that there should also exist some relationship between their shear cracking loads, and this will be discussed in section 6.1.3.

Under uniform loading it was observed that more than one diagonal tension crack may form in either half of the beam as shown for Beam B 14 in Figure

6.7.b; some of these cracks may develop from flexure cracks as shown for Beam D 14 in Figure 6.7.e. These two cases are similar to the cases of Beams A12 and A10 as shown in Figures 5.1.l and 5.1.f respectively. This crack pattern can also be seen in the photographs of Arthur et al[48].

The critical diagonal tension crack for all the I-beams tested under uniform loading in this investigation formed on a line through a reaction. In this respect they showed behaviour similar to that of the reinforced rectangular beams reported by Leonhardt and Walther[61] and to that of the prestressed I-beams tested by Arthur et al[48]. None of them showed the shear-compression mode of failure observed in Kar's[43] prestressed rectangular beams. Thus it may be concluded that as well as the span to effective depth ratio, the magnitude of prestress and the web breadth play an important role in determining the mode of failure under uniform loading.

Note: Readers are reminded of the footnote to page x where it is stated that when expressions containing the term $1000V_c$ are used in Chapters 6 to 8, these expressions will only be dimensionally correct when V_c is expressed in kN , f'_{ct} in N/mm^2, and other dimensions in mm.

CHAPTER 6

ANALYSIS OF TEST RESULTS

6.1. Prediction of the Diagonal Tension Cracking Load.

6.1.1. Diagonal tension cracking load and ultimate shear failure load.

Under some ranges of variables, the ultimate shear failure load, for a beam without shear reinforcement, was equal to the first diagonal tension cracking load, and the beam could either fail to sustain further increase in loading or collapse simultaneously with the formation of the diagonal tension crack. For a different range of variables it might exceed the cracking load by a substantial amount as shown in the second last column of Table 5.1. Since the magnitude of the ultimate shear failure load depends on the final mode of shear failure and the latter was shown in Section 5.1 to be a function of many indeterminate variables, it seems necessary to limit the useful capacity in shear of a beam without shear reinforcement to the first diagonal tension cracking load, and this will be defined as the shear force at which the diagonal tension crack will start to affect the behaviour of the beam (36).

6.1.2. Prediction of the first diagonal tension cracking load under one- or two-point loading.

As mentioned in Section 4.1, the experimental programme was planned to bring out the effect of each of the dimensionless variables shown in equation 3.5 re-written below:

$$\frac{V_c}{b_w d\ f'_{ct}} = F_2\left(\frac{f_{cp}}{f'_{ct}}\ ,\ \frac{b}{b_w}\ ,\ \frac{h_f}{d},\ \frac{a_v}{d}\right) \qquad (3.5)$$

where V_c corresponds to the shear force at the formation of a diagonal tension crack which develops when the diagonal-tension stress (principal tensile stress) exceeds the tensile strength of the concrete. The effect of the stresses normal to the longitudinal axis, which are usually ignored by present codes of practice[30,32], is taken care of by the variable $({}^{a}v/d)$. Thus equation 3.5 is basically a principal tension criterion.

Figure 6.1 shows the relationship between $1000\ V_c/(b_w d\ f'_{ct})$ and f_{cp}/f'_{ct} for four cross-sections and one value of ${}^{a}v/d$ for each. Despite the scatter in the test results which may be due to the random occurrence of voids and flaws resulting from imperfect compaction, a linear relationship could be assumed to exist in which the ordinate increases as f_{cp}/f'_{ct} increases. This could be formulated as:

$$\frac{1000\ V_c}{f'_{ct}\, b_w d} = A + B\,\frac{f_{cp}}{f'_{ct}} \qquad (6.1)$$

where the values of A and B for a given cross-section depend on the value of ${}^{a}v/d$. Values of A and B depend also upon the way in which the tensile strength of concrete is evaluated, as the latter can be determined in a variety of ways. The ratio A/B was taken as unity by Sozen et al[36], Evans and Schumacher[40] and Arthur[44], when the tensile strength of concrete was taken to be approximately equal to f'_{ct}. So, by taking A/B as unity, equation 6.1 could be modified

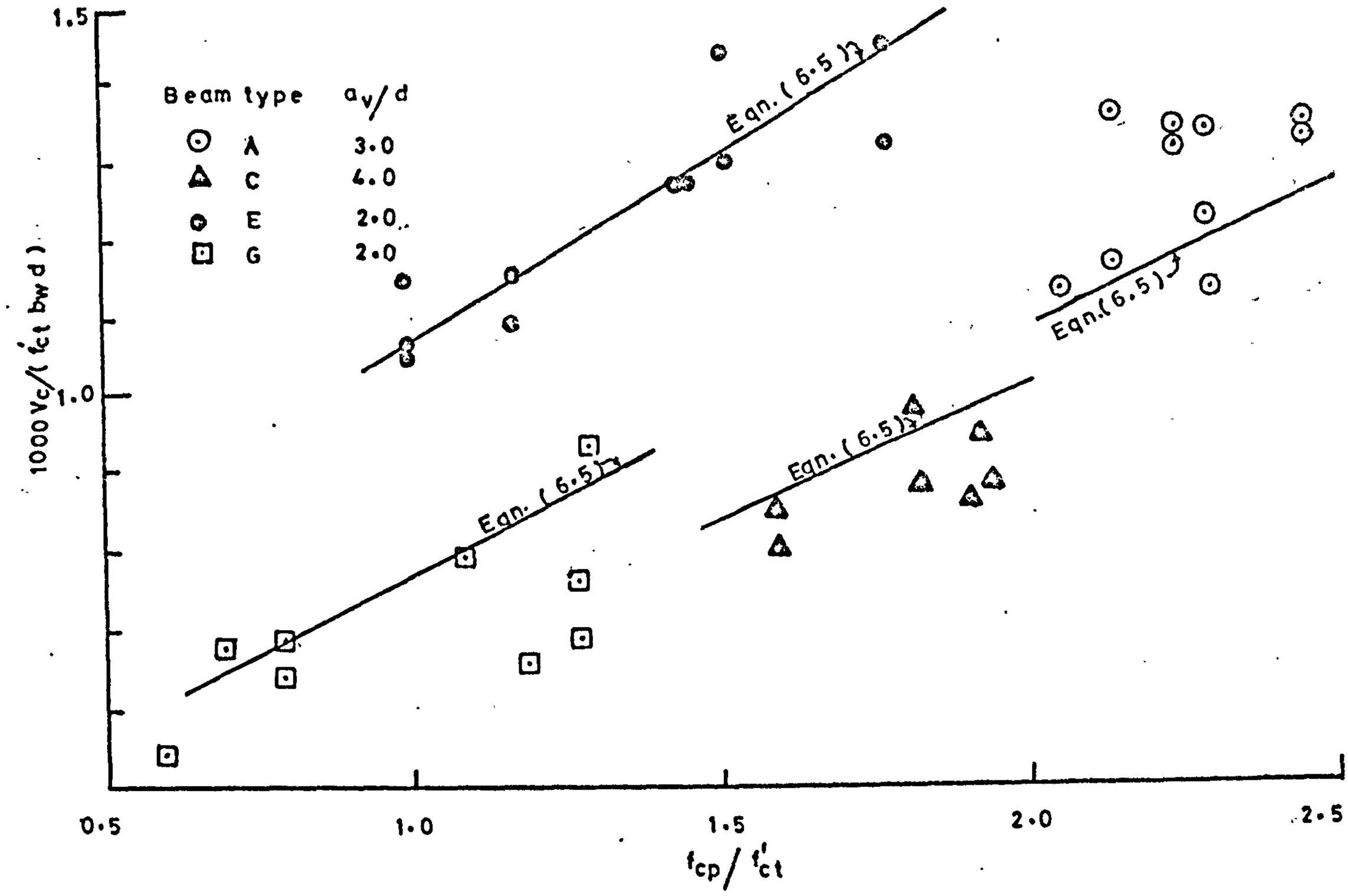

Figure 6.1: Effect of f_{cp}/f'_{ct} upon V_c

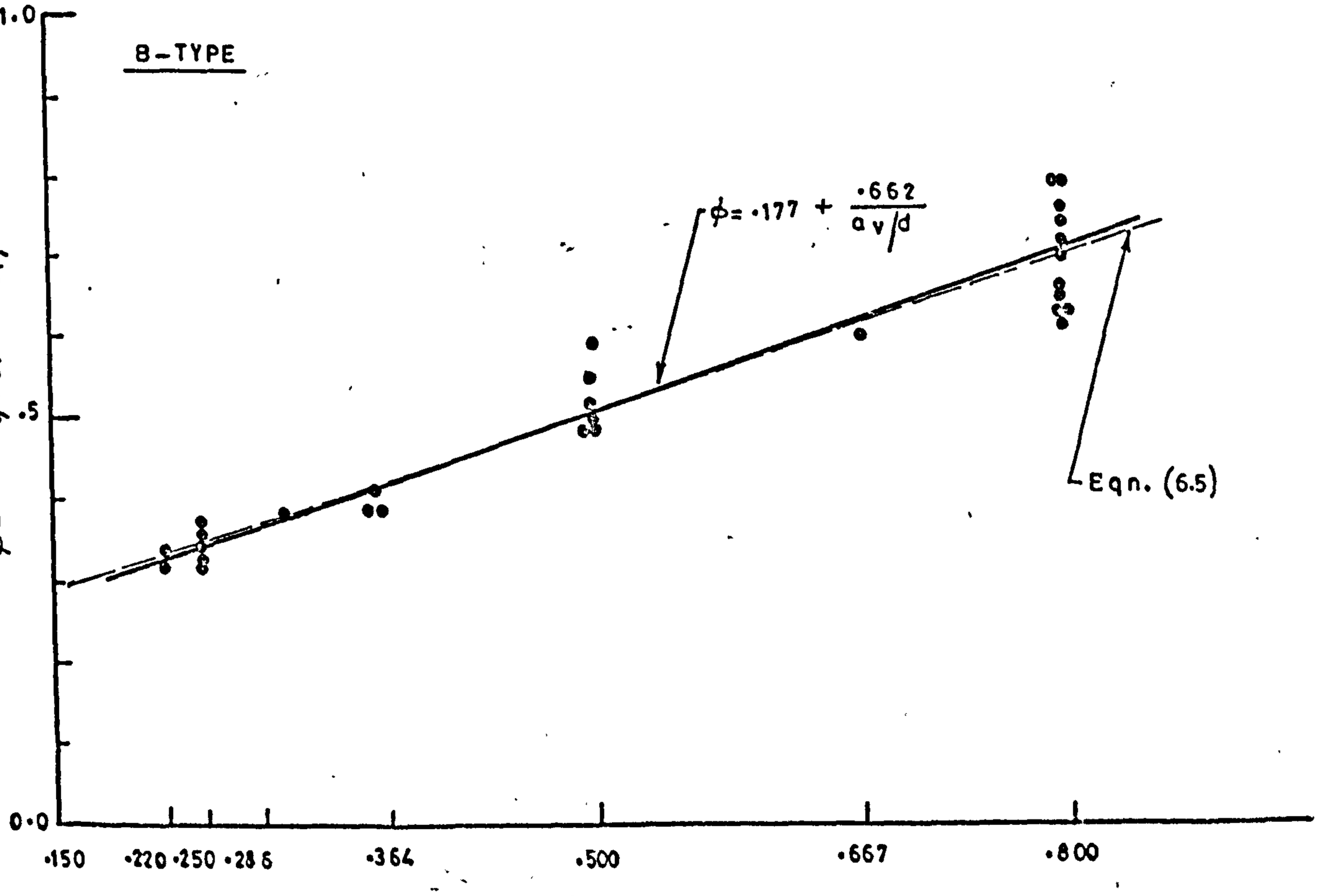

Figure 6.2: Effect of $a_{v/d}$ upon V_c
(Results for type B beams)

to have the following form:

$$\frac{1000\ V_c}{f'_{ct}\left(1 + \frac{f_{cp}}{f'_{ct}}\right)} = F_3\left(\frac{a_v}{d}, \frac{h_f}{d}, \frac{b}{b_w}\right) = \emptyset \qquad (6.2)$$

where F_3 is a functional notation.

The test data obtained from type B beam over a wide range of $^{a}v/d$ ratios were plotted in Figure 6.2. These test data demonstrate that cracking shear force, V_c, is inversely proportional to $^{a}v/d$ ratio.

Figure 6.3 shows a linear relationship between $\emptyset$ and $^{h}f/d$ for a given value of $^{a}v/d$. For a given value of $^{h}f/d$, the value of $\emptyset$ increases as b/b_w increases. This leads to the assumption that the flange projections contribute to the value of $\emptyset$. They may be related in the following form:

$$\emptyset = C + D\left(\frac{b}{b_w} - 1\right)\frac{h_f}{d} \qquad (6.3)$$

in which the second term on the R.H.S. is proportional to the area of flange projections. Both C and D depend on $^{a}v/d$. Figure 6.4 shows this linear relationship between $\emptyset$ and $\left(\frac{b}{b_w} - 1\right)\frac{h_f}{d}$ for a given value of $^{a}v/d$.

Therefore the final semi-empirical expression for the diagonal cracking load can be written as:

$$\frac{1000\ V_c}{b_w d\ f'_{ct}} = \left(1 + \frac{f_{cp}}{f'_{ct}}\right)\left(B' + \frac{C'}{a_{v/d}}\right)\left(D' + \left(\frac{b}{b_w} - 1\right)\frac{h_f}{d}\right) \qquad (6.4)$$

the ratio C/D being taken constant for simplicity.

Using a least-squares method based on the data plotted in Figure 6.4 the value of D' was found to be 1.50. Similarly B' and C' were found to be 0.10 and

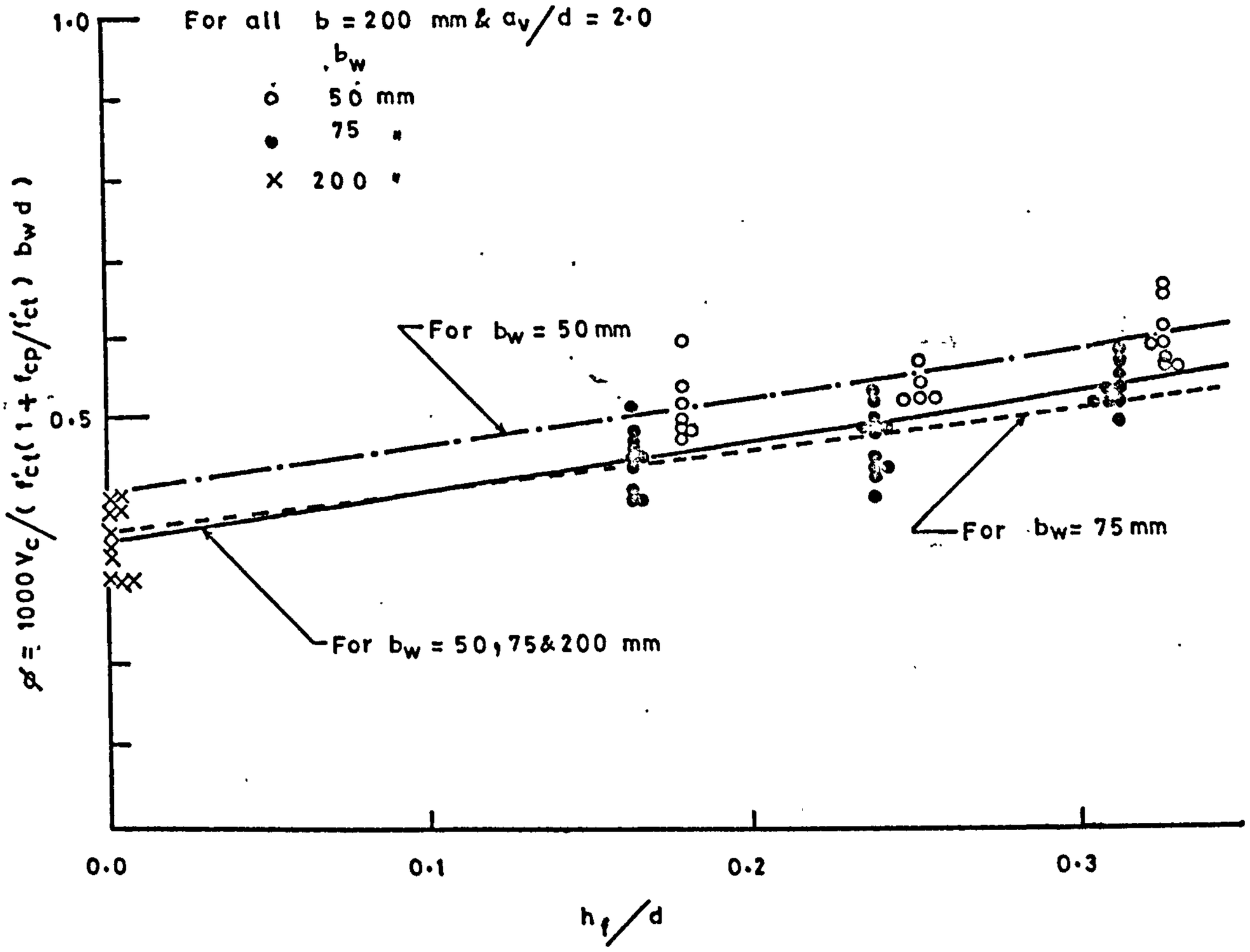

Figure 6.3: Effect of $h_{f/d}$ on V_c

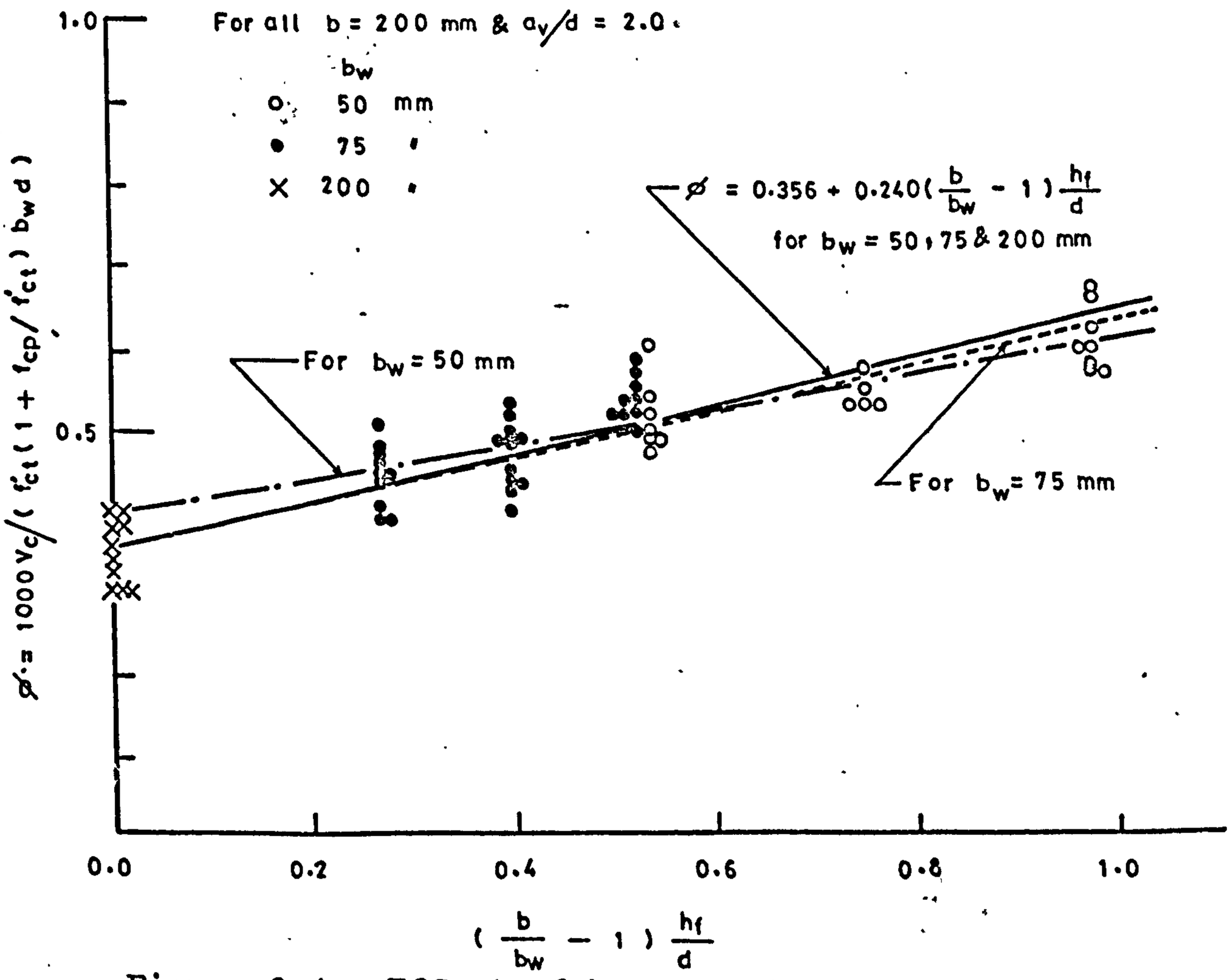

Figure 6.4: Effect of $h_{f/d}$ and $b_{/b_w}$ on V_c

0.31 respectively from the data plotted in Figure 6.5. Accordingly equation 6.4 may be written as:

$$\frac{1000\ V_c}{f'_{ct}\left(1 + \frac{f_{cp}}{f'_{ct}}\right) b_w d\left[1.5 + \left(\frac{b}{b_w} - 1\right)\frac{h_f}{d}\right]} = 0.10 + \frac{0.31}{a_{v/d}} = \psi \qquad (6.5)$$

The ratios of the experimental values of V_c to the values predicted by equation 6.5 to all the test results obtained in this investigation under one - or two-point loading gave a mean value of 0.98 with standard deviation of 0.09.

Figure 6.5 shows that the curve tends to be horizontal at higher values of $a_{v/d}$, i.e. the rate of decrease of ψ tends to be zero at higher values of $a_{v/d}$. This shows that, for the specimens whose failure in shear was not initiated by flexural cracks, the effect of stress normal to the longitudinal axis due to the load and the reactions is either becoming constant or diminishing at higher values of $a_{v/d}$. This is illustrated by Figure 6.6 which shows the variation of the stress normal to the longitudinal axis, fyy, just prior to the formation of the diagonal tension crack with $a_{v/d}$ ratio at different levels of f_{cp}/f'_{ct} for type B beam assumed to be in the centroidal axis in the vicinity of the mid shear span. These relationships were derived from the principal tension equation. If the principal tensile stress, f_t, is taken as positive, elastic theory gives

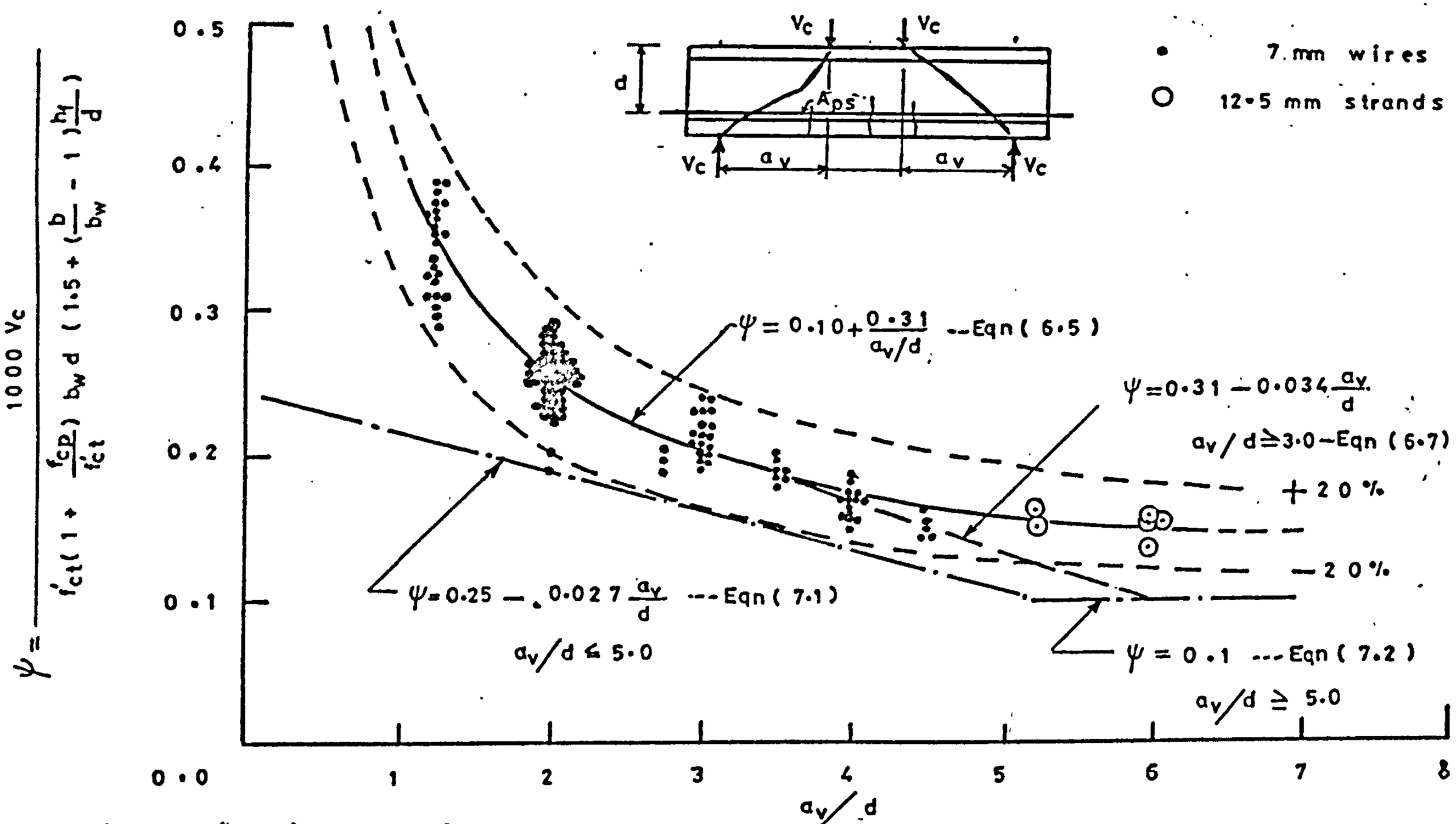

Figure (6.5): Experimental results: Diagonal cracking load and beam properties in terms of $a_{v/d}$ ratio.

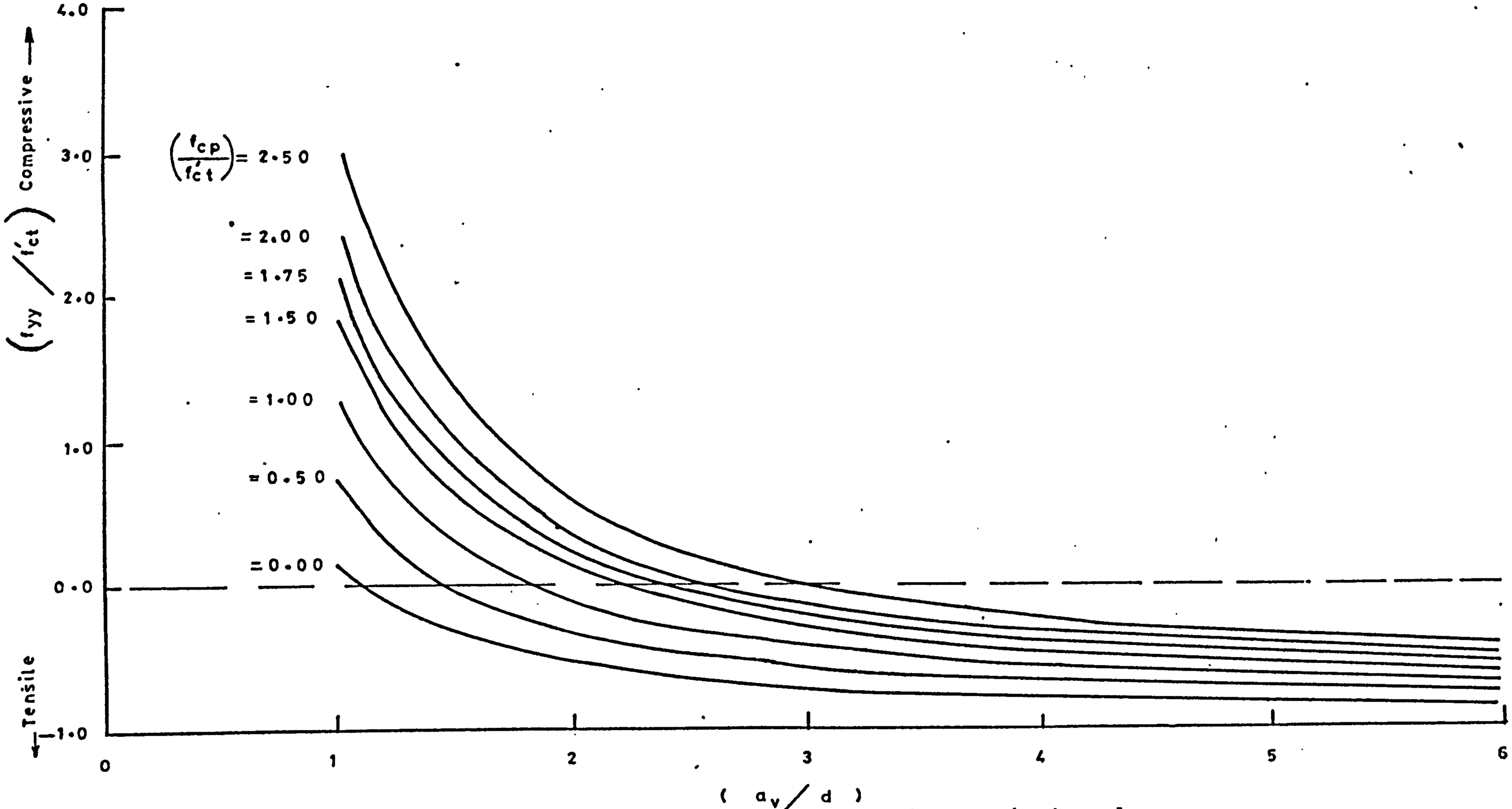

Figure (6.6). Variation of stress normal to the longitudinal axis based on equation (6.5) and type B beam.

$$f_t = -\frac{f'_{cp} + f_{yy}}{2} + \sqrt{\frac{(f_{cp} - f_{yy})^2}{4} + v^2_{xy\ max}} \qquad (6.6')$$

where $v_{xymax} = \frac{V_c \quad Q}{I \quad b_w}$

Putting $f_t = f'_{ct}$ and rearranging, equation 6.6′ can be written as:

$$\frac{f_{yy}}{f'_{ct}} = \frac{v^2_{xy\ max}}{f^2_{ct}\left(1 + f_{cp}/f'_{ct}\right)} - 1 \qquad (6.6)$$

where $v_{xy\ max}$ is the maximum shear stress just prior to the diagonal cracking and is determined from the value of V_c given by equation 6.5 . Thus Figure 6.6 shows that equation 6.5 predicts, for a given value of f_{cp}/f'_{ct}, nearly constant values for f_{yy} at values of $a_v/d \geq 3.0$. Figure 6.6 also shows that the use of the principal tension equation taking f_{yy} as zero may lead to an overestimate of the value of V_c at higher values of a_v/d especially with low levels of f_{cp}/f'_{ct}. This is indicated by the fact that Figure 6.6 gives tensile values for f_{yy} at higher values of a_v/d and low values of f_{cp}/f'_{ct}.

Under certain sets of material and cross-section variables, some specimens at high a_v/d ratios exhibit shear failures initiated by flexural cracks, as illustrated in Figures 5.1.b and 5.1.h to 5.1.j. In such cases, any reduction in the diagonal cracking load with increase in a_v/d may be attributed to the influence of the flexural cracks, as they reduce the stiffness of the specimen. The load-deflection curves for such specimens confirm this, as they show

a definite reduction in slope, indicating a reduction in stiffness beyond a point corresponding to the occurrence of flexural cracks. This is shown for Beam B9 in Figure 5.2 and for Beam C10 in Figure 5.3. This was taken into account by BSCP 110: 1972[30] and by ACI (318-71)[32]. Both of these codes give two expressions for calculating V_c, one for sections uncracked in flexure and the other for those cracked in flexure. However, despite the general indication that shear-compression is likely to occur with $^{a}v/d > 3.0$ the strand-stressed I - beams with f_{cp} ranging between 2.45 and 2.81 N/mm^2 tested at $^{a}v/d$ of 5.25 and 6.0 all failed by diagonal tension cracking, the experimental value of the diagonal cracking shear force being accurately predicted by equation 6.5 as shown in Figure 6.5 by circles. But as a design expression should be the logical outcome of research of this nature, a general solution for diagonal cracking taking into account tne effect of flexure cracks is felt to be desirable. For design purposes this could be done empirically by assuming the rate of decrease of ψ with increase in $^{a}v/d$ to be constant and equal to the rate of decrease at $^{a}v/d = 3.0$ for all values of $^{a}v/d > 3.0$. This is justified because for all beams tested at $^{a}v/d = 3.0$, the ultimate shear failure load resulting from a sudden major diagonal-tension crack was sensibly the same as that at the formation of the inclined tension

crack (usually flexure-shear crack), as shown in the second last column in Table 5.1 . A tangent to the curve in Figure 6.5 at $^{a}v/d = 3.0$ gives the following expression

$$\psi = \frac{1000\ V_c}{f'_{ct}\left(1 + \frac{f_{cp}}{f'_{ct}}\right) b_w\ d\left[1.5 + \left(\frac{b}{b_w} - 1\right)\frac{h_f}{d}\right]} = 0.31 - 0.034\ \frac{a_v}{d}$$

$$\text{for } \frac{a_v}{d} > 3.0 \qquad (6.7)$$

Equation 6.7 is shown in Figure 6.5 and its limitations will be discussed later on when it will be compared with other published experimental results.

6.1.3. Prediction of first diagonal tension cracking load in a uniformly loaded beam.

6.1.3.1. General:

This project was extended to cover the uniformly distributed load case, as this constitutes a practical type of loading, in order to discover whether the results already obtained in the case of one - or two-point loads could be applied in the case of the uniformly distributed load.

In this investigation all the uniformly loaded beams cracked on a line through a reaction as shown in Figures 6.7.a to 6.7.e and the distance from the support to the point of intersection of this inclined tension crack with the centroidal axis was found to bear some relation to $^{l}/_{d}$ ratio, as shown in Figure 6.8. Figure 6.9 shows the relationship between the distance from the support to the failure section in the compression face as reported by Kar[42,43], Hanson

Figure 6.7: Shear Crack Patterns under Uniform Loading (formation of a diagonal tension crack on a line through a reaction in a uniformly loaded prestressed I-beam)

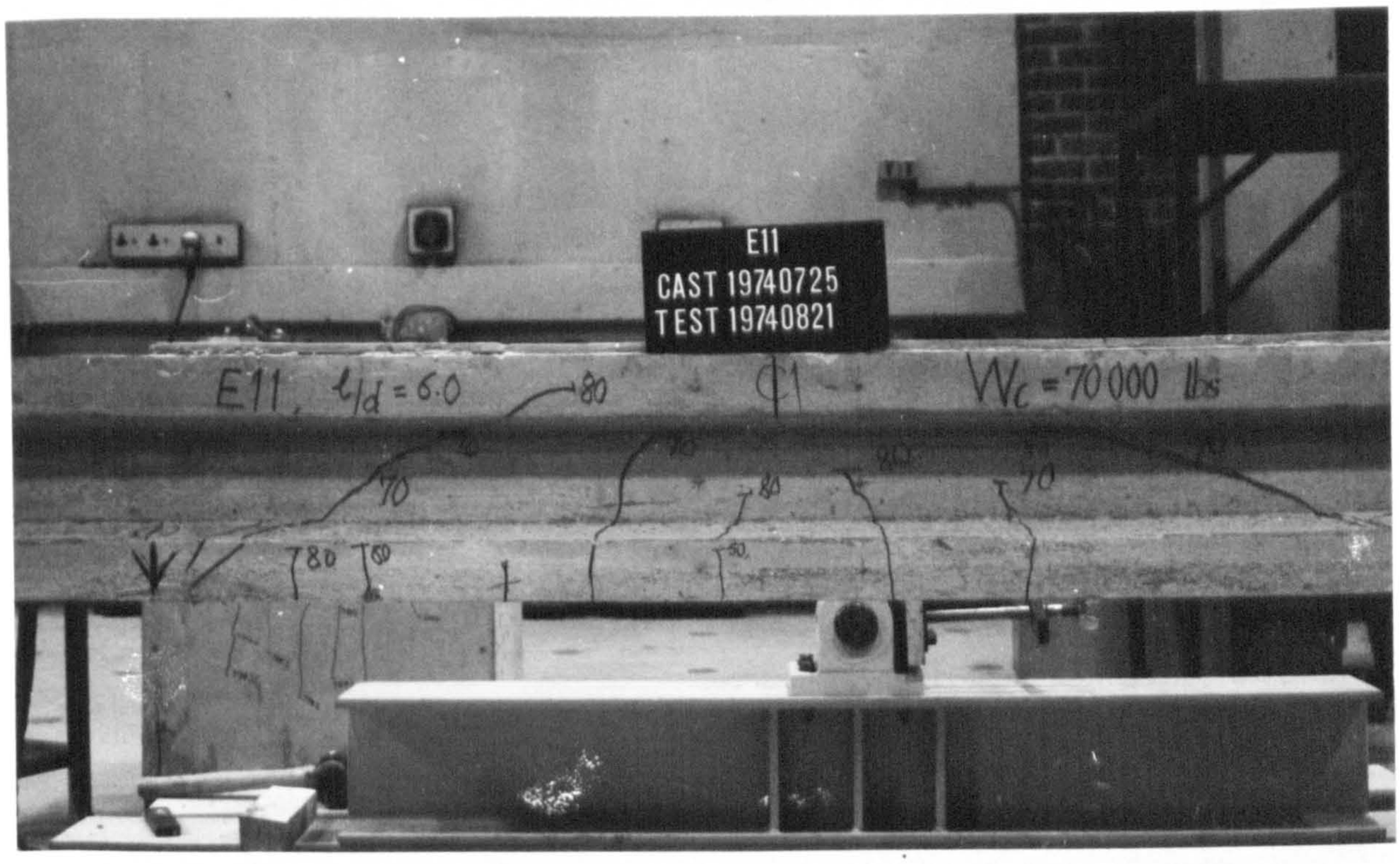

Figure 6.7.a: Beam E11, $l/d = 6.0$

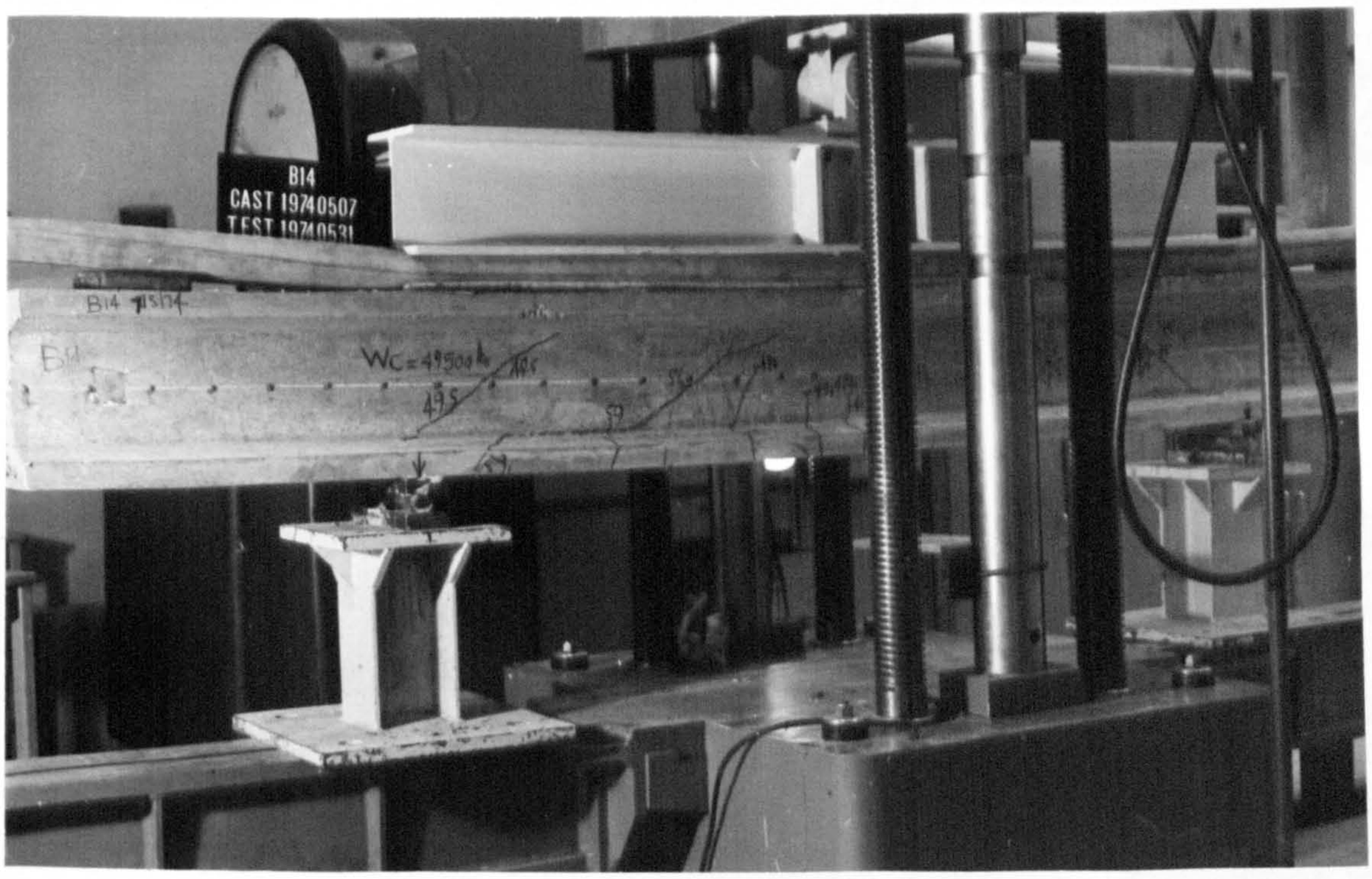

Figure 6.7.b: Beam B14, $l/d = 7.28$

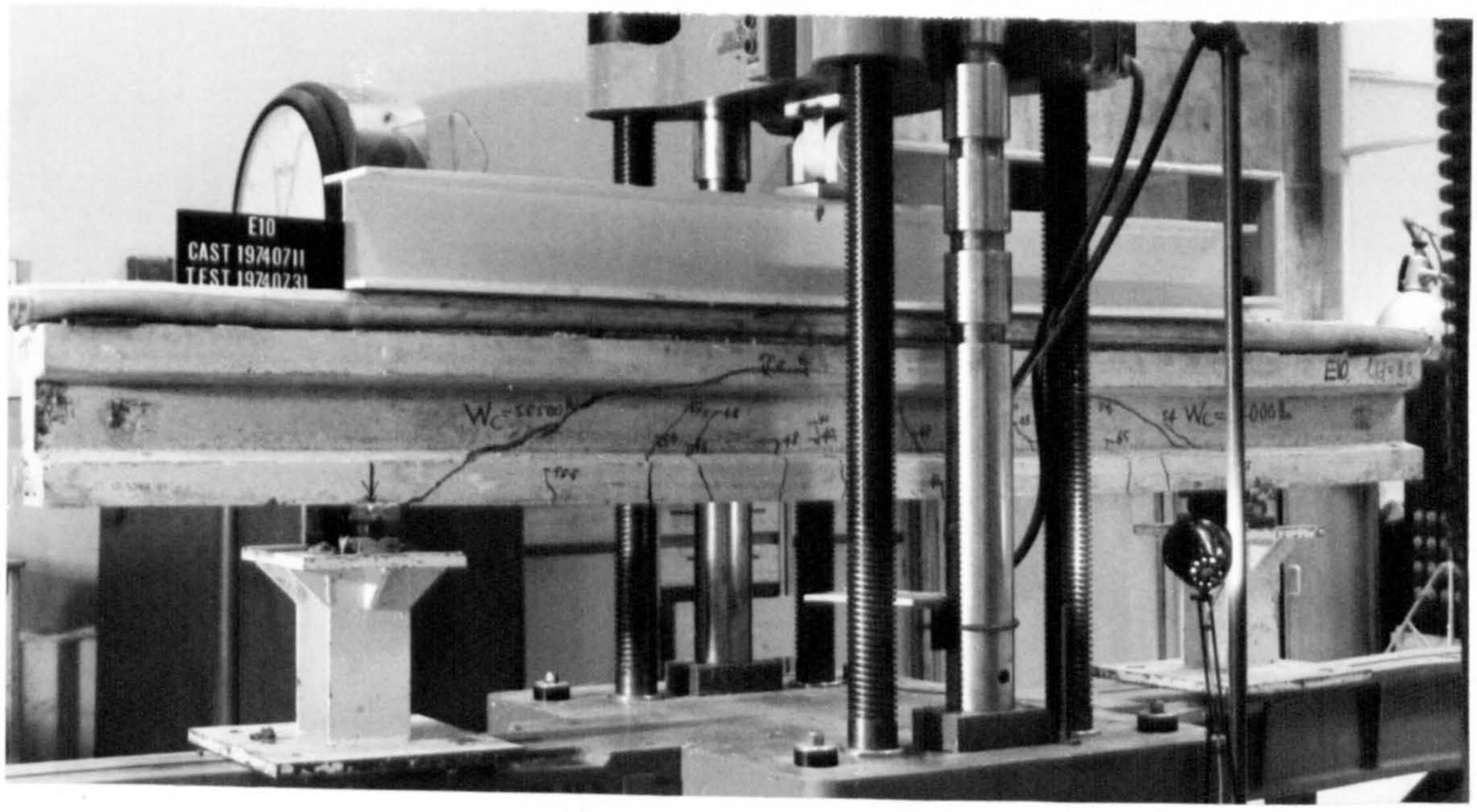

Figure 6.7.c: Beam E10, ℓ/d = 8.0

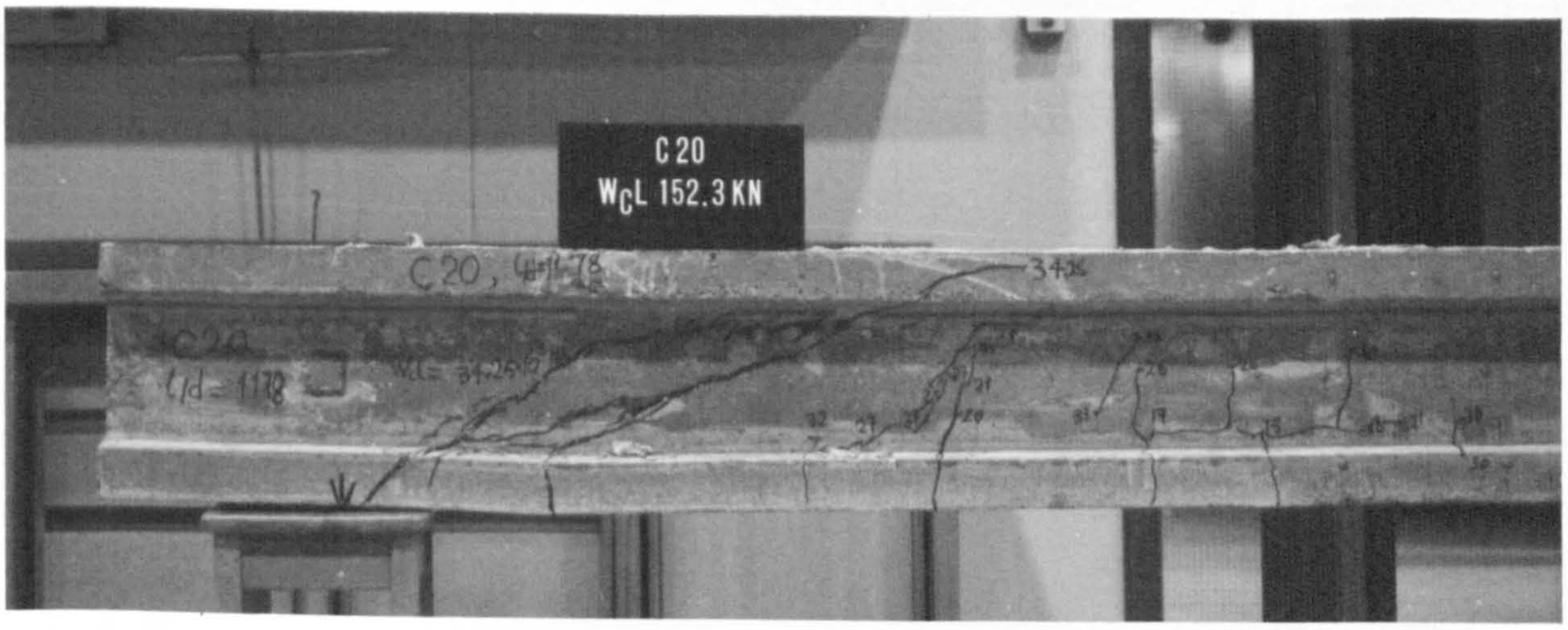

Figure 6.7.d: Beam C20, ℓ/d = 11.78

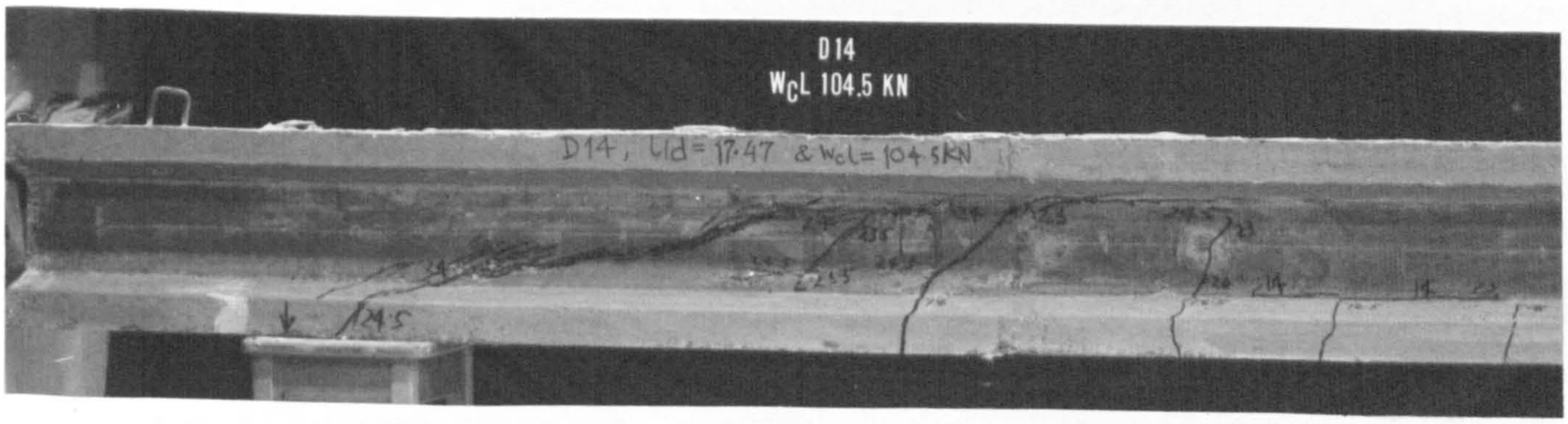

Figure 6.7.e: Beam D14, ℓ/d = 17.47

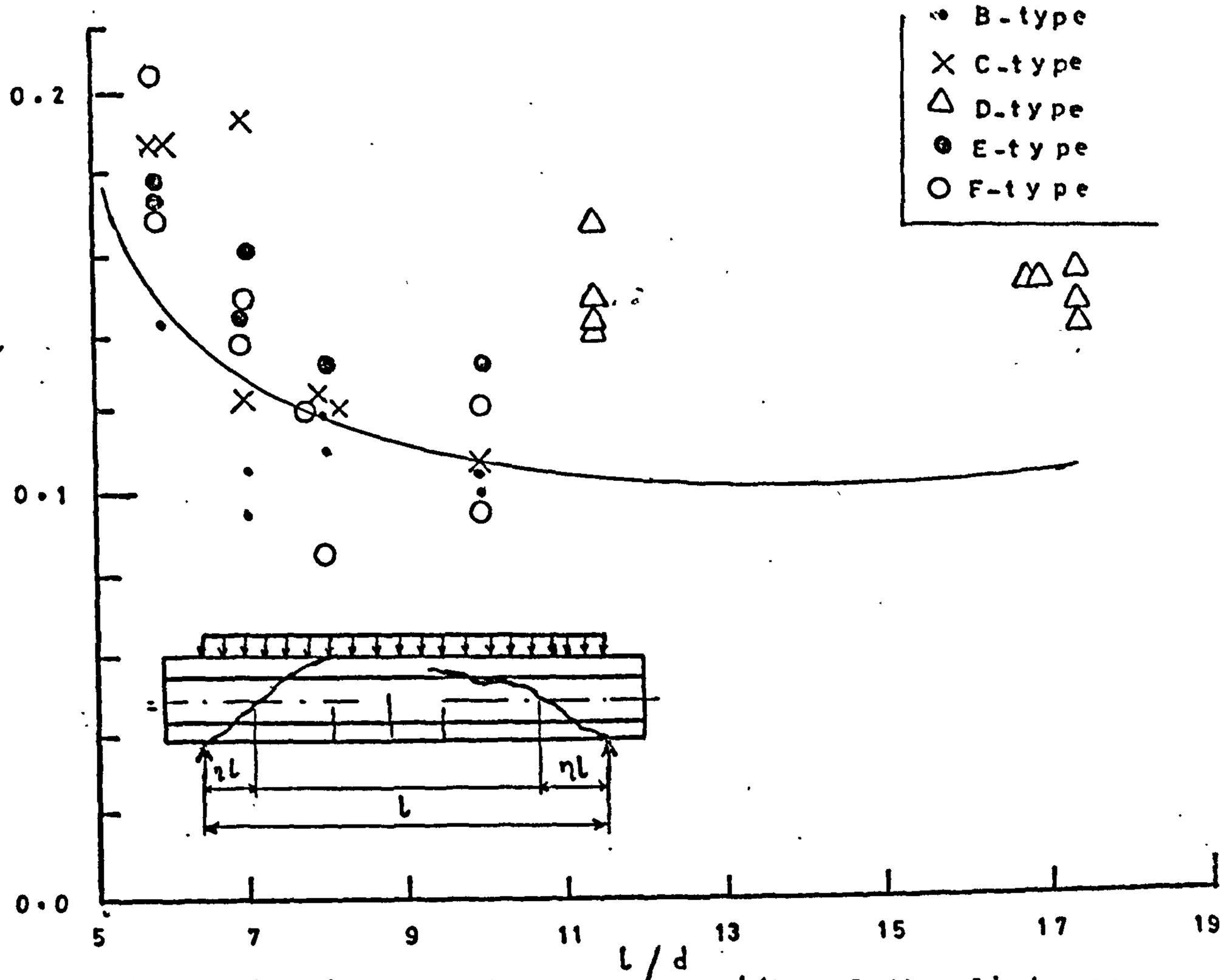

Figure (6.8): Relation between l/d and the distance from the support to the intersection of the diagonal crack with the centroidal axis.

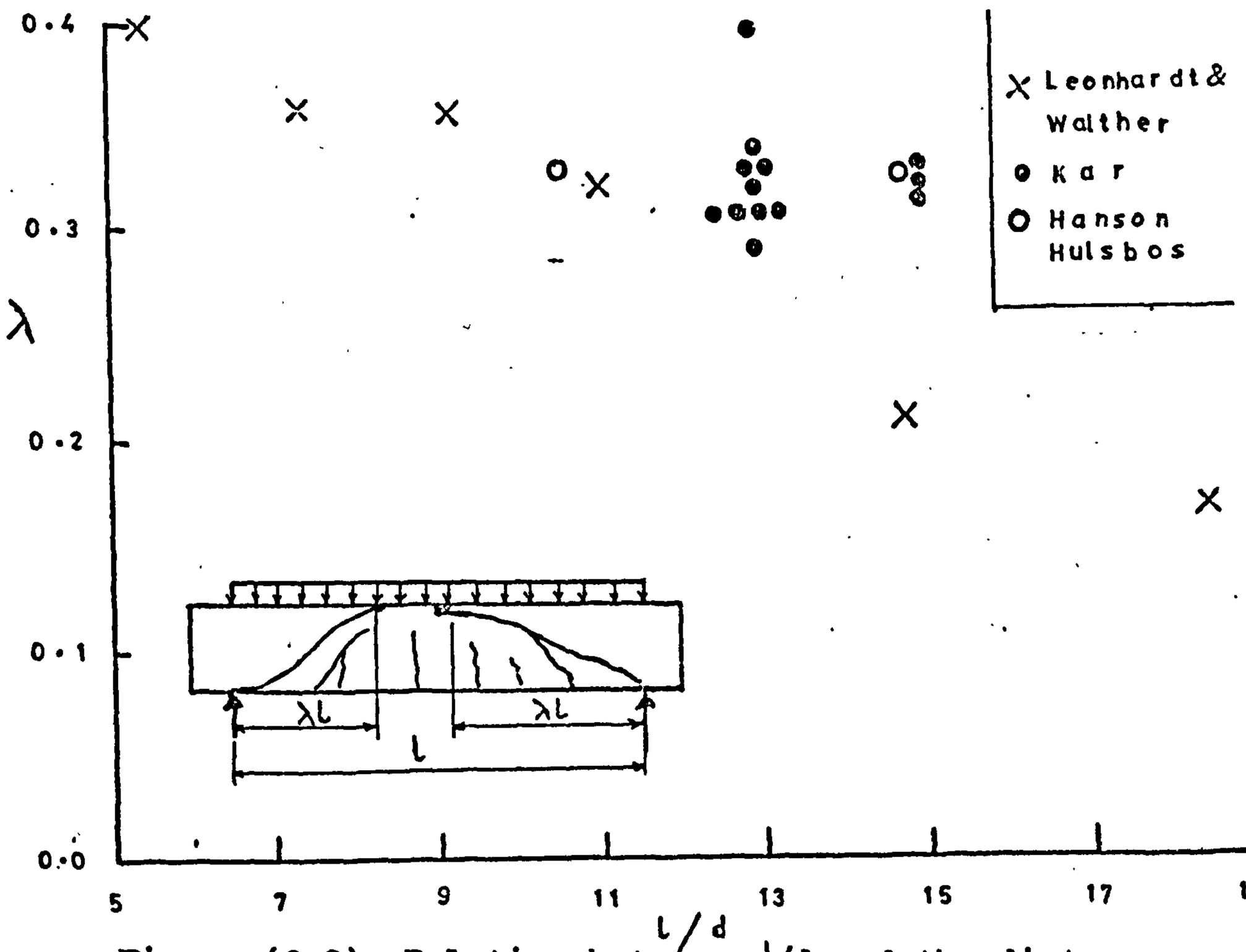

Figure (6.9): Relation between l/d and the distance from the support to the failure section in the compression face.

and Hulsbos[47] and Leonhardt and Walther[61]. Leonhardt and Walther's results were obtained from ordinary reinforced concrete beams which cracked on a line through the reaction, but Hanson and Hulsbos' results and Kar's were for failures caused by flexure-shear crack. The latter had an average value of $0.33l$ from the nearest support.

From Figures 6.8 and 6.9, it may be concluded that, for beams that crack through a reaction, the position of the critical section is a function of l/d, while for those in which failure is initiated by a flexure-shear crack the failure sections in the compression face will occur at a distance of about $0.33l$ from a support.

6.1.3.2. <u>Prediction of the diagonal cracking load, $q_c l$, under uniformly distributed load from the one - or two-point loading results.</u>

By using the moment-shear ratio term $\left(\frac{M}{V}\right)_c$ instead of a_v in equation 6.5, then the latter will become:

$$V_c = K\left(0.10 + \frac{0.31}{(M/Vd)_c}\right) \qquad (6.8)$$

where $K = f'_{ct}\left(1 + \frac{f_{cp}}{f'_{ct}}\right)\frac{b_w\, d}{1000}\left[1.5 + \left(\frac{b}{b_w} - 1\right)\frac{h_f}{d}\right]$

V_c is assumed to be the shear force at the critical section, i.e. at a distance $\lambda_c l$ from the nearest support of a simply supported beam with a uniformly distributed load. If q_c is the load per unit length at cracking, then

$$V_c = \frac{q_c l}{2}\left(1 - 2\lambda_c\right) \qquad (6.9)$$

$$M_c = \frac{q_c \lambda_c l^2}{2} \left(1 - \lambda_c\right) \qquad (6.10)$$

$$\text{and} \left(\frac{M}{V_d}\right)_c = \frac{\lambda_c l}{d} \left(\frac{1 - \lambda_c}{1 - 2\lambda_c}\right) \qquad (6.11)$$

By substituting equations 6.9 and 6.11 into equation 6.8, we will have:

$$\frac{q_c l}{2}\left(1 - 2\lambda_c\right) = K\left(0.10 + \frac{0.31\ (1 - 2\lambda_c)}{l/d\ \lambda_c(1 - \lambda_c)}\right)$$

or

$$q_c l = 2K\left(\frac{0.10}{1 - 2\lambda_c} + \frac{0.31}{l/d\ \lambda_c(1 - \lambda_c)}\right) \qquad (6.12)$$

Then the section of least shear resistance according to equation 6.5 will be obtained by differentiating equation 6.12 with respect to λ_c and equating to zero, so we get:

$$\frac{dq_c l}{d\lambda_c} = 2k\left(\frac{2 \times 0.1}{(1 - 2\lambda_c)^2} - \frac{0.31\ (1 - 2\lambda_c)}{l/d\ \lambda_c^2(1 - \lambda_c)^2}\right) = 0$$

or

$$0.2\ l/d\ \lambda_c^2\left(1 - \lambda_c\right)^2 = 0.31\ \left(1 - 2\ \lambda_c\right)^3$$

After rearranging we get:

$$\lambda_c^4 + \left(\frac{12.40}{l/d} - 2\right)\lambda_c^3 + \left(1 - \frac{18.60}{l/d}\right)\lambda_c^2 +$$

$$\frac{9.30\lambda_c}{l/d} - \frac{1.55}{l/d} = 0 \qquad (6.13)$$

The solution of the above equation will give the value of λ_c which will result in a minimum value for $q_c l$ in equation 6.12. The solution of equation 6.13 is obtained using the Newton-Raphson iterative formula.(89) The values of λ_c for different values for

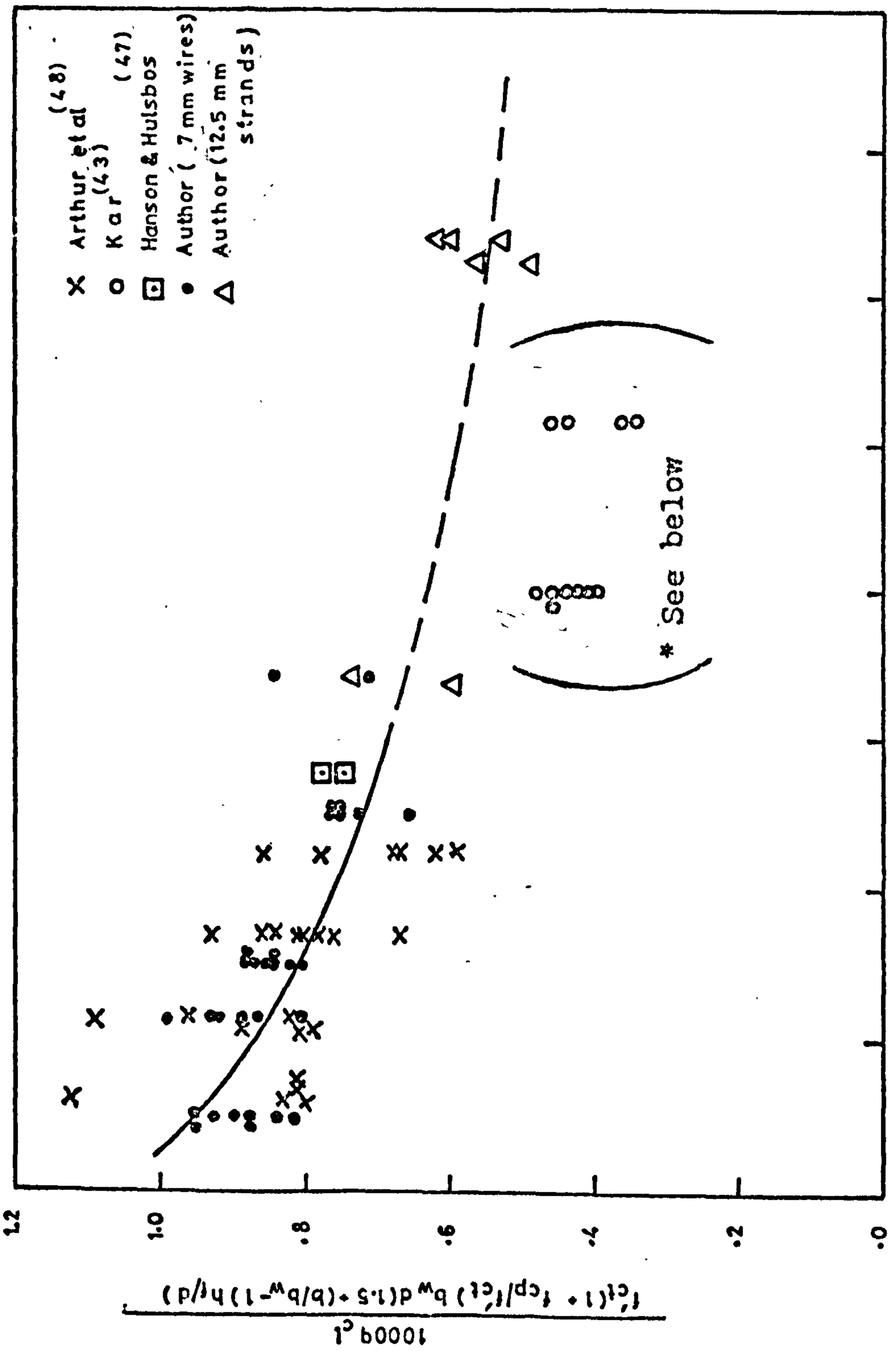

Figure (6.10) Experimental results. Diagonal cracking load, $q_c l$, and beam properties in terms of l/d.

* Kar's beams failed in shear-compression. See Table (7.4).

l/d ratios are shown in Table 6.1 below:

Table 6.1

l/d	λ_c	$\left(\frac{M}{Vd}\right)_c$		$\frac{q_c l}{K}$
6.00	.244	.360	l/d	.9508
6.18	.243	.358	l/d	.9345
7.28	.233	.334	l/d	.8511
8.00	.228	.323	l/d	.8080
8.42	.224	.316	l/d	.7859
9.00	.221	.308	l/d	.7590
9.52	.218	.301	l/d	.7366
10.00	.216	.298	l/d	.7182
13.00	.200	.267	l/d	.6310
15.00	.192	.252	l/d	.5911
20.00	.175	.222	l/d	.5224

The last column of Table 6.1, $\frac{q_c l}{K}$, is plotted in Figure 6.10 together with the present experimental results and those reported by other investigators (42,43,47,48).

6.1.3.3. Development of an expression for predicting $q_c l$ using the experimental results of the uniformly loaded beams.

An alternative approach to the attempt above, to adjust the results for point loaded beams to suit the uniformly loaded case, is to attempt to develop an expression for the uniformly loaded case entirely independently.

Starting with an equation similar to equation 6.2 one can write:

$$\frac{1000\, q_c l}{f'_{ct}\left(1 + \frac{f_{cp}}{f'_{ct}}\right) b_w\, d} = F_4\left(\frac{b}{b_w}, \frac{h_f}{d}, \frac{l}{d}\right) \qquad (6.14)$$

where F_4 is a functional notation. Equation 6.14 can be rewritten as follows:

$$\frac{1000\, q_c l}{f'_{ct}\left(1 + \frac{f_{cp}}{f'_{ct}}\right) b_w\, d} = A\left(\frac{b}{b_w} - 1\right)\frac{h_f}{d} + B \qquad (6.15)$$

where the term $A\left(\frac{b}{b_w} - 1\right)\frac{h_f}{d}$ reflects the effect of the flanges of an I - section on the value of $q_c l$. 'A' can either be a constant or a function of l/d and B is a function of l/d.

Figure 6.11 shows the relationship between

$\frac{1000\, q_c l}{f'_{ct}\left(1 + \frac{f_{cp}}{f'_{ct}}\right) b_w\, d}$ and $\left(\frac{b}{b_w} - 1\right)\frac{h_f}{d}$ for different values of l/d. The straight lines indicate that different values for A and B apply for the different l/d ratios.

Figure 6.12 shows the plot of A and B derived from Figure 6.11 in terms of l/d. Because of the scatter of A - values with l/d, no general trend for A with respect to l/d can be formulated. Thus an average value of 0.75 for A - values was chosen. The value of B can be represented by the equation:

$$B = \frac{6.74}{l/d} + 0.36 \qquad (6.16)$$

Thus equation 6.15 will become:

$$\frac{1000\, q_c l}{f'_{ct}\left(1 + \frac{f_{cp}}{f'_{ct}}\right) b_w\, d} = 0.36 + 0.75\left(\frac{b}{b_w} - 1\right)\frac{h_f}{d} + \frac{6.74}{l/d} \qquad (6.17)$$

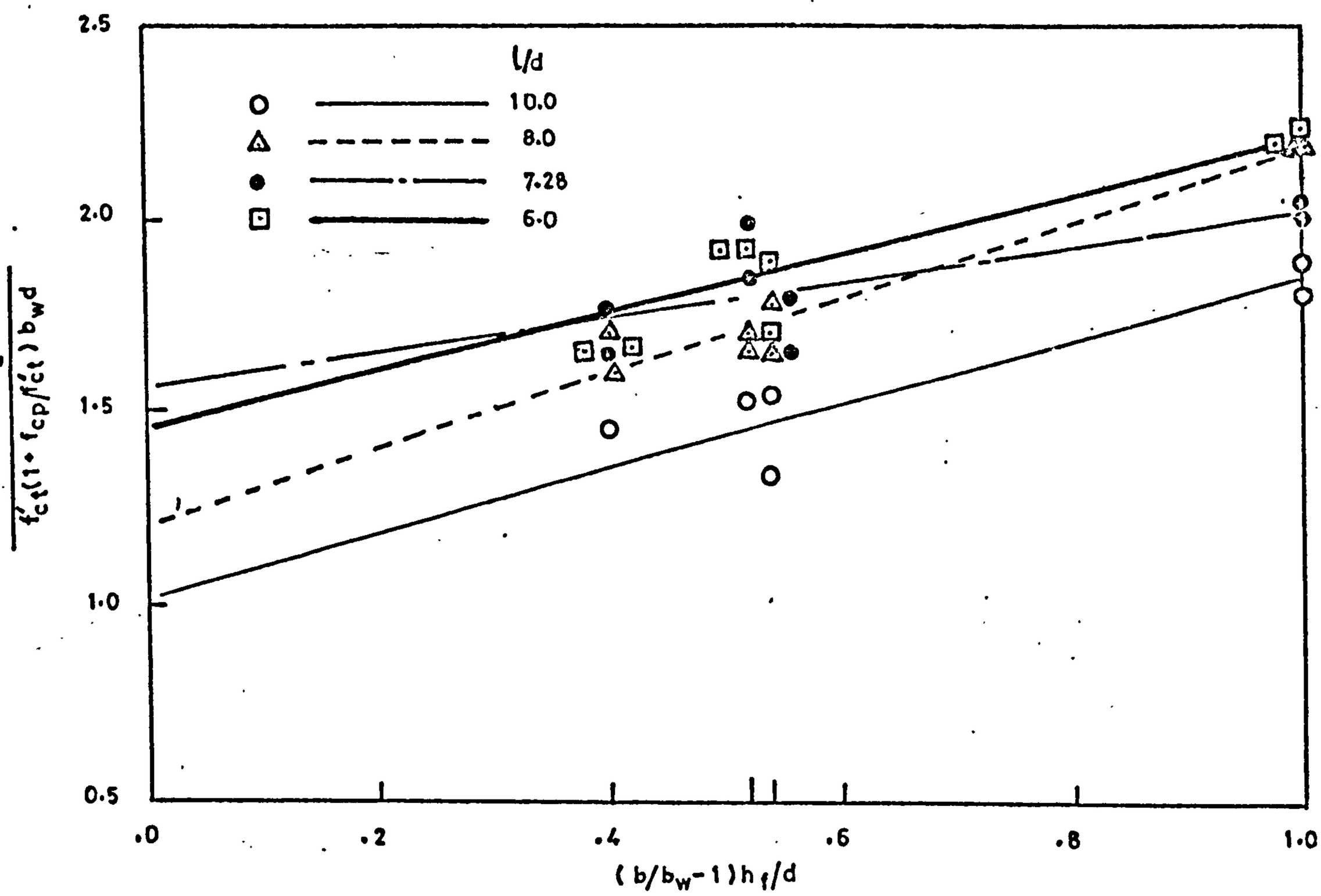

Figure 6.11: Effect of beam properties on diagonal cracking load.

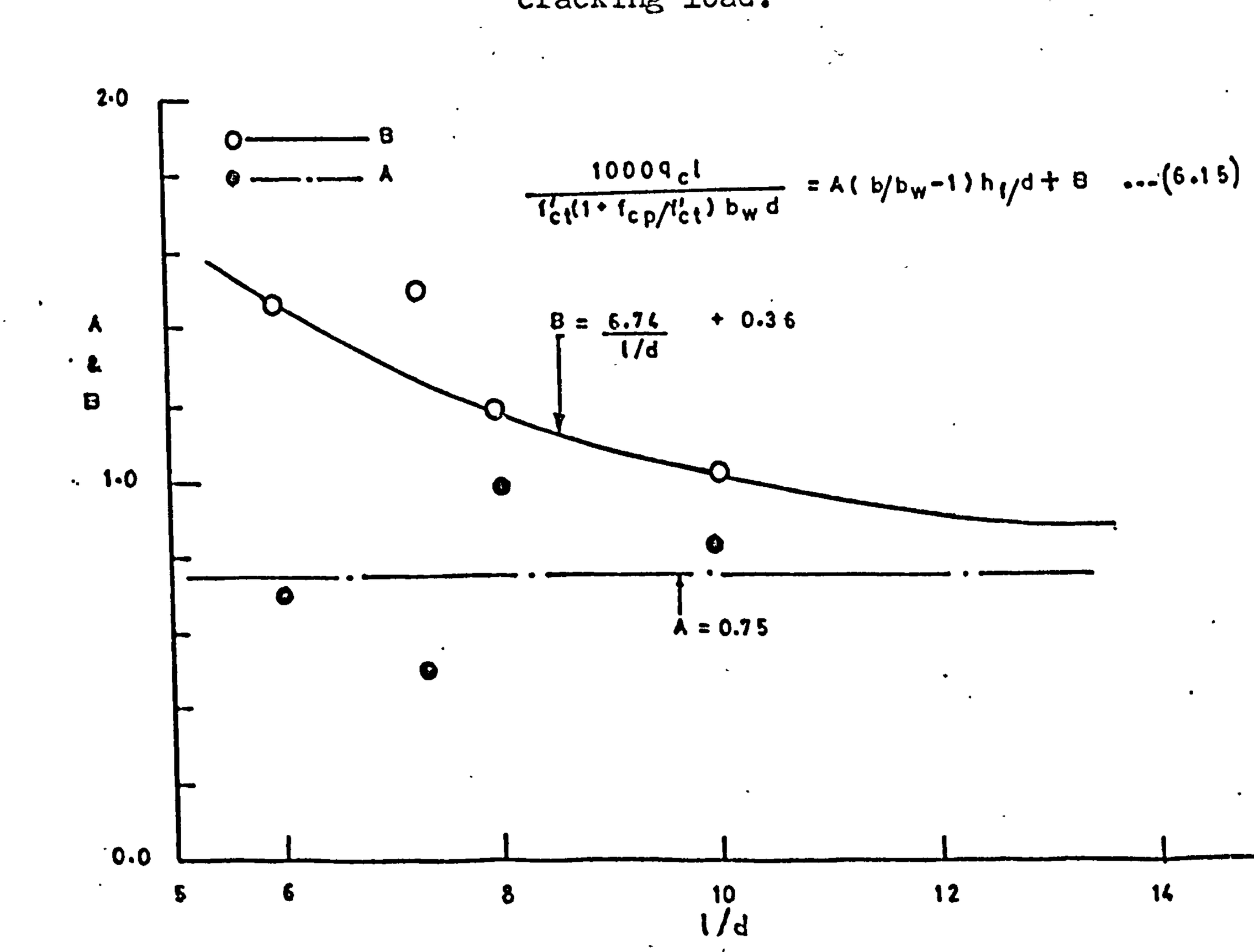

Figure 6.12: Diagonal cracking load and beam properties in terms of l/d.

6.1.3.4. Comparison between equations 6.12 and 6.17.

Equations 6.12 and 6.17 were used independently to predict the value of the cracking load, $^{q}c^{l}$, for all the tests in this series and the results published by others[42,43,47,48]. The values predicted were compared with the corresponding experimental values and the results are shown in Table 6.2. The mean value of the ratio of the experimental load to calculated load and corresponding standard deviation are also shown for each set of data in Table 6.2. There is little difference between the values predicted by the two equations, and this confirms that all the assumptions made in deriving equation 6.12 from equation 6.5 were reasonable. Accordingly equation 6.12 can be used for predicting the diagonal cracking load, $^{q}c^{l}$, in the case of a uniformly loaded beam.

6.2. Prediction of Shear-compression Failure Load:

6.2.1. General.

Equations 6.5 and 6.12 predicted the first diagonal tension cracking load reasonably well for all the beams in which shear cracking was not influenced by the presence of flexure cracks. At higher $^{a}v/d$ ratios the resistance of the web section to the formation of major diagonal tension cracks is high because the breadth, b_w, is very thick as in rectangular sections or because the prestress level,

TABLE 6.2

Comparison of results of tests on uniformly loaded beams with values predicted by diagonal tension equations (6.12) and (6.17)

Author	Beam mark	$\frac{l}{d}$	Ratio $\frac{q_c l \text{ Expt.}}{q_c l \text{ Calc.}}$	
			Eqn. 6.12	Eqn. 6.17
Present Investigation	B12	10.00	1.05	1.07
			0.91	0.93
	13	8.00	1.00	1.03
			1.08	1.11
	14	7.28	0.95	0.97
			1.04	1.07
	15	6.00	0.98	1.00
			0.88	0.91
	C13	10.00	1.06	1.09
	14	8.00	1.05	1.07
			1.06	1.08
	15	7.28	1.01	1.03
			1.10	1.12
	16	6.00	0.92	0.93
			0.92	0.93
	20	11.78	1.27	1.29
	D10	"	1.08	1.07
	11a	17.78	1.10	1.04
	11b	"	0.98	0.92
			1.13	1.06
	12	11.78	1.10	1.10
			0.90	1.89
	13	17.47	0.90	0.84
	14	"	1.03	0.96
	E 9	10.00	1.05	1.07
	10	8.00	1.01	1.04
			1.04	1.07

TABLE 6.2 (Cont'd)

Author	Beam mark	$\frac{l}{d}$	Ratio $\frac{q_c l \text{ Expt.}}{q_c l \text{ Calc.}}$ Eqn. 6.12	Eqn. 6.17
Present Investigation	E11	6.00	1.00	1.03
			1.00	1.03
	12	7.28	1.16	1.20
			1.08	1.11
	F6	10.00	1.06	1.07
			1.00	1.01
	7	8.00	1.09	1.13
			1.09	1.13
	8	6.00	0.95	1.00
			0.85	0.91
	9	7.28	0.95	0.99
			0.97	1.01
Mean value of ratio			1.021	1.034
Standard deviation			.085	.089
Hanson and Hulsbos[47]	F17	10.58	1.07	1.08
			1.11	1.12
Arthur et al[48]	C9	9.52	0.84	0.86
	10	7.28	0.95	0.96
			1.05	1.07
	12	9.52	0.80	0.82
	13	8.42	0.88	0.90
			0.93	0.95
	14	9.52	0.90	0.93
			1.06	1.09
	15	8.42	0.77	0.79
			0.90	0.92
	16	7.28	0.92	0.94
			0.97	0.99

TABLE 6.2 (Cont'd)

Author	Beam mark	$\frac{l}{d}$	Ratio $\frac{q_c l \text{ Expt.}}{q_c l \text{ Calc.}}$ Eqn. 6.12	Equn. 6.17
Arthur et al[48]	C17	6.18	0.85	0.86
			0.89	0.91
	D 6	8.42	0.97	0.99
			1.03	1.06
	7	9.52	0.93	0.95
	8	7.28	1.12	1.14
	9	6.18	0.87	0.87
			0.87	0.87
	10	6.18	0.88	0.88
	11	8.42	1.02	1.05
			1.07	1.09
	E 5	9.52	1.17	1.21
	6	8.42	1.09	1.11
	7	7.28	1.28	1.29
	8	6.18	1.18	1.18
	9	8.42	0.99	1.01
			1.18	1.20
Mean value of ratio			0.98	1.00
Standard deviation		-	.126	.128
Kar[43]	A-U-2	13.10	0.68	0.73
	-3	"	0.77	0.82
	-4	"	0.71	0.76
	-5	"	0.66	0.71
	-6	"	0.74	0.79
	-8	"	0.74	0.79
	-9	"	0.73	0.79
	-11	"	0.64	0.69
	B-U-1	15.30	0.71	0.82
	-2	"	0.59	0.69
	-4	"	0.74	0.86
	-5	"	0.58	0.67
Mean value of ratio			0.69	0.76
Standard deviation		.124	0.061	0.061

f_{cp}, is very high. In such cases, for example that of rectangular beams at relatively high a_v/d or l/d ratios[42,43], the ultimate failure in shear is frequently shear-compression initiated by a flexure-shear crack. In this type of failure it is difficult to define precisely the first diagonal tension crack and hence the load at which it occurs. In the following sections an attempt will be made to calculate the shear-compression failure load which in turn will be compared either with equation 6.5 or with equation 6.12 as appropriate. It is recommended that the lesser be taken as the limit of usefulness in shear of a beam without shear reinforcement.

To achieve this object, it is necessary to have full knowledge of the stress-strain behaviour of concrete in compression and to find a simple but appropriate failure criterion for concrete in the compression zone.

6.2.2. Equation for the stress-strain curve of concrete in compression.

The stress-strain curve for concrete in compression is adequately represented by a parabola, either terminating at a maximum stress f_o corresponding to a strain ε_o, or continuing beyond this point at a constant stress equal to the maximum, up to a limiting strain ε_u.

The exact geometry of the stress-strain curve is dependent on a large number of factors, the most

significant of which are the concrete mix, the strain rate and duration of loading[90] and the strain gradient across the concrete[91,92]. In design methods it is impracticable to take proper account of the effects of the rate of loading and the strain gradient upon the stress-strain characteristics, and therefore most of the expressions given for the stress-strain curves are in terms of concrete crushing strength alone. The stress-strain curves for differing concrete strengths are generally, for convenience, taken to be geometrically similar and are expressed in the form:

$$f/f_o = F_5(\varepsilon / \varepsilon_o) \qquad (6.18)$$

where F_5 is a functional notation. An example of this type is given by Desayi and Krishnan[93] as:

$$f/f_o = 2\varepsilon/\varepsilon_o\left[1+(\varepsilon/\varepsilon_o)^2\right] \qquad (6.19)$$

As it is normal in design to consider only the rising branch and the part over which the stress is approximately constant, the idealized stress-strain curve given by BSCP 110: Part 1: 1972[30] will be used here. This curve is shown in Figure 6.13 and can be represented by the following equations:

$$f = 5.5 \times 10^3 \sqrt{f_{cu}} \times \varepsilon - 11.29 \times 10^6 \varepsilon^2 \text{ for } \varepsilon \leq \varepsilon_o$$

$$f = 0.67 f_{cu} \quad \text{for } \varepsilon_o \leq \varepsilon \leq 0.0035$$

$$\text{where } \varepsilon_o = 0.244 \times 10^{-3} \sqrt{f_{cu}} \qquad (6.20)$$

6.2.3. Failure criterion for the shear-compression zone:

The strength of an element in the compression zone depends on the normal flexure stress f_{xx}, the shearing stress v_{xy}, and the stress normal to the longitudinal

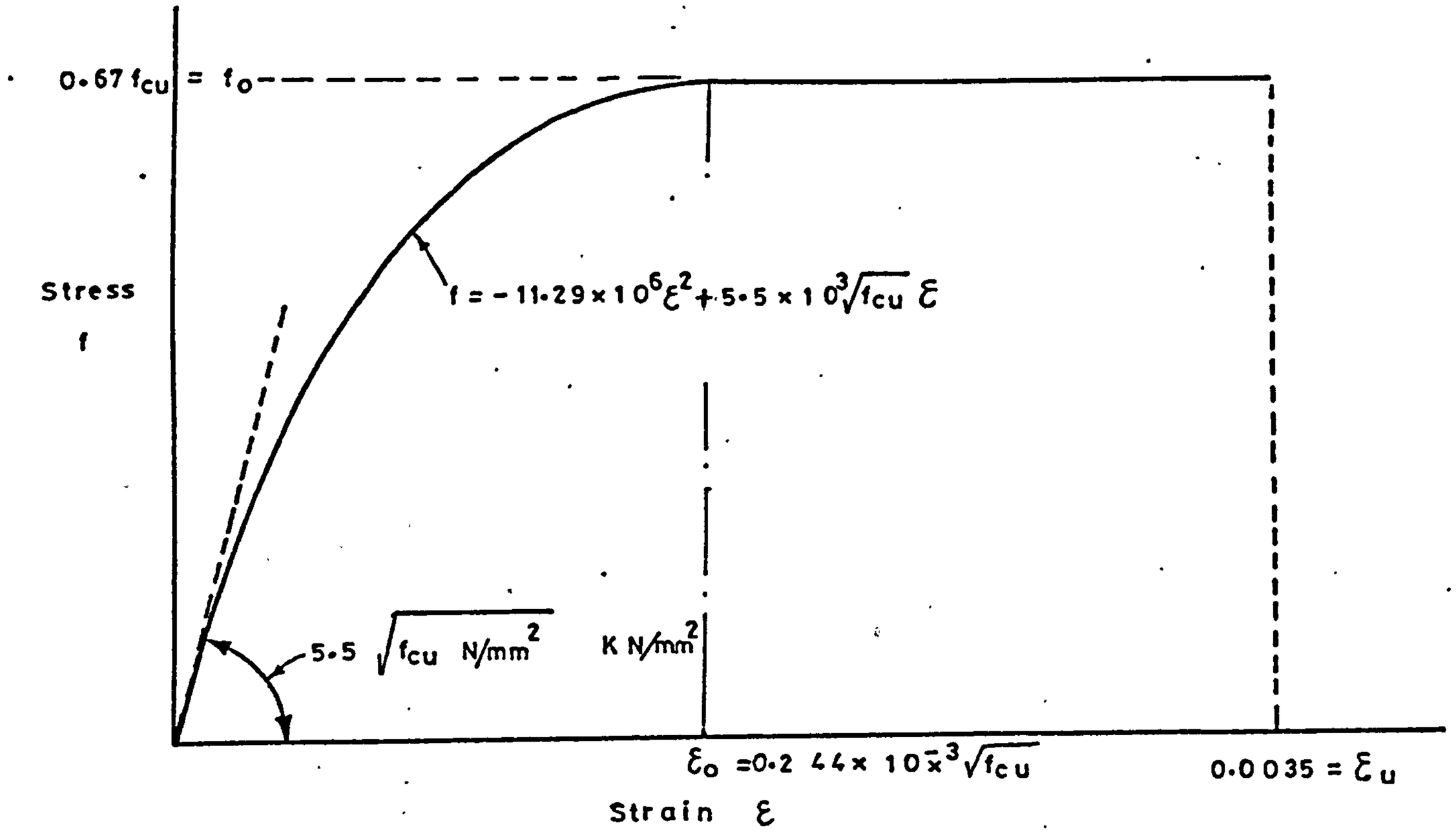

Figure 6.13: The idealized stress-strain curve for concrete in compression
(BSCP 110: Part 1: 1972[30])

axis f_{yy}. The first two of these stresses are related to one another by the configuration of loading so that their effect can be taken into account by the effective moment-shear ratio $\left(\frac{M}{V}\right)_c$.

Full consideration of the strength of concrete under a complex state of stress is outside the scope of this investigation, and further discussion will be based on the Mohr failure theory. Mohr's theory has been found to be valid for biaxial stresses[25,69], and this is generally the state of stress in the compression zone of concrete beam. So in order to establish the relation between normal and shearing stresses which, when acting together, cause failure to occur in the compression zone, the shape of Mohr's failure envelope should be known.

Various suggestions about the shape of the envelope have been made in the past, and this is discussed in Section 3.6. In this investigation a straight line envelope to Mohr's circles of failure, based on pure tension and pure compressive strength circles was adopted. By using the geometric relationships derived from that envelope together with the principal stress equation, the following expression was derived for the failure criterion in the compression zone.

$$\left(\frac{v_{xy}}{f'_t}\right)^2 = \frac{\gamma}{(\gamma+1)^2}\left[\gamma + (\gamma-1)\left(\frac{f_{xx}}{f'_t} + \frac{f_{yy}}{f'_t}\right) + \frac{(\gamma+1)^2}{\gamma} \times \frac{f_{xx}}{f'_t} \cdot \frac{f_{yy}}{f'_t} - \left(\frac{f_{xx}}{f'_t} + \frac{f_{yy}}{f'_t}\right)^2\right] \qquad (6.21)$$

where γ is the ratio between uniaxial compressive and uniaxial tensile stress, i.e. $\gamma = f'_c/f'_t$.

The derivation of equation 6.21 is given in Appendix E.

Shear-compression failure is observed either at high values of a_v/d where the failure loads are not high enough to produce any appreciable value of f_{yy} or in rectangular sections with moderate shear spans where the value of f_{yy}, if it is assumed to be inversely proportional to b, will be small. Neglecting f_{yy} in equation 6.21 may thus lead to a small error on the safe side, and equation 6.21 will be reduced to the following form:

$$\left(\frac{v_{xy}}{f'_t}\right)^2 = \frac{\gamma}{(1+\gamma)^2}\left[\gamma + (\gamma - 1)\frac{f_{xx}}{f'_t} - \left(\frac{f_{xx}}{f'_t}\right)^2\right] \qquad (6.22)$$

The value of γ can be obtained from equation 4.2 as:

$$\gamma = \frac{f'_c}{f'_t} = \frac{22.4\ f_{cu}}{f_{cu} + 40.6\ N/mm^2} \qquad (6.23)$$

and f'_c is taken here as $0.8\ f_{cu}$ and $f'_t = f'_{ct}$

so $f'_t = 0.8\ f_{cu}/\gamma$ (6.24)

For simplicity, from Figures 6.13 and 6.14.a, f_{xx} is taken as f_{av} where f_{av} is the average normal flexure stress in the compression zone given by:

$$f_{av} = k_1 \times 0.67\ f_{cu} \qquad (6.25)$$

where k_1 is the ratio between average normal flexure stress and the maximum normal flexure stress.

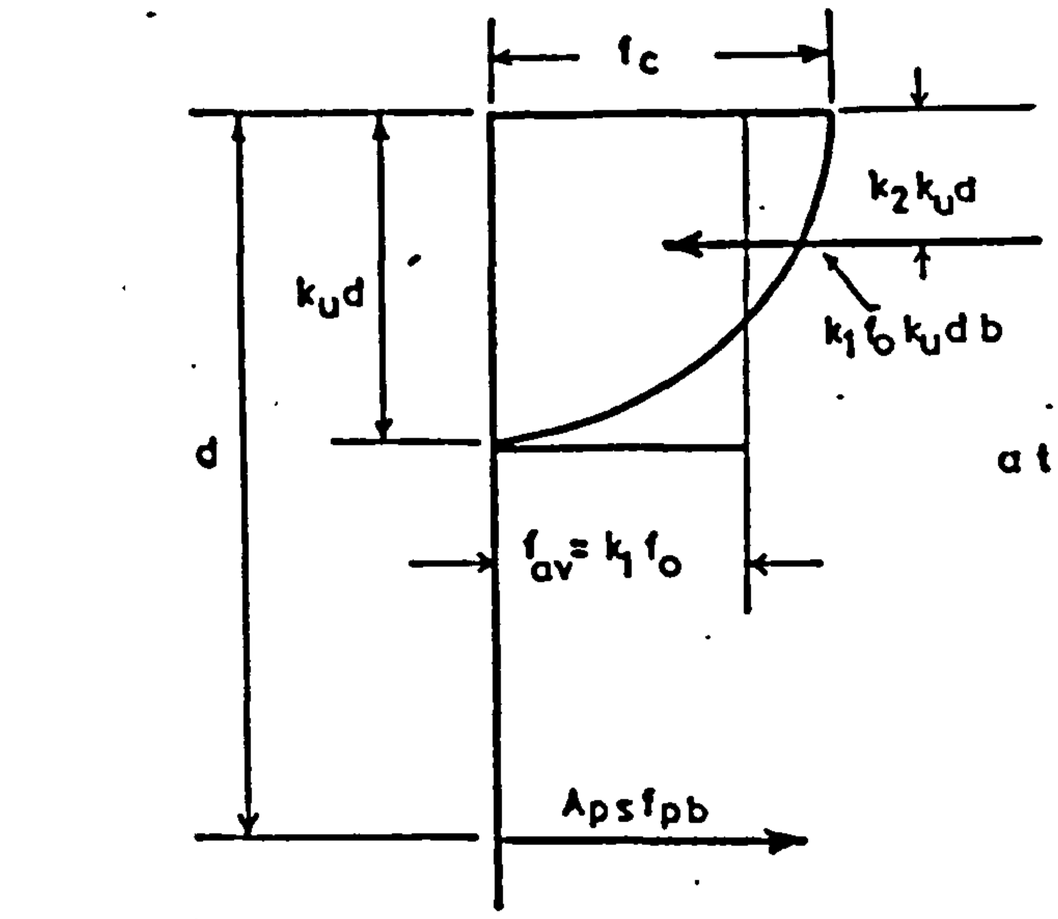

(a) Forces and normal stress (bending), f_{xx}, distribution.

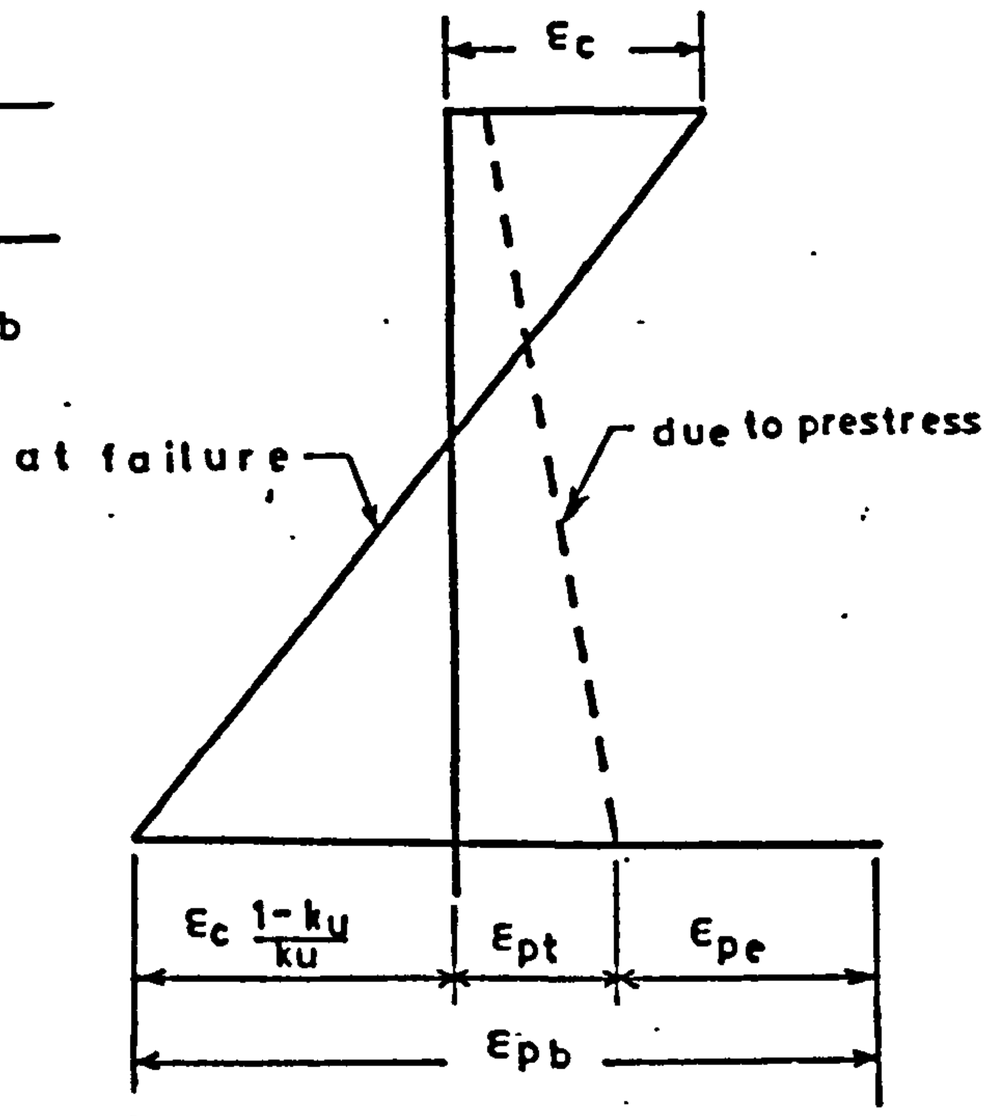

(b) Concrete and tendons strains at failure

Figure 6.14

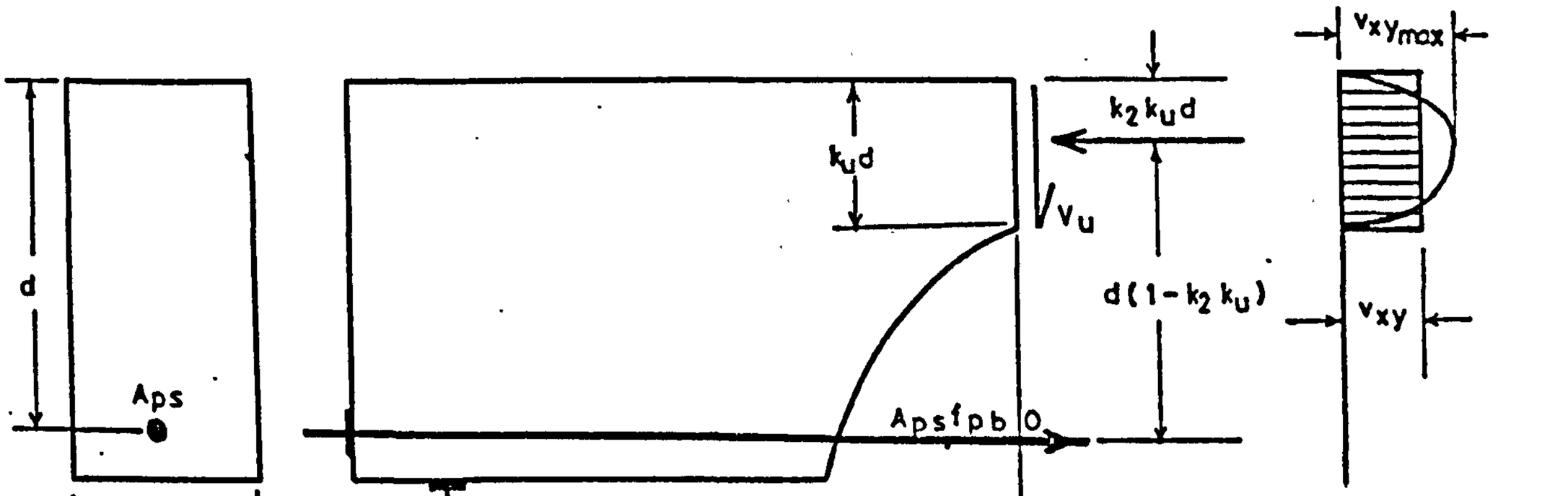

Figure 6.15

k_1 is a function of the value of $\varepsilon_c/\varepsilon_o$ at the extreme compressed fibre (see Section 6.2.6.).

By substituting equations 6.24 and 6.25 into equation 6.22 we will have:

$$\left(\frac{v_{xy}}{f_{cu}}\right)^2 = \frac{1}{(1+\gamma)^2}\left[0.64 + 0.536\ (\gamma - 1)\ k_1 - 0.449\ \gamma k_1^2\right] \qquad (6.26)$$

Equation 6.26 is a failure criterion for an element in the compression zone under normal and shear stresses.

6.2.4. Equilibrium condition:

Referring to Figure 6.15.a, and neglecting the dowel action of the longitudinal reinforcement and the vertical component of the force due to aggregate interlock on the inclined crack, one can write from the equilibrium of external and internal moments that:

$$a_v V_u = 0.67\ k_1\ f_{cu}\ k_u\ d\ b\ d\ (1 - k_2 k_u) \qquad (6.27)$$

and from equilibrium of vertical forces:

$$V_u = v_{xy}\ k_u\ d\ b \qquad (6.28)$$

where k_u is the ratio of the neutral axis depth to effective depth and k_2 is the ratio of the depth to the line of action of the normal compressive force to the neutral axis depth.

From equations 6.27 and 6.28 we get:

$$\frac{v_{xy}}{f_{cu}} = \frac{0.67.k_1\ (\ 1 - k_2\ k_u)}{a_{v/d}} \qquad (6.29)$$

To determine the value of the average shear stress, but not the position of the neutral axis itself, it

is reasonable to adopt the simplified assumption[25,26] that $(1 - k_2 k_u) = 0.9$ (6.30)

By combining equations 6.26, 6.29 and 6.30 we get:

$$k_1^2 \left(\frac{(1+\gamma)^2}{(a_v/d)^2} + 1.24\gamma \right) - 1.48\,(\gamma - 1)\,k_1 - 1.77 = 0 \qquad (6.31)$$

So V_u can be calculated using equations 6.28, 6.29 and 6.31 if the neutral axis depth factor, k_u, is known.

6.2.5. Neutral axis depth factor k_u:

The tendon strain ε_{pb} at failure may be considered to be made up of two parts: (a) the strain ε_{pe} due to f_{pe} and (b) the additional strain ε_{pa} produced by the applied loading as shown in Figure 6.14.b . Thus

$$\varepsilon_{pb} = \varepsilon_{pe} + \varepsilon_{pa} \qquad (6.32)$$

Assuming an idealized case of perfect bonding between steel and concrete, ε_{pa} can be written as:

$$\varepsilon_{pa} = \varepsilon_c \left(\frac{1 - k_u}{k_u} \right) + \frac{f_{pt}}{E_c} \qquad (6.33)$$

Substituting equation 6.33 into equation 6.32 then

$$\varepsilon_{pb} = \varepsilon_{pe} + \alpha \varepsilon_o \left(\frac{1 - k_u}{k_u} \right) + \frac{f_{pt}}{E_c} \qquad (6.34)$$

where $\alpha = \frac{\varepsilon_c}{\varepsilon_o}$

From equation 6.34

$$k_u = \frac{\alpha\ \varepsilon_o}{\varepsilon_{pb} + \varepsilon_o - \varepsilon_{pe} - \frac{f_{pt}}{E_c}} \qquad (6.35)$$

Referring to Figure 6.14.a and applying the equilibrium

conditions:

$$0.67\, k_1\, f_{cu}\, k_u\, d\, b = A_{ps}\, f_{pb} \qquad (6.36)$$

From equations 6.35 and 6.36

$$f_{pb} = \frac{0.67 \alpha \varepsilon_o\, k_1 f_{cu}\, b\, d}{A_{ps}\,(\varepsilon_{pb} + \alpha\varepsilon_o - \varepsilon_{pe} - \frac{f_{pt}}{E_c})} \qquad (6.37)$$

The value of $\alpha (= \varepsilon_c/\varepsilon_o)$ can be determined from Section 6.2.6, and equation 6.37 can be solved graphically using the stress-strain curve of the tendon on a strain compatibility basis. Having found f_{pb} and hence the tendon strain at failure ε_{pb}, then k_u can be calculated from equation 6.35.

6.2.6. Evaluation of k_1 and k_2 in terms of $\varepsilon_c/\varepsilon_o\ (= \alpha)$ and their limitations:

Referring to Figures 6.13 and 6.14 a, and by definition:

$$k_1 = \frac{\int_o^{\varepsilon_c} f\ d\varepsilon}{\varepsilon_c\ f_o}$$

$$= \frac{3\alpha - 1}{3\alpha} \qquad (6.38)$$

for $1.0 \leqslant \alpha \leqslant \dfrac{0.0035}{0.244 \times 10^{-3} \times \sqrt{f_{cu}}}$

and k_2 by definition is equal to:

$$k_2 = \frac{1}{k_1\, f_o\, \varepsilon_c^2} \int_o^{\varepsilon_c} (\varepsilon_c - \varepsilon) f\, d\varepsilon$$

$$= \frac{1}{4\alpha(3\alpha - 1)}\,(6\alpha^2 - 4\alpha + 1) \qquad (6.39)$$

for $1.0 \leqslant \alpha \leqslant \dfrac{0.0035}{0.244 \times 10^{-3} \times \sqrt{f_{cu}}}$

where $\alpha = \frac{\varepsilon_c}{\varepsilon_o}$ and $\varepsilon_o \leq \varepsilon_c \leq 0.0035$

6.2.7. Evaluation of V_u:

k_1, k_2 and k_u can be calculated as shown in the previous Sections, and therefore $(1 - k_2 k_u)$ can be determined. If the latter differs considerably from 0.9 (see equation 6.30), then the new value of $(1 - k_2 k_u)$ should be used in equation 6.29 to construct equation 6.26. This will lead to a new value of k_1. This procedure should be repeated till there is a reasonable agreement between the calculated and the assumed value of $(1 - k_2 k_u)$. V_u can then be calculated using the final values of k_1, k_2 and k_u in equations 6.29 and 6.28.

6.2.8. Prediction of shear-compression failure load in a uniformly loaded simply supported beam.

6.2.8.1. Failure section and equilibrium condition:

The position at which failure will occur in the shear-compression case in a simply supported uniformly loaded beam is not immediately apparent. The process of flexure-shear cracking is progressive and does not stop suddenly when a crack reaches a particular section, but the crack tends to progress towards the centre of the span.

Neglecting the effect of aggregate interlock the shaar crack should theoretically progress with increasing load until the shear resistance of the concrete at its head is equal to the external shear force. The length of the crack should thus increase with increasing

load.

Assume that the failure plane in shear-compression lies at a distance $\lambda_u l$ from the nearest support. Then by referring to Figure 6.15.b, and neglecting the dowel force and aggregate interlock, one can write from the equilibrium of external and internal moments that:

$$\frac{q_u l^2 \lambda_u}{2} - \frac{q_u \lambda_u^2 l^2}{2} = 0.67\, k_1 f_{cu} k_u\, d\, b\, d\, (1-k_2 k_u) \qquad (6.40)$$

and from equilibrium of vertical forces:

$$\frac{q_u l}{2} - q_u \lambda_u l = v_{xy}\, k_u\, b\, d \qquad (6.41)$$

Combining equation 6.40 and equation 6.41, gives:-

$$\frac{v_{xy}}{f_{cu}} = \frac{0.67\, k_1\, (1 - k_2\, k_u)(1 - 2\lambda_u)}{l/d\ \lambda_u\ (1 - \lambda_u)} \qquad (6.42)$$

As mentioned before, experiments showed that uniformly loaded simply supported beams which failed in shear-compression, had critical sections at a distance $0.33l$ from a support. Hence putting $\lambda u = 0.33$ in equation 6.42 , gives:-

$$\frac{v_{xy}}{f_{cu}} = \frac{k_1\, (1 - k_2\, k_u)}{l/d} \qquad (6.43)$$

Assuming $(1 - k_2 k_u) = 0.9$ and combining equations 6.26 and 6.43, gives:-

$$k_1^2 \left(\frac{(1+\gamma)^2}{(l/d)^2} + 0.554\,\gamma\right) - 0.662\,(\gamma - 1)\, k_1 - 0.79 = 0 \qquad (6.44)$$

The solution of equation 6.44 yields values for k_1 for $f_{cu} \geqslant 30.0$ N/mm^2 and for all values of $l/d \geqslant 7.0$, which are all greater than

$$1 - \frac{0.33 * 0.0035}{0.244 \times 10^{-3}\sqrt{f_{cu}}}$$

which is the maximum value for k_1 (see equation 6.38). Hence for all values of $l/d \geqslant 7.0$ and $f_{cu} \geqslant 30.0$ N/mm^2, the value of k_1 should be limited to the maximum value of k_1 given above. The value of k_u can be calculated from equations 6.35 and 6.37 and by substituting the values of k_1, k_2 and k_u into equations 6.42 and 6.28, V_u, the shear force at the critical section, can be calculated.

To determine the value of $q_u l$ from V_u, it will be assumed that this value of V_u is the shear force at a distance 0.5 d from the critical section measured in the direction of decreasing bending moment.

Hence

$$V_u = \frac{q_u l}{2} - q_u \left(\frac{l}{3} - \frac{d}{2} \right)$$

$$\text{or } q_u l = \frac{6\ V_u\ l/d}{l/d + 3} \qquad (6.44)$$

A more conservative assumption is to take V_u at d from the critical section . This gives

$$V_u = \frac{q_u l}{2} - q_u \left(\frac{l}{3} - d \right)$$

$$\text{or } q_u l = \frac{6\ V_u\ l/d}{l/d + 6} \qquad (6.45)$$

Equations 6.44 and 6.45 will be discussed later in Section 7.5.2 when they will be compared with experi-

mental results.

6.3. Comparison between Diagonal Tension Equation and Shear-compression Equation.

6.3.1. One - or two-point loading case:

A typical specimen of the general dimensions of the type C beams used in the tests and stressed by seven 7 mm diameter wires was studied in order to study the results predicted by equations 6.5 and 6.28 for various values of concrete strength, pre-stress and shear span to effective depth ratio.

Figures 6.17.1 and 6.17.2 show the value of shear force at failure as predicted by the diagonal tension equation 6.5, the shear-compression equation 6.28 and ultimate flexure[94], as a function of $^{a}v/d$. In Figure 6.17.1 ^{f}cu was taken as 50.0 N/mm^2 and ^{f}cp was chosen as 3, 5 and 7 N/mm^2. Figure 6.17.1 shows that, within these ranges of variables, beams of type C will never fail in shear-compression. Figure 6.17.2 shows the effect of varying ^{f}cu between 35.0 and 45.0 N/mm^2, with ^{f}cp constant at 5.0 N/mm^2, on the mode of failure of specimen C. This case, too, shows that diagonal tension is the dominant mode of failure of a type C specimen. For $^{a}v/d > 5.0$, ultimate flexural failure will be reached before diagonal tension failure can occur.

6.3.2. Uniformly distributed load case:

For this case two typical specimens were studied, one with the general dimensions of type D in the present

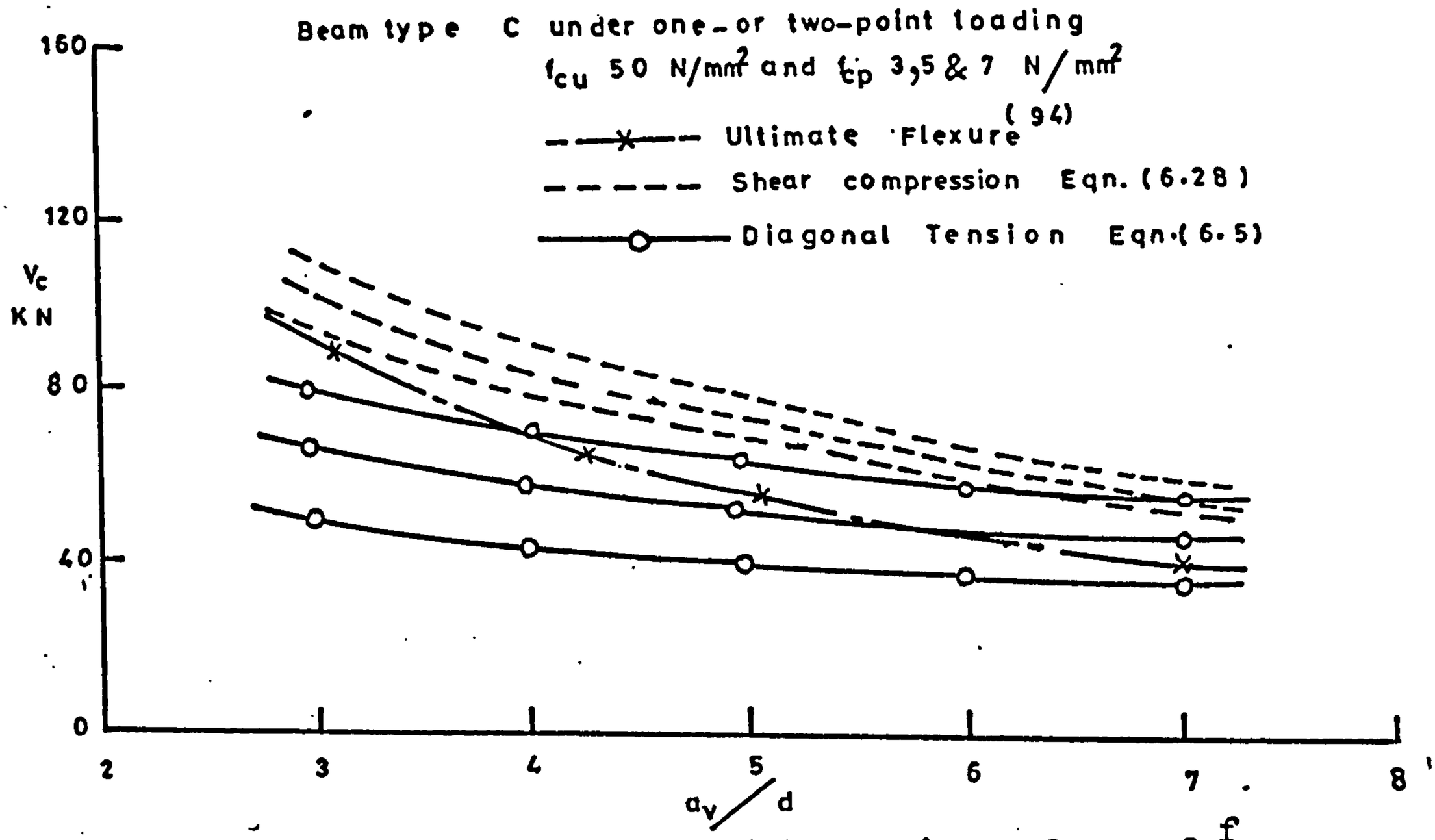

Figure 6.17.1: Type C beam with varying values of f_{cp} and $a_{v/d}$ (Concrete strength constant)

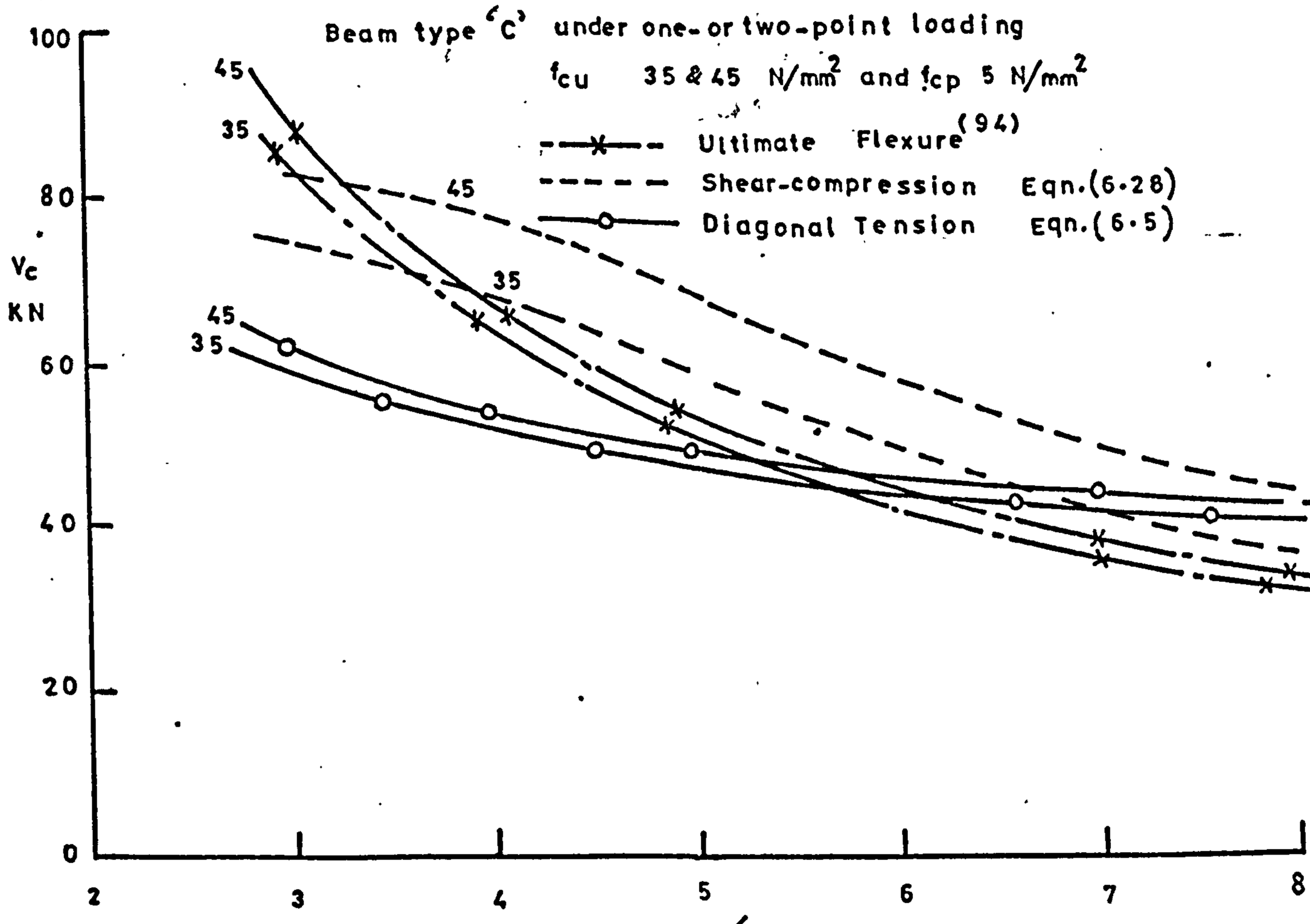

Figure 6.17.2: Type C beam with varying values of f_{cu} and $a_{v/d}$ (Prestress constant)

Figure 6.17. Point-loaded beams. Effect of f_{cp}, f_{cu} and $a_{v/d}$ on mode of failure and shear force at failure or type C beam.

series of tests stressed by two 12.5 mm diameter strands, and the other similar to type A-U-5 reported by Kar[43]. For the D type beam with b_w = 50 mm, f_{cu} was taken as 50.0 N/mm^2 and f_{cp} was varied from 2.0 to 5.0 N/mm^2. For the A-U-5 type with b = 125 mm, f_{cu} was assumed to be 45.0 N/mm^2. Figure 6.18.1, for the D type beam, shows that diagonal tension is the dominant mode of failure for $f_{cp} < 4.0$ N/mm^2, but that flexure failure will become the mode of failure at $f_{cp} \geq 5.0$ N/mm^2 and $l/d \geq 12.0$. As the breadth of the web increases or in a rectangular case as shown in Figure 6.18.2 for the A-U-5 type beams, shear-compression is dominant for $l/d < 10$ and f_{cp} = 2.0 N/mm^2. For $f_{cp} >$ 2.0 N/mm^2 and $l/d > 8.0$, flexure failure will dominate. For $f_{cp} \leq 2.0$ and $l/d > 10.0$ the shear-compression failure and flexure failure overlap. For f_{cp} = 0 and for all values of $l/d \leq 20$ the diagonal tension failure is dominant. This latter case can also be observed in Leonhardt and Walther's photographs for rectangular beams of b = 190 mm.

From the above it can be concluded that the web breadth plays an important role in determining the mode of failure in a uniformly loaded case. From the case studied which is shown in Figure 6.18.1 and confirmed by experiments in this investigation in the higher range of l/d on type D-beam, it can be concluded that the shear-compression type of failure observed in

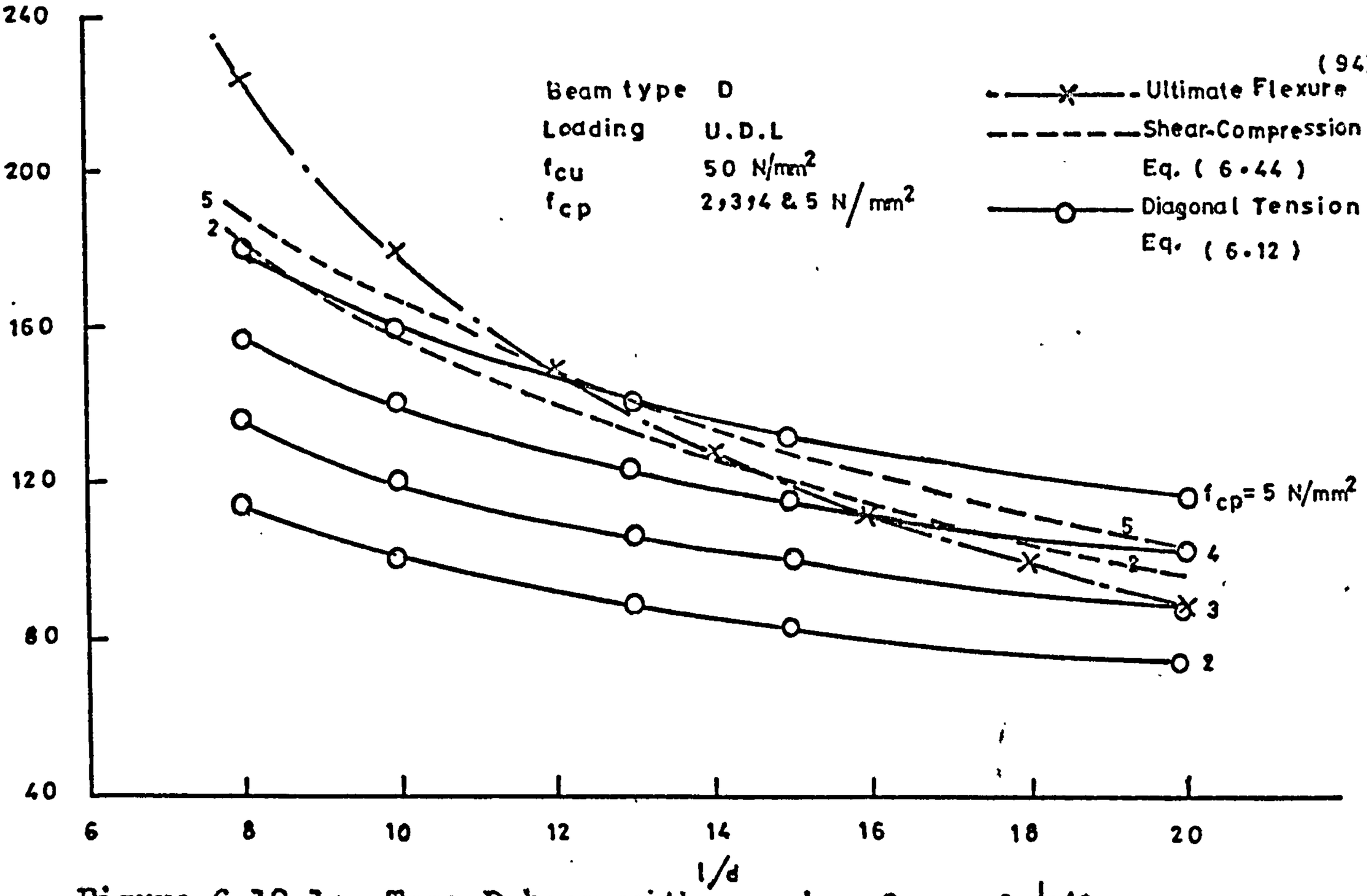

Figure 6.18.1: Type D beam with varying f_{cp} and l/d
(Concrete strength constant)

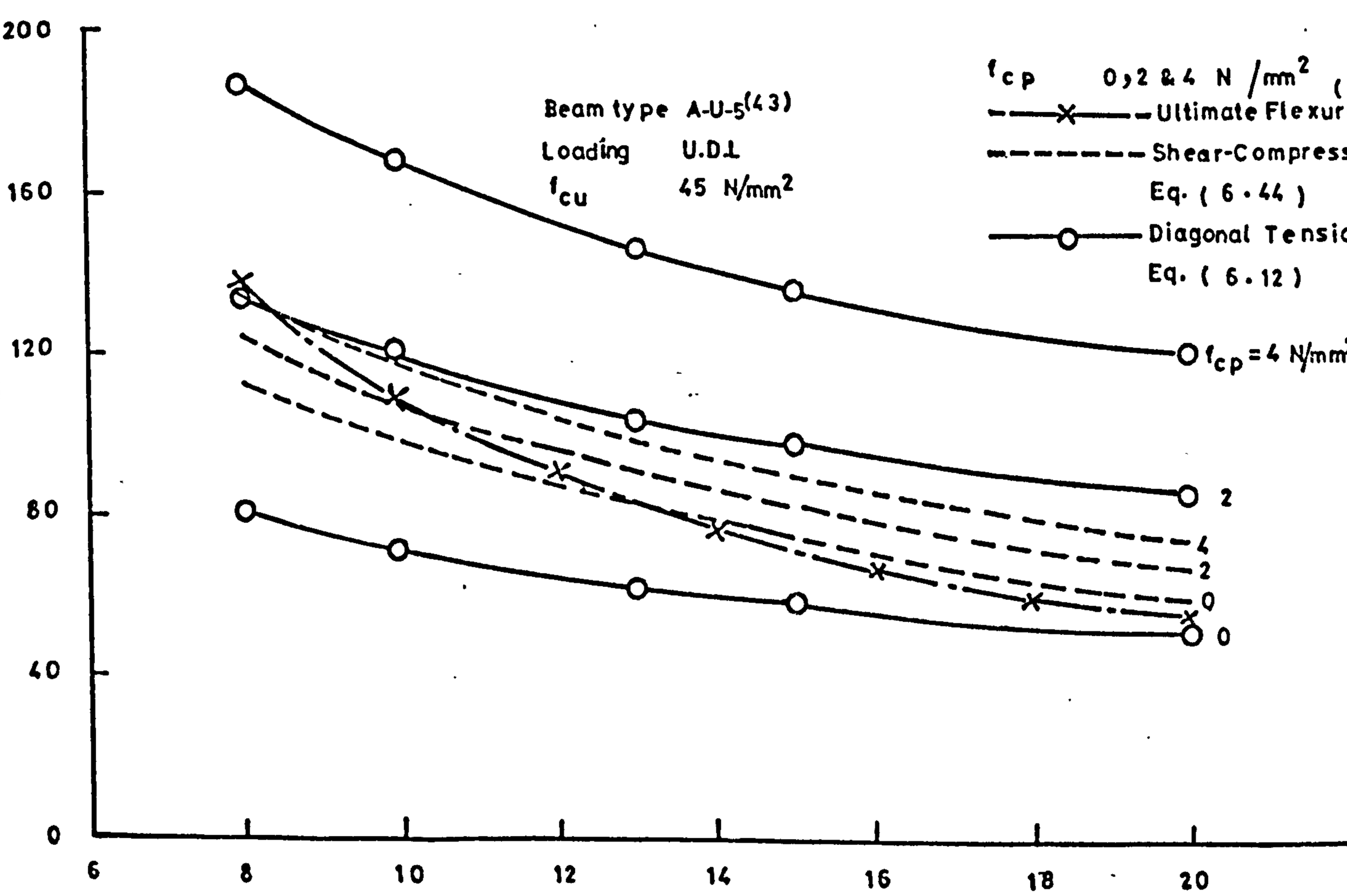

Figure 6.18.2 Kar's type (A-U-5) beam with varying f_{cp} and l/d
(concrete strength constant)

Figure 6.18 Uniformly-loaded beams. Effect of beam properties and l/d on mode of failure and shear force at failure.

Kar's rectangular beams will never occur at all l/d ranges for sections with $b_{w/d} \leq 0.25$.

CHAPTER 7

COMPARISON WITH OTHER RESULTS AND DESIGN RULES

7.1. BSCP 110: Part 1: 1972[30] and ACI (318 - 71) Building Code[32] Design Equations.

Equations (45) and (46) of CP 110: Part 1: 1972 contain partial safety factors of 1.50 relative to concrete strength and 1.25 relative to the prestressing force. For the purpose of this comparison, these safety factors incorporated in the Code have been removed, giving:-

$$V_{co} = 0.67\ b_w\ hf_t\sqrt{1 + \frac{f_{cp}}{f_t}}$$ Code equation (45)

where $f_t = 0.36\sqrt{f_{cu}}$

and $$V_{cr} = \left(1 - 0.55\ \frac{f_{pe}}{f_{pu}}\right)\sqrt{1.5}\ v_c\ b_w d + \frac{M_o}{(\ a_{v/d} - 0.5)\ d}$$

Code equation (46)

where $$M_o = f_{pt}\ \frac{I}{y}$$

The shear force at diagonal cracking should be taken as the lesser of the Code equations (45) and (46).

If the dead load is neglected and straight tendons are assumed, the ACI (318-71) Building Code gives under a web-shear crack, the ultimate shear resistance of a section as V_{cw} where:

$$V_{cw} = \emptyset\ b_w d\left(0.29\sqrt{0.8\ f_{cu}} + 0.3\ f_{cp}\right)$$ ACI equations (11-3 and 11-12)

and V_{ci} as an upper limit to the ultimate shear strength of a section under flexure-shear where:

$$V_{ci} = \emptyset\ \ b_w d\left(0.05\sqrt{0.8\ f_{cu}} + \frac{I}{y}\ \frac{(0.5\sqrt{0.8\ f_{cu}} + f_{pe})}{b_w\ d^2\left(\frac{a_v}{d}\right)}\right)$$

ACI equations (11-3 and 11-11)

To permit comparison, the capacity reduction factor Ø was removed and the lesser of the above two expressions was taken as the shear force at diagonal cracking.

7.2. Comparison of Equations 6.5 and 6.7 for one- or two-point Loading with Published Equations and Code Rules.

To compare equations 6.5 and 6.7 with other published design equations and code rules, two typical specimens were studied, one with the general dimensions of type B in the tests and the other with those of type F, both being stressed by means of seven 7 mm diameter indented wires. The concrete strength and the prestressing force were chosen to be within the practical range. The concrete cube strength was taken as 50.0 N/mm^2 in both cases.

For B type beam, f_{cp} was taken as 8.0 N/mm^2 and f_{pe}/f_{pu} as 0.55. For the F type, f_{cp} was taken as 6.0 N/mm^2 and f_{pe}/f_{pu} as 0.58. The value of the cracking load predicted by each of the published expressions as a function of $^{a}v/d$ was evaluated and the results were plotted as shown in Figures 7.1 and 7.2, together with the shear force corresponding to ultimate flexural moment[94].

For the B type beam (^{h}f = 47.5 mm), Figure 7.1, the expressions of Sethunarayanan[34], Sozen et al[36], and Evans and Schumacher[40] overestimate V_c, but Sozen[36] et al come out with close agreement at $^{a}v/d > 5.0$, and the expressions of Arthur[44] and Jena and Pannell[52] underestimate V_c over the whole

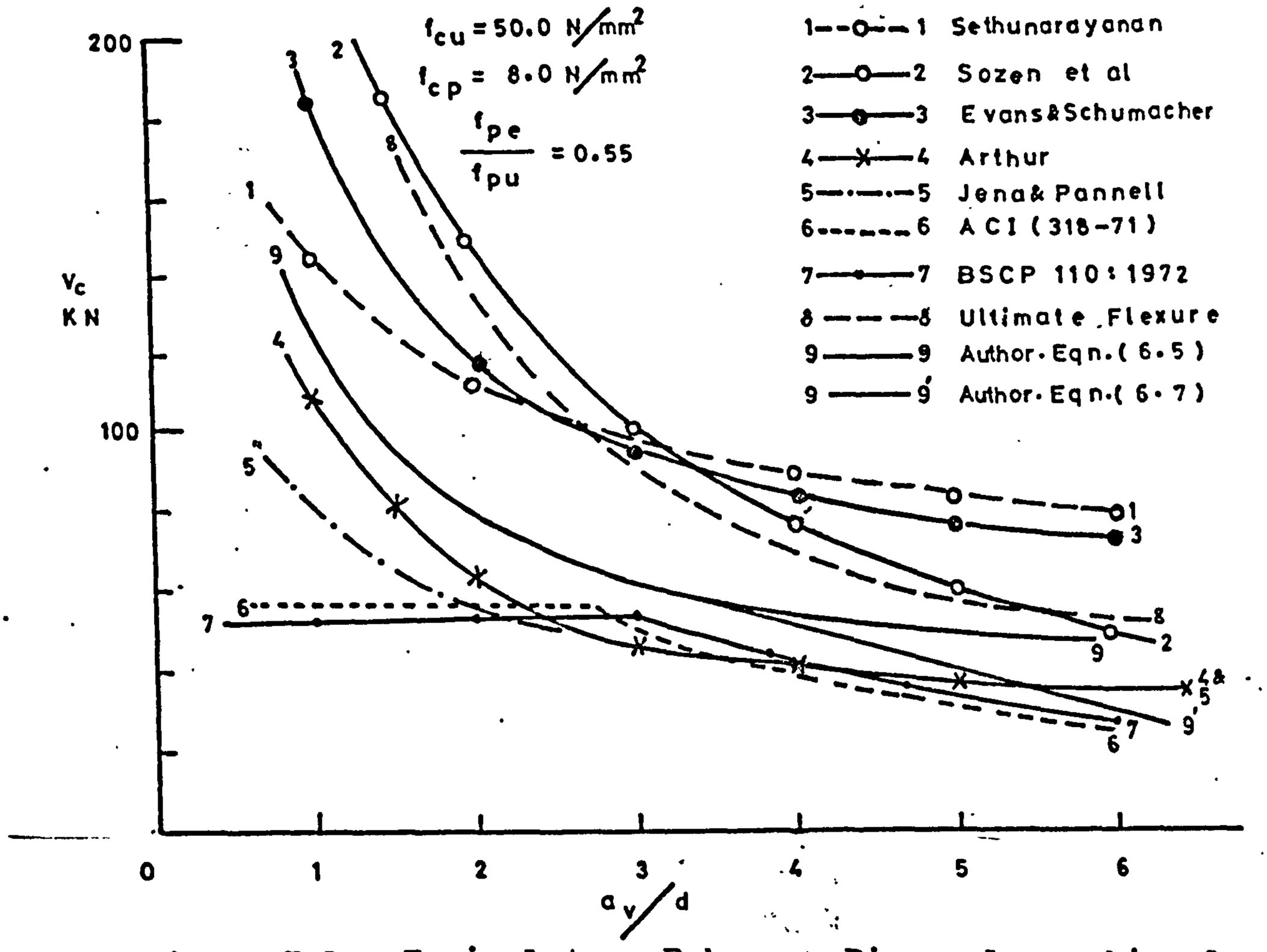

Figure 7.1: Typical type B-beam. Diagonal cracking load as predicted by published expressions and design rules in terms of $a_{v/d}$

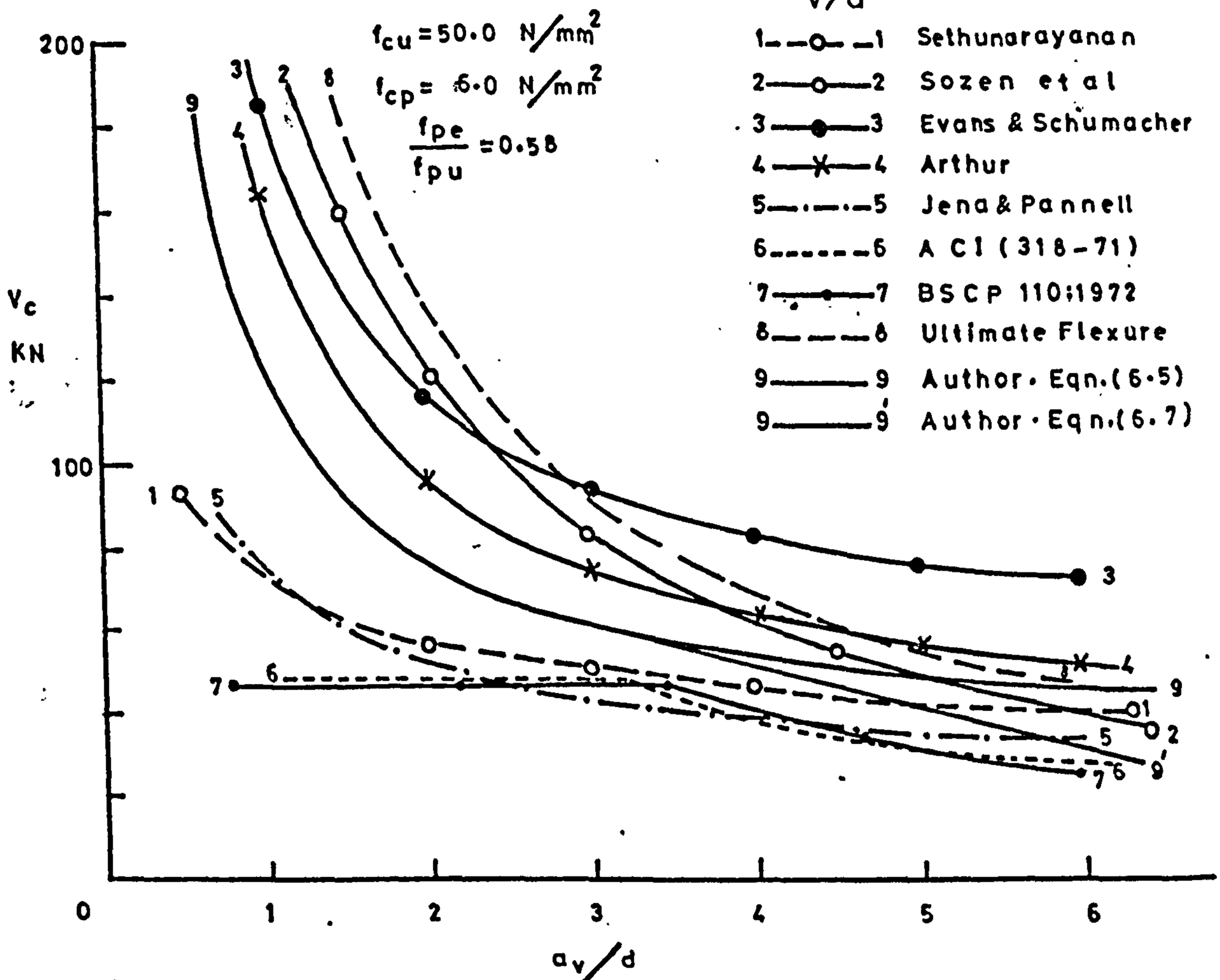

Figure 7.2: Typical type F-beam. Diagonal cracking load as predicted by published expressions and design rules in terms of $a_{v/d}$

range of $^{a}v/d$. Both BSCP 110: 1972 and ACI (318-71) are conservative for $^{a}v/d < 2.0$, but give results close to the modified curve (equation 6.7) at higher values of $^{a}v/d$.

Figure 7.2 shows the comparison based on the F type beam with a thicker flange (h_f = 87.5 mm). Here Sethunarayanan and Jena and Pannell give conservative predictions whilst Evans and Schumacher and Arthur overestimate the value of V_c. Sozen et al show some agreement for $^{a}v/d > 4.0$. BSCP 110: 1972 and ACI (318-71) Building Code underestimate the value of V_c at $^{a}v/d < 2.0$, but they are close to the modified curve (equation 6.7) for $^{a}v/d > 3.0$. Both the British and the American Codes of necessity, being design rules, stipulate lower bounds to the expected range of test results, so they would be expected to appear conservative.

7.3. Comparison of Equation 6.5 for one- or two-point Loading with Published Test Results:

Figures 7.3.1 and 7.3.2 and Table 7.1.1 show a comparison between equation 6.5 and test results reported by different authors[34-36, 41-45, 47,49] for various rectangular, I and hollow sections with different concrete strength, prestressing levels and $^{a}v/d$ ratios. Some of these beams were of zero prestressing force[36,49] and others contained web reinforcement[47,49].

From Figure 7.3.1 and Table 7.1.1 it can be seen that, of the beams reported by Hanson and Hulsbos[47] and Bennett et al[49] with web reinforcement, the test

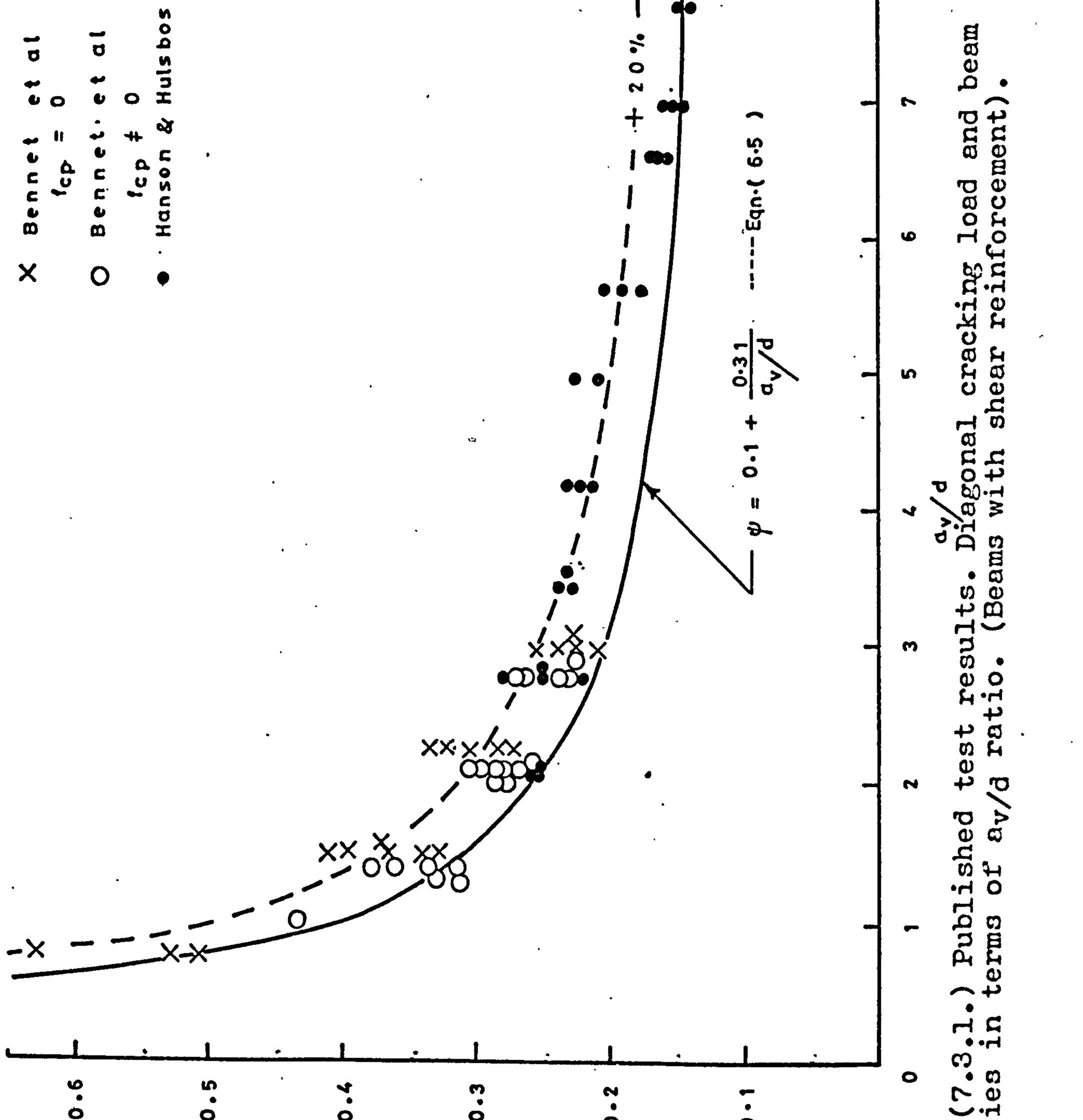

Figure (7.3.1.) Published test results. Diagonal cracking load and beam properties in terms of a_v/d ratio. (Beams with shear reinforcement).

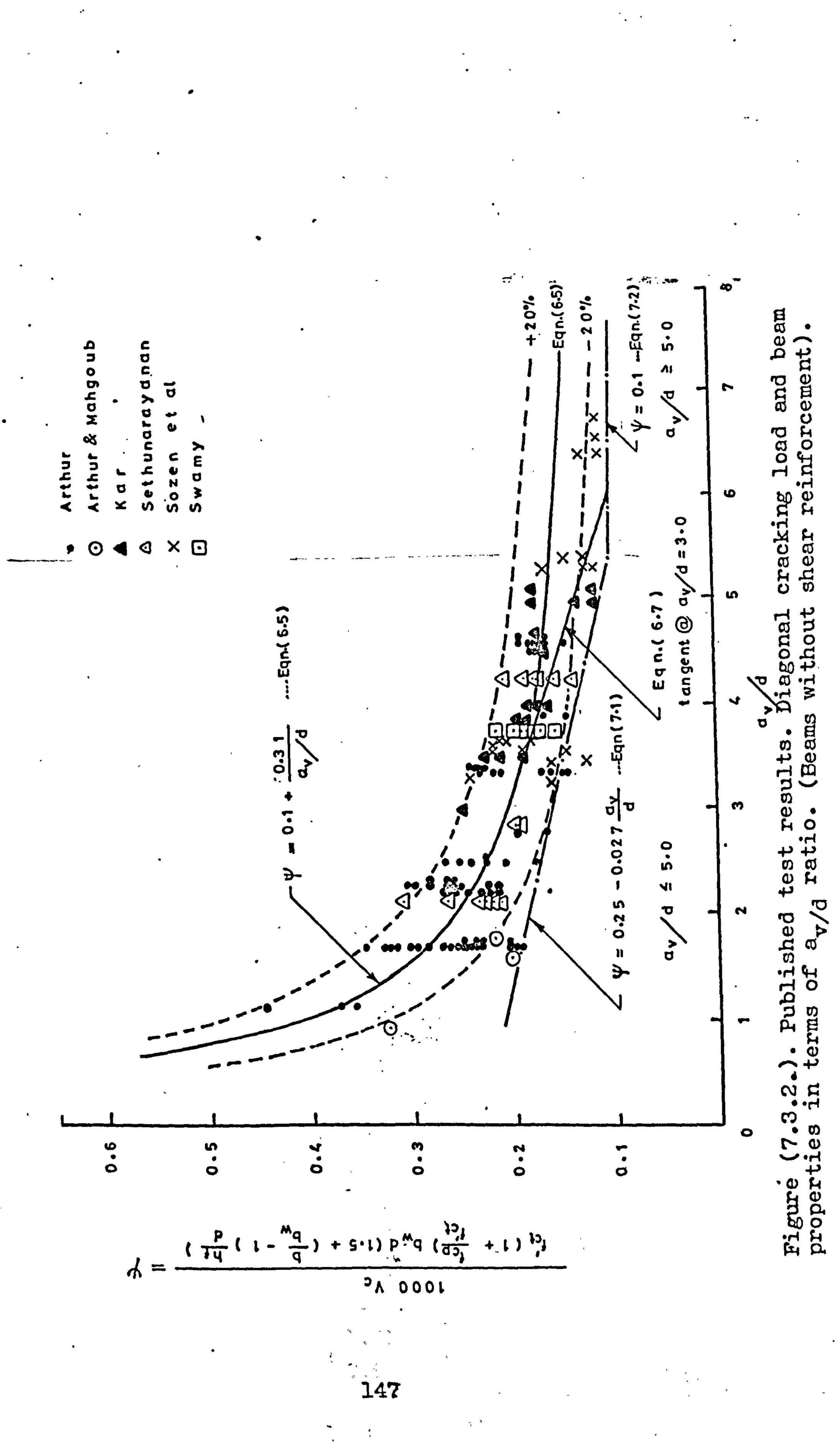

Figure (7.3.2.). Published test results. Diagonal cracking load and beam properties in terms of a_v/d ratio. (Beams without shear reinforcement).

$$\psi = \frac{f'_{ct}\left(1 + \frac{f'_{cp}}{f'_{ct}}\right) b_w d\,(1.5 + (\frac{b}{b_w} - 1)\frac{h_f}{d})}{1000\ V_c}$$

TABLE 7.1.1.

Comparison of test results for beams under one-or two-point loads by other investigators[34,36,41,43 - 45,47,49] with values calculated with the diagonal tension cracking equation(6.5).

Author	Beam mark	$\frac{a_v}{d}$	$\frac{V_c \text{ Expt.}}{V_c \text{ Calc.}}$	Author	Beam mark	$\frac{a_v}{d}$	$\frac{V_c \text{ Expt.}}{V_c \text{ Calc.}}$
[34] Sethuna-rayanan	1	2.84	0.94	[36] Sozen et al $f_{cp} \neq 0$	C1233	3.57	1.17
	2	4.26	0.90		1257	3.63	1.14
	9	"	1.20		2231	3.31	1.25
	10	2.12	0.89		2240	3.65	1.11
	11	2.13	1.25	[36] Sozen et al $f_{cp} = 0$	B3211	3.46	0.64
	13A	2.12	0.92		19	3.53	0.71
	13B	4.24	1.07		31	3.53	0.99
	14	2.83	0.92		34	3.56	0.86
	15A	2.13	0.86		41	3.40	0.92
	15B	4.26	0.82		54	3.47	0.85
	17A	2.13	1.07		C3211	3.25	.89
	17B	4.26	1.01		22	3.60	1.05
	21A	2.13	0.95		37	3.60	1.07
	21B	4.26	1.00		42	3.56	0.77
					50	3.37	0.87
[36] Sozen et al $f_{cp} \neq 0$	A1143	6.55	0.73		80	3.60	1.06
	1151	6.40	0.86				
	1153	6.73	0.77	[41] Swamy	S1	3.75	1.04
	1196	6.42	0.73		SII	"	1.19
	B1120	5.29	0.79		SIII	"	1.08
	1129	5.40	0.78		SIV	"	0.94
	1140	"	0.91		SV	"	0.86
	1210	3.24	0.81		SVI	"	1.02
	1261	3.64	1.10				
	2126	5.29	0.73	Kar[43]	A-1	5.00	0.74
	2265	3.62	0.96		-2	"	0.73
	3115	5.29	1.04		-4	3.50	1.20
	3231	3.53	1.01		-5	3.00	1.22
	3254	3.47	0.85		-6	4.00	0.98

TABLE 7.1.1. (Cont'd)

Author	Beam mark	$\frac{a_v}{d}$	$\frac{V_{c\ Expt.}}{V_{c\ Calc.}}$	Author	Beam mark	$\frac{a_v}{d}$	$\frac{V_{c\ Expt.}}{V_{c\ Calc.}}$
Kar[43]	A-7	3.86	1.07	(44) Arthur	A24	3.43	1.19
	-8	4.14	0.98		25	"	1.25
	-9	3.86	1.03		26	"	1.21
	-10	5.00	1.07		B1	3.36	0.82
	-12	4.00	1.00		2	"	0.88
	B-3	3.50	1.11		3	2.52	1.02
	-4	4.00	0.92		"	"	1.11
	-5	4.50	0.97		4	1.68	1.12
	-6	4.67	1.06		5	2.52	1.18
	-7	3.50	1.00		6	1.68	0.86
	-9	5.00	0.84		7.	"	0.87
	-10	5.00	1.09		"	"	1.22
(44) Arthur					8	2.52	1.02
	A1	2.28	1.09		"	"	1.07
	2	4.57	1.06		9	3.36	0.75
	4	"	0.97		"	"	0.77
	5	2.28	1.26		10	1.68	1.03
	6	"	1.27		"	"	1.11
	8	"	1.09		"	1.12	0.98
	9	"	1.13		11	3.36	1.10
	10	"	1.19		"	"	1.20
	"	"	1.12		12	2.24	0.92
	11	"	1.08		"	"	0.96
	12	"	1.06		C1	1.68	1.00
	13	"	1.19		"	"	1.05
	17	4.57	1.12		2	1.12	0.94
	18	"	1.06		3	2.24	1.09
	19	"	0.87		"	"	1.12
	"	"	1.12		6	1.12	1.18
	20	"	1.05		7	2"24	0.89
	"	"	1.05		"	"	0.93
	21	"	1.03		"	"	0.90
	22	"	0.98		"	"	1.02
	23	3.43	1.23		8	1.68	0.86

TABLE 7.1.1 (Cont'd)

Author	Beam mark	$\frac{a_v}{d}$	$\frac{V_c \text{ Expt.}}{V_c \text{ Calc.}}$
(44) Arthur	C8	1.68	0.95
	"	"	0.14
	D1	3.36	1.21
	2	3.92	0.82
	3	2.52	0.78
	"	"	0.91
	4	1.68	0.69
	"	"	0.70
	"	"	0.82
	"	"	0.91
	5	"	0.70
	"	"	0.84
	"	"	0.90
	"	"	0.88
	E1	2.80	0.79
	2	"	0.93
	3	3.92	0.93
	4	1.68	0.66
	"	"	0.80
	"	"	0.81
	"	"	0.82
Arthur & (45) Mahgoub	1	1.68	0.70
	2	1.76	0.80
	3	0.91	0.73
Hanson & (47) Hulsbos (with web reinforcement)	FXI	3.39	1.26
	"	"	1.19
	F1	2.12	1.08
	"	"	1.05
	2	2.82	1.35
	"	"	1.19
	3	"	1.20
	"	"	1.08
	5	3.52	1.24
Hanson & (47) Hulsbos (with web reinforcement)	F6	7.05	0.99
	"	"	1.11
	7	4.24	1.33
	"	"	1.28
	8	"	1.24
	9	5.64	1.15
	"	6.34	1.04
	10	4.94	1.31
	"	"	1.20
	13	5.64	1.33
	"	"	1.21
	14	6.35	1.12
	"	"	1.07
	15	7.05	1.02
	16	7.76	1.02
	"	"	0.99
(49) Bennett et al (with web reinforcement) f_{cp}= 0	A03	0.75	1.00
	13	1.50	1.12
	23	2.25	1.41
	33	3.00	1.25
	B02	0.75	1.23
	12	1.50	1.07
	22	2.25	1.17
	C03	0.75	1.04
	13	1.50	1.31
	23	2.25	1.20
	33	3.00	1.12
	D13	1.50	1.21
	23	2.25	1.37
	33	3.00	1.03
	E13	1.50	1.21
	33	3.00	1.17
	F13	1.50	1.36
	23	2.25	1.30
	33	3.00	1.12

TABLE 7.1.1. (Cont'd)

Author	Beam mark	$\frac{a_v}{d}$	$\frac{V_c \text{ Expt.}}{V_c \text{ Calc.}}$
(49) Bennett et al (with web reinforcement) $f_{cp} \neq 0$	G23	2.00	1.10
	33	3.00	1.14
	H13	1.40	1.06
	23	2.10	1.11
	23	2.80	1.30
	33	1.00	1.07
	J12	2.00	1.14
	22	2.10	1.14
	K13	1.40	1.14
	23	2.10	1.21
	33	2.80	1.14
	L13	1.40	1.19
	23	2.10	1.23
	33	2.80	1.26
	M13	1.40	0.99
	13	"	1.04
	23	2.10	1.15
	33	2.80	1.11
	N13	1.40	0.99
	23	2.10	1.07

TABLE 7.1.1. (Cont'd)

Mean value of ratio and standard deviation.

Author	No. of results	Mean Value of ratio	Standard deviation
Sethunarayanan	14	0.99	0.125
Sozen et al $f_{cp} \neq 0$	18	0.93	0.171
Sozen et al $f_{cp} = 0$	12	0.89	0.138
Swamy	6	1.02	0.114
Kar	17	1.00	0.136
Arthur	76	1.00	0.155
Hanson and Hulsbos (with web reinforcement)	25	1.16	0.114
Bennett et al (with web reinforcement) $f_{cp} = 0$	19	1.19	0.119
Bennett et al (with web reinforcement) $f_{cp} \neq 0$	20	1.13	0.082

results were more or less within or slightly above the + 20% bound. This may mean that the presence of web reinforcement has a negligible effect upon the value of cracking load calculated according to equation 6.5. Figure 7.3.2, for beams without web reinforcement, shows that at higher values of $^{a}v/d$, some tests reported by Sozen et al[36] seem to lie below the lower bound (-20%) of equation 6.5, but not outside the modified curve given by equation 6.7. On the other hand about 90% of the tests reported by Kar[42,43] on rectangular beams failing in shear-ccmpression at $3.0 \leqslant {}^{a}v/d \leqslant 5.0$, gave cracking load values above the lower bound (-20%) of equation 6.5 as shown on Table 7.2 column 7. So it can be seen from Figure 7.3.2 that equation 6.7, after being multiplied by a reduction factor of 0.8, can be taken as a lower bound for predicting the cracking load value for design purposes for $^{a}v/d < 5.0$ and that for $^{a}v/d > 5.0$ the effect of $^{a}v/d$ can be ignored. Thus, for $^{a}v/d \leqslant 5.0$

$$\frac{1000\ V_c}{f'_{ct}\left(1 + \frac{f_{cp}}{f'_{ct}}\right) b_w\ d\left[1.5 + \left(\frac{b}{b_w} - 1\right)\frac{h_f}{d}\right]} = 0.25 - .027\ \frac{a_v}{d} \qquad (7.1)$$

whilst for $^{a}v/d > 5.0$

$$\frac{1000\ V_c}{f'_{ct}\left(1 + \frac{f_{cp}}{f'_{ct}}\right) b_w\ d\left[1.5 + \left(\frac{b}{b_w} - 1\right)\frac{h_f}{d}\right]} = 0.1 \qquad (7.2)$$

7.4. Comparison of the Shear-compression Equation 6.28 with Experimental Results and other Published Shear-compression Equations.

7.4.1. Some of test results in this investigation and some others reported by Kar[43] and Arthur[44] on rectangular and I - section beams show that the final mode of shear failure for those specimens was shear-compression failure initiated by a flexure-shear crack. The ratio of the experimental to the predicted shear force at failure is shown in Table 7.2 column 8. The experimental values of 81% of test results were within ± 20% of the calculated values given by equation 6.28.

7.4.2. Comparison of equation 6.28 with other published shear-compression equations:

To compare equation 6.28 with other published expressions[40,43], the test results of Kar's[43] prestressed concrete beams were studied. The comparison was made between the experimental and the calculated value predicted by each expression as shown in Table 7.3 which also shows the mean value of that ratio and the standard deviation in each case. The scatter of the experimental to calculated values in terms of a_v/d is shown in Figure 7.4. From Table 7.3 and Figure 7.4, equation 6.28 seems to predict the shear force at shear-compression failure reasonably well when compared with Kar's expression which was derived from the same experimental data from which this comparison was made. Kar's expression is tedious, and Evans and Schumacher's[40] expressions, i.e. equations 2.25 - 2.28 have their limitations as they are governed by the percentage of the main steel, ρ, as discussed

TABLE 7.2.

Comparison of results of tests on beams failing in shear-compression under one- or two-point loads by Kar[43], Arthur[44] and the present investigator, with equation (6.5) and shear-compression equation (6.28).

(1) Beam mark	(2) f_{cu} N/mm^2	(3) f_{cp} N/mm^2	(4) $\frac{a_v}{d}$	(5) V_c Expt. KN	(6) V_u Expt. KN	(7) $\frac{V_c \text{ Expt.}}{V_c \text{ Calc.}}$	(8) $\frac{V_u \text{ Expt.}}{V_u \text{ Calc.}}$
(43) (Kar)							
A-1	44.9	2.57	5.00	22.0	26.4	0.74	0.95
-2	43.5	2.07	5.00	19.6	24.0	0.73	0.96
-4	36.0	2.65	3.50	40.1	55.0	1.20	1.31
-5	43.0	3.35	3.00	51.4	68.5	1.22	1.27
-6	35.0	1.57	4.00	24.5	38.2	0.98	1.12
-7	37.8	2.64	3.86	34.3	45.0	1.07	1.02
-8	42.7	4.03	4.14	39.2	43.1	0.98	0.94
-9	42.3	4.66	3.86	46.5	53.9	1.03	1.04
-10	39.8	4.66	5.00	34.3	40.1	1.07	0.98
-12	43.6	3.29	4.00	36.7	43.6	1.00	1.02
B-3	36.4	2.45	3.50	24.5	28.4	1.11	0.93
-4	40.0	2.42	4.00	19.6	28.9	0.92	1.01
-5	35.0	2.06	4.50	17.6	25.5	0.97	0.98
-6	37.7	2.98	4.67	23.0	26.9	1.06	0.93
-7	41.4	3.28	3.50	26.4	39.7	1.00	1.17
-9	41.6	3.28	5.00	19.1	26.0	0.84	0.94
-10	44.3	4.14	5.00	28.4	33.3	1.09	1.12
(44) Arthur							
D2	56.7	5.09	3.92	37.8	50.3	0.82	0.83
E3	53.3	5.05	3.92	48.5	52.7	0.93	0.85
G6 *	49.7	3.88	3.00	94.5	98.0	0.84	0.97
C19 *	51.0	2.45	5.25	31.1	54.5	1.03	0.91

* Author's beams.

TABLE 7.3

Comparison of the shear-compression equation(6.28) and other published expressions[40,43] with experimental results obtained by Kar[43] on rectangular prestressed concrete beams.

Beam mark	$\frac{a_v}{d}$	Experimental shear-compression failure load / Calculated shear-compression failure load		
		Equation 2.25[40]	Equation 6.28	Kar[43]
A-1	5.00	1.25	0.95	0.96
-2	5.00	1.24	0.96	1.03
-4	3.50	1.11	1.31	1.19
-5	3.00	1.05	1.27	1.16
-6	4.00	1.09	1.12	1.18
-7	3.86	1.00	1.02	1.07
-8	4.14	0.85	0.94	0.92
-9	3.86	0.94	1.04	1.01
-10	5.00	0.92	0.98	0.98
-12	4.00	0.84	1.02	1.05
B-3	3.50	0.85	0.93	0.88
-4	4.00	0.93	1.01	0.99
-5	4.50	0.95	0.98	1.08
-6	4.67	1.05	0.93	0.96
-7	3.50	1.03	1.17	1.10
-9	5.00	0.96	0.94	1.01
-10	5.00	1.12	1.12	1.19
mean		1.011	1.041	1.045
standard deviation	0.127		0.118	0.095

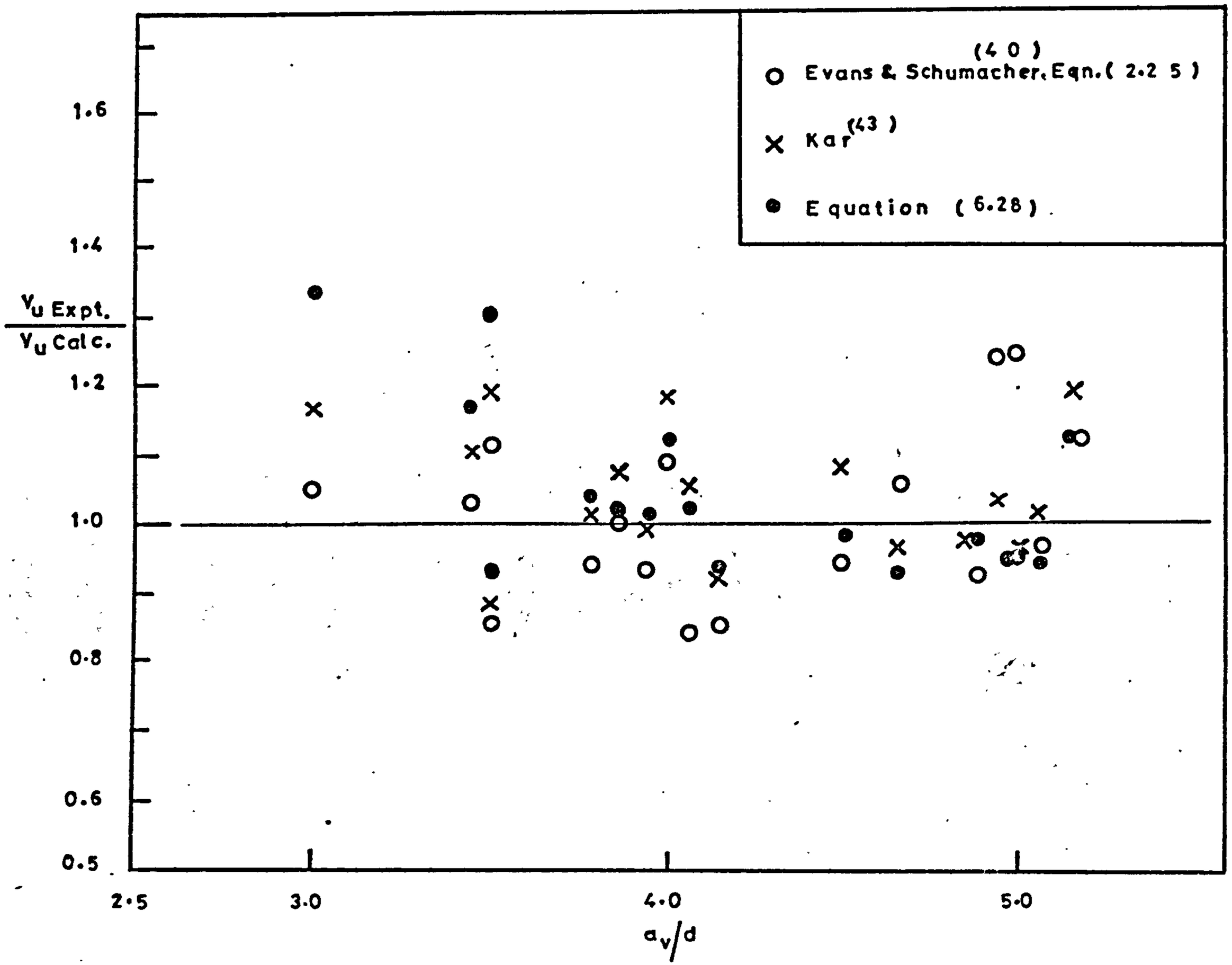

Figure 7.4: Ratio of experimental to calculated shear force at shear-compression failure in terms of $a_{v/d}$ ratio.

in Section 2.5.2.5.

As mentioned in Section 6.1, because of the many variables involved in determining the final mode of failure in shear for beams without shear reinforcement, and because of indeterminate nature of some of these variables, for design purposes the useful capacity of such beams in shear under one - or two-point loads should be limited to the values given by equations 7.1 and 7.2.

7.5. Comparison of the Expressions Developed for Uniformly Loaded Beams with Test Results and Published Expressions.

7.5.1. Comparison of the diagonal tension equation 6.12 and test results.

Figure 6.10 shows the test results in the present investigation and those reported by others[43,47,48] on rectangular and I - section beams plotted with equation 6.12. Table 6.2 shows this scatter in the form of a comparison between the experimental and calculated diagonal tension cracking load predicted by equation 6.12. From Table 6.2 and Figure 6.10, it can be seen that all the experimental results obtained by Hanson and Hulsbos[47], Arthur et al[48] and this investigation for the diagonal tension cracking load were within $\pm$ 20% of the value given by equation 6.12, even for those specimens tested at l/d as high as 17.78 (D-type beam stressed with two 12.5 mm strands). In this investigation a common feature in all those beams was that the

diagonal crack opened on a line either through or in the vicinity of a reaction, as mentioned in Section 6.1.3.1. On the other hand, Kar's[43] specimens which were of rectangular cross-section, all failed in shear-compression initiated by a flexure-shear crack. His experimental results are also shown in Figure 6.10 for the sake of comparison with equation 6.12. The overestimation of cracking load given by equation 6.12 in such instances is shown in Table 7.4 column 7. Equation 6.12 even predicts values greater than the shear-compression failure load as can be seen by comparing columns 6 and 7 of Table 7.4, but this is to be expected since the final mode of failure was not diagonal tension cracking. The only exceptional case was (A-U-9), with zero prestressing force, in which case the diagonal tension cracking load predicted by equation 6.12 was 0.78 of the experimental ultimate shear-compression failure load. This case was discussed in section 6.3.2, and was illustrated by the example given in Figure 6.18.2.

7.5.2. Comparison of the shear-compression equations 6.44 and 6.45 with Kar's[43] test results.

Kar's rectangular beams were found to fail in shear-compression before the formation of the diagonal tension cracks. In the previous section it was pointed out that values predicted by equation 6.12 were greater than the experimental shear-compression failure loads. The expressions developed for the shear-compression

TABLE 7.4

Comparison of results of tests on uniformly loaded rectangular beams by Kar[43] failing in shear-compression with values calculated by shear-compression equations (6.44) and (6.45)

(1) Beam mark	(2) f_{cu} N/mm^2	(3) f_{cp} N/mm^2	(4) $\frac{l}{d}$	(5) $q_c l$ Expt KN	(6) $q_u l$ Expt. KN	(7) $q_c l$ Calc. KN Eqn. 6·12	(8) $\frac{q_u l}{q_u l}$ Expt. / Eqn. 6.45	(9) $\frac{q_u l}{q_u l}$ Expt. / Calc. Eqn. 6.44
A-U-2	44.3	1.96	12.87	69.9	91.0	102.8	0.98	0.82
-3	48.3	3.35	"	103.2	128.8	134.0	1.23	1.03
-4	45.7	4.02	"	103.2	119.9	145.4	1.15	0.96
-5	35.9	3.23	"	81.0	97.7	122.7	1.17	0.99
-6	35.9	3.34	"	92.1	116.6	124.5	1.34	1.13
-8	34.8	2.64	"	81.0	107.8	109.5	1.30	1.10
-9	38.0	0.00	"	42.1	74.3	57.7	1.03	0.86
-11	42.3	4.02	"	108.8	125.5	170.0	1.19	1.06
B-U-1	48.3	3.28	15.00	63.9	80.6	90.0	1.21	1.07
-2	42.3	4.14	"	57.9	65.0	98.1	1.05	0.90
-4	45.7	4.15	"	75.0	79.4	101.4	1.18	1.01
-5	39.6	3.33	"	47.2	62.8	81.4	1.09	0.94
			Mean value of ratio				1.16	0.99
			Standard deviation				0.107	0.096

failure load in Section 6.2.8, equations 6.44 and 6.45 were used to predict the shear-compression failure load for Kar's beams, and the results of comparison with the experimental values are shown in Table 7.4 columns 8 and 9. Column 9 shows that the values predicted by equation 6.44 are in reasonable agreement with the experimental values, while equation 6.45 gave conservative predictions, as shown in column 8. Thus it can be concluded that the value of the total uniformly distributed load at shear-compression failure can well be predicted by equation 6.44.

Hence, for design purposes, the total uniformly distributed load at failure should be limited to 0.8 times the lesser of that given by equations 6.12 and 6.44.

7.5.3. Comparison of the diagonal tension equations with other published expressions.

A comparison between equations 6.12 and 6.17 developed for predicting the total uniformly distributed load at diagonal tension cracking and that given by Arthur et al[48], equation 2.37, is shown in Figures 7.5 and 7.6, together with the experimental results obtained from type B and F beams in this investigation. Arthur et al's equation 2.37 tends to underestimate the value of $q_c l$ for $l/d > 9.0$ as it predicts a zero value at $l/d = 12.47$ (see Section 2.5.3.3.). For the type B beams, which were of small flange depth compared with those reported by Arthur

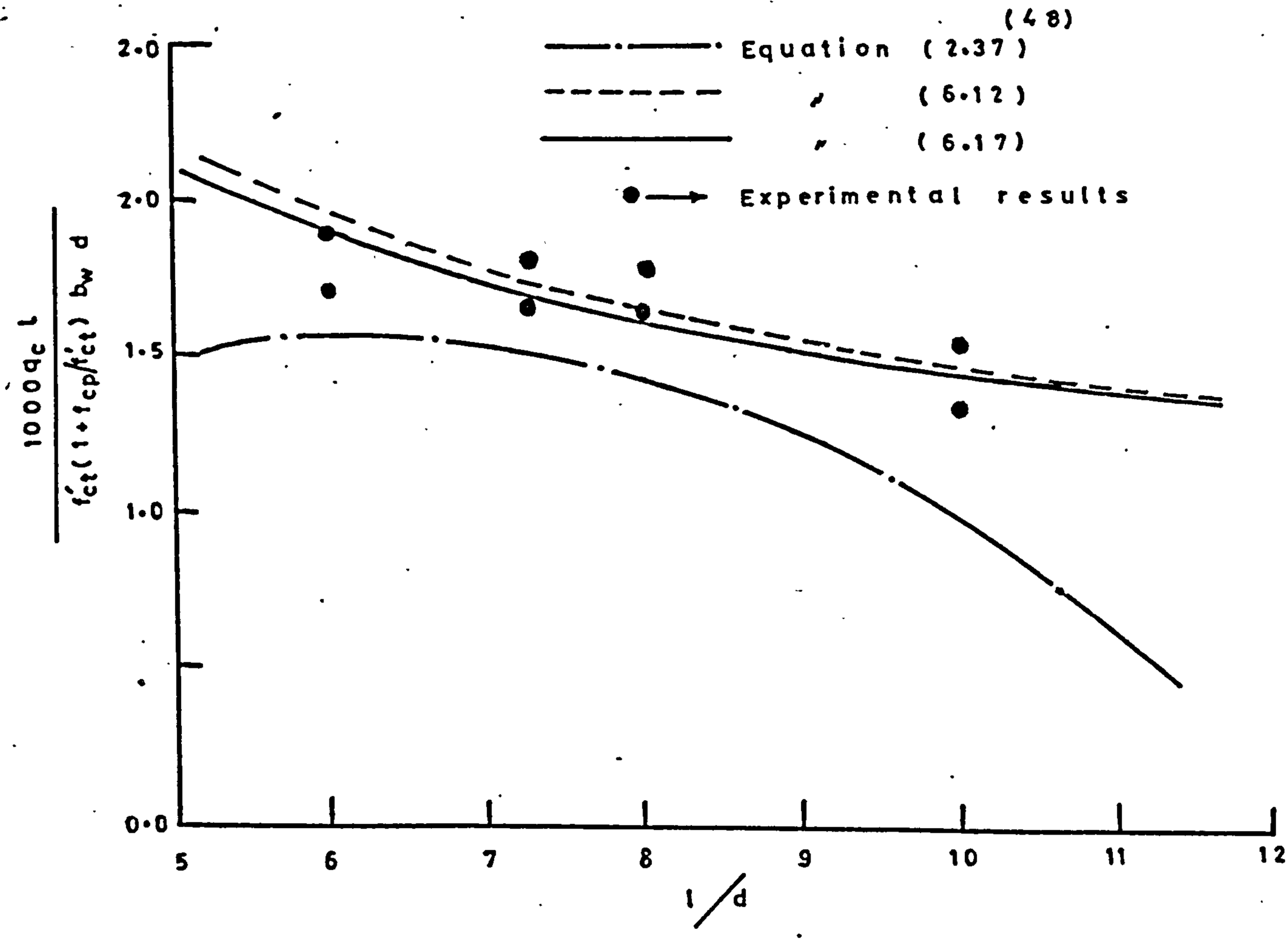

Figure 7.5.a. Type B beam.

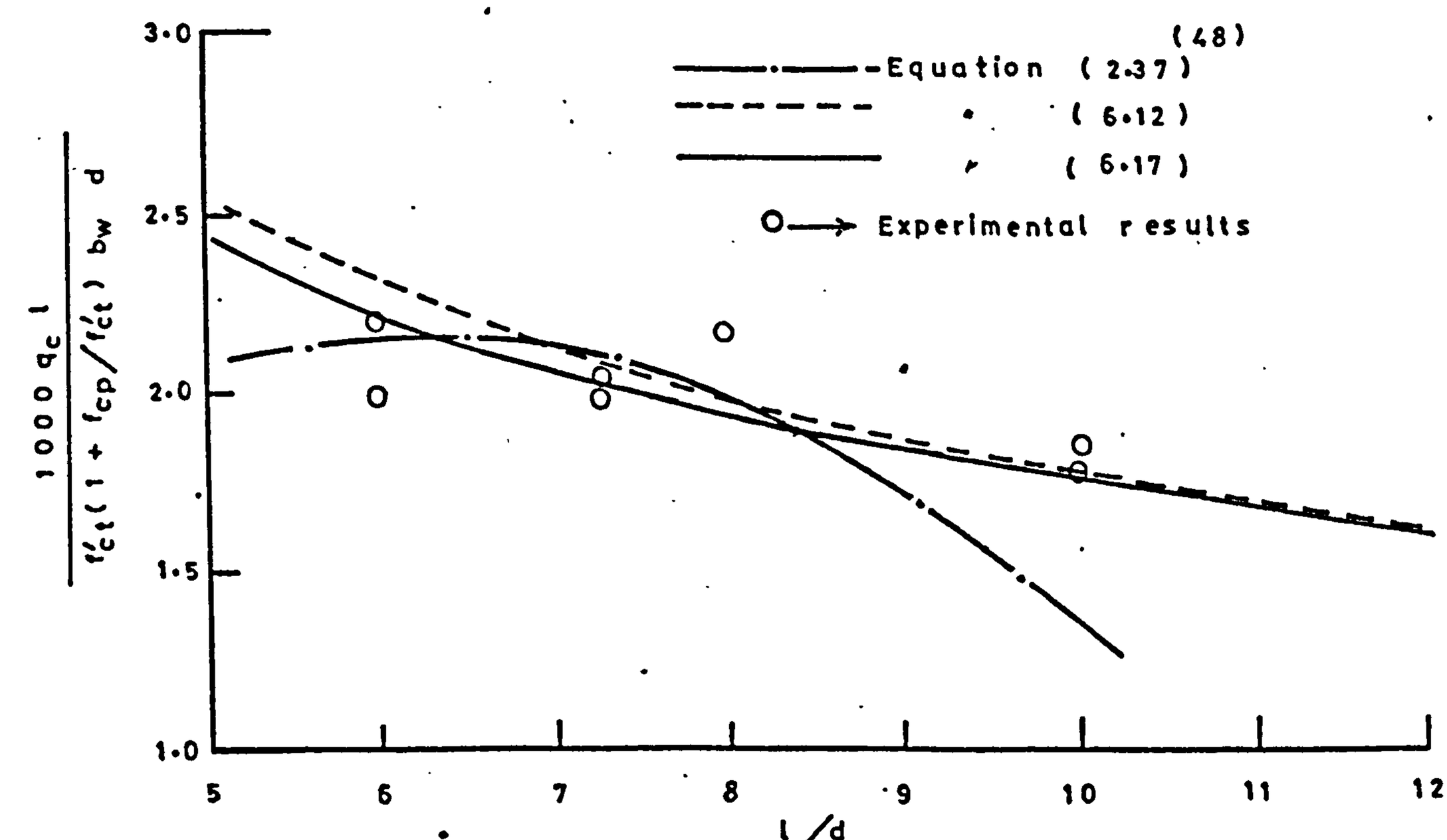

Figure 7.5.b. Type F beam.

Figure 7.5. Comparison of results of tests on type B and type F beams under uniform load with the proposed and Arthur et al[48] expressions for diagonal tension cracking load, $q_c l$.

et al, equation 2.37 underestimates at all L/d values. This is because, as mentioned in Section 2.5.3.3, of the arbitrary choice of the coefficient and the constant which describes the geometry of the flange.

CHAPTER 8

CONCLUSICNS AND RECOMMENDATIONS FOR FURTHER RESEARCH

8.1. Conclusions:

For the number of specimens tested and the range of variables tackled in this investigation, the following conclusions may be drawn:-

8.1.1. Distinctly different characteristics of behaviour were shown by the specimens after the formation of the diagonal tension crack. This behaviour could not be predicted from a knowledge of $^{a}v/d$ or $^{l}/d$ alone.

8.1.2. Because there are, at present, indeterminate variables controlling any margin of shear strength beyond inclined cracking, the useful ultimate shear strength of prestressed concrete beams without shear reinforcement should be limited to the inclined cracking shear force.

8.1.3. The flange projections of an I - section can contribute up to 40% of the value of the inclined cracking shear force depending on their configuration.

8.1.4. The diagonal tension cracking load can be predicted to an accuracy of ± 20% by the following expressions.

8.1.4.1. Under one - or two-point loading.

$$\frac{1000\ V_c}{f'_{ct}\ b_w\ d} = \left(1 + \frac{f_{cp}}{f'_{ct}}\right)\left[1.5 + \left(\frac{b}{b_w} - 1\right)\frac{h_f}{d}\right]\left(0.10 + \frac{0.31}{a_{v/d}}\right)$$

Equation (6.5)

where $\left(\frac{b}{b_w} - 1\right)\frac{h_f}{d} \not> 1.0$

8.1.4.2: Under uniformly distributed load:

$$\frac{1000\, q_c l}{f'_{ct}\, b_w\, d} = 2\left(1 + \frac{f_{cp}}{f'_{ct}}\right)\left[1.5 + \left(\frac{b}{b_w} - 1\right)\frac{h_f}{d}\right] \times \left(\frac{0.10}{1-2\lambda_c} + \frac{0.31}{l/d\ \lambda_c(1-\lambda_c)}\right)$$

Equation (6.12)

where λ_c is given by:-

$$\lambda_c^4 + \left(\frac{12.40}{l/d} - 2\right)\lambda_c^3 + \left(1 - \frac{18.6}{l/d}\right)\lambda_c^2 + \frac{9.30\lambda_c}{l/d} - \frac{1.55}{l/d} = 0$$

Equation (6.13)

and $\left(\frac{b}{b_w} - 1\right)\frac{h_f}{d} \not> 1.0$

The values of λ_c as a function of l/d is shown in Table 6.1 and the relation of $q_c l$ with l/d (equation 6.12) is shown graphically in Figure 6.10

8.1.5. The shear-compression failure load, based on Mohr's criterion of failure using a straight line envelope, can be calculated to within ± 20% using the following equations:-

8.1.5.1. Under one - or two-point loading:

$$V_u = v_{xy}\, k_u\, b\, d$$ Equation (6.28)

where

$$\left(\frac{v_{xy}}{f_{cu}}\right)^2 = \frac{1}{(1+\gamma)^2}\left[0.64 + 0.536\ (\gamma - 1)\ k_1 - 0.449\,\gamma\, k_1^2\right]$$

and k_1 is given by: Equation (6.26)

$$k_1^2\left(\frac{(1+\gamma)^2}{(a_v/d)^2} + 1.24\gamma\right) - 1.48\ (\gamma - 1)\ k_1 - 1.77 = 0$$

Equation (6.31)

$$k_u = \frac{\alpha \varepsilon_o}{\varepsilon_{pb} + \alpha\varepsilon_o - \varepsilon_{pe} - \frac{f_{pt}}{E_c}} \qquad \text{Equation (6.35)}$$

8.1.5.2. Under uniformly distributed load:

$$q_u l = \frac{6\ V_u\ l/d}{l/d + 3} \qquad \text{Equation (6.44)}$$

where $V_u = v_{xy}\ k_u\ b\ d$ as Equation (6.28)

and v_{xy} is given by equation 6.26 shown in (8.1.5.1), where

$$k_1 = 1 - \frac{0.33 \times 0.0035}{0.244 \times 10^{-3} \sqrt{f_{cu}}}$$

for $f_{cu} \geqslant 30.0\ N/mm^2$ and $l/d \geqslant 7.0$

k_u is given by equation 6.35 shown in (8.1.5.1).

8.1.6. The Code rules of BSCP 110: Part 1: 1972 and ACI (318-71) are rather conservative at lower $^{a}v/d$ ratios. The other published expressions tend to over-estimate the value of the cracking load at lower $^{a}v/d$ ratios.

8.1.7. When published test results are compared with equations 6.5, 6.7, 6.12, 6.28 and 6.44, close agreement is obtained over a wide range of variables. Compared with beams having shear reinforcement, the effect of the latter upon the value of the cracking shear force predicted by equation 6.5 is negligible.

8.1.8. For design purposes, the following expressions may be used:-

8.1.8.1. Under one - or two-point loading

$$\frac{1000\ V_c}{f'_{ct}\left(1+\frac{f_{cp}}{f'_{ct}}\right) b_w\, d\left[1.5+\left(\frac{b}{b_w}-1\right)\frac{h_f}{d}\right]} = 0.25 - 0.027\,\frac{a_v}{d}$$

Equation (7.1)

for $\frac{a_v}{d} \leq 5.0$

$= 0.10$ for $\frac{a_v}{d} > 5.0$ Equation (7.2)

where $\left(\frac{b}{b_w}-1\right)\frac{h_f}{d} \not> 1.0$

8.1.8.2. Under uniformly distributed load:
The lesser of the values given by equations 6.12 and 6.44 multiplied by a reduction factor of 0.80.

8.1.9. From the experimental observations, it seems necessary to provide a thin-webbed section with $b_{w/d} \leq 0.33$ at $2.0 \leq a_{v/d} \leq 4.0$ with a minimum amount of web reinforcement which will increase ductility and reduce considerably the likelihood of a sudden and catastrophic shear failure.

8.1.10. The experiments conducted on type D - beam under uniformly distributed load and the case studied in Figure 6.18.1 showed that shear-compression failure will never occur in uniformly loaded beams with $b_{w/d} \leq 0.25$ for all l/d values.

8.2. <u>Recommendations for Further Research</u>:

8.2.1. Equation 6.5 was developed from tests on beams with $\left(\frac{b}{b_w}-1\right)\frac{h_f}{d} \not> 1.0$ which are the types of beams most commonly used in general building construction, but it is questionable, at the present stage, if we could allow the flange projections to contribute

more than 40% to the value of V_c for higher values of $\left(\frac{b}{b_w} - 1\right) \frac{h_f}{d}$. Tang[97] quoted some long span box girder bridges of $\frac{b}{b_w} > 12.0$. Hence further investigation is needed on box beams with $b/b_w > 4.0$.

8.2.2. Some shear tests on full-scale prestressed concrete box beams are necessary to study the scale effect on equation 6.5. A few of these tests have been reported[45].

8.2.3. The shear failure behaviour of box beams and T-beams under uniformly distributed load should be investigated.

8.2.4. A slower rate of loading might be expected to lead to a lower shear cracking load. Beam E4 in Figure 5.1.g is an example of this possibility. Hence the effects of different rates of loading should be studied.

8.2.5. Equation 6.5 could be modified to predict the cracking load for the type of loading shown in Figure 8.1. The end reaction $q_c n l$, for such loading will be assumed to be given by the following equation:

$$\frac{q_c \, n \, l}{f'_{ct}\left(1 + \frac{f_{cp}}{f'_{ct}}\right) b_w \, d \left[1.5 + \left(\frac{b}{b_w} - 1\right)\frac{h_f}{d}\right]} = n\left(\frac{0.10}{(n-\lambda_c)} + \frac{0.62}{\lambda_c (2n-\lambda_c) l/d}\right) \qquad (8.1)$$

where $\lambda_c l$ is the distance of the critical section from a reaction and is given by the following equation:

$$\lambda_c^4 + \left(\frac{12.4}{l/d} - 4n\right)\lambda_c^3 + \left(4n^2 - \frac{37.2}{l/d}\right)\lambda_c^2 + 37.2n^2\lambda_c - \frac{12.4n^3}{l/d} = 0 \qquad (8.2)$$

Further research is needed covering this type of loading to verify equation 8.1.

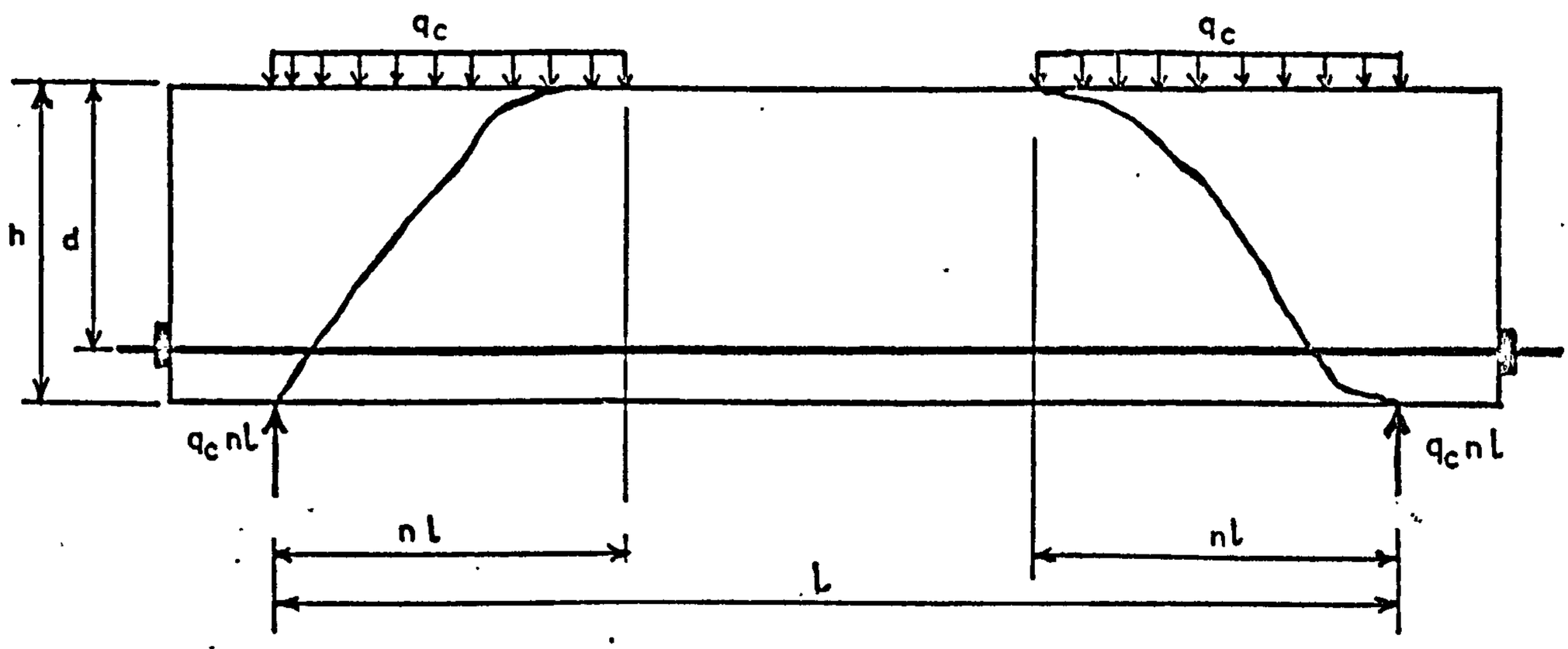

Figure 8.1

Appendix A

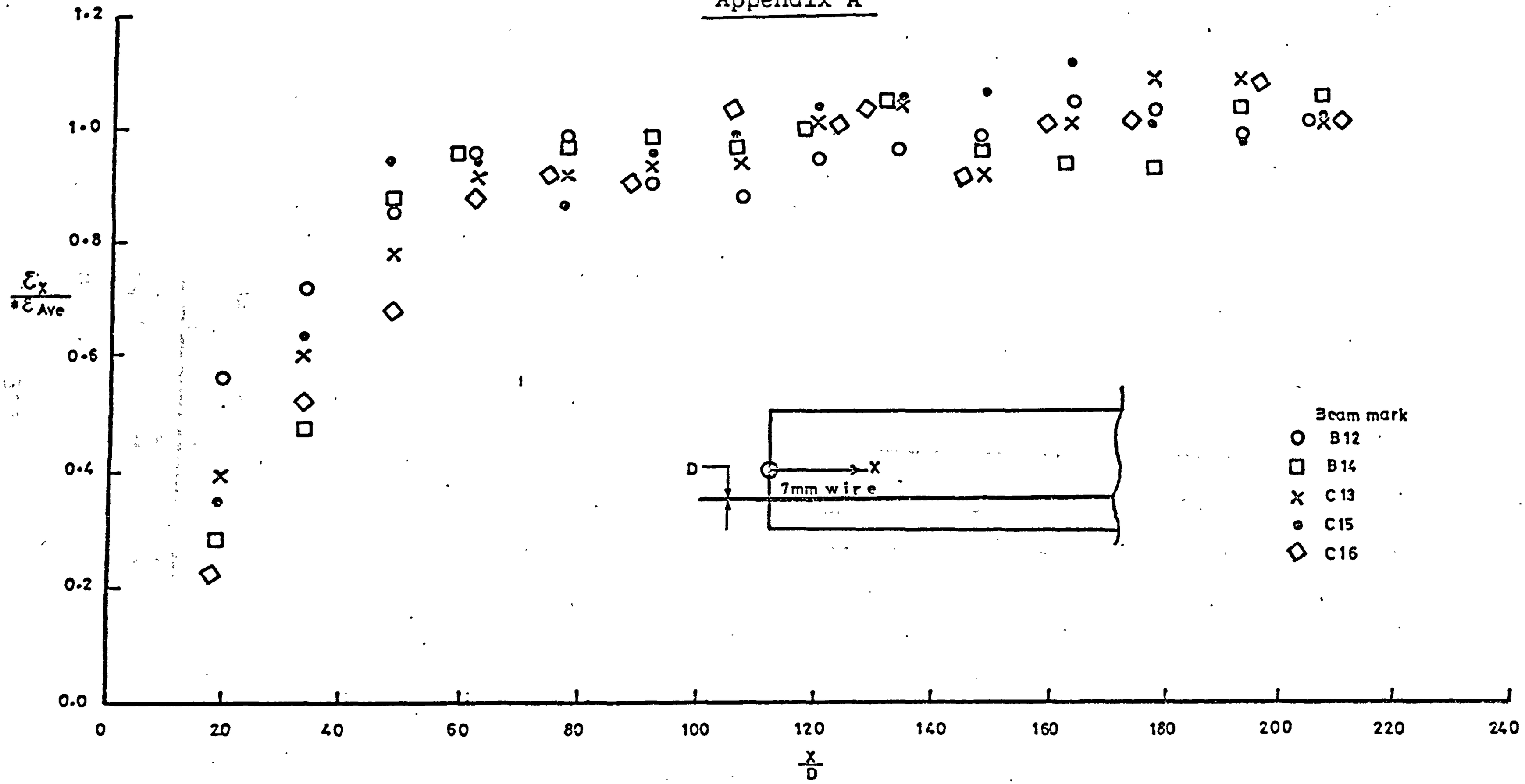

Figure A.1 : Transmission length with 7 mm diameter indented wire

$*\varepsilon_{Ave}$ = Average of all strains measured at $\frac{X}{D} > 100$

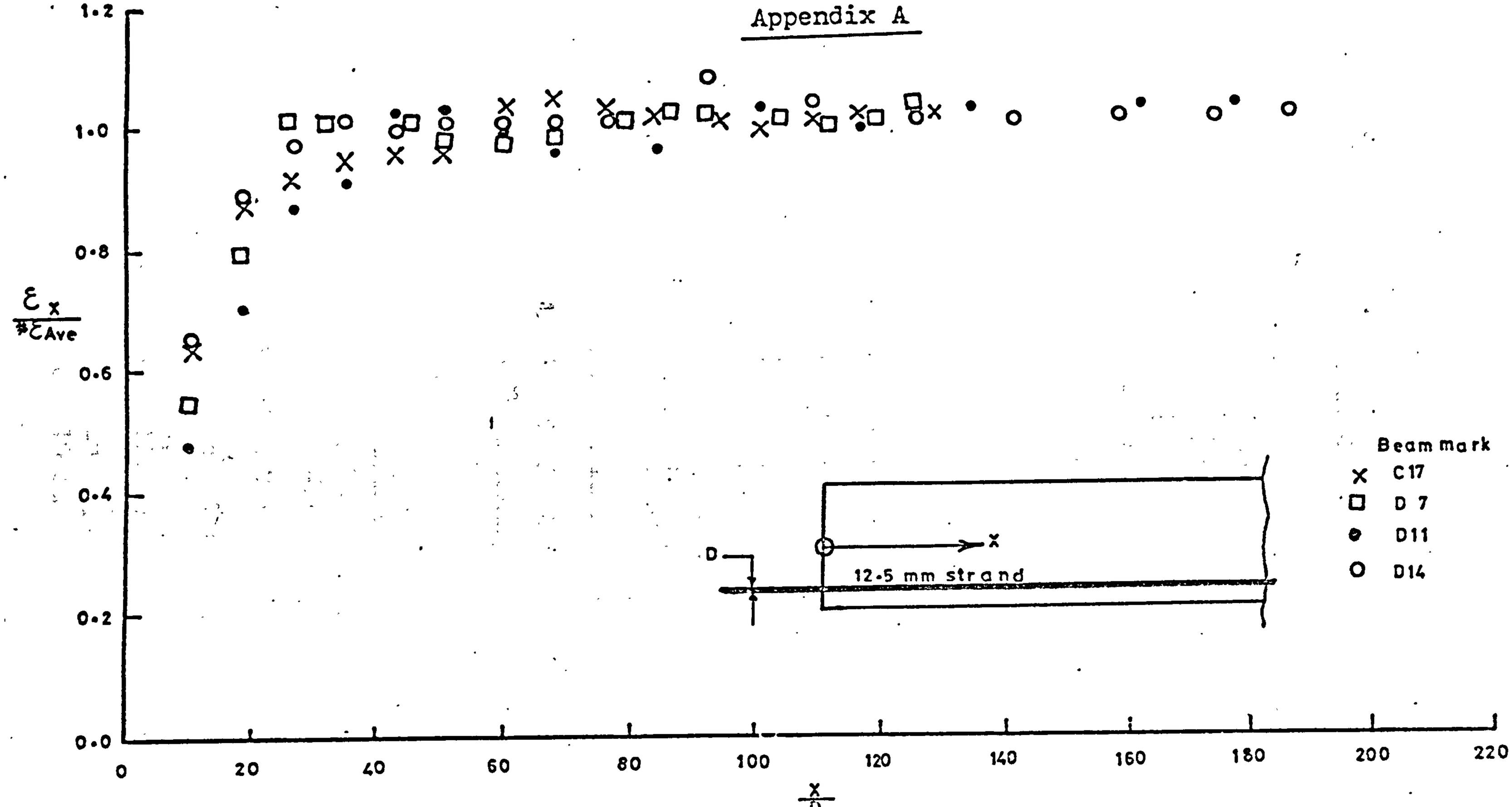

Figure A.2 : Transmission length with 12.5 mm diameter strand.

$*\varepsilon_{Ave}$ = Average of all strains measured at $\frac{X}{D} > 50$

APPENDIX B

B.1 Estimation of Prestress Losses in a Typical Beam

B.1.2. Geometric and material properties of the specimen

Beam mark	Age at test in days	Cement type	Cement content kg/m^3	Water cement ratio (W/C)	Humidity	f_{ci} N/mm^2	f_{cu} at test N/mm^2	Prestressing steel
A1	26	R.H.P.C.	500	0.40	Normal air	43.4	51.5	7mm indented wires

A_{ps} mm^2	Average $\varepsilon_{spi} \times 10^5$ mm/mm	E_s KN/mm^2	Average f_{pi} KN/mm^2	$A_c \times 10^{-3}$ mm^2	$I \times 10^{-7}$ mm^2	Perimeter exposed mm	Eccentricity (e) mm
269.5	546	200	109.2	33.44	34.97	1205	46.4

B.1.3. Estimation of the losses in accordance with BSCP 110: Part 1: 1972[30].

B.1.3.1. Elastic losses:

$$A_{ps} f_{ptr.} = \frac{A_{ps} f_{pi}}{1 + \frac{E_s}{E_{ci}} A_{ps} \left(\frac{1}{A_c} + \frac{e^2}{I}\right)}$$

$$A_{ps} f_{pi} = 294.3 \text{ KN}$$

$E_{ci}(f_{cu} = 43.4) = 32 \text{ KN/mm}^2$ (Table 1, BSCP 110)

$\frac{E_s}{E_{ci}} = 6.25$, $\frac{1}{A_c} = 299 \times 10^{-7}$, $\frac{e^2}{I} = 61.6 \times 10^{-7}$

and $\frac{1}{A_c} + \frac{e^2}{I} = 360.6 \times 10^{-7} \text{ mm}^{-2}$

$$A_{ps}f_{ptr} = \frac{294.3}{1 + 6.25 \times 269.5 \times 360.6 \times 10^{-7}} = \frac{294.3}{1.061}$$

= 277.5 KN i.e. Prestressing force in the wires after elastic shortening.

B.1.3.2. Relaxation, shrinkage and creep losses:

Shrinkage strain (Table 41) $= 300 \times 10^{-6}$

Specific creep (Clause 4.8.2.5.) $= \frac{1}{2} \times 48 \times 10^{-6} = 24 \times 10^{-6}$ mm/N^2

Prestressing force at transfer = 277.5 KN

Relaxation loss (from BS 2691: 1969) = 5%

= 13.9 KN

Average force during loss period = $277.5 - \frac{13.9}{2} = 270.6$ KN

B.1.3.3. First approximation.

Average stress in concrete at centroid of steel

$$= 270.6 \times 10^{3} \times \left(\frac{1}{A_c} + \frac{e^2}{I}\right) N/mm^2$$

$= 9.76$ N/mm^2

creep strain $= 9.76 \times 24 \times 10^{-6}$ mm/mm

$= 23.4 \times 10^{-5}$ mm/mm.

creep + shrinkage strain $= (30.0 + 23.4) \times 10^{-5}$

$= 53.4 \times 10^{-5}$ mm/mm.

Steel stress loss = 107 N/mm^2

Steel force loss $= 107 \times 269.5 \times 10^{-3}$ KN

= 28.8 KN

$A_{ps} f_{pe}$ (approximately) $= 277.5 - (13.9 + 28.8)$ KN

= 234.8 KN

B.1.3.4. Estimation of the effective prestressing force:

Average force during loss period $= 277.5 - \frac{(13.9 + 28.8)}{2}$

= 256.2 KN

Average stress in concrete at centroid of steel $= 256.2 \times 10^{-3} \times \left(\frac{1}{A_c} + \frac{e^2}{I}\right) N/mm^2$

$= 9.24$ N/mm^2

Creep strain $= 9.24 \times 24 \times 10^{-6}$ mm/mm

$= 22.2 \times 10^{-5}$ mm/mm

Creep + shrinkage strains $= (30.0 + 22.2) \times 10^{-5}$ mm/mm

$= 52.2 \times 10^{-5}$ mm/mm

Steel stress loss $= 104$ N/mm^2

Steel force loss $= 28.1$ KN

$\therefore A_{ps} f_{pe} = 277.5 - (13.9 + 28.1) = \underline{235.5 \text{ KN}}$

Total loss at test $= 100 - \frac{235.5}{294.5} \times 100$

$= \underline{20.0\%}$

B.1.4. Estimation of losses using CEB - FIP Recommendations[27].

B.1.4.1. Elastic losses:

$$A_{ps} f_{ptr} = \frac{294.3}{1 + \frac{E_s}{E_{ci}} A_{ps}\left(\frac{1}{Ac} + \frac{e^2}{I}\right)}$$

$E_{ci} = 6.6 \sqrt{0.8 f_{cu}}$ KN/mm^2 (Clause R 12 · 22)

$= 38.9$ KN/mm^2

$\frac{E_s}{E_{ci}} = 5.14$

$$A_{ps} f_{ptr} = \frac{294.3}{1 + 5.14 \times 269.5 \times 360.6 \times 10^{-7}}$$

$$= \frac{294.3}{1 + .05} = 280.3 \text{ KN}$$

i.e. Prestressing force in the wires after elastic shortening.

B.1.4.2. Creep strain: f (Clause R 12.31)

$$f = \left(\frac{\text{Stress in concrete at centroid of prestressing steel} \times \phi_t}{}\right) / E_{c\,28}$$

where ϕ_t is the creep coefficient

$E_{c\,28}$ = secant modulus of concrete at 28 days

ϕ_t is the product of five partial coefficients, each given in a form of a chart (see Figure B.1).

$$\phi_t = k_c\ k_d\ k_b\ k_e\ k_t$$

where

k_c depends on the environmental conditions and it gives the effect of drying under load, which is very large if the relative humidity is low.

k_d represents the combined effects of ageing and hydration as a function of the type of cement used.

k_b depends on the mix. It includes the effects of water cement ratio and cement content.

k_e covers the influence of the size and shape of the member in delaying drying.

k_t shows the development of creep with time, including the delaying effect of the larger sections.

In this case:

k_c = 2.30 (Normal air)

k_d = 0.70 (R.H.P. Cement and 21 day loading, detensioned after 5 days).

k_b = 1.00 (Water/cement ratio = 0.40 and cement content = 500 kg/m^3)

k_e is a function of the theoretical thickness e_m

where

$$e_m = \frac{\text{Area of section}}{\frac{1}{2}\text{ perimeter in contact with atmosphere}}$$

$$= \frac{33.44 \times 10^3}{60.25 \times 10^2}\ \text{cm} = 5.6\,\text{cm}$$

$\therefore\ k_e = 1.20$

k_t = 0.40 (e_m = 5.6 and time under load = 21 days)

$\therefore\ \phi_t = 2.3 \times 0.7 \times 1.0 \times 1.2 \times 0.4$

$= 0.773$

Figure B.1 : CEB-FIP Recommendations

Charts for the Estimation of Creep and Shrinkage

Coefficient k_c (environmental conditions).

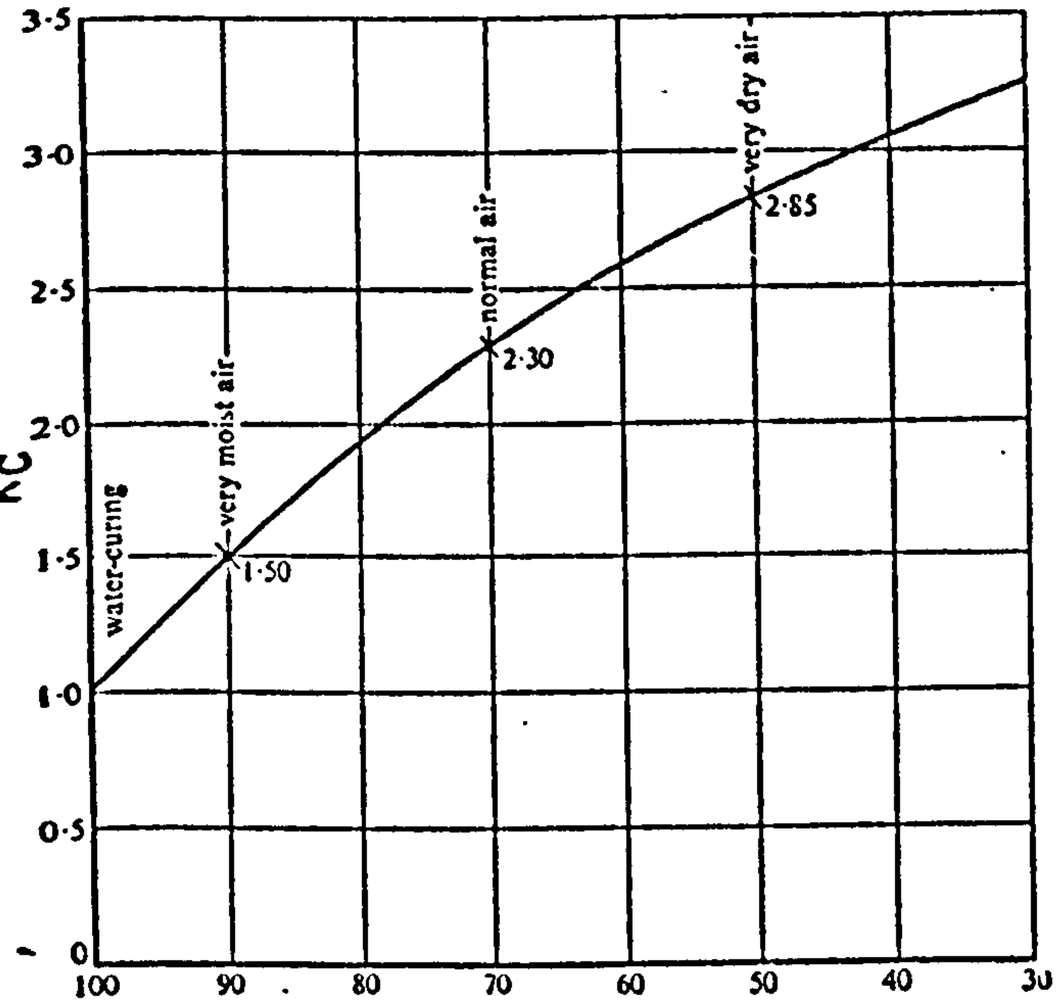

Coefficient k_d (hardening at the age of loading).

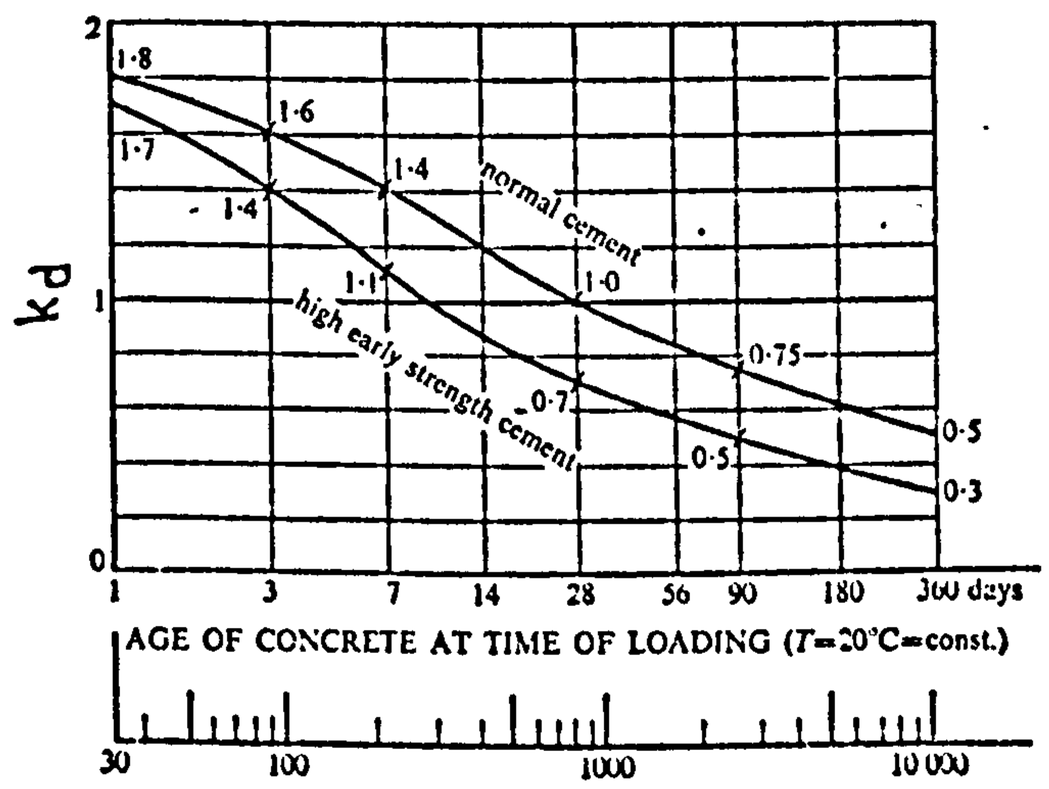

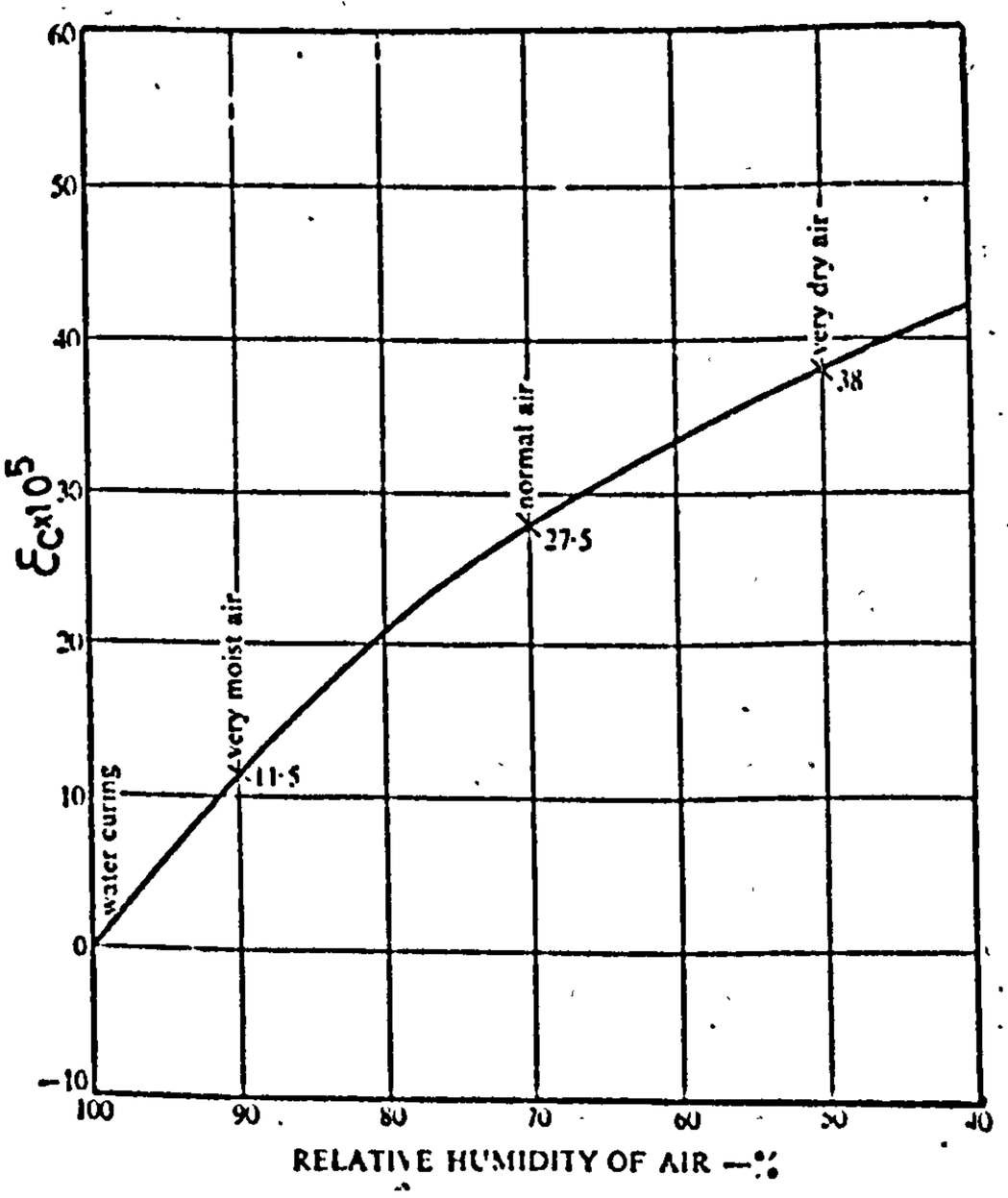

Coefficient k_b (composition of the concrete).

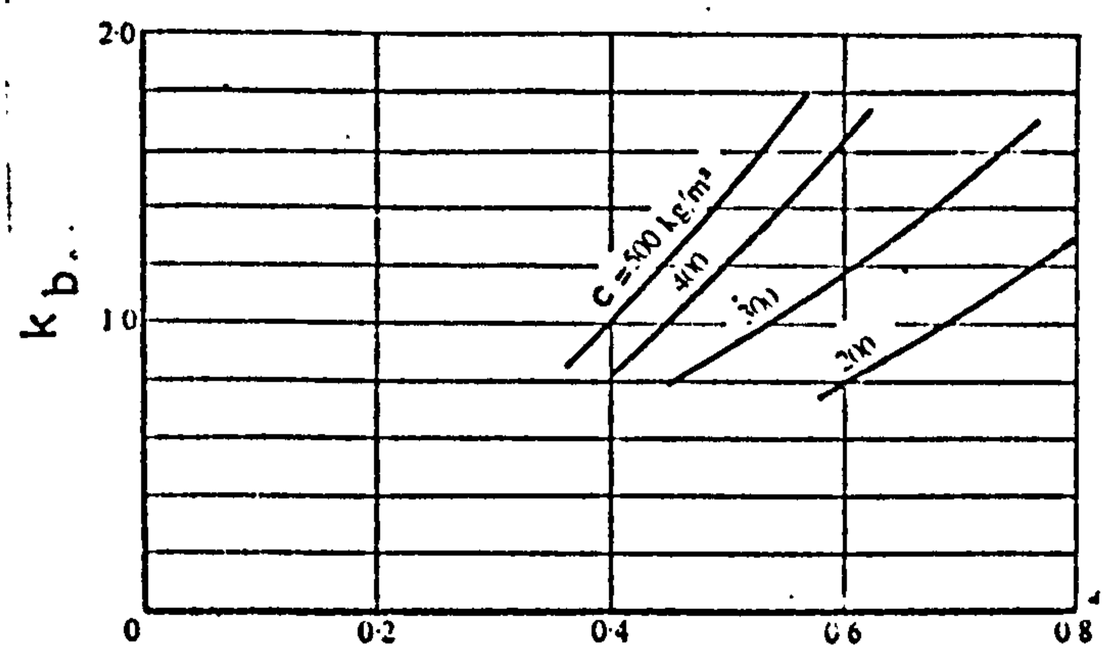

Coefficient k_t (variation as a function of time)

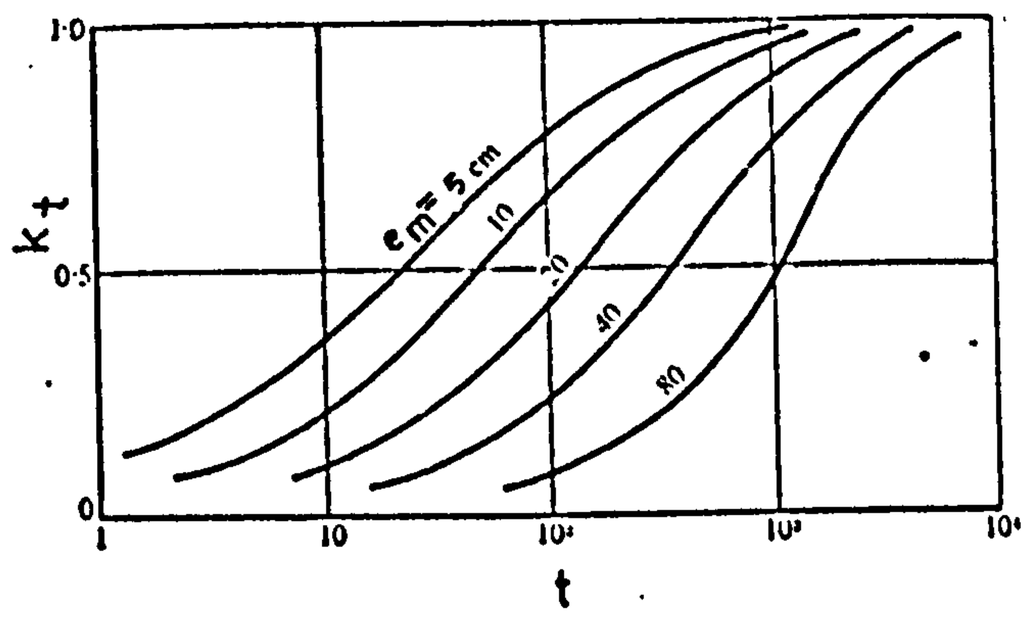

(t represents the number of days after the application of loads).

Coefficient k_e (theoretical thickness).

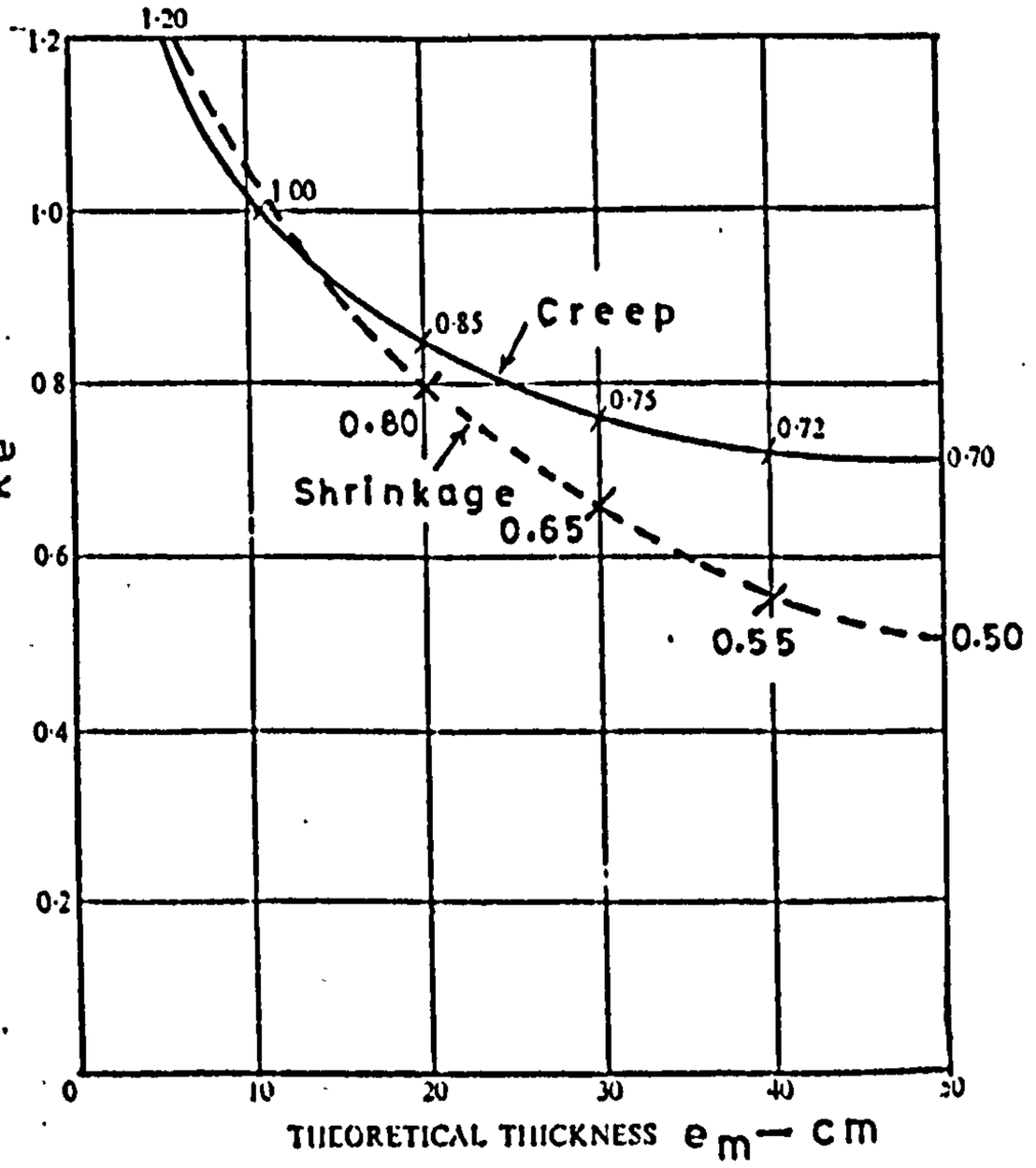

B.1.4.3.. Shrinkage strain ε_r (Clause R 12.32)

$$\varepsilon_r = \varepsilon_c k_b\, k_e\, k_p\, k_t$$

where

ε_c depends on the environment

k_b as for creep

k_e depends on the theoretical thickness of the member e_m (Approximately equals to the creep values)

k_p depends on the percentage of the steel and is given as $\frac{100}{100 + 20\rho}$ to allow for restraint due to steel.

k_t defines the development of shrinkage as a function of time (as for creep).

In this example

$\varepsilon_c = 27.5 \times 10^{-5}$

$$k_p = \frac{100}{100 + \frac{20 \times 269.5 \times 100}{33.44 \times 1000}} = 0.86$$

k_b, k_e and k_t as for creep.

$$\therefore \varepsilon_r = 27.5 \times 10^{-5} \times 1.0 \times 1.2 \times 0.86 \times 0.4$$

$$= \underline{11.4 \times 10^{-5}} \text{ mm/mm.}$$

B.1.4.4. <u>First approximation of losses:</u>

The relaxation loss is given by CEB (Clause R 11.22) as a function of time by a straight-line law of logarithmic type by:

$$\log \frac{\Delta \sigma_{ap,\,t}}{\sigma_{ap,\,o}} = k_1 + k_2 \log t$$

where $\Delta \sigma_{ap,t}$ represents the loss through relaxation at time t (hours) and $\sigma_{ap,o}$ the initial tension. The values of the coefficients k_1 and k_2 depend on the type of prestressing steel.

For simplicity of calculations, the relaxation loss will be assumed as 5% (as given by BS 2691: 1969)

$\therefore$ Relaxation loss = 14.0 KN

Average force during loss period = $280.3 - \frac{14.0}{2}$

= 273.3 KN

Average stress in concrete at centroid of steel

$$= 273.3 \times 10^3 \times \left(\frac{1}{A_c} + \frac{e^2}{I}\right) \text{ N/mm}^2$$

$$= 9.87 \text{ N/mm}^2$$

$\therefore$ creep strain = $\frac{9.87 \times 0.773}{E_{c\,28}}$

$E_{c\,28} = 6.6 \sqrt{0.8 \times 52.0} = 42.6$ KN/mm^2

f_{cu28} estimated as 52.0 N/mm^2

$\therefore$ creep strain = $\frac{9.87 \times .773}{42.6 \times 10^3} = \underline{17.9 \times 10^{-5}}$ mm/mm

creep + shrinkage strain = $(17.9 + 11.4) \times 10^{-5}$ mm/mm

$= 29.3 \times 10^{-5}$

Steel stress loss = 58.6 N/mm^2

Steel force loss = 15.8 KN

$A_{ps}\ f_{pe}$ (Approximately) = 280.3 - (14.0 + 15.8)

= 250.5 KN

B.1.4.5. Estimation of the effective prestressing force:

Average force during loss period

$= 280.3 - \frac{(14.0 + 15.8)}{2}$

= 265.4 KN

Average stress in concrete at centroid of the steel = 9.57 N/mm^2

Creep strain = 17.4×10^{-5} mm/mm

Creep + shrinkage strain = $(17.4 + 11.4) \times 10^{-5}$

$= 28.8 \times 10^{-5}$

Steel stress loss = $57.6\ N/mm^2$

Steel force loss = 15.5 KN

$A_{ps} f_{pe} = 280.3 - (14.0 + 15.5)$

$= 250.8$ KN

Total loss at test = $100 - \frac{250.8}{294.5} \times 100$

$= \underline{15.0\%}$

B.1.5. Total losses estimated from surface strain measurement on speciman A1 = 16.0%.

The CEB and BSCP 110 Recommendations were applied to 12 specimens covering the four seasons of the year, the cross-sections used, the prestressing tendons employed and different types of concrete mix. CEB Recommendations were always very close to the values estimated from surface strain measurement. BSCP 110 in all these cases studied overestimated the values of the prestressing losses. In all the calculations of the prestressing losses in this investigation, the losses estimated from the surface strain measurements were used.

Use of the CEB - FIP Recommendations requires some knowledge about the environmental conditions and this may not be known to the designer.

The overestimation of the losses given by the crude figures of CP 110 is on the safe side. Hence in the author's opinion, CP 110 is most suitable for design, at least for the time being.

Appendix C

TABLE C.1

Calculations steps in analysis of one-or two-point load cases

Beam mark	$\frac{h_f}{d}$	$\frac{b}{b_w}$	α	f'_{ct} N/mm^2	$\frac{f_{cp}}{f'_{ct}}$	$\frac{a_v}{d}$	β		γ		$\frac{V_c \text{Expt.}}{V_c \text{Calc.}}$	
							East	West	East	West	East	West
A1	.165	2.667	.275	3.29	2.25	3.00	.4098	-	.2309		1.14	-
"	"	"	"	"	"	"	-	.4080	-	.2299	-	1.13
2	"	"	"	3.39	1.99	3.50	.3200	-	.1800	-	.95	-
3	"	"	"	3.42	1.85	2.00	.4089	-	.2304	-	-	.90
"	"	"	"	"	"	"	-	.4015	-	.2263	-	.89
"	"	"	"	"	2.18	"	.4679	-	.2636	-	1.03	-
4	"	"	"	3.34	2.04	"	.5069	-	.2856	-	1.12	-
"	"	"	"	"	"	"	-	.4033	-	.2272	-	.89
"	"	"	"	"	"	"	.4672	.4464	.2632	.2515	1.03	.99
5	"	"	"	3.42	1.95	"	.4377	-	.2466	-	.97	-
"	"	"	"	"	"	"	-	.4711	-	.2654	-	1.04
"	"	"	"	"	2.13	"	.4809	.4494	.2709	.2532	1.06	.99
"	"	"	"	"	"	"	.4640	-	.2614	-	1.03	-
6	"	"	"	3.56	2.06	3.00	-	.3696	-	.2082	-	1.02
7	"	"	"	3.27	2.30	"	.3706	-	.2088	-	1.03	-
"	"	"	"	"	"	"	.3438	.4056	.1937	.2285	.95	1.12
8	"	"	"	2.47	3.01	"	-	.4080	-	.2299	-	1.13
"	"	"	"	"	"	"	.3891	-	.2192	-	1.08	-
9	"	"	"	2.98	2.46	"	-	.3839	-	.2163	-	1.06
"	"	"	"	"	"	"	-	.3859	-	.2174	-	1.07
10	"	"	"	3.05	2.15	"	.4308	.3669	.2427	.2067	1.19	1.02
11	"	"	"	2.91	1.85	3.50	.3240	.3550	.1825	.2000	.97	1.06
"	"	"	"	"	"	"	.3374	-	.1901	-	1.01	-
12	"	"	"	2.75	2.13	"	.3511	.3248	.1978	.1830	1.05	0.97
B1	.179	4.000	.537	3.10	1.90	4.00	.3267	.3738	.1604	.1835	.90	1.03
2	"	"	"	3.26	2.17	"	.3464	.3575	.1701	.1755	.96	.99
3	"	"	"	3.52	1.93	2.00	.4884	.5215	.2398	.2560	.94	1.00
"	"	"	"	"	"	"	"	.5439	-	.2670	-	1.05
4	"	"	"	3.19	2.21	"	.4881	.4992	.2397	.2451	.94	.96
"	"	"	"	"	2.30	"	.5980	.4854	.2936	.2383	1.15	.93
5	"	"	"	3.28	1.71	4.5	.3397	-	.1668	-	.99	-

TABLE C.1 (Cont'd)

Beam mark	$\frac{h_f}{d}$	$\frac{b}{b_w}$	α	f'_{ct} N/mm^2	$\frac{f_{cp}}{f'_{ct}}$	$\frac{a_v}{d}$	β		γ		$\frac{V_c \text{ Expt.}}{V_c \text{ Calc.}}$	
							East	West	East	West	East	West
B6	.179	4.000	.537	3.31	1.81	1.25	.6503	.6339	.3192	.3112	.92	.89
"	"	"	"	"	"	"	.7610	.7252	.3736	.3560	1.07	1.02
7	"	"	"	3.25	1.95	"	.7006	.7006	.7006	.3439	.99	.99
"	"	"	"	"	"	"	.7979	.6638	.3917	.3259	1.13	.94
"	"	"	"	"	"	"	-	.6724	-	.3301	-	.95
8	"	"	"	3.23	1.95	"	.6187	.6189	.3037	.3037	.87	.87
"	"	"	"	"	"	"	.7443	.7977	.3654	.3916	1.05	1.13
9	"	"	"	3.30	1.71	4.50	.3142	-	.1542	-	.91	-
10	"	"	"	3.23	2.32	3.50	.3916	-	.1922	-	1.02	-
"	"	"	"	"	"	1.50	.5951	-	.2921	-	.95	-
11	"	"	"	3.36	2.34	2.75	.3889	-	.1909	-	.90	-
"	"	"	"	"	"	"	.3960	.4188	.1944	.2056	.91	.97
C1	.241	2.667	.401	3.24	1.78	2.00	-	.4902	-	.2580	-	1.01
"	"	"	"	"	"	"	.4874	-	.2565	-	1.01	-
"	"	"	"	"	2:07	"	.5172	.4439	.2722	.2336	1.01	.92
2	"	"	"	3.11	1.91	1.25	.5208	.6797	.2741	.3597	.79	1.03
"	"	"	"	"	"	"	.7170	.7170	.3774	.3774	1.08	1.08
3	"	"	"	3.45	1.83	4.00	-	.3124	-	.1644	-	.93
4	"	"	"	3.35	1.91	"	-	.2982	-	.1563	-	.88
5	"	"	"	3.27	1.73	2.00	-	.4357	-	.2293	-	.90
"	"	"	"	"	"	"	.4872	.4782	.2564	.2517	1.01	.99
"	"	"	"	"	"	"	.4536	-	.2387	-	.94	-
"	"	"	"	"	"	"	.5230	-	.2753	-	1.08	-
6	"	"	"	3.33	1.94	1.25	.6125	.6579	.3224	.3463	.93	1.00
"	"	"	"	"	"	"	-	.6571	-	.2985	-	.86
"	"	"	"	"	"	"	-	.5559	-	.2926	-	.84
"	"	"	"	"	"	"	.7273	.6809	.3828	.3584	1.10	1.03
7	"	"	"	3.26	1.80	"	.5566	.6364	.2929	.3349	.84	.96
"	"	"	"	"	"	"	-	.5506	-	.2898	-	.83
"	"	"	"	"	"	"	.6606	.7024	.3477	.3697	1.00	1.06
8	"	"	"	3.06	2.04	2.00	-	.3970	-	.2089	-	.82
"	"	"	"	"	"	"	.4362	-	.2296	-	.90	-
"	"	"	"	"	"	"	-	.5009	-	.2636	-	1.03

TABLE C.1 (Cont'd)

Beam mark	$\frac{h_f}{d}$	$\frac{b}{b_w}$	α	f'_{ct} N/mm^2	$\frac{f_{cp}}{f'_{ct}}$	$\frac{a_v}{d}$	β		γ		$\frac{V_{c\,Expt.}}{V_{c\,Calc.}}$	
							East	West	East	West	East	West
C9	.241	2.667	.401	3.01	1.90	1.25	.6102	.6102	.3212	.3212	.92	.92
"	"	"	"	"	"	"	.7227	.7227	.3804	.3804	1.09	1.09
10	"	"	"	2.96	1.95	4.00	-	.3025	-	.1592	-	.90
11	"	"	"	3.06	1.60	"	.3267	.3090	.1719	.1626	.97	.92
* 12	"	"	"	2.70	1.93	"	.3256	.3358	.1714	.1767	.96	1.00
D1	.255	4.00	.764	3.19	2.00	2.00	.5269	.5269	.2326	.2326	.91	.91
"	"	"	"	"	"	"	.5625	.5269	.2483	.2326	.97	.91
2	"	"	"	3.21	2.01	"	-	.5385	-	.2377	-	.93
3	"	"	"	3.35	1.60	3.00	.3372	.3953	.1489	.1745	.73	.86
4	"	"	"	3.29	1.53	4.50	.3280	-	.1448	-	.86	-
5	"	"	"	3.06	1.74	4.00	.3951	-	.1745	-	.98	-
6	"	"	"	3.39	1.58	3.00	.4418	-	.1951	-	.96	-
7	"	"	"	2.73	1.03	6.00	.5614	.3744	.2339	.1560	1.54	1.03
8	"	"	"	3.04	.89	"	-	.3620	-	.1508	-	.99
9	"	"	"	3.27	.83	5.25	.3639	-	.1516	-	.95	-
E1	.314	2.667	.524	3.74	1.17	3.00	.4377	.4414	.2159	.2178	1.06	1.07
"	"	"	"	"	"	"	.4483	-	.2212	-	1.09	-
"	"	"	"	"	"	2.00	.5307	.5022	.2618	.2478	1.03	.97
2	"	"	"	3.33	1.00	"	-	.5252	-	.2591	-	1.02
"	"	"	"	"	"	"	.5761	-	.2842	-	1.11	-
"	"	"	"	"	"	"	-	.5312	-	.2621	-	1.03
3	"	"	"	3.37	1.45	"	-	.5202	-	.2566	-	1.01
"	"	"	"	"	"	"	-	.5202	-	.2566	-	1.01
"	"	"	"	"	1.53	"	.5127	.5707	.2529	.2815	.99	1.10
4	"	"	"	3.29	1.57	4.00	.3372	.3468	.1664	.1711	.94	.96
5	"	"	"	3.17	1.79	"	-	.3858	-	.1903	-	1.07
"	"	"	"	"	"	2.00	.4732	.5169	.2334	.2550	.92	1.00
6	"	"	"	3.22	1.96	3.00	.4892	.4245	.2413	.2094	1.19	1.03
7	"	"	"	3.10	1.80	"	-	.3869	-	.1909	-	.94
"	"	"	"	"	"	"	.3996	-	.1971	-	.97	-
"	"	"	"	"	"	"	.4182	-	.2063	-	1.01	-
* 8	"	"	"	3.52	1.52	4.00	-	-	-	-	-	-
C17	.283	2.667	.472	2.73	.93	6.00	.3110	-	.154	-	1.03	-
18	"	"	"	3.04	.82	6.00	-	.2730	-	.138	-	.91
19	"	"	"	3.27	.75	5.25	-	.3200	-	.162	-	1.02

* Note: C17,C18, and C19 are shown in the bottom of the page.

TABLE C.1 (Cont'd)

Beam mark	$\frac{h_f}{d}$	$\frac{b}{b_w}$	α	f'_{ct} N/mm^2	$\frac{f_{cp}}{f'_{ct}}$	$\frac{a_v}{d}$	β		γ		$\frac{V_c \text{ Expt.}}{V_c \text{ Calc.}}$	
							East	West	East	West	East	West
F1	.330	4.000	.990	3.14	1.45	4.00	.4057	.2911	.1629	.1169	.92	.66
2	"	"	"	3.21	1.46	"	.3946	.3792	.1585	.1523	.89	.86
3	"	"	"	3.41	1.50	2.00	.5741	.5936	.2306	.2384	.90	.93
"	"	"	"	"	1.57	"	.6123	.6527	.2459	.2621	.96	1.03
4	"	"	"	3.28	1.70	"	.5684	.5684	.2283	.2283	.90	.90
"	"	"	"	"	1.79	"	.5910	.6557	.2373	.2632	.93	1.03
5	"	"	"	3.33	1.00	4.5	-	.3526	-	.1416	-	.84
G1	.000	1.000	.000	3.80	.80	2.00	.3558	-	.2367	-	.93	-
"	"	"	"	"	"	"	.3825	-	.2550	-	1.00	-
2	"	"	"	3.40	1.10	"	.3760	-	.2507	-	.98	-
3	"	"	"	3.34	.60	"	-	.2958	-	.1972	-	.77
"	"	"	"	"	"	"	-	.3427	-	.2285	-	.90
"	"	"	"	"	.70	"	.4036	-	.2691	-	1.06	-
4	"	"	"	3.35	1.06	4.00	-	-	-	-	-	-
5	"	"	"	2.94	1.27	2.00	-	.3035	-	.2023	-	.79
"	"	"	"	"	1.27	2.00	-	.3363	-	.2242	-	.88
6	"	"	"	3.23	1.20	3.00	.2552	-	.1701	-	.84	-
"	"	"	"	"	"	2.00	-	.3002	-	.2001	-	.78
"	"	"	"	"	1.30	"	.4073	-	.2715	-	1.06	-
7	"	"	"	3.26	1.04	1.50	-	-	-	-	-	-
8	"	"	"	3.39	1.13	2.00	-	-	-	-	-	-

Notes.

1. $\alpha = \left(\frac{b}{b_w} - 1\right) \frac{h_f}{d}$, $\beta = \frac{1000\ V_c}{f'_{ct}\left(1 + \frac{f_{cp}}{f'_{ct}}\right) b_w\ d}$ and

$$\gamma = \frac{1000\ V_c}{f'_{ct}\left(1 + \frac{f_{cp}}{f'_{ct}}\right) b_w\ d \left[1.5 + \left(\frac{b}{b_w} - 1\right)\frac{h_f}{d}\right]}$$

2. $\frac{V_c \text{ Expt.}}{V_c \text{ Calc.}} = \frac{V_c \text{ Experimental}}{V_c \text{ Calculated using equation 6.5}}$

Appendix D

TABLE D.1

Calculations steps in analysis of uniformly distributed load case.

Beam mark	$\frac{h_f}{d}$	$\frac{b}{b_w}$	α	f'_{ct} N/mm^2	$\frac{f_{cp}}{f'_{ct}}$	$\frac{a_v}{d}$	β'		γ'		q_c Expt. / q_c Calc.	
							East	West	East	West	East	West
B12	.179	4.000	.537	3.09	1.45	10.0	1.530	1.330	.7511	.6530	1.05	.91
13	"	"	"	2.93	1.61	8.0	1.643	1.643	.8066	.8710	1.00	1.08
14	"	"	"	3.13	1.94	7.28	1.642	1.806	.8060	.8860	.95	1.04
15	"	"	"	2.93	2.15	6.0	1.891	1.891	.9280	.840	.98	.88
C13	.241	2.667	.401	3.13	1.21	10.0	1.447	-	.7620	-	1.06	-
14	"	"	"	3.11	1.24	8.0	1.605	1.702	.8450	.856	1.05	1.06
15	"	"	"	3.13	1.62	7.28	1.638	1.774	.8620	.934	1.01	1.10
16	"	"	"	2.93	1.84	6.0	1.663	1.663	.8750	.875	.92	.92
20	.283	"	.472	2.67	1.05	11.78	1.649	-	.8362	-	1.27	-
D10	.300	4.000	.900	2.67	1.11	11.78	1.718	-	.7158	-	-	1.08
11a	"	3.450	.735	3.45	0.90	17.78	1.333	-	.5963	-	-	1.10
11b	"	"	"	3.41	0.90	"	1.184	1.367	.5298	.6116	0.98	1.13
12	"	"	"	3.64	1.07	11.78	1.627	1.312	.7280	.5870	1.10	0.90
13	"	"	"	3.11	1.06	17.47	1.091	-	.4881	-	.90	-
14	"	"	"	3.02	1.14	"	-	1.239	-	.5544	-	1.03
E 9	.314	2.667	.524	2.91	1.42	10.0	1.524	-	.7520	-	1.05	-
10	"		"	2.95	1.46	8.0	1.662	1.707	.8200	.8420	1.01	1.04
11	"		"	3.10	1.61	6.0	1.934	1.934	.9540	.9540	1.00	1.00
12	"		"	3.00	1.49	7.28	2.007	1.858	.9900	.9170	1.16	1.08
F 6	.330	4.000	.990	2.98	1.38	10.0	1.891	1.796	.7590	.7210	1.06	1.00
7	"	"	"	2.91	1.52	8.0	2.198	2.198	.8830	.8830	1.09	1.09
8	"	"	"	2.95	1.71	6.0	2.229	2.079	.8950	.8110	.95	.85
9	"	"	"	3.01	1.50	7.28	2.008	2.053	.8060	.8240	.95	.97

Notes:

1. $\alpha = (b/b_w - 1)\, h_f/d$, $\beta' = (1000\, q_c l)/(f'_{ct}\,(1 + f_{cp}/f'_{ct})\, b_w d)$

   $\gamma' = (1000\, q_c l)/(f'_{ct}\,(1 + f_{cp}/f'_{ct})\, b_w d(1.5 + (b/b_w - 1)\, h_f/d)$

2. $$\frac{q_c l \text{ Expt.}}{q_c l \text{ Calc.}} = \frac{q_c l \text{ Experimental}}{q_c l \text{ Calculated using equation 6.12}}$$

Appendix E

E.1 Mohr's Failure Criterion Assuming a Straight Line Envelope:

From the geometrical relations in Figure E.1, and taking compression as positive.

$f_1 + f_2 = 2\,\overline{OC}$, $\quad \overline{OC} = \overline{CE} - \overline{OE}$ where $\overline{CE} = \overline{CD}$

$\frac{f_1 - f_2}{2}$ cosec θ since $\overline{CD} = \frac{f_1 - f_2}{2}$ and $\overline{OE} = c \cot \theta$

$\therefore \overline{OC} = \frac{f_1 - f_2}{2}$ cosec θ - $c \cot \theta$

or $2\,\overline{OC} = f_1 + f_2 = (f_1 - f_2)$cosec- $2c \cot \theta$ (1)

With the same sign convention, the following expressions can be deduced from the well known principal stresses:

$$f_1 - f_2 = f_{xx} + f_{yy}$$

$$f_1 + f_2 = \sqrt{(f_{xx} - f_{yy})^2 + 4\,v_{xy}^2} \qquad (2)$$

From (1) and (2)

$$\sqrt{(f_{xx} - f_{yy})^2 + 4\,v_{xy}^2} = (f_{xx} + f_{yy})\,\text{cosec} - 2c \cot \theta \qquad (3)$$

From the geometrical relations in Figure E.2 with compression taken as positive

$\overline{GQ} = \overline{HK} = \frac{f'_c}{2} - \overline{PQ}$ where $\overline{PQ} = \frac{f'_c - f'_t}{2}$ $\sin\theta$

$\therefore \overline{GQ} = \frac{f'_c}{2} - \frac{f'_c - f'_t}{2}$ $\sin\theta$ (4)

and $\overline{HK} = -\frac{f'_t}{2} = \frac{f'_c}{2} - \frac{f'_c - f'_t}{2}$ $\sin\theta$ (5)

From (5)

$$\frac{f'_c}{f'_t} = -\frac{1 + \sin\theta}{1 - \sin\theta} \qquad (6)$$

Solving (6) for θ gives $\theta = \sin^{-1} \frac{f'_c + f'_t}{f'_c - f'_t}$ (7)

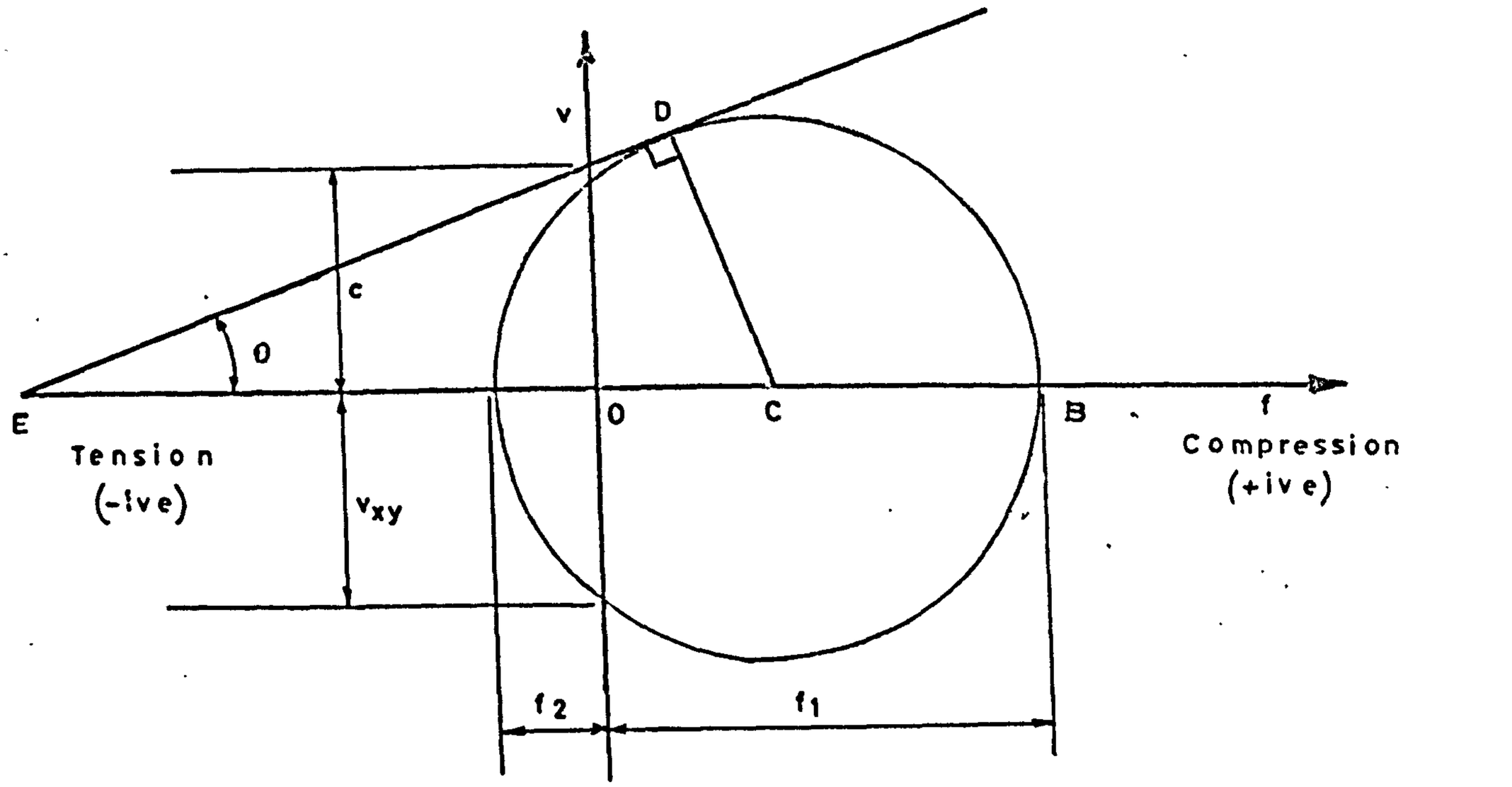

Figure E.1

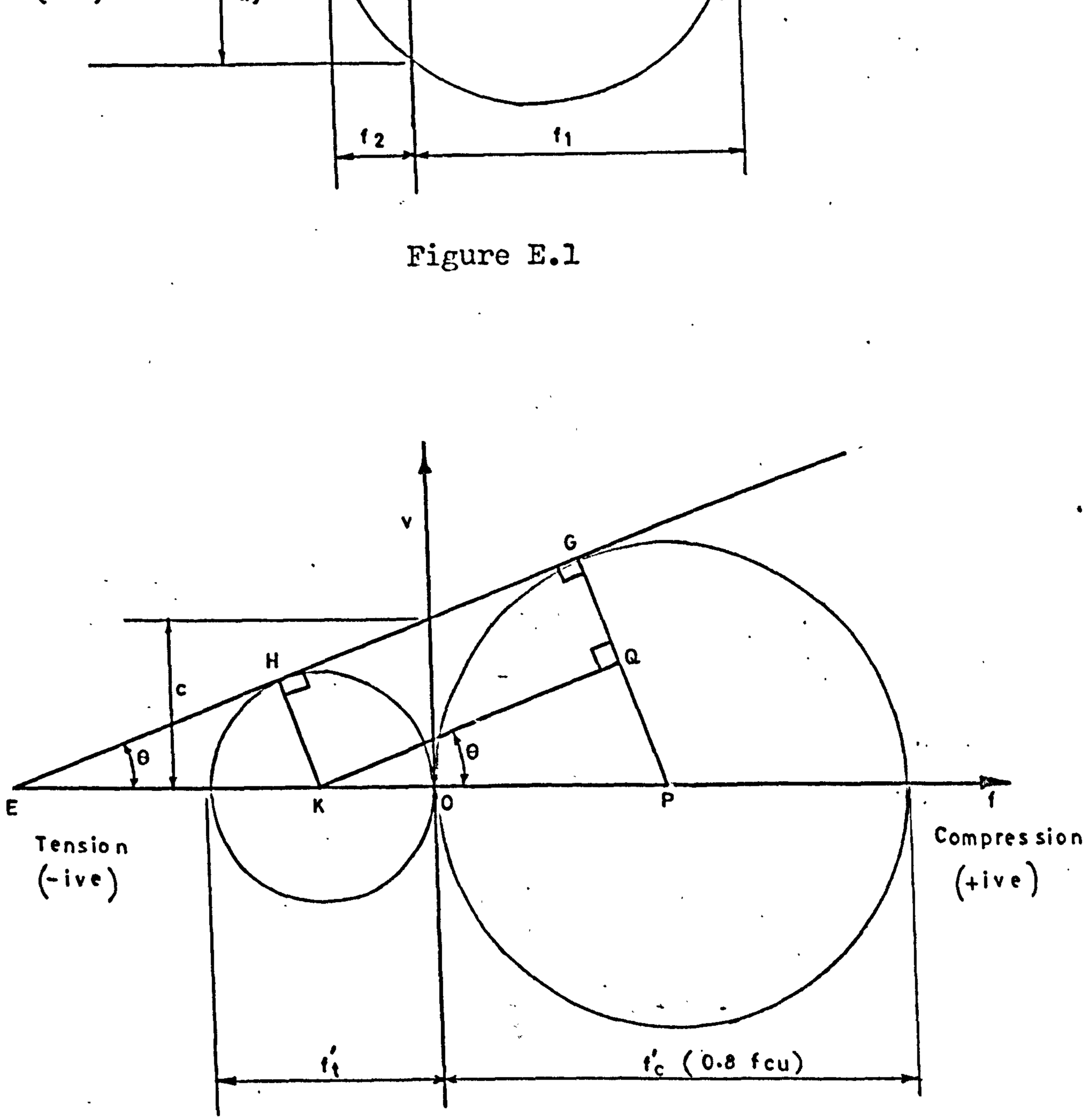

Figure E.2

From Figure E .2 :

$$\overline{OE} = \overline{EK} + \overline{OK} \text{ where } \overline{EK} = -\frac{f'_t}{2}\operatorname{cosec}\theta \text{ and } \overline{OK} = -\frac{f'_t}{2}$$

$$\therefore \overline{OE} = -\frac{f'_t}{2}\frac{(1+\sin\theta)}{\sin\theta}$$

$$\tan\theta = \frac{c}{OE} = -\frac{2c\sin\theta}{f'_t(1+\sin\theta)}$$

or

$$c = -\frac{f'_t(1+\sin\theta)}{2\cos\theta} \qquad (8)$$

From (7) and (8)

$$c = \sqrt{-\frac{f'_c f'_t}{2}} \qquad (9)$$

Substituting (7) and (9) into (3), we get:

$$\sqrt{(f_{xx}-f_{yy})^2+4v_{xy}^2} = \frac{(f_{xx}+f_{yy})(f'_c-f'_t)}{(f'_c+f'_t)} + \frac{2f'_c f'_t}{(f'_c+f'_t)}$$

or

$$(f'_c+f'_t)^2\left((f_{xx}-f_{yy})^2+4v_{xy}^2\right) = (f_{xx}+f_{yy})^2(f'_c-f'_t)^2 + 4f'^2_t f'^2_c + 4f'_t f'_c(f_{xx}+f_{yy})(f'_c-f'_t)$$

After simplifying, rearranging, dividing by f'^4_t and substituting γ as $\left|\frac{f'_c}{f'_t}\right|$ we get:

$$\left(\frac{v_{xy}}{f'_t}\right)^2 = \frac{\gamma}{(\gamma+1)^2}\left[\gamma + (\gamma-1)\left(\frac{f_{xx}}{f'_t}+\frac{f_{yy}}{f'_t}\right) + \left(\frac{(\gamma+1)^2}{\gamma}\right)\times \left(\frac{f_{xx}}{f'_t}\cdot\frac{f_{yy}}{f'_t}\right) - \left(\frac{f_{xx}}{f'_t}+\frac{f_{yy}}{f'_t}\right)^2\right] \qquad (6.21)$$

REFERENCES

1. SHEAR STUDY GROUP. The shear strength of reinforced concrete beams. London, Institution of Structural Engineers, January 1969. pp. 1 -170.

2. A.S.C.E. - A.C.I. COMMITTEE 426. The shear strength of reinforced concrete members. Proceedings of the American Society of Civil Engineers. Vol. 99, No. ST 6. June 1973. pp. 1091 - 1187.

3. ANDERSON, B.G. Rigid frame failures. Journal of the American Concrete Institute. Proceedings Vol. 53, No. 7. January 1957. pp. 625 - 636.

4. MAHGOUB, M.O. Shear strength of prestressed concrete beams without web reinforcement. Magazine of Concrete Research. Vol. 27, No. 93. December 1975. pp. 219 - 228.

5. HOGNESTAD, E. What do we know about diagonal tension and web reinforcement in concrete? Urbana, University of Illinois, Engineering Experiment Station, 1951. Circular Series No. 64, pp. 47.

6. A.C.I. - A.S.C.E. COMMITTEE 326. Shear and diagonal tension. Journal of the American Concrete Institute. Proceedings Vol. 59, Nos. 1 - 3. January to March 1962. pp. 1 - 30, 277 - 333 and 353 - 395.

7. BRESLER, B. and MACGREGOR, J.G. Review of concrete beams failing in shear. Proceedings of the American Society of Civil Engineers. Vol. 93, No. ST. 1. February 1967. pp. 343 - 372.

8. GVOZDEV, A.A. Research on prestressed concrete in U.S.S.R. and neighbouring European countries. Fifth Congress of the Federation Internationale de la Precontrainte, Paris, 1966. London, 1967. pp. 12 - 29.

9. CLARK, A.P. Diagonal tension in reinforced concrete beams. Journal of the American Concrete Institute. Proceedings Vol. 48, No. 2. October 1951. pp 145 - 156.

10. TALBOT, A.N. Tests on reinforced concrete beams: Resistance to web stresses. Urbana, University of Illinois, Engineering Experiment Station, January 1901. pp. 85. Bulletin No. 29.

11. MOODY, K.G., VIEST, I.M., ELSTNER, R.C., and HOGNESTAD, E. Shear strength of reinforced concrete beams. Journal of the American Concrete Institute. Proceedings Vol. 51, Nos. 4 and 5. December 1954 and January 1955. pp. 317 - 332 and 417 - 434.

12. ELSTNER, R.C., MOODY, K.G., VIEST, I.M. and HOGNESTAD, E. Shear strength of reinforced beams: Tests of restrained beams with web reinforcement. Journal of the American Concrete Institute. Proceedings Vol. 51, No. 6. February 1955. pp. 525 - 539.

13. MOODY, R.G. and VIEST, I.M. Shear strength of reinforced concrete beams: Analytical studies. Journal of the American Concrete Institute. Proceedings Vol. 51, No. 7. March 1955. pp. 697 - 730.

14. MORROW, J. and VIEST, I.M. Shear strength of reinforced concrete frame members without web reinforcement. Journal of the American Concrete Institute. Proceedings Vol. 53, No. 9. March 1957. pp. 833 - 869.

15. KESLER, C.E. Statistical relation between cylinder, modified cube and beam strength of plain concrete. Proceedings of the American Society for Testing Materials. Vol. 54. 1954. pp. 1178 - 1187.

16. WHITNEY, C.S. Ultimate shear strength of reinforced concrete flat slabs, footings, beams and frame members without shear reinforcement. Journal of the American Concrete Institute. Proceedings Vol. 54, No. 4. October 1957. pp. 265 - 298.

17. TAUB, J. and NEVILLE, A.M. Resistance to shear of reinforced concrete beams. Journal of the American Concrete Institute. Proceedings Vol. 57, Nos. 2 - 5. August - November 1960. pp. 193 - 220, 315 - 336, 443 - 463 and 517 - 532.

18. SMITH, R.B.L. The interaction of moment and shear on the failure of reinforced concrete beams without web reinforcement. Civil Engineering and Public Works Review. Vol. 61, Nos. 719, 720 and 721. June - August 1966. pp. 723 - 725, 869 - 872 and 967 - 970.

19. KREFELD, W.J. and THURSTON, C.W. Studies of the shear and diagonal tension strength of simply supported reinforced concrete beams. Journal of the American Concrete Institute. Proceedings Vol. 63, No. 3. March 1966. pp. 451 - 476.

20. DESAYI, P. A method for determining the shear strength of reinforced concrete beams with small $a_{v/d}$ ratios. Magazine of Concrete Research, Vol. 26, No. 86. March 1974. pp. 29 - 38.

21. LAUPA, A., SIESS, C.P., and NEWMARK, N.M. Strength in shear of reinforced concrete beams. Urbana, University of Illinois, Engineering Experiment Station, March 1955. pp. 73, Bulletin No. 428.

22. WATSTEIN, D. and MATHEY, R.G. Strains in beams having diagonal cracks. Journal of the American Concrete Institute. Proceedings Vol. 55, No. 6. December 1958. pp. 717 - 728.

23. KANI, G.N.J. The riddle of shear failure and its solution. Journal of the American Concrete Institute. Proceedings Vol. 61, No. 4. April 1964. pp. 441 - 467.

24. REGAN, P.E. Combined shear and bending of reinforced concrete members. Thesis submitted to the University of London for the degree of Ph.D. April 1967. pp. 722.

25. WALTHER, R. Calculation of the shear strength of reinforced and prestressed concrete beams by the shear failure theory. Beton-und Stahlbetonbau. Vol. 57, No.11. November, 1962. pp. 261 - 271. English translation by C.V. Amerongen. London, Cement and Concrete Association. 1964. pp. 28. C & CA Translation No. Cj 110.

26. OJHA, S.K. The shear strength of rectangular reinforced and prestressed concrete beams. Magazine of Concrete Research. Vol. 19, No. 60. September 1967. pp. 173 - 184.

27. COMITE EUROPEEN du BETON - FEDERATION INTERNATIONALE de la PRECONTRAINTE. International recommendations for the design and construction of concrete structures. London, Cement and Concrete Association, 1970. Principles and recommendations. pp. 80.

28. GVOZDEV, A.A., DMITRIEV, S.A. and KALATOUROV,B.A. Russian limit design method for prestressed concrete. A contribution in French to a meeting of the F.I.P.- C.E.B. Joint Committee No. 1, Venice, 1963. English translation by C.V. Amerongen. London, Cement and Concrete Association. 1964. pp. 16. C & CA Translation No. Cj. 117.

29. SIGALOV, E. and STRONGIN, S. Reinforced concrete. Moscow, Foreign Languages Publishing House, 1962. pp. 393.

30. BRITISH STANDARDS INSTITUTION. CP 110: Part 1: 1972. The Structural use of concrete. Part 1. Design, materials and workmanship. London. pp. 154.

31. BRITISH STANDARDS INSTITUTION. CP 115: 1959. The structural use of prestressed concrete in buildings. London. pp. 44.

32. AMERICAN CONCRETE INSTITUTE. ACI 318 - 71. Building code requirements for reinforced concrete. Detroit, American Concrete Institute, 1971. pp. 78.

33. HICKS, A.B. The influence of shear span and concrete strength upon the shear resistance of a pre-tensioned prestressed concrete beam. Magazine of Concrete Research. Vol.10, No. 30. November 1958. pp. 115 - 122.

34. SETHUNARAYANAN, R. Ultimate strength of pre-tensioned I beams in combined bending and shear. Magazine of Concrete Research. Vol. 12, No. 35. July 1960. pp. 83 - 90.

35. SETHUNARAYANAN, R. Ultimate strength of pre-stressed beams in combined bending and shear. A paper presented to the International Conference on Shear, Torsion and Bond in Reinforced and Prestressed Concrete, Coimbatore, India, 1969. pp.20.

36. SOZEN, M.A., ZWOYER, E.M. and SIESS, C.P. Strength in shear of beams without web reinforcement. Urbana, University of Illinois, Engineering Experiment Station, April 1959. pp. 69. Bulletin No. 452.

37. EVANS, R.H. and HOSNY, A.H.H. The shear strength of post-tensioned prestressed concrete beams. Third Congress of the Federation Internationale de la Precontrainte, Berlin, 1958. London, 1958. pp. 112 - 132.

38. WALTHER, R. The shear strength of prestressed concrete beams. Third Congress of the Federation Internationale de la Precontrainte, Berlin, 1958. London, 1958. pp. 80 - 100.

39. WARNER, R.F. and HALL, A.S. The shear strength of concrete beams without web reinforcement. Third Congress of the Federation Internationale de la Precontrainte, Berlin, 1958. London, 1958. pp. 101 - 111.

40. EVANS, R.H. and SCHUMACHER, E.G. Shear strength of prestressed beams without web reinforcement Journal of the American Concrete Institute. Proceedings Vol. 60, No. 11. November 1963. pp. 1621 - 1642.

41. SWAMY, N. Some aspects of the diagonal cracking failure of prestressed hollow beams without web reinforcement. The Indian Concrete Journal. Vol. 38, No. 9. September 1964. pp. 328 - 333.

42. KAR, J.N. Diagonal cracking in prestressed concrete beams. Proceedings of the American Society of Civil Engineers. Vol. 94, No. ST1. January 1968. pp. 83 - 109.

43. KAR, J.N. Shear strength of prestressed concrete beams without web reinforcement. Magazine of Concrete Research. Vol. 21, No. 68. September 1968. pp. 159 - 170.

44. ARTHUR, P.D. The shear strength of pre-tensioned I - beams with unreinforced webs. Thesis submitted to the University of St. Andrews for the degree of Ph.D. June 1968. pp.84.

45. ARTHUR, P.D. and MAHGOUB, M.O. Shear test on full-scale prestressed concrete box beams. Proceedings of the Institution of Civil Engineers. Part 2. Research and Theory. Vol. 59. September 1975. pp. 535 - 540.

46. WILBY, C.B. and NAZIR, C.P. Shear strength of uniformly loaded prestressed concrete beams. Civil Engineering and Public Works Review. Vol. 59, No. 693. April 1964. pp. 457 - 461.

47. HANSON, J.M. and HULSBOS, C.L. Ultimate shear tests of prestressed concrete I beams under concentrated and uniform loadings. Journal of the Prestressed Concrete Institute. Vol. 9, No. 3. June 1964. pp. 15 - 28.

48. ARTHUR, P.D., BHATT, P. and DUNCAN, W. Experimental and analytical studies on the shear failure of pretensioned I beams under distributed loading. Journal of the Prestressed Concrete Institute. Vol. 18, No. 1. January - February 1973. pp. 50 - 67.

49. BENNETT, E.W., ABDUL-AHAD, H.Y., and NEVILLE, A.M. Shear strength of reinforced and prestressed concrete beams subject to moving loads. Journal of the Prestressed Concrete Institute. Vol. 17, No. 6. November - December 1972. pp. 58 - 69.

50. MACGREGOR, J.G., SOZEN, M.A. and SIESS, C.P. Strength of prestressed concrete beams with web reinforcement. Journal of the American Concrete Institute. Proceedings. Vol. 62. No. 12 December 1965. pp. 1503 - 1519.

51. MACGREGOR, J.G., SOZEN, M.A., and SIESS, C.P. Effect of draped reinforcement on behaviour of prestressed concrete beams. Journal of the American Concrete Institute. Proceedings Vol. 57, No. 6. December 1960. pp. 649 - 677.

52. JENA, B. and PANNELL, F.N. The diagonal cracking strength of continuous prestressed concrete beams. Magazine of Concrete Research. Vol. 24, No. 78. March 1972. pp. 3 - 14.

53. BHATT, P. The diagonal cracking strength of prestressed I beams with unreinforced webs. Building Science. Vol. 9, No. 4. December 1974. pp. 315 - 323.

54. MOAYER, M. and REGAN, P.E. Shear strength of prestressed and reinforced concrete T beams. Shear in reinforced concrete. Detroit, American Concrete Institute, 1974. Publication SP - 42. Vol. 1. pp. 183 - 213.

55. DEWAR, J.D. The indirect tensile strength of concrete of high compressive strength. London, Cement and Concrete Association. March 1964. pp. 12. Technical Report TRA/377.

56. ZIENKIEWICZ, O.C. The finite element method in engineering science. London, McGraw Hill, 1971. pp. 521.

57. NILSON, A.H. Nonlinear analysis of reinforced concrete by the finite element method. Journal of the American Concrete Institute. Proceedings Vol. 65, No. 9. September 1968. pp. 757-766.

58. SCORDELIS, A.C., NGO, D. and FRANKLIN, H.A. Finite element study of reinforced concrete beams with diagonal tension cracks. Shear in reinforced concrete. Detroit, American Concrete Institute, 1974. Publication SP - 42. Vol. 1. pp. 79 - 102.

59. HOUDE, J. and MIRZA, M.S. A finite element analysis of shear strength of reinforced concrete beams. Shear in reinforced concrete. Detroit, American Concrete Institute, 1974. Publication SP - 42 Vol. 1. pp. 103 - 128.

60. FERGUSON, P.M. and THOMPSON, J.N. Diagonal tension in T - beams without stirrups. Journal of the American Concrete Institute. Proceedings Vol. 49, No. 7. March 1953. pp. 665 - 676.

61. LEONHARDT, F. and WALTHER, R. The Stuttgart shear tests. Beton-und Stahlbetonbau. Vol. 56, No. 12. 1961 and Vol. 57, Nos. 2, 3, 6, 7 and 8. 1962. English translation by C.V. Amerongen. London, Cement and Concrete Association, 1964. pp. 134. C & CA Translation No. Cj 111.

62. PLACAS, A. and REGAN, P.E. Shear failures of reinforced concrete beams. Journal of the American Concrete Institute. Proceedings Vol. 68, No. 10. October 1971. pp. 763 - 773.

63. KANI, G.N.J. How safe are our large reinforced concrete beams? Journal of the American Concrete Institute. Proceedings Vol. 64, No. 3. March 1967. pp. 128 - 141.

64. TAYLOR, H.P.J. Shear strength of large beams. Proceedings of the American Society of Civil Engineers. Vol. 98, No. ST 11. November 1972. pp. 2473 - 2490.

65. WRIGHT, P.J.F. Comments on an indirect tensile test on concrete cylinders. Magazine of Concrete Research. Vol. 7, No. 20. July 1955. pp. 87 - 96.

66. OLADAPO, I.O. Cracking and failure in plain concrete beams. Magazine of Concrete Research. Vol. 16, No. 47. June 1964. pp. 103 - 110.

67. GOODE, C.D. and HELMY, M.A. The strength of concrete under combined shear and direct stress. Magazine of Concrete Research. Vol. 19, No. 59. June 1967. pp. 105 - 112.

68. BRESLER, B. and PISTER, K.S. Strength of concrete under combined stress. Journal of the American Concrete Institute. Proceedings Vol. 55, No. 3. September 1958. pp. 321 - 345.

69. COWAN, H.J.The strength of plain, reinforced and prestressed concrete under the action of combined stresses,with particular reference to combined bending and torsion of rectangular sections. Magazine of Concrete Research. Vol. 5, No. 14. December 1953. pp. 75 - 86.

70. KRAHL, N.W., KHACHATURIAN, N., and SIESS, C.P. Stability of tensile cracks in concrete beams. Proceedings of the American Society of Civil Engineers. Vol. 93, No. ST 1. February 1967. pp. 235 - 254.

71. KUPFER, H., HILSDORF, H., and RÜSCH, H. Behaviour of concrete under biaxial stresses. Journal of the American Concrete Institute. Proceedings Vo. 66, No. 8. August 1969. pp. 656 - 666.

72. LIU, T.C.Y., NILSON, A.H. and SLATE, F.O. Biaxial stress-strain relations for concrete. Proceedings of the American Society of Civil Engineers. Vol. 98, No. ST 5. May 1972. pp. 1025 - 1034.

73. NADAI, A. Theory of flow and fracture of solids. Vol. I. Second edition. New York, McGraw Hill Inc., 1950. pp.572.

74. GURALNICK, S.A. Strength of reinforced concrete beams. Transactions of the American Society of Civil Engineers. Vol. 125, Part I, Paper No. 3036. 1960. pp. 603 - 645.

75. SHEIKH, M.A., de PAIVA, H.A.R. and NEVILLE, A.M. Calculation of flexure - shear strength of prestressed concrete beams. Journal of the Prestressed Concrete Institute. Vol. 13, No. 1. February 1968. pp. 68 - 85.

76. MUKHOPADHYAY, M. and SEN, B.R. Ultimate load analysis of reinforced concrete members with plain web under combined flexure, shear and axial force. Building Science. Vol. 9, No. 3. September 1974. pp. 167 - 174.

77. GUYON, Y. Prestressed concrete. Vol. II. Statically indeterminate structures. London, Contractors Record Ltd., 1960, pp.741.

78. LANGHAAR, H.L. Dimensional analysis and theory of models. New York, John Wiley and Sons Inc. London, Chapman and Hall Ltd., 1951. pp.166.

79. IYENGAR, K.T.S.R., RANGAN, B.V. and PALANISWAMY, R. Some factors affecting shear strength of reinforced concrete beams. Indian Concrete Journal. Vol. 42, No. 12. December 1968. pp. 499 - 505.

80. ROAD RESEARCH LABORATORY. Design of concrete mixes. Second edition. London, H.M.S.O., 1950. pp.16. Road Note No. 4.

81. HURD, M.K. Formwork for concrete. Second edition. Detroit, American Concrete Institute, 1969. pp.364. ACI Special Publication No. 4.

82. MARSHALL, W.T. and MATTOCK, A.H. Control of horizontal cracking in the ends of pre-tensioned,prestressed concrete girders. Journal of the Prestressed Concrete Institute. Vol. 7, No. 5. October 1962. pp. 56 - 74.

83. LEONHARDT, F. Prestressed concrete. Design and construction. Second edition. Berlin, Wilhelm Ernst and Sohn, 1964. pp.677.

84. MORICE, P.B. Full scale test on a prestressed concrete beam. Engineering. Vol. 177, No. 4613. 25 June 1954. pp. 815 - 817.

85. BATE, S.C.C. et al. Handbook on the Unified Code for structural concrete (CP 110: 1972). London, Cement and Concrete Association, 1972. pp.153.

86. HSU, T.T.C., SLATE, F.O., STURMAN, G.M. and WINTER, G. Micro-cracking of plain concrete and the shape of the stress-strain curve. Journal of the American Concrete Institute. Proceedings. Vol. 60, No. 2. February 1963. pp. 209 - 224.

87. HSU, T.T.C. Mathematical analysis of shrinkage stresses in a model of hardened concrete. Journal of the American Concrete Institute. Proceedings Vol. 60, No. 3. March 1963. pp. 371 - 390.

88. HSU, T.T.C. and SLATE, F.O. Tensile bond strength between aggregate and cement paste or mortar. Journal of the American Concrete Institute. Proceedings Vol. 60, No. 4. April 1963. pp. 465 - 486.

89. BALFOUR, A. and McTERNAN, A.J. The numerical solution of equations. London. Heinemann Educational. 1967. pp. 85.

90. RÜSCH, H. Researches toward a general flexural theory for structural concrete. Journal of the American Concrete Institute. Proceedings Vol. 57, No.1. July 1960. pp. 1 - 28.

91. STURMAN, G.M., SHAH, S.P. and WINTER, G. Effects of flexural strain gradients on micro-cracking and stress-strain behaviour of concrete. Journal of the American Concrete Institute. Proceedings Vol. 62, No. 7. July 1965. pp. 805 - 822.

92. CLARK, L.E., GERSTLE, K.H., and TULIN, L.G. Effect of strain gradient on the stress-strain curve of mortar and concrete. Journal of the American Concrete Institute. Proceedings Vol. 64, No. 9. September 1967. pp. 580 - 586.

93. DESAYI, P. and KRISHNAN, S. Equation for the stress-strain curve of concrete. Journal of the American Concrete Institute. Proceedings Vol. 61, No. 3. March 1964. pp. 345 - 350.

94. SMITH, I.A. Calculations of ultimate moment capacities of prestressed concrete beam. Computer program No. 1070. Civil Engineering Department, University of Glasgow. 1974.

95. CARINO, N.J. and SLATE, F.O. Limiting tensile strain criterion for failure of concrete. Journal of the American Concrete Institute. Proceedings Vol. 73, No. 3. March 1976. pp. 160 - 165.

96. JONES, L.L. A theoretical solution for the ultimate strength of rectangular reinforced concrete beams without stirrups. A paper presented to the European Committee for Concrete at Wiesbaden, 1963. pp. 12.

97. TANG, MAN-CHUNG. Shear design of large concrete box girders. Shear in reinforced concrete. Detroit, American Concrete Institute, 1974. Publication SP - 42. Vol. 1. pp. 305 - 319.